

In cooperation with the
SAN GORGONIO PASS WATER AGENCY

Geology, Ground-Water Hydrology, Geochemistry, and Ground-Water Simulation of the Beaumont and Banning Storage Units, San Geronio Pass Area, Riverside County, California



Scientific Investigations Report 2006–5026

U.S. DEPARTMENT OF THE INTERIOR
U.S. GEOLOGICAL SURVEY

*Cover photo: San Geronio Pass Water Agency Recharge Facility, Cherry Valley, California.
Photo by Allen Christensen, U.S. Geological Survey.*

Geology, Ground-Water Hydrology, Geochemistry, and Ground-Water Simulation of the Beaumont and Banning Storage Units, San Gorgonio Pass Area, Riverside County, California

By Diane L. Rewis, Allen H. Christensen, Jonathan C. Matti, Joseph A. Hevesi,
Tracy Nishikawa, and Peter Martin

Prepared in cooperation with the San Gorgonio Pass Water Agency

Scientific Investigations Report 2006–5026

**U.S. Department of the Interior
U.S. Geological Survey**

U.S. Department of the Interior
P. Lynn Scarlett, Acting Secretary

U.S. Geological Survey
P. Patrick Leahy, Acting Director

U.S. Geological Survey, Reston, Virginia: 2006

For product and ordering information:

World Wide Web: <http://www.usgs.gov/pubprod>

Telephone: 1-888-ASK-USGS

For more information on the USGS--the Federal source for science about the Earth, its natural and living resources, natural hazards, and the environment:

World Wide Web: <http://www.usgs.gov>

Telephone: 1-888-ASK-USGS

Any use of trade, product, or firm names is for descriptive purposes only and does not imply endorsement by the U.S. Government.

Although this report is in the public domain, permission must be secured from the individual copyright owners to reproduce any copyrighted materials contained within this report.

Suggested citation:

Rewis, D.L., Christensen, A.H., Matti, J.C., Hevesi, J.A., Nishikawa, Tracy, and Martin, Peter, 2006, Geology, ground-water hydrology, geochemistry, and ground-water simulation of the Beaumont and Banning storage units, San Geronio Pass area, Riverside County, California: U.S. Geological Survey Scientific Investigations Report 2006-5026, 173 p.

Contents

Abstract.....	1
Introduction.....	2
Purpose and Scope	5
General Description of Study Area	5
Acknowledgments	6
Geology.....	7
Previous Geologic Studies	7
Geologic Units	7
Crystalline Basement Rocks	7
Late Cenozoic Sedimentary Deposits.....	12
Older Sedimentary Deposits (QTso).....	12
Younger Sedimentary Deposits (Qsu, Qsl)	12
Quaternary Surficial Deposits (Qvo, Qo, Qy, and Ql).....	13
Geologic Structure.....	13
Faults	15
Banning Fault.....	15
San Gorgonio Pass Fault Zone	15
Cherry Valley Fault.....	16
Banning Barrier Faults.....	16
Beaumont Plain Fault Zone	17
San Timoteo Canyon Fault.....	17
Wildwood Canyon Fault.....	18
Folds	18
Ground-Water Hydrology	18
Storage Unit Characterization	18
Definition of Aquifers	20
Natural Ground-Water Recharge.....	21
INFILv3 Model Description.....	21
INFILv3 Model Area and Discretization	22
INFILv3 Model Inputs	22
Climate and Meteorological Data	22
Digital Map Files and Attribute Tables	28
Topographic Parameters	28
Spatially Distributed Vegetation and Root-Zone Parameters	28
Spatially Distributed Soil Parameters	28
Spatially Distributed Bedrock and Deep-Soil Parameters	30
INFILv3 Model Coefficients.....	34
INFILv3 Model Calibration	35
Annual and Seasonal Discharge	35
Monthly Discharge	35
Daily Mean Discharge	37
Storm Event Total Discharge.....	37

INFILv3 Model Results	39
Water Balance for San Timoteo Creek, Portrero Creek, and San Gorgonio River Surface-Water Drainage Basins	39
Water Balance for the Beaumont and Banning Storage Units	39
Water Balance for the Sub-Drainage Basins Upstream of the Beaumont and Banning Storage Units	41
Effects of Urbanization on Simulated Average Annual Ground-Water Recharge and Surface-Water Outflow	51
Data Required to Simulate Urbanization Affects Using INFILv3	51
Urban-Area INFILv3 Model Results	54
INFILv3 Model Limitations	54
Summary of INFILv3 Results	55
Natural Discharge.....	55
Ground-Water Pumpage	57
Artificial Recharge	57
Return Flow of Applied Water.....	59
Septic-Tank Seepage	59
Artificial Recharge Ponds	60
Ground-Water Levels and Movement.....	60
1926–27 Conditions	61
1955 Conditions.....	65
1967 Conditions.....	65
2000 Conditions.....	65
Water-Level Change.....	65
Geochemistry.....	66
General Water-Quality Characteristics.....	66
Chemical Character of Ground Water.....	70
Determining the Source of Water to Wells	70
Source and Age of Ground Water.....	74
Stable Isotopes of Oxygen and Hydrogen	74
Tritium	75
Carbon-14.....	75
Ground-Water Simulation Model	78
Model Objectives and Assumptions	78
Model Discretization	79
Spatial Discretization	79
Temporal Discretization	79
Boundary Conditions	79
Aquifer Properties.....	86
Hydraulic Conductivity and Transmissivity.....	88
Vertical Conductance.....	88
Specific Yield and Storage Coefficient.....	88
Faults	93
Simulated Model Recharge	93
Areal recharge	93
Mountain-Front Recharge.....	96

Simulated Artificial Recharge.....	98
Return Flow of Crop and Golf-Course Irrigation	98
Return Flow of Landscape Irrigation in Banning and Beaumont	98
Septic-Tank Seepage and Return Flow of Landscape Irrigation in the Cherry Valley Area	98
Model Discharge.....	101
Model Calibration	101
Steady-State Calibration	101
Transient Calibration	106
Model Calibration Results	106
Water Budgets	107
Sensitivity Analysis.....	110
Model Limitations.....	122
Particle-Tracking and Flow Paths	122
Simulation of Future Water-Management Scenarios.....	125
Water-Management Scenario 1.....	125
Water-Management Scenario 2.....	125
Water-Management Scenario 3.....	142
Water-Management Scenario 4.....	142
Summary and Conclusions.....	142
References Cited.....	145
Appendix.....	150

Figures

Figure 1. Map showing location of study area and watershed boundaries, San Gorgonio Pass, Riverside County, California.....	3
Figure 2. Map showing the study area boundary, the San Gorgonio Pass Water Agency boundary, and storage unit boundaries, San Gorgonio Pass, Riverside County California.....	4
Figure 3. Graph showing population in Banning, Beaumont, and Cherry Valley for 1920–2003, San Gorgonio Pass area, Riverside County, California. Data from California Department of Finance (2006)	5
Figure 4. Graphs showing annual precipitation and cumulative departure of precipitation from mean at Beaumont, 1876–2004, San Gorgonio Pass area, Riverside County, California	6
Figure 5. Map showing the generalized geology of the San Gorgonio Pass area, Riverside County California.....	8
Figure 6. Schematics showing generalized geologic cross sections for the San Gorgonio Pass area, Riverside County, California.....	9
Figure 7. Map showing regional geologic structure of the San Gorgonio Pass area, Riverside County California.....	14
Figure 8. Map showing the storage units and hydrologic areas of the San Gorgonio Pass area, Riverside County California.....	19
Figure 9. Schematic showing conceptual model of net infiltration illustrating the layered root-zone water-balance model for the San Gorgonio Pass area, Riverside County California.....	22

Figure 10. Map showing the San Timoteo Creek, Potrero Creek, and San Gorgonio River surface-water drainage basins used for the INFILv3 simulation, San Gorgonio Pass area, Riverside County, California.....	23
Figure 11. Map showing surface-water sub-drainage basins upstream of the Beaumont and Banning storage units simulated using INFILv3, San Gorgonio Pass area, Riverside County, California.....	25
Figure 12. Map showing location of climate stations of the National Climatic Data Center (NCDC) in the Southern California region (EarthInfo, Inc., 2004)	26
Figure 13. Map showing vegetation type and coverage used for the INFILv3 simulation of the San Gorgonio Pass area, Riverside County, California	29
Figure 14. Map showing State Soil Geographic Database (STATSGO) soil units used for the INFILv3 simulation, San Gorgonio Pass area, Riverside County, California	31
Figure 15. Geologic map used for the INFILv3 simulation of the San Gorgonio Pass area, Riverside County, California.....	33
Figure 16. Graph showing measured and simulated streamflow at Little San Gorgonio Creek gage (11056500) for total annual, total monthly, and daily mean discharge, San Gorgonio Pass area, Riverside County, California	36
Figure 17. Map showing average annual precipitation simulated by the INFILv3 model of the San Gorgonio Pass area, Riverside County, California	44
Figure 18. Map showing average annual snowfall simulated by the INFILv3 model of the San Gorgonio Pass area, Riverside County, California	45
Figure 19. Map showing average annual evapotranspiration simulated by the INFILv3 model of the San Gorgonio Pass area, Riverside county, California	46
Figure 20. Map showing average annual runoff simulated by the INFILv3 model for natural conditions and the difference in simulated net runoff between urban-modified and natural conditions, San Gorgonio Pass area, Riverside County, California	47
Figure 21. Map showing average annual net infiltration simulated by the INFILv3 model for natural conditions and the difference in simulated average annual net infiltration between urban-area modified and natural conditions, San Gorgonio Pass area, California.....	49
Figure 22. Graphs showing the annual precipitation, runoff, outflow, evapotranspiration, and recharge simulated by the INFILv3 model for Little San Gorgonio Creek sub-drainage basin, San Gorgonio Pass area, Riverside County, California	51
Figure 23. Map showing impervious area simulated in the urban-area INFILv3 model of the San Gorgonio Pass area, Riverside County, California.....	52
Figure 24. Map showing approximate areas of flowing springs and wells during 1926–27 and areas of artificial recharge from septic-tank seepage, irrigation return flow from the irrigation of crops, golf courses, and landscape in the San Gorgonio Pass area, California.....	56
Figure 25. Graphs showing ground-water pumpage from the Beaumont and Banning storage units by area, Beaumont–Cherry Valley Water District, City of Banning Water Company, and cumulative ground-water pumpage from the Beaumont and Banning storage units for 1927–2003, San Gorgonio Pass area, Riverside County, California.....	58
Figure 26. Estimated and reported annual rates of artificial recharge applied at land surface by area, type, 1927–2003, and the estimated annual totals and cumulative totals of artificial recharge applied at land surface, and reaching the water table, 1927–2074, San Gorgonio Pass area, Riverside County, California rea location	60

Figure 27. Maps showing ground water-level contours for 1926–27, 1955, and 1967 for the Beaumont storage unit and surrounding area, San Gorgonio Pass area, Riverside County, California	62
Figure 28. Map showing ground water-levels for Spring 2000 for the Beaumont and Banning storage units and surrounding area, San Gorgonio Pass area, Riverside County, California.....	63
Figure 29. Graphs showing water-level hydrographs and pumpage by area for the Beaumont and Banning storage units, San Gorgonio Pass area, Riverside County, California	64
Figure 30. Map showing wells in the water-quality monitoring network and fluoride and nitrate concentrations as nitrogen in samples from selected production and monitoring wells, San Gorgonio Pass area, Riverside County, California	67
Figure 31. Graphs showing trilinear diagrams for samples from selected production and monitoring wells in the Beaumont and Banning storage units and surrounding area, San Gorgonio Pass area, Riverside County, California	68
Figure 32. Map showing stiff diagrams and dissolved-solids concentrations for samples from selected production and monitoring wells in the Beaumont and Banning storage units and surrounding area, San Gorgonio Pass area, Riverside County, California.....	69
Figure 33. Geologic cross sections <i>A–A'</i> and <i>C–C'</i> showing Stiff diagrams and perforated intervals for selected wells, San Gorgonio Pass area, Riverside County, California.....	71
Figure 34. Graphs showing trilinear diagrams for samples collected from temporary wells installed during the construction of well 2S/1W-27P2, from well 2S/1W-27P2 after construction, from well 3S/1E-17C1, and from 550 feet and 1,000 feet below land surface in well 3S/1E-17C1, San Gorgonio Pass area, Riverside County, California.....	73
Figure 35. Graph showing stable isotope data for selected wells in the Beaumont and Banning storage units and surrounding area, San Gorgonio Pass area, Riverside County, California	76
Figure 36. Map showing carbon-14 and tritium data for selected wells in the Beaumont and Banning storage units and surrounding area, San Gorgonio Pass area, Riverside County, California	77
Figure 37. Map showing the ground-water flow model grid for the Beaumont and Banning storage units, San Gorgonio Pass area, Riverside County, California	80
Figure 38. Map showing the active model grid and boundary conditions for the ground-water model for model layer 1 and model layer 2, San Gorgonio Pass area, Riverside County, California	81
Figure 39. Generalized model cross sections <i>A–A'</i> and <i>B–B'</i> showing vertical discretization of the ground-water flow model, San Gorgonio Pass area, Riverside County, California.....	83
Figure 40. Map showing the bottom altitudes for model layer 1 and model layer 2, San Gorgonio Pass area, Riverside County, California	84
Figure 41. Time-varying and cumulative mass-balance errors simulated by the ground-water flow model, San Gorgonio Pass area, Riverside County, California.....	86
Figure 42. Map showing distribution of transmissivity values for model layer 1 and model layer 2 for the steady-state ground-water flow model, and the percent decrease in transmissivity between the steady state and year-2003 for model layer 1	89
Figure 43. Map showing distribution of vertical conductance (VCONT) for the ground-water flow model between model layers 1 and 2, San Gorgonio Pass area, Riverside County, California.....	92

Figure 44. Map showing distribution of storage coefficient values for model layer 2 in the transient ground-water flow model, San Gorgonio Pass area, Riverside County, California	94
Figure 45. Map showing the distribution of areal recharge cells for the ground-water flow model, San Gorgonio Pass area, Riverside County, California	95
Figure 46. Graph showing departure of tree-ring indices for southern California (1458–1966), cumulative departure of precipitation at Beaumont (1875–2003), and wet and dry climatic periods for the INFILv3 simulation period (water years 1926–2003), San Gorgonio Pass area, Riverside County, California	97
Figure 47. Map showing the distribution of pumpage and return flow cells in the ground-water flow model, San Gorgonio Pass area, Riverside County, California	100
Figure 48. Map showing the measured water levels for 1926–27 and simulated hydraulic-head contours for the calibrated steady-state ground-water flow model for (A) model layer 1 and (B) model layer 2, San Gorgonio Pass area, Riverside County, California.	102
Figure 49. Maps showing measured Spring 2000 water levels and simulated hydraulic-head contours for the calibrated transient-state ground-water flow model for model layer 1 and model layer 2, San Gorgonio Pass area, Riverside County, California	104
Figure 50. Graphs showing measured water levels and simulated hydraulic heads and residuals and sum of residuals for the calibrated ground-water flow model, 1926–2003, San Gorgonio Pass area, Riverside County, California	109
Figure 51. Graphs showing measured and simulated hydraulic heads for selected wells, and pumpage by model area, for Area 1, Areas 2 and 3, Area4, and Area 5, San Gorgonio Pass area, Riverside County, California	110
Figure 52. Graphs showing the simulated recharge flux, discharge flux, cumulative recharge, and cumulative discharge, 1926–2003, San Gorgonio Pass area, Riverside County, California	115
Figure 53. Maps showing the simulated water budget for simulated steady-state conditions and year-2003 conditions, San Gorgonio Pass area, Riverside County, California	119
Figure 54. Graph showing the sensitivity of selected ground-water model parameters, San Gorgonio Pass area, Riverside County, California	121
Figure 55. Map showing backward particle tracking of particles under steady-state conditions starting at selected production wells, San Gorgonio Pass area, Riverside County, California	124
Figure 56. Graphs showing pumpage and simulated hydraulic heads from 2000–2013 for water-management scenario 1, scenario 2, scenario 3, and scenario 4, San Gorgonio Pass area, Riverside County, California	138
Appendix Figure 1. Map showing location of wells referenced in this report, San Gorgonio Pass, Riverside County, California.....	151

Tables

Table 1. Area and altitude of surface-water drainage basins and surface-water sub-drainage basins upstream of and including the Beaumont and Banning storage units modeled using INFILv3 for the San Gorgonio Pass area, Riverside County, California	24
Table 2. Climate stations in the Southern California Region with daily climate records maintained by the National Climatic Data Center (NCDC) and used to develop the INFILv3 model of the San Gorgonio Pass area, Riverside County, California	27

Table 3. Estimated vegetation cover and root densities used to define the root-zone parameters for the INFILv3 model of the San Gorgonio Pass area, Riverside County, California.....	30
Table 4. Initial and calibrated soil parameter values used as input to the INFILv3 model of the San Gorgonio Pass area, Riverside County, California	32
Table 5. Estimated root-zone porosity, initial, and final (calibrated) saturated hydraulic conductivity for bedrock and deep soil parameters used in the INFILv3 model of the San Gorgonio Pass area, Riverside County, California.....	32
Table 6. Average monthly precipitation and maximum and minimum regression model coefficients and statistics for spatially distributing daily climate inputs as a function of altitude and point measurements of average monthly precipitation in the INFILv3 model of the San Gorgonio Pass area, Riverside County, California	34
Table 7. Measured and INFILv3-simulated total annual (water-year), total monthly, daily mean, and storm event total discharge, San Gorgonio Pass area, Riverside County, California.....	38
Table 8A. Summary of INFILv3 simulated water-balance results for natural conditions in the San Gorgonio Pass area, Riverside County, California, 1930–2001	40
Table 8B. Summary of INFILv3 simulated water-balance results for urban-area modified conditions in the San Gorgonio Pass area, Riverside County, California, 1930–2001	42
Table 9. Urbanization parameters for drainage basins and sub-drainage basins upstream of and including the Beaumont and Banning storage units modeled using INFILv3 for the San Gorgonio Pass area, Riverside County, California	53
Table 10. Summary of initial and calibrated parameter estimates used in the ground-water flow model of the San Gorgonio Pass area, Riverside County, California	87
Table 11. Mountain-front recharge simulated in the ground-water flow model of the San Gorgonio Pass area, Riverside County, California	99
Table 12. Comparisons of measured spring water levels and simulated hydraulic heads for steady-state and transient conditions(1926–2003), areas, pumping periods, and decade for the San Gorgonio Pass area, Riverside County, California	108
Table 13. Water budget for the calibrated steady-state model and for selected periods of the transient-state model of the San Gorgonio Pass area, Riverside County, California.....	114
Table 14. Estimated and simulated residence times of ground water in selected cells during steady-state conditions using backward particle tracking, San Gorgonio Pass area, Riverside County, California.....	123
Table 15. Simulated water budgets for water management scenario 1, scenario 2, scenario 3, and scenario 4 for the San Gorgonio Pass area, Riverside County, California.....	126
Appendix Table 1. Well construction data for selected wells, San Gorgonio Pass area, Riverside County, California.....	152
Appendix Table 2. Well construction, specific capacity, and transmissivity data for selected wells, San Gorgonio Pass area, Riverside County, California.....	156
Appendix Table 3. Reported or estimated pumpage for wells in the Beaumont and Banning Storage Units and total pumpage for the Edgar Canyon, Banning Bench and Banning Canyon Storage Units, San Gorgonio Pass, Riverside County, California, 1927–2003.....	158

Conversion Factors, Datum, Abbreviations. Acronyms, and Organizations

Multiply	By	To obtain
Length		
inch (in.)	2.54	centimeter (cm)
inch (in.)	25.4	millimeter (mm)
inch per foot (in/ft)	8.33	centimeter per meter (cm/m)
foot (ft)	0.3048	meter (m)
mile (mi)	1.609	kilometer (km)
Area		
acre	4,047	square meter (m ²)
acre	0.004047	square kilometer (km ²)
square foot (ft ²)	0.09290	square meter (m ²)
square mile (mi ²)	2.590	square kilometer (km ²)
Volume		
gallon (gal)	3.785	liter (L)
gallon per day (gal/d)	0.003785	cubic meter per day(m ³ /d)
acre-foot (acre-ft)	1,233	cubic meter (m ³)
Flow rate		
acre-foot per year (acre-ft/yr)	1,233	cubic meter per year (m ³ /yr)
foot per second (ft/s)	0.3048	meter per second (m/s)
ft ³ /s	0.02832	cubic foot per second
square foot per day (ft ² /d)	0.3048	square meter per day (m ² /d)
foot per year (ft/yr)	0.3048	meter per year (m/yr)
inch per year (in/yr)	25.4	millimeter per year (mm/yr)
Hydraulic conductivity		
foot per second (ft/s)	0.3048	meter per second(m/sec)
foot per day (ft/d)	0.3048	meter per day (m/d)

Temperature in degrees Fahrenheit (°F) may be converted to degrees Celsius (°C) as follows:

$$^{\circ}\text{C}=(^{\circ}\text{F}-32)/1.8$$

Water-quality and unsaturated-zone data are generally reported in metric units. The use of dual units in this report is intended to facilitate application of the data by maintaining the integrity of the original units of measurement.

Vertical coordinate information is referenced to the North American Vertical Datum of 1988 (NAVD 88).

Horizontal coordinate information is referenced to the North American Datum of 1983 (NAD 83).

Vertical coordinate information is referenced to the National Geodetic Vertical Datum of 1929 (NGVD 29).

Altitude, as used in this report, refers to distance above the vertical datum.

*Transmissivity: The standard unit for transmissivity is cubic foot per day per square foot times foot of aquifer thickness [(ft³/d)/ft²]ft. In this report, the mathematically reduced form, foot squared per day (ft²/d), is used for convenience.

Specific conductance is given in microsiemens per centimeter at 25 degrees Celsius (μS/cm at 25 °C).

Data for the isotopes oxygen-18 and deuterium are reported in delta (δ) notation as per mil (parts per thousand); tritium data are reported in tritium units (TU); carbon-14 data are reported as per-cent modern carbon (pmc).

Abbreviations and Acronyms

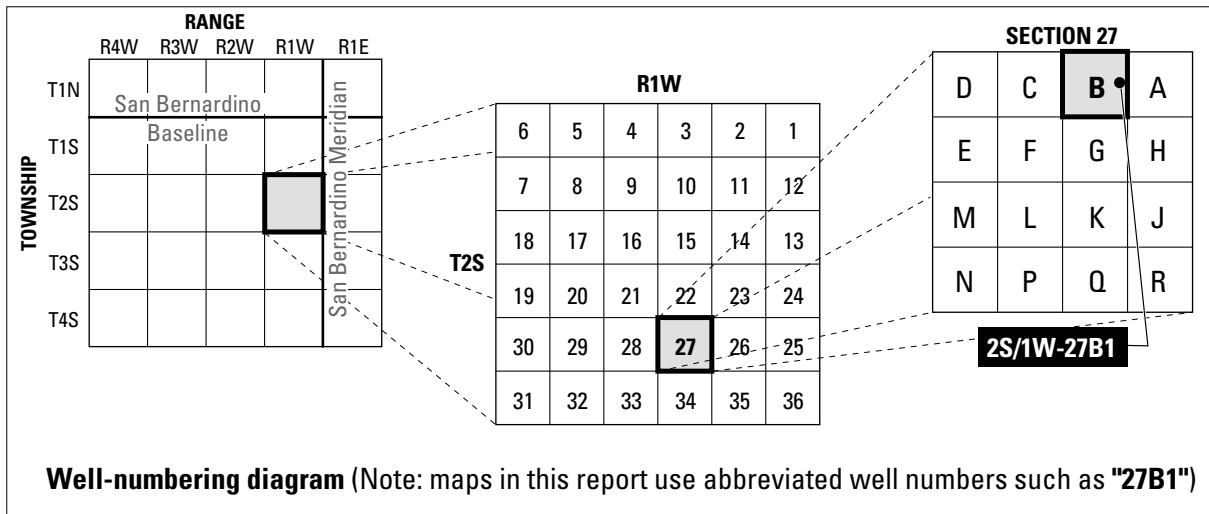
asl, above sea level
 ^{14}C , carbon-14
 δD , delta deuterium
 $\delta^{18}\text{O}$, delta oxygen-18
 $^{\circ}$, degrees
DEM, digital elevation model
GAP, California Gap Analysis Program
GHB, general-head conductance
 h_c , hydraulic conductivity
INFILv3, distributed-parameter watershed model
 K_h , hydraulic conductivity
 K_v , vertical hydraulic conductivity
MCL, maximum contaminant level
ME, mean error
MSE, mean-square error
m, meter
 m^2 , square meter
meq/L, milliequivalents per liter
MODFLOW-96, ground-water flow model
MODPATH, particle tracking program
MUID, map unit identifier
NCDC, National Climatic Data Center
NWISweb, USGS National Water Information System Web page
pmc, percent modern carbon
Ql, landslide deposits
Qo, older deposits
Qsl, younger sedimentary deposit, lower member
Qsu, younger sedimentary deposit, upper member
QTso, older sedimentary deposits
Qvo, very old deposits
Qy, younger deposits
RMSE, root-mean-square error
S, storativity
SGPWA, San Geronio Pass Water Agency
STATSGO, state soil geographic database
 S_s , specific storage
 S_y , specific yield
TU, tritium units
VCONT, vertical conductance
VSMOW, Vienna Standard Mean Ocean Water

Organizations

BCVWD, Beaumont–Cherry Valley Water District
BWD, Banning Water District
CADWR, California Department of Water Resources
SGPWA, San Geronio Pass Water Agency
SWP, California State Water Project
USEPA, U.S. Environmental Protection Agency
USGS, U.S. Geological Survey

Well-Numbering System

Wells are identified and numbered according to their location in the rectangular system for the subdivision of public lands. Identification consists of the township number, north or south; the range number, east or west; and the section number. Each section is divided into sixteen 40-acre tracts lettered consecutively (except I and O), beginning with "A" in the northeast corner of the section and progressing in a sinusoidal manner to "R" in the southeast corner. Within the 40-acre tract, wells are sequentially numbered in the order they are inventoried. The final letter refers to the base line and meridian. In California, there are three base lines and meridians; Humboldt (H), Mount Diablo (M), and San Bernardino (S). All wells in the study area are referenced to the San Bernardino base line and meridian (S) Well numbers consist of 15 characters and follow the format 002S001W027B001. In this report, well numbers are abbreviated and written 2S/1W-27B1. Wells in the same township and range are referred to only by their section designation, 27B1. The following diagram shows how the number for well 2S/1W-27B1 is derived.



This page intentionally left blank.

Geology, Ground-Water Hydrology, Geochemistry, and Ground-Water Simulation of the Beaumont and Banning Storage Units, San Gorgonio Pass Area, Riverside County, California

By Diane L. Rewis, Allen H. Christensen, Jonathan Matti, Joseph A. Hevesi, Tracy Nishikawa, and Peter Martin

Abstract

Ground water has been the only source of potable water supply for residential, industrial, and agricultural users in the Beaumont and Banning storage units of the San Gorgonio Pass area, Riverside County, California. Ground-water levels in the Beaumont area have declined as much as 100 feet between the early 1920s and early 2000s, and numerous natural springs have stopped flowing. In 1961, the San Gorgonio Pass Water Agency (SGPWA) entered into a contract with the California State Department of Water Resources to receive 17,300 acre-feet per year of water to be delivered by the California State Water Project (SWP) to supplement natural recharge. Currently (2005), a pipeline is delivering SWP water into the area, and the SGPWA is artificially recharging the ground-water system using recharge ponds located along Little San Gorgonio Creek in Cherry Valley with the SWP water. In addition to artificial recharge, SGPWA is considering the direct delivery of SWP water for the irrigation of local golf courses and for agricultural supply in lieu of ground-water pumpage. To better understand the potential hydrologic effects of different water-management alternatives on ground-water levels and movement in the Beaumont and Banning storage units, existing geohydrologic and geochemical data were compiled, new data from a basin-wide ground-water level and water-quality monitoring network were collected, monitoring wells were installed near the Little San Gorgonio Creek recharge ponds, geohydrologic and geochemical analyses were completed, and a ground-water flow simulation model was developed.

The San Gorgonio Pass area was divided into several storage units on the basis of mapped or inferred faults. This study addresses primarily the Beaumont and Banning storage units. The geologic units in the study area were generalized into crystalline basement rocks and sedimentary deposits. The

younger sedimentary deposits and the surficial deposits are the main water-bearing deposits in the San Gorgonio Pass area. The water-bearing deposits were divided into three aquifers: (1) the perched aquifer, (2) the upper aquifer, and (3) the lower aquifer based on lithologic and downhole geophysical logs.

Natural recharge in the San Gorgonio Pass area was estimated using INFILv3, a deterministic distributed-parameter precipitation-runoff model. The INFILv3 model simulated that the potential recharge of precipitation and runoff in the Beaumont and Banning storage units was about 3,710 acre-feet per year and that the potential recharge in 28 sub-drainage basins upstream of the storage units was about 6,180 acre-feet per year.

The water supply for the Beaumont and Banning storage units is supplied by pumping ground water from wells in the Canyon (Edgar and Banning Canyons), Banning Bench, Beaumont, and Banning storage units. Total annual pumpage from the Beaumont and Banning storage units ranged from about 1,630 acre-feet in 1936 to about 20,000 acre-feet in 2003. Ground-water levels declined by as much as 100 feet in the Beaumont storage unit from 1926–2003 in response to ground-water pumping of about 450,160 acre-feet during this period.

Since ground-water development began in the San Gorgonio Pass area, there have been several sources of artificial recharge to the basin including return flow from applied water on crops, golf courses, and landscape; septic-tank seepage; and infiltration of storm runoff diversions and imported water into recharge ponds. Return flow from applied water and septic-tank seepage was estimated to reach a maximum of about 8,100 acre-feet per year in 2003. Owing to the great depth of water in much of study area (in excess of 150 feet), the return flow and septic-tank seepage takes years to decades to reach the water table.

2 Geology, Ground-Water Hydrology, Geochemistry, and Ground-Water Simulation, San Gorgonio Pass Area, California

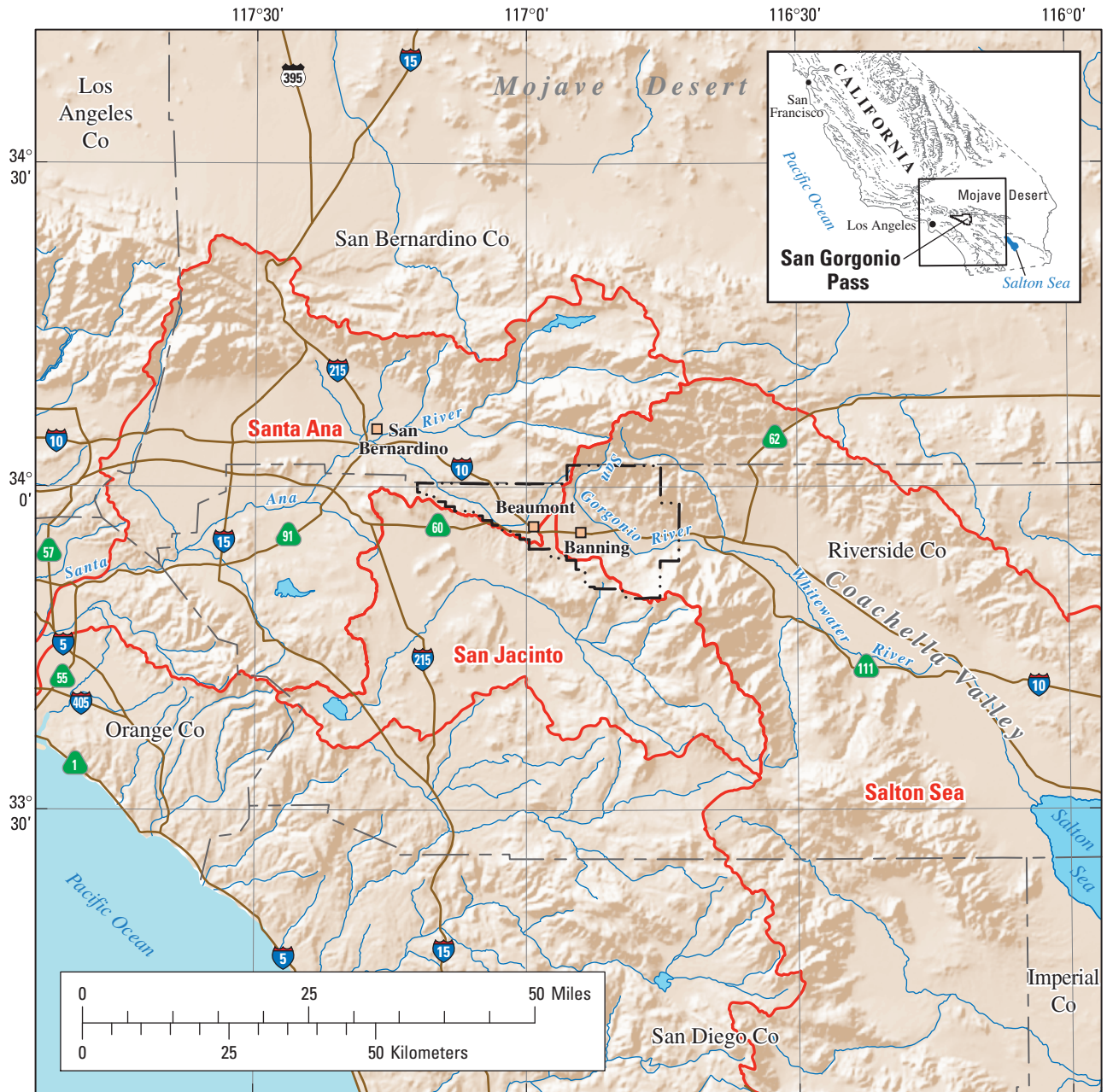
Stable-isotope data indicate that the source of ground-water recharge was precipitation from storms passing through the San Gorgonio Pass as opposed to runoff from the higher altitudes of the San Bernardino Mountains. In addition, these data indicate that little if any of the ground water in the fractured crystalline rocks flows across the Banning Fault into the Beaumont storage unit. Tritium concentrations indicate that little to no recharge has reached the water table since 1952 in most areas of the Beaumont and Banning storage units. In general, the uncorrected carbon-14 ages of ground water sampled from wells in the Beaumont, Banning, and surrounding storage units ranged from about 400 to 17,500 years before present. The older water was sampled in southeastern part of Beaumont storage unit and in the Banning storage unit, and ranged from 1,900 to 17,500 years before present.

To better understand the dynamics of ground-water flow and the potential effects of water-level changes resulting from artificial recharge in the San Gorgonio Pass area, a regional-scale, numerical ground-water flow model was developed using MODFLOW-96. This model will be used by water managers to help manage the ground-water resources in the San Gorgonio Pass area. Results of the steady-state simulation indicate that the total inflow rate, or recharge, was about 6,590 acre-feet per year with about 3,710 acre-feet per year from areal recharge, about 2,670 acre-feet per year from mountain-front recharge, and about 210 acre-feet per year from the surrounding older sedimentary deposits. The simulated water budget for 1926–2003 indicates that of the total simulated volume of water pumped from the aquifer (450,160 acre-feet), about 50 percent was derived from depletion of ground-water storage (222,660 acre-feet), about 21 percent was derived from the reduction of underflow to the Cabazon and San Timoteo storage units (about 96,280 acre-feet), about 19 percent was derived from a reduction of ground-water outflow to the stream channels draining the San Timoteo storage unit (about 86,030 acre-feet), about 8 percent was derived from irrigation return flows and septic-tank seepage (about 36,780 acre-feet), and about 2 percent was derived from an increase in ground-water underflow from the surrounding older sedimentary deposits (about 8,410 acre-feet).

The calibrated ground-water flow model was used to simulate the effects of four water-management scenarios being considered by SGPWA for the period 2004–13. In general, the results of the water-management scenarios indicate that artificial recharge in the Little San Gorgonio Creek recharge ponds primarily benefits the area north of the Cherry Valley Fault. For the scenario that used SWP water in lieu of ground water for golf course irrigation and for agricultural use, hydraulic heads increased by about 50 feet. None of the water-management scenarios significantly benefited the Banning storage unit.

Introduction

Ground water has been the only source of potable water supply for residential, industrial, and agricultural users in the Beaumont and Banning areas of the San Gorgonio Pass, Riverside County, California (*fig. 1*). Ground-water levels near Beaumont declined as much as 100 feet (ft) between the early 1920s and early 2000s and numerous natural springs have stopped flowing in the San Timoteo storage unit (Bloyd, 1971). Boyle Engineering Corporation, (1995) attributed the water-level declines to (1) dry periods in the basin since ground-water development began; (2) increased ground-water pumping to support residential and agricultural needs; (3) basin exports; (4) upstream water development that has reduced basin recharge; and (5) subsurface drainage into the Colorado River Aqueduct San Jacinto Tunnel. In 1961, the San Gorgonio Pass Water Agency (SGPWA) contracted with the California State Department of Water Resources to receive 17,300 acre-ft/yr of water to be delivered by the California State Water Project (SWP) to supplement natural recharge. Currently (2005), a pipeline is delivering SWP water into the area and the SGPWA is artificially recharging the ground-water system with the SWP water using recharge ponds located along Little San Gorgonio Creek in the Cherry Valley area (*fig. 2*). In addition, the SGPWA is considering the direct delivery of SWP water for the irrigation of local golf courses and for agricultural supply in lieu of ground-water pumpage. The SGPWA is concerned about the effects of alternative water-management scenarios on ground-water levels and movement.



Base from U.S. Geological Survey digital data, 1:100,000, 1981-89; Universal Transverse Mercator Projection (NGVD 29), Zone 11.

EXPLANATION

- **San Jacinto** Watershed boundary and name
- . . . — San Gorgonio Pass Water Agency boundary
- Major roads
- Major stream channels

Figure 1. Map showing location of study area and watershed boundaries, San Gorgonio Pass, Riverside County, California.



Figure 2. Map showing the study area boundary, the San Gorgonio Pass Water Agency boundary, and storage unit boundaries, San Gorgonio Pass, Riverside County California.

Purpose and Scope

In 1997, the U.S. Geological Survey (USGS) and the SGPWA entered into a cooperative agreement to investigate the feasibility and potential hydrologic effects of artificially recharging the ground-water system with water from the SWP using artificial recharge ponds in the Cherry Valley area. The feasibility of artificial recharge at the Little San Gorgonio Creek recharge ponds was investigated by Ellett (2002) and Flint and Ellett (2004). The purpose of this study is to improve the understanding of hydrogeology and geochemistry of the Beaumont and Banning storage units and the potential hydrologic effects of artificial-recharge alternatives. The study compiled existing geohydrologic and geochemical data; collected new data from basin-wide ground-water level and water-quality monitoring networks; drilled and installed monitoring wells near the Little San Gorgonio Creek recharge ponds; mapped the surficial geology; and defined the geology, ground-water hydrology, and geochemistry of the Beaumont and Banning storage units. These data were used to develop and calibrate a three-dimensional, numerical ground-water flow model for steady-state and transient conditions. A particle-tracking program was used to simulate the direction and travel times of ground-water flow. The calibrated model was used to evaluate the potential effects of four different water-management scenarios.

General Description of Study Area

The SGPWA service area is about 210 square miles (mi²) of semi-arid badlands, alluvial plains, benches and canyon watersheds. The study area is located in the San Gorgonio

Pass, southern California, which is about 85 mi east of Los Angeles (*fig. 1*). Boyd (1971) divided the San Gorgonio Pass area into the Beaumont, Banning, Cabazon, Calimesa, San Timoteo, South Beaumont, Banning Bench, Singleton, and Canyon (Edgar Canyon, Banning Canyon, Hathaway Canyon, Potrero Canyon, and Millard Canyon) storage units (*fig. 2*). This study addresses primarily the Beaumont and Banning storage units (*fig. 2*), which are bounded by the San Bernardino Mountains to the north, the San Jacinto Mountains to the south, and the San Timoteo Badlands to the southwest.

The area was first settled by non-Native Americans in the late 1800s with the construction of the Southern Pacific Railroad through San Timoteo Canyon, over San Gorgonio Pass, and into the Coachella Valley. Communities within the SGPWA service area include the southern part of Calimesa, Beaumont, Cherry Valley, Banning, and Cabazon (*fig. 2*). The population in the communities of Beaumont, Banning, and Cherry Valley has grown from about 3,200 in 1920 to about 47,600 in 2004 (*fig. 3*). Agriculture (fruit orchards, irrigated pasturelands, and poultry farms) was the primary land use until the early 1950s when suburban development began to extend eastward out of Los Angeles and San Bernardino Counties.

The area has a transitional climate characterized by the marine coastal influences to the west and arid Mojave Desert influences to the east, with low rainfall amounts, hot summers, and cool winters. The long-term average annual precipitation at Beaumont (1876–2004) is 18.32 inches (in.) (*fig. 4*), most of which is lost through evapotranspiration; the total average annual pan evaporation rate ranges from 55 to 72 in/yr (California Irrigation Management Information System, 2002). Most precipitation comes as winter storms from the Pacific Ocean or tropical storms from the east and southeast.

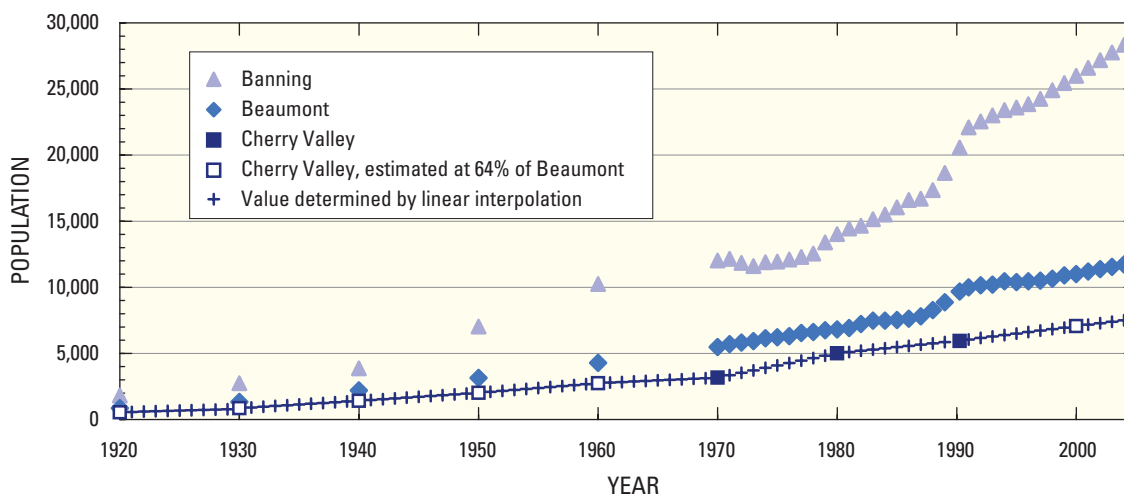


Figure 3. Graph showing population in Banning, Beaumont, and Cherry Valley for 1920–2003, San Gorgonio Pass area, Riverside County, California. Data from California Department of Finance (2006).

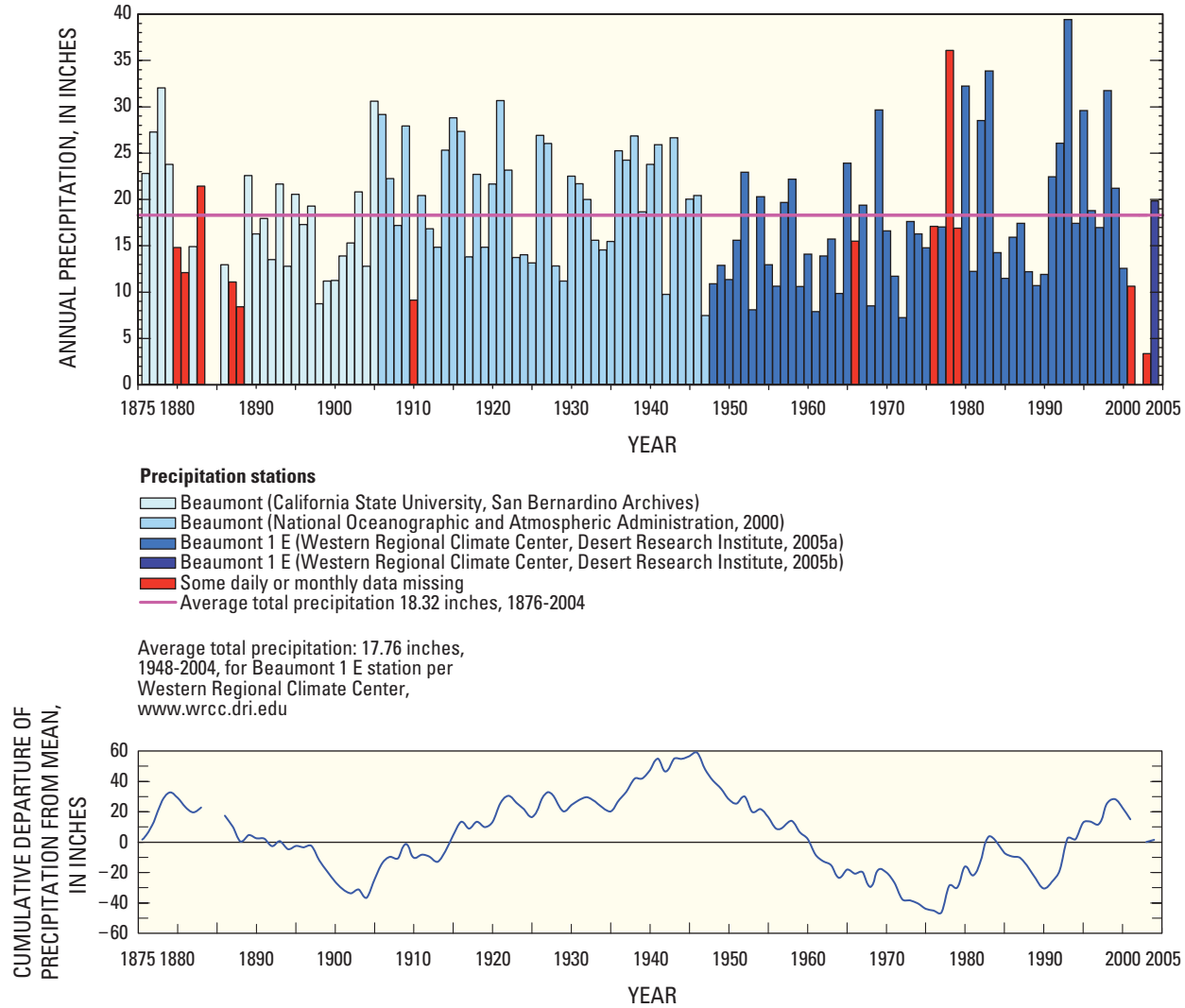


Figure 4. Graphs showing annual precipitation and cumulative departure of precipitation from mean at Beaumont, 1876–2004, San Gorgonio Pass area, Riverside County, California. NOAA, National Oceanic and Atmospheric Association; WRCC DRI, Western Regional Climate Center, Desert Research Institute.

Noble and Little San Gorgonio Creeks and other small watershed drainages in the western part of the study area flow into San Timoteo Creek which is part of the Santa Ana River watershed drainage that flows toward Los Angeles and into the Pacific Ocean. Smith Creek, Montgomery Creek, and the San Gorgonio River in the eastern part of the study area flow southeast and south into the Salton Sea (figs. 1 and 2).

Acknowledgments

The authors acknowledge the many individuals and agencies in the San Gorgonio Pass area that contributed technical support and data to this work. The cooperation and assistance

of the San Gorgonio Pass Water Agency in providing funding for the study and supplying data on water levels and pumpage are gratefully acknowledged. The Beaumont–Cherry Valley Water District (BCVWD) and the Banning Water District (BWD) provided access to their property and valuable hydrologic data. The geologic mapping in the area was completed as part of the National Cooperative Geologic Mapping Program and the Earthquake Hazards Program in cooperation with the California Division of Mines and Geology and the U.S. Forest Service (San Bernardino National Forest).

Geology

The geology of the study area was defined by summarizing and revising previously published geologic maps of the storage unit, evaluating seismic-stratigraphic surveys, and correlating geophysical and geological logs from existing wells and from logs of monitoring wells constructed for this study.

Previous Geologic Studies

Many previous investigators have contributed to understanding the geologic framework of the study area. Frick (1921) described Tertiary sedimentary rocks of the San Timoteo Badlands. Vaughan (1922), in a regional investigation of the San Bernardino Mountains, briefly described faults and geologic units in San Gorgonio Pass. Fraser (1931) described crystalline rocks of the San Jacinto Mountains, including those exposed south of the Beaumont storage unit, and revised some of Frick's interpretations for late Cenozoic sedimentary deposits in the San Timoteo Badlands. Allen (1957) provided the first detailed investigation of geologic materials and geologic structures in the greater San Gorgonio Pass region, and Dibblee (1964, 1968, 1975, 1982) added to the knowledge of the regional geologic setting through his many maps and reports describing the San Bernardino and San Jacinto Mountains. Geophysical studies include gravity investigations (Willingham, 1981; Blanck, 1987; Christensen, 2000) and seismic-reflection and seismic-refraction investigations (Catchings and others, 1999; Gandhok and others, 2000). Matti and others (1985, 1992) delineated the geologic structure of the greater San Gorgonio Pass region, including strands of the San Andreas Fault system and the San Gorgonio Pass Fault zone. Matti and Morton (1993) used this work to interpret the geologic history of the San Andreas Fault system in the San Gorgonio Pass area and elsewhere in southern California. Geologic mapping presented by Morton (1999) covers the west part of the study area. Late Cenozoic sedimentary deposits of the San Timoteo Badlands have been examined by several graduate students (English, 1953; Shuler, 1953; Larsen, 1962; Albright, 1997); various authors have studied vertebrate fossils collected from these deposits (Frick, 1921; May and Repenning, 1982; Reynolds and Reeder, 1986, 1991; Albright, 1999). Hehn and others (1996) and Albright (1999) conducted magnetostratigraphic investigations of the San Timoteo Badlands succession.

Geologic Units

A generalized geologic map of the Beaumont and Banning storage units and surrounding area is shown in *figure 5*. For purposes of this investigation, the geologic units are generalized into crystalline basement rocks and late Cenozoic sedimentary deposits from detailed geologic mapping and stratigraphic studies conducted for this report by the U.S.

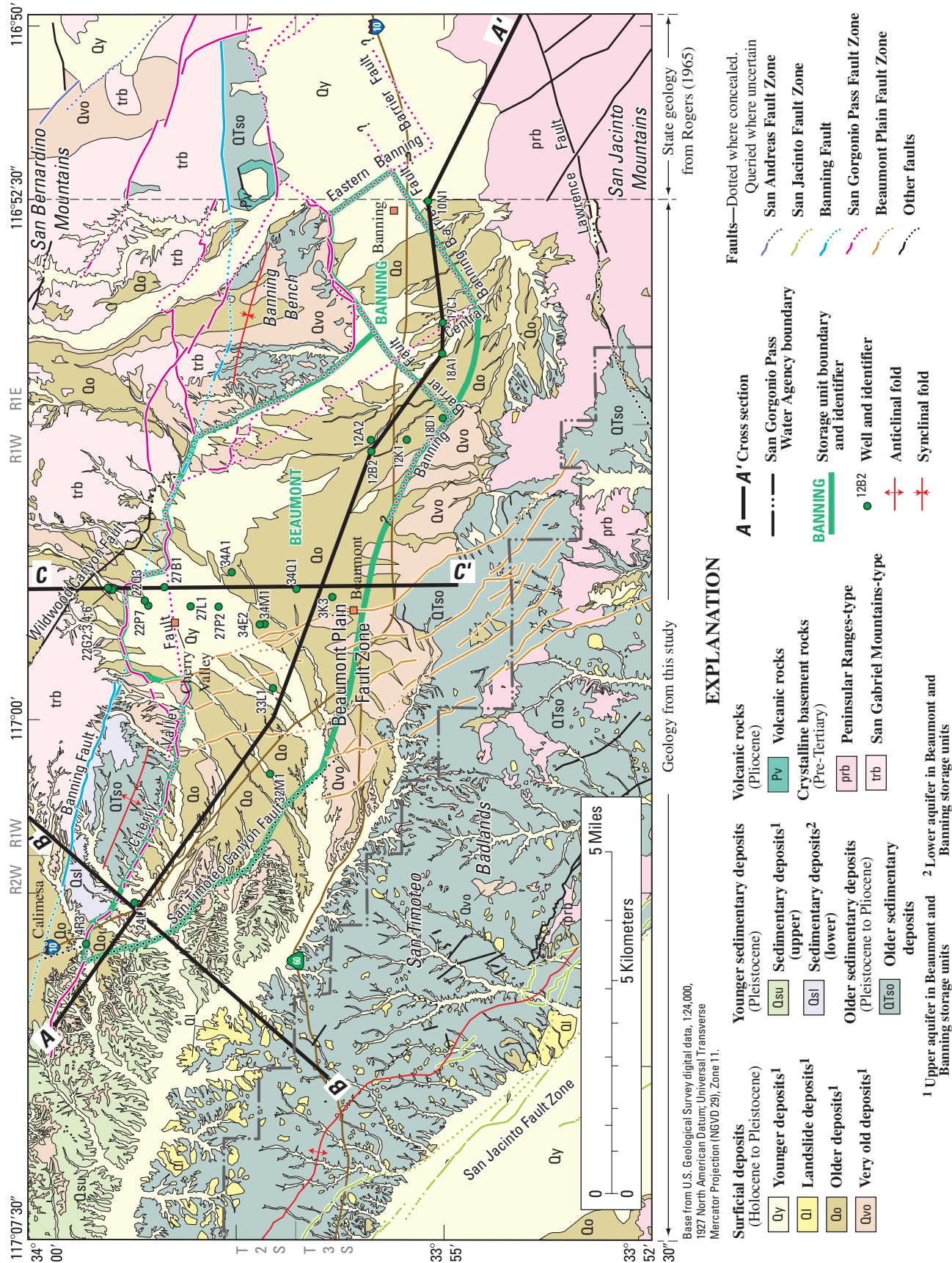
Geological Survey (J.C. Matti and D.M. Morton, unpub. data, 2000–2004). Geologic sections showing structural and stratigraphic relations in the study area are presented in *figure 6*.

Crystalline Basement Rocks

Crystalline rocks occur beneath and around the margins of the Beaumont and Banning storage units and are referred to as basement rocks because they form a hard, low-permeability foundation for more permeable sedimentary materials subsequently deposited within the storage unit. The basement rocks can be subdivided into two distinctive groups (Matti and others, 1992; Matti and Morton, 1993): rocks of Peninsular Ranges-type south of the Banning Fault, and rocks of San Gabriel Mountains-type north of the Banning Fault (*figs. 5 and 6*).

Crystalline rocks of Peninsular Ranges-type crop out in the San Jacinto Mountains and in the foothills south of the Beaumont and Banning storage units, and are inferred to occur in the subsurface beneath the storage units. Rocks of Peninsular Ranges-type are shown in *figure 5* as a single unit (unit prb), but they actually consist of two main rock types: (1) Mesozoic (Cretaceous) plutonic rocks of various granitoid compositions, and (2) older metasedimentary rocks that consist of bodies and screens of marble and quartzofeldspathic biotite gneiss and schist. The plutonic rocks are part of the Cretaceous San Jacinto intrusive complex described by Hill (1984, 1988; Hill and Silver, 1988; Hill and others, 1988). In general, rocks of Peninsular Ranges-type are very hard, slightly to moderately weathered, and not extensively fractured. Although exposed just south of the Beaumont and Banning storage units, northward these rocks plunge steeply into the subsurface and lie deep beneath the storage units. Gravity data (Langenheim and others, 2005) indicate that rocks of Peninsular Ranges-type are deeper than 4,500 ft beneath the western part of the Beaumont storage unit.

Crystalline rocks of San Gabriel Mountains-type are known to occur only north of the Banning Fault, where they underlie watersheds that drain southward into the Beaumont and Banning storage units. The rocks are compositionally and texturally heterogeneous, but on the geologic map are grouped within a single unit (*fig. 5*, unit trb). The terrane consists mainly of plutonic granitoid rocks that are granodioritic to tonalitic in composition. Much of this rock has mylonitic and cataclastic fabrics created when the rock was deformed by ductile and brittle-ductile shearing, stretching, and squeezing. In some exposures the rock has gneissic compositional layering. The terrane is intruded by numerous felsic dikes, most of which are aplitic or pegmatitic. In general, basement rocks of San Gabriel Mountains-type are highly weathered and are cut by fractures that locally are abundant and closely spaced. In places, the rock is so fractured that it crumbles readily.



Base from U.S. Geological Survey digital data, 1:24,000, 1927 North American Datum, Universal Transverse Mercator Projection (NGVD 29), Zone 11.

Geology from this study

State geology from Rogers (1965)

EXPLANATION

Surficial deposits (Holocene to Pleistocene)

- Qy Younger deposits¹
- Qs1 Landslide deposits¹
- Qo Older deposits¹
- Qvo Very old deposits¹

Younger sedimentary deposits (Pleistocene)

- Qsu Sedimentary deposits¹ (upper)
- Qsl Sedimentary deposits² (lower)

Older sedimentary deposits (Pleistocene to Pliocene)

- QIso Older sedimentary deposits

Volcanic rocks (Pliocene)

- Pv Volcanic rocks

Crystalline basement rocks (Pre-Tertiary)

- prb Peninsular Ranges-type
- trb San Gabriel Mountains-type

Faults—Dotted where concealed. Queried where uncertain

- San Andreas Fault Zone
- San Jacinto Fault Zone
- Banning Fault
- San Gorgonio Pass Fault Zone
- Beaumont Plain Fault Zone
- Other faults

A—A' Cross section

- San Gorgonio Pass Water Agency boundary
- Storage unit boundary and identifier
- Well and identifier
- Anticlinal fold
- Synclinal fold

BANNING

- 12B2
- Well and identifier
- Anticlinal fold
- Synclinal fold

1 Upper aquifer in Beaumont and Banning storage units

2 Lower aquifer in Beaumont and Banning storage units

Figure 5. Map showing the generalized geology of the San Gorgonio Pass area, Riverside County California.

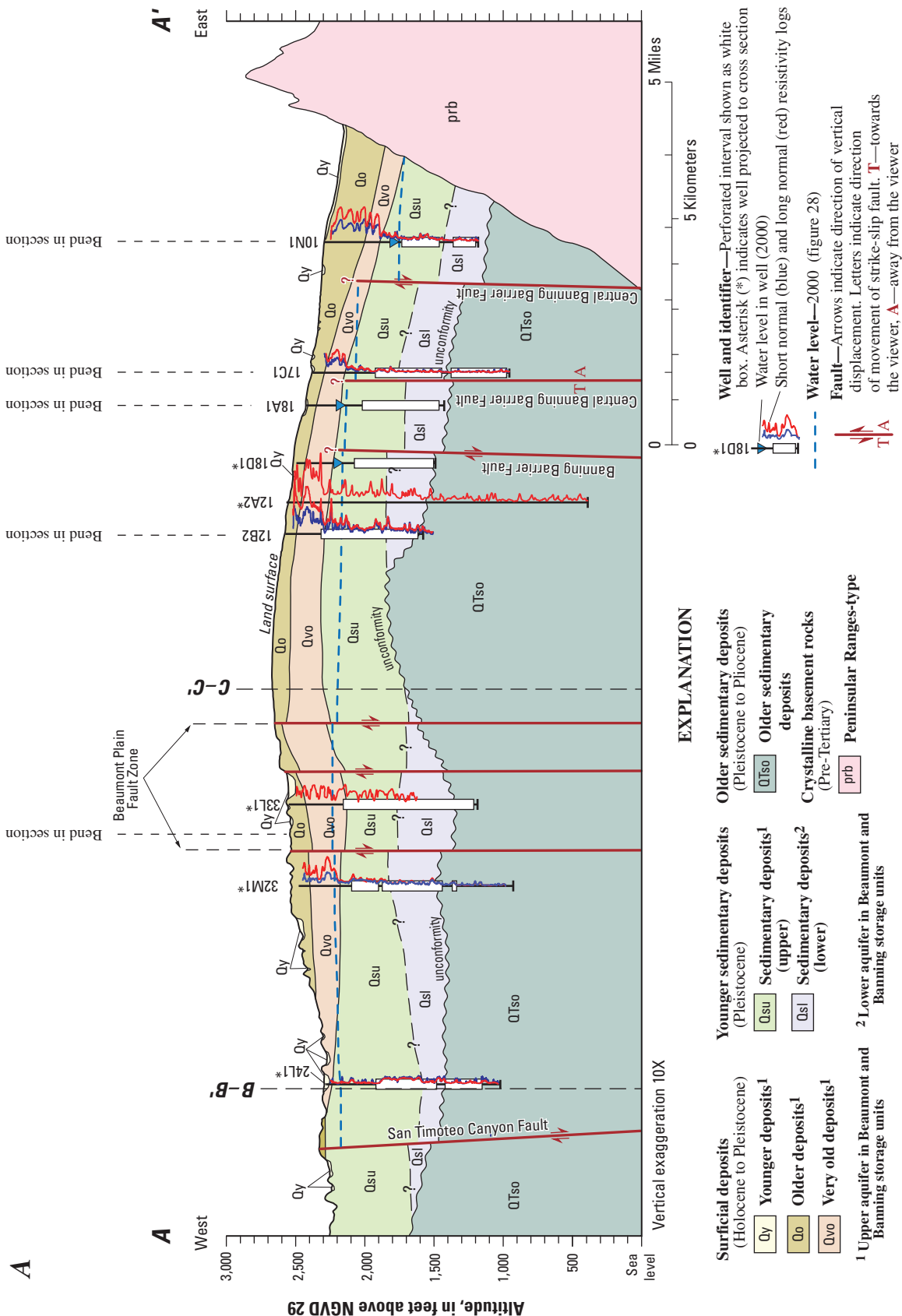


Figure 6. Schematics showing generalized geologic cross sections for the San Gorgonio Pass area, Riverside County, California. A, A-A'.

B

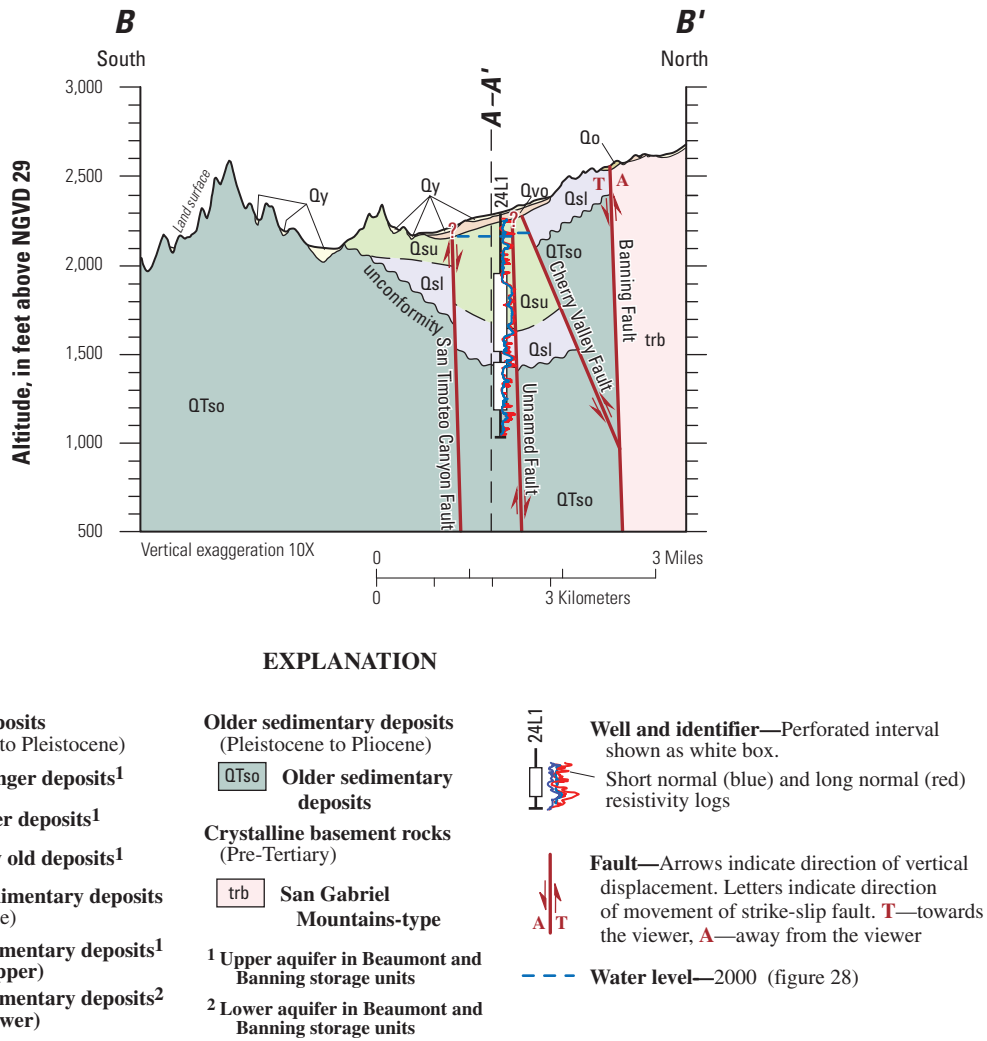
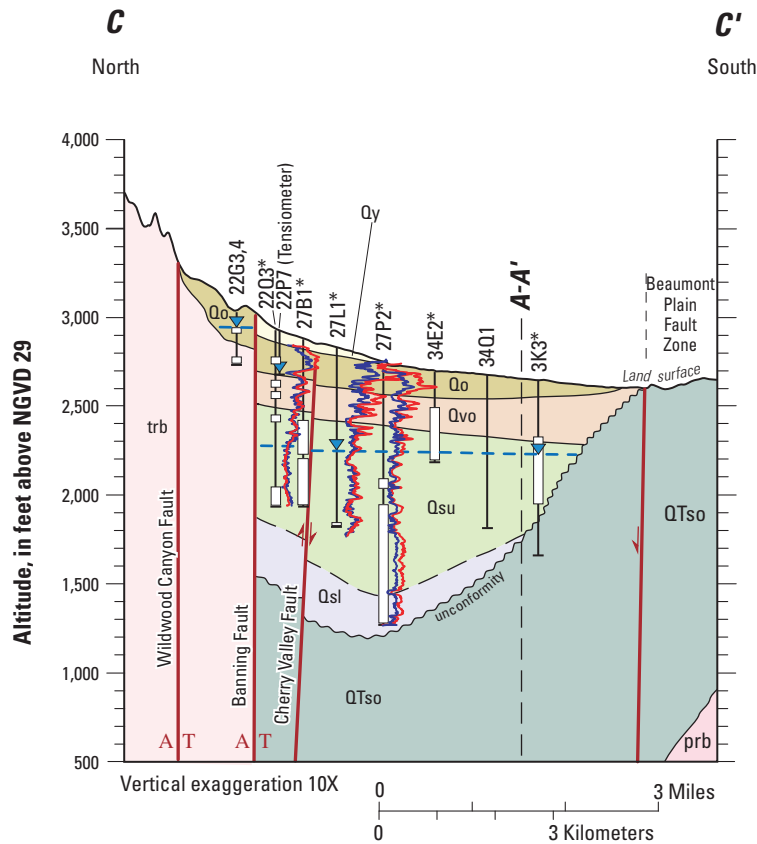


Figure 6. Continued. B, B-B'.

C



EXPLANATION

Surficial deposits
(Holocene to Pleistocene)

- Qy Younger deposits¹
- Qo Older deposits¹
- Qvo Very old deposits¹

Younger sedimentary deposits
(Pleistocene)

- Qsu Sedimentary deposits¹ (upper)
- Qsl Sedimentary deposits² (lower)

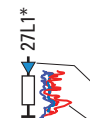
¹ Upper aquifer in Beaumont and Banning storage units
² Lower aquifer in Beaumont and Banning storage units

Older sedimentary deposits
(Pleistocene to Pliocene)

- QTso Older sedimentary deposits

Crystalline basement rocks
(Pre-Tertiary)

- prb Peninsular Ranges-type
- trb San Gabriel Mountains-type



Well and identifier—Perforated interval shown as white box. Asterisk (*) indicates well projected to cross section
 Water level in well (2000)
 Short normal (blue) and long normal (red) resistivity logs

--- **Water level**—2000 (figure 28)



Fault—Arrows indicate direction of vertical displacement. Letters indicate direction of movement of strike-slip fault. **T**—towards the viewer, **A**—away from the viewer

Figure 6. Continued. C, C-C'

Late Cenozoic Sedimentary Deposits

Sedimentary deposits in the study area can be divided into a number of individual map units that have distinct to subtle lithologic differences. For the purposes of this report, these various map units were grouped into three major sedimentary units: (1) older sedimentary deposits, (2) younger sedimentary deposits, and (3) surficial deposits. This subdivision reflects fundamental differences in porosity and permeability between the different deposits.

Within the Beaumont and Banning storage units both the older and younger sedimentary units mainly are concealed by surficial deposits. However, the older unit crop out extensively in the San Timoteo Badlands to the south and southwest (*fig. 5*). The Badlands parallel the San Jacinto Fault, extending more than 20 miles (mi) northwestward from the study area. Canyons and arroyos eroded into the Badlands during the last million years or so (Morton and others, 1990; Kendrick, 1999, Kendrick and others, 2002) reveal a gently to moderately dipping sequence of nonmarine sediment and sedimentary rock deposited on crystalline rocks of Peninsular Ranges-type. These deposits accumulated during a period of region-wide sedimentation that probably began in late Miocene time (about 7 or 8 million years ago) and continued intermittently through middle Pleistocene time (about 700,000 years ago). The sedimentary deposits have been deformed into a major anticline that plunges gently to the northwest for much of its extent (Morton, 1999).

Older Sedimentary Deposits (QTso)

Deposits grouped within the older sedimentary deposits (*fig. 5*, unit QTso) include parts of two formations: (1) the Mt. Eden beds of Frick (1921) and (2) older parts of the San Timoteo beds of Frick (1921). These deposits are well exposed in the San Timoteo Badlands (*fig. 5*). However, owing to regional deformation caused by anticlinal folding and faulting, the older deposits are present only in the subsurface of the Beaumont and Banning storage units. The older sedimentary deposits are buried as deeply as 1,500 ft beneath the Cherry Valley area. North of the storage units, the older beds were brought to the surface by faulting and folding related to the San Gorgonio Pass Fault Zone (*fig. 5*), and they are exposed locally in uplifts such as the Banning Bench and in the foothills west of Cherry Valley.

Although the older sedimentary deposits (unit QTso) have considerable lithologic variability, the various rock and sediment types are similar in their greater degree of compaction, consolidation, and cementation relative to younger sedimentary materials. Typical lithologies include

- well-consolidated to cemented, light-gray to very pale-brown, well-sorted fine- to coarse-grained sand and sandstone;
- sheet-like layers of well-consolidated to indurated, light-gray pebble-cobble gravel and conglomerate as much as 30 ft thick containing clasts of granitic, gneissic, mylonitic, and hypabyssal rock of San Gabriel Mountains-type;

- well-consolidated and compacted, greenish-gray mudstone and silty very fine-grained sand and sandstone;
- reddish-colored siltstone and fine-grained sand and sandstone that locally are clay-rich; some intervals may be paleosols.

The older sedimentary deposits were identified in the subsurface on the basis of borehole electrical logs. The older deposits are characterized by low resistivity (*fig. 6*) and minimal separation between the short-(16-in.) and long-(64-in.) normal resistivity logs. The low resistivities were attributed to relatively high percentages of fine-grained constituents (clay and silt). The minimal separation probably is related to the high degree of compaction and consolidation of these deposits, which would limit mud invasion during drilling (mud invasion would result in the short-normal resistivity log being less resistive than the long-normal resistivity log).

Sediments that comprise the older sediments were transported by streams draining various highland areas and deposited on lowland floodplains surrounding isolated hills and mountains (inselbergs) of crystalline rock of Peninsular Ranges-type. The ancient floodplain that deposited the older sediments was a network of braided sandy and gravelly streams separated by overbank areas of finer sandy and silty sediment. The ancient streams emptied into standing bodies of water (ponds and lakes) that are represented now by greenish-gray clay and silt layers exposed in the hillsides. Most of the sediment that forms the older sedimentary deposits was derived from crystalline rocks of San Gabriel Mountains-type that were situated north and northwest of the San Timoteo Badlands (Matti and Morton, 1993, *fig. 7H-7K*).

Younger Sedimentary Deposits (Qsu, Qsl)

Materials grouped within the younger sedimentary deposits represent the upper part of the San Timoteo beds identified by Frick (1921). These deposits are divided into a lower member (unit Qsl) and an upper member (units Qsu) on the basis of geologic properties, hydraulic characteristics, and borehole electrical logs (*fig. 6*).

Unit Qsl is exposed only in the hills north of the Cherry Valley Fault (*figs. 5 and 6B*). There, moderately folded beds of unit Qsl rest unconformably on tightly folded beds of the older sedimentary unit. Elsewhere, unit Qsl is concealed deep in the subsurface, where it is identified on the basis of subtle electrical-log properties. Unit Qsu is well exposed in the hills north of San Timoteo Canyon and south of Calimesa, where it comprises beds that dip gently (5° to 10°) northward. In this exposure, the lower contact of unit Qsu is concealed by young alluvial sediments of San Timoteo Canyon (*fig. 6B*). However, regional relations indicate that beds assigned to unit Qsu unconformably overlie unit QTso. These relations suggest that units Qsl and Qsu accumulated on the north side of the anticline in the San Timoteo Badlands sedimentary sequence, with beds of Qsl and Qsu progressively lapping onto the landscape that evolved on top of the developing fold.

Where exposed north of the Cherry Valley Fault, unit Qsl consists of very pale brown to yellowish-brown sand and sandstone interbedded with gravel and conglomerate containing clasts of locally derived basement rock of San Gabriel Mountains-type. The sediments generally are poorly sorted, with clasts ranging in size up to 1.5 ft. On average, the beds dip north and northwest about 20°, although they dip more steeply adjacent to the Banning Fault. In general, sedimentary material in unit Qsl is more consolidated than that in unit Qsu.

Unit Qsu consists of grayish- to yellowish-brown colored sand and gravel layers; locally these are cemented into ledge-forming beds of sandstone and conglomerate. Toward the top of the unit, the beds are darker brown and the upper member can be difficult to distinguish from overlying alluvial units of similar color. Locally, unit Qsu is cut by caliche-lined faults and fractures; where it lies beneath overlying alluvial units or beneath a capping residual-soil horizon, the upper part of the unit is laced with irregular seams and zones of white to light-gray caliche or calcrete. In borehole lithologic logs, gray to brown sand and gravel of unit Qsu can be distinguished fairly easily from more consolidated and lithologically more heterogeneous beds of the older sedimentary deposits (unit QTso). Materials of unit Qsu are not so easily distinguished in borehole cuttings from overlying surficial deposits of units Qvo and Qo.

Borehole electrical logs indicate that the younger sedimentary deposits are more resistive than the underlying older sedimentary deposits (*fig. 6*). The higher resistivity values are attributed to the deposits containing only small amounts of fine-grained constituents (clay and silt). Most logs show a slight decrease in resistivity in the lower part of the younger sedimentary deposits, indicating an increase in the quantity of fine-grained deposits and (or) ground water of higher salinity. This shift in resistivity was used in dividing the younger sedimentary deposits into upper and lower parts that are believed to coincide with units Qsu and Qsl as mapped at the surface. Hydrologic and geochemical data presented later in this report support separation of the younger sedimentary deposits into two subunits.

Deposition of units Qsl and Qsu departed from patterns established during the period represented by older sedimentary deposits. Beginning about 1.5 million years ago, beds of unit QTso began to be folded into an anticlinal uplift (Morton, 1999) whose axis parallels the San Jacinto Fault Zone (*fig. 6B and C*). These events led to formation of the Calimesa–Cherry Valley Basin, a depositional sag that developed on the northeast flank of the evolving fold that was uplifting older deposits of the San Timoteo sequence (including QTso). The subsiding basin formed a depositional trough for sand, gravel, and mud of the younger sedimentary deposits (units Qsl and Qsu).

These sediments appear to have buttressed depositionally against the landscape formed by the developing fold (*fig. 5*). Streams that carried sediments of units Qsl and Qsu probably flowed west and east around and parallel to the crest of this highground.

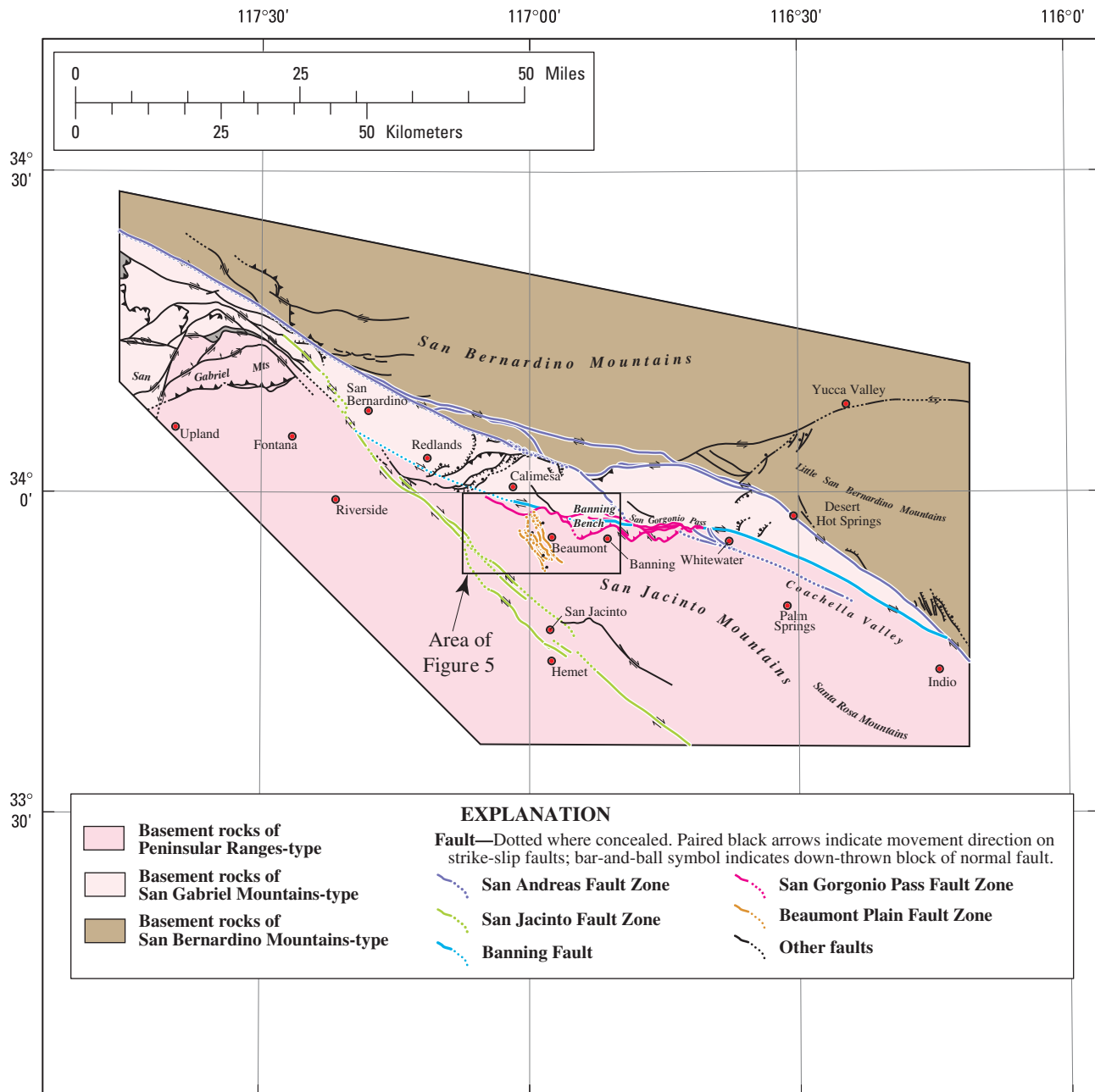
Quaternary Surficial Deposits (Qvo, Qo, Qy, and Ql)

Sediments that have accumulated at the land surface over the last half million years or so are widespread in the study area. In this report these surficial deposits are divided into four groups: (1) very old deposits (unit Qvo), (2) older deposits (unit Qo), younger deposits (unit Qy), and landslide deposits (Ql). Each unit represents a different age of surficial materials, except for landslide deposits, which may correlate with any of the other three. Within each unit, various kinds of deposits are lumped together, including sand and gravel deposits that occur in river and creek bottoms or that form valley floors; loose rubble that lies on hillslopes; and various kinds of landslides and other slope-movement materials that occur on hillsides. In general, all these materials are unconsolidated; that is, they have not been compacted or cemented into sedimentary rock. However, consolidation tends to increase with increasing age and depth of burial so that surficial materials in the subsurface of the study area are somewhat more consolidated than those occurring at the land surface. In general, surficial sedimentary materials consist of interlayered sand and gravel deposits, with intermittent layers of clay, silt, and fine sand.

The surficial deposits are characterized by high resistivity on the borehole electrical logs (*fig. 6*). The high resistivity is attributed to high amounts of coarse-grained sediments (sand and gravel) with minor amounts of fine-grained sediments and to unsaturated conditions (most of the surficial deposits are above the water table).

Geologic Structure

Geologic structures in the study area are within the San Andreas Fault system—a family of geologic structures (faults, folds) that interact together as an integrated complex (*fig. 7*)—in southern California. The modern trace of the San Andreas Fault itself lies just north of the study area along the base of the San Bernardino Mountains. Geologic research has demonstrated that the San Andreas Fault per se is but one of many geologic structures that has distributed strain throughout a broad region during the last few million years. Faults in the study area are part of this regional structural complex and have orientations and movement histories that reflect their role in the regional system.



Modified from Matti and others (1985) and Matti and Morton (1993).

Figure 7. Map showing regional geologic structure of the San Gorgonio Pass area, Riverside County California.

Faults

Banning Fault

The Banning Fault is an important element of the overall structural setting of the study area. The major movement along this fault occurred during late Miocene time (about 10 to 5 million years ago), when it produced right-lateral strike-slip movements as part of the San Andreas Fault system (Matti and others, 1992; Matti and Morton, 1993). Since that time, strike-slip activity shifted to the San Andreas Fault zone to the north, and the Banning Fault has not been a major tectonic element. However, the fault locally has produced contractional reverse-slip displacements that have deformed sedimentary rocks to the south.

The Banning Fault today consists of western, central, and eastern segments, each of which has a unique geologic and geomorphic setting and records a distinctive tectonic and depositional history during Quaternary time (Matti and others, 1992; Matti and Morton, 1993). The Quaternary tectonic events have obscured the distribution and history of the ancestral Banning Fault that originally formed a single continuous strike-slip trace throughout the three geographic segments.

The central, or San Gorgonio Pass, segment of the Banning Fault extends east-southeast from Calimesa and defines the northern boundary of the Singleton storage unit. Traced eastward, the fault forms the southern boundary of the canyon storage units (*fig. 2*). This segment largely is obscured by Quaternary surficial deposits, and has been modified by Quaternary reverse, thrust, and tear faults of the San Gorgonio Pass Fault Zone.

Where the Banning Fault is exposed in the study area, the fault generally dips steeply north and juxtaposes crystalline rocks of San Gabriel Mountains-type against late Cenozoic sedimentary deposits; these exposures represent the ancestral trace of the fault in the study area. The fault usually forms a distinct plane between a zone of crushed and sheared crystalline rock to the north and deformed sedimentary rocks to the south; the zone of crushed rock locally is as much as 15 ft wide.

In the foothills, along the northern boundary of the Singleton storage unit, the Banning Fault juxtaposes sheared basement rocks against older beds of unit QTso that are steeply dipping to overturned adjacent to the fault zone. Eastward across the northern boundary of the Beaumont storage unit, the trace of the fault is concealed by various generations of Quaternary surficial deposits, and its subsurface location must be inferred based on geophysical data. Farther east, in the Banning Bench storage unit, the fault juxtaposes crystalline basement rocks against unit QTso (the San Timoteo beds of Frick, 1921); the older sedimentary deposits are deformed into moderate to steep dips for a distance of several hundred meters south of the fault. Along the east and west sides of San Gorgonio River, the fault places sheared basement rocks of

San Gabriel Mountains-type against unit QTso (the Hathaway Formation of Allen, 1957); on the west side of San Gorgonio River the beds of unit QTso are overturned adjacent to the fault.

Where concealed by surficial deposits along the northern boundary of the Beaumont storage unit, structural relations between the Banning Fault and geologic units to the south and north are assumed to be the same as on Banning Bench. Where defined by gravity and surface-resistivity measurements, the concealed fault is interpreted to dip steeply northward, and juxtaposes basement rocks on the north against sedimentary materials to the south (*fig. 6C*).

In the study area and eastward into San Gorgonio Pass, the ancestral Banning Fault has been reactivated by or obscured by Quaternary reverse and thrust faults of the San Gorgonio Pass Fault Zone. For example, in the vicinity of Cherry Valley, fault scarps we attribute to the San Gorgonio Pass Fault Zone create curving landforms that do not represent the Banning Fault itself but reflect younger tectonism.

San Gorgonio Pass Fault Zone

Matti and others (1985) applied the name San Gorgonio Pass Fault Zone to a group of Quaternary reverse, thrust, and tear faults that extends from the Whitewater area westward to the Calimesa area (*fig. 7*). This fault zone is associated spatially with the Banning Fault, but its evolution has no relationship to that of the Banning Fault except where the latter has been reactivated by movements on the younger system.

In map view (*figs. 5 and 7*), the San Gorgonio Pass Fault Zone has a distinctive zig-zag character caused by repetition of a distinctive fault geometry—an L-shaped fault pattern in which the shorter base of the “L” is oriented eastward to north-eastward and the elongate staff of the “L” northwestward. The east-oriented segments are moderately dipping reverse faults in the west half of the fault zone and shallowly dipping thrust faults in the east half. The northwest-oriented segments appear to be vertical wrench or tear faults having oblique right-lateral displacements. These segments have approximately the same orientation as active right-lateral faults in the region.

In the study area, faults of the San Gorgonio Pass Fault Zone have produced many tectonically controlled landforms, of which the Banning Bench is a classic example (*fig. 5*). The Banning Bench is an uplifted block of older sedimentary deposits bounded along its south margin by an east-trending thrust or reverse fault and along its west margin by a northwest-trending high-angle oblique-slip fault having a combination of right-lateral slip and reverse dip slip. The Banning Bench has been uplifted in the last 100,000 years or so, and is being dissected by streams such as Montgomery Creek. Tectonic landforms attributable to the San Gorgonio Pass Fault Zone can be traced intermittently northwestward from the Banning Bench (*fig. 5*). Along their entire extent, faults of the San Gorgonio Pass Fault Zone break and displace the older Banning Fault in the subsurface.

All the faults of the San Gorgonio Pass Fault Zone have been active in late Quaternary time. Some faults in the San Gorgonio Pass Fault Zone may have been active only in the Pleistocene; others have been active throughout the late Pleistocene and Holocene and have generated ground ruptures as recently as a few thousand years ago (J.C. Tinsley and J.C. Matti, U.S. Geological Survey, unpub. trench data, 1986). Faults for which displacement during the Holocene is confirmed have been identified only in the eastern part of the San Gorgonio Pass Fault Zone east of Beaumont; faults in the western part of the zone between Beaumont and Calimesa appear to have been active only in late Pleistocene time.

Cherry Valley Fault

The Cherry Valley Fault as defined by Boyd (1971, pl. 1) appears to be a strand of the San Gorgonio Pass Fault Zone. Although originally recognized on the basis of ground-water measurements, the Cherry Valley Fault locally has surface expression. Between Cherry Valley and Calimesa, faults of the Cherry Valley zone form discontinuous, west-northwest-trending scarps and lineaments that bound the south margin of an uplift cored by older sedimentary deposits (unit QTso) (*fig. 6B*). The scarp trends west across Interstate Highway 10 and ends just south of Calimesa (*fig. 5*). Where trenched by geological consultants, the fault plane that forms these scarp segments dips gently northward as shallow as 15°. In the Cherry Valley area, the position of the Cherry Valley Fault is poorly constrained because the topographic scarps defining the structure are subdued and have been modified by agricultural activities. Moreover, the structure largely is concealed beneath alluvium deposited by Noble and Little San Gorgonio Creeks.

In the Cherry Valley area, three lines of evidence constrain the subsurface location of the fault: (1) aquifer test results, (2) correlation of discontinuous scarps, and (3) seismic reflection and refraction profiles. A 5-day aquifer test was conducted in the Cherry Valley area in 1991 to determine the hydraulic properties of the aquifer system (Boyle Engineering Corporation, 1992). During the test, ground water was pumped from well 2S/1W-27B1 (BCVWD well 16), and water levels were measured in wells 2S/1W-22Q3 (referred to as test well 2 by Boyle Engineering Corporation) and 2S/1W-27L1 (referred to as test well 1 by Boyle Engineering Corporation) (*fig. 5*). Results of the test indicate that the water-level drawdown in well 22Q3 was significantly greater than the drawdown in well 27L1. If the transmissivity of the aquifer penetrated by these wells is assumed constant, a barrier must exist between the observation wells to account for this large difference in measured drawdown between them, with wells 27B1 and 22Q3 on the north side of the barrier and well 27L1 on the south side of the barrier. A fault is the most likely origin of this barrier, and it probably is a continuation of the Cherry Valley Fault defined by Boyd (1971, pl. 1). In the Cherry Valley area, the fault

most likely is a reverse fault having up-on-the-north displacement, and thus, it is compatible with the orientation and movement style of other faults of the San Gorgonio Pass Fault Zone.

The trend of the proposed extension of the Cherry Valley Fault follows discontinuous arcuate fault scarps at the west edge of Cherry Valley and at the mouth of Noble Creek. The similar age of alluvium the scarps disrupt, their similar faulting style, and the apparent need for a fault to explain the large water-level difference between wells 27B1 and 27L1 during the aquifer test suggest that the scarps may be formed by a single fault that trends between them.

In 1997 and 1998, the U.S. Geological Survey, in cooperation with SGPWA, completed seismic reflection and refraction profiles in the Cherry Valley area to help define the geohydrology (Catchings and others, 1999; Gandhok and others, 2000). Numerous faults were identified on the seismic profiles along Little San Gorgonio Creek between wells 27B1 and 27L1 (Catchings and others, 1999). South of well 27B1, a series of faults were interpreted to cumulatively offset the sedimentary deposits by as much as 160 ft, with up-on-the-north displacement. Geologic materials modeled with a seismic velocity of about 2,600 ft/s appear to be thicker on the south side of this fault zone than on the north side, and reflectors appear to be more diffuse on the south side. These relations are consistent with a north-dipping reverse-slip fault that was active while the sediment was being deposited. The diffuse reflectors in the downthrown block, adjacent to the interpreted reverse fault, may be the result of drag-folding deformation and fault-wedge detritus.

Banning Barrier Faults

Boyd (1971) postulated that a fault separates the Beaumont and Banning storage units southeast of Beaumont because water levels on the Beaumont side of the proposed fault (northwest side) were as much as 50 ft higher than levels on the Banning side (southeast side) (Boyd, 1971, pl. 2) (*fig. 5*). Subsequent investigators have referred to this as the Banning Barrier. Boyd (1971, pl. 1, 2) postulated that the Banning Barrier is a southwestward extension of the west-trending reverse fault that bounds the south margin of the Banning Bench [interpreted by Matti and others (1985, 1992) as being part of the San Gorgonio Pass Fault Zone]. However, in contrast to faults that bound the Banning Bench, the Banning Barrier has no surface landform expression. Consequently, it is not reasonable to expect that the Banning Barrier is an extension of the fault bounding the south margin of the Banning Bench. Water-level and geochemical data collected since Boyd (1971) completed his investigation indicate that multiple ground-water barriers are associated with the Banning storage unit. In this report, these barriers are interpreted to be multiple strands of the San Gorgonio Pass Fault Zone (*fig. 5*) that are older than the Banning Bench structures, and hence are concealed by surficial deposits of the Beaumont Plain.

The Banning Barrier is referred to as the Banning Barrier Fault in this report. This fault is inferred to be a north-dipping reverse fault similar to other reverse and thrust faults that form east-trending legs of the L-shaped pattern that characterizes the San Gorgonio Pass Fault Zone. The other leg of the fault set is inferred to trend west-northwest along the southern boundary of the Beaumont storage unit. To account for other observed water-level differences between wells in the Banning storage unit, two additional L-shaped fault sets are inferred to exist and are referred to as the Central Banning Barrier Fault and the Eastern Banning Barrier Fault in this report (*fig. 5*). The resulting subsurface pattern of faults and associated folds depicted on the geologic map (*fig. 5*) and in the geologic cross sections (*fig. 6A*) is complex, but is compatible with fault and fold geometries observed at the surface elsewhere in the study area and with water-level differences observed in the Banning storage unit. The lack of surface expression indicates that these faults are older than the faults that bound the Banning Bench. It is for this reason that faults in this part of the study area are depicted as not extending to land surface (*figs. 5, 6A*).

Beaumont Plain Fault Zone

Matti and others (1985, 1992) applied the name Beaumont Plain Fault Zone to a series of northwest-trending en echelon faults that break late Pleistocene surficial deposits (units Qo and Qvo) in the western part of the Beaumont storage unit (*fig. 5*). Faults of the Beaumont Plain Fault Zone are subparallel to the McInnes Fault and related structures shown by Boyd (1971, pl. 1). The term McInnes Fault is not used in this report because surface expression of the fault or associated structures could not be confirmed where Boyd (1971, pl. 1) depicts them south and southwest of Beaumont. Instead, en echelon fault scarps of the Beaumont Plain Fault Zone trend more northwesterly through the town of Beaumont and farther west.

Faults of the Beaumont Plain Fault Zone form mainly east-facing scarps in late Pleistocene surficial deposits. The faults trend subparallel to right-lateral strike-slip faults of the San Andreas Fault system, but at a more northwesterly trend than these structures. Matti and others (1985, 1992) interpreted the Beaumont Plain Fault Zone as a belt of normal dip-slip faults possibly having an oblique right-slip component. Matti and others (1985) cited as evidence for normal dip-slip geometry several closely-spaced en echelon faults northwest of Beaumont Avenue, whose opposing west- and east-facing scarps bound a down-dropped block that appears to form a graben-like structure. Trenching investigations indicate that fault geometry is consistent with normal dip slip displacements (Rasmussen and Associates, 1978).

Faults of the Beaumont Plain Fault Zone were identified in U.S. Geological Survey seismic reflection and refraction profiles along Noble Creek (Gandhok and others, 2000,

figs. 26a, 27a, b). Displaced reflection boundaries in the profiles appear to define upthrown and downthrown blocks, the shape and distribution of which is similar to those expected for horst and graben complexes. Not all of the imaged structures can be recognized on the surface of the Beaumont Plain either because they are concealed by alluvium younger than the faulting or because they may have been obliterated by agricultural and urban activities. Geometric and kinematic relations among faults of the Beaumont Plain Fault Zone and those of the San Gorgonio Pass Fault Zone have not been established.

San Timoteo Canyon Fault

The San Timoteo Canyon Fault trends west-northwest from south of Beaumont to the Calimesa area (*fig. 5*). To the southeast, the fault appears to splay into multiple structures that break the older sedimentary deposits (unit QTso); to the northwest, it appears to end at the westernmost extension of the San Gorgonio Pass Fault Zone (Cherry Valley Fault) south of Calimesa.

Evidence for the San Timoteo Canyon Fault is both direct and indirect. South of Beaumont, a series of aligned west-northwest-trending scarps indicates a fault that drops very old surficial deposits (unit Qvo) and the unit of older sedimentary deposits (unit QTso) down on the east relative to counterparts to the west. The scarps have the same general orientation and displacement sense as those of the Beaumont Plain Fault Zone, but are older and have a more westerly trend. West-northwest of San Timoteo Creek, the existence and position of the San Timoteo Canyon Fault are inferred indirectly from geologic and stratigraphic evidence. Low hills west of the inferred trace of the fault expose beds of unit Qsu capped by a reddish residual soil that marks an old Quaternary landscape surface. This combination of geologic features is not observed anywhere east and northeast of the inferred trace of the San Timoteo Canyon Fault. The fault is interpreted to drop the upper San Timoteo sequence and its capping residual soil into the subsurface east of the fault (*fig. 6B*). The location of the San Timoteo Canyon Fault in part coincides with areas where springs have been documented historically, where section *B-B'* intersects the fault (*figs. 5, 6B*). Water-level data indicate the presence of a barrier to flow in the western part of the Beaumont storage unit, which is inferred to be a splay of the San Timoteo Canyon Fault (*figs. 5, 6B*).

The structural significance of the San Timoteo Canyon Fault is not clear. It has down-on-the-east displacements that probably reflect a normal dip-slip origin. In this regard, and in its generally northwest orientation, the fault is similar to the fault strands of the Beaumont Plain Fault zone. The fault probably was active during deposition of units Qsl and Qsu, but does not break surficial unit Qvo or younger surficial units.

Wildwood Canyon Fault

The Wildwood Canyon Fault trends northwestward from the mouth of Noble Creek (*fig. 5*). The fault forms scarps in late Pleistocene alluvium but it does not appear to disrupt Holocene alluvial deposits in the study area. Fault scarps alternate between north- and south-facing, a characteristic of strike-slip structures. Interaction between the Wildwood Canyon Fault and structures of the San Gorgonio Pass Fault Zone is not clear: the former may be the northwestward extension of a wrench fault that tears through the upper part of the San Gorgonio Pass Fault Zone.

Folds

A major northwest-trending anticline can be traced for much of the length of the San Timoteo Badlands; this fold affects all rock units in the exposed sedimentary sequence (*fig. 5*) (Morton, 1999). The anticline is asymmetric, with a steeply dipping south limb and gently dipping north limb. For much of its extent, the fold axis plunges gently to the northwest.

In the Singleton storage unit, between the Cherry Valley Fault and the Banning Fault, beds of the older sedimentary deposits (unit QTso) have been warped into a northwest-trending anticlinal fold whose axis roughly parallels the two faults. Similar to the San Timoteo Badlands anticline, the Singleton storage unit fold is asymmetric, with a steep south limb that locally is overturned and a more shallow dipping north limb.

Beneath the Banning Bench, the middle member of the San Timoteo beds have been warped into several minor folds and a major syncline situated just south of the Banning Fault.

Ground-Water Hydrology

The ground-water hydrology of the Beaumont storage unit was defined by summarizing previously published research (California Department of Water Resources, 1963; Bloyd, 1971; Boyle Engineering Corporation, 1990; and Geoscience Support Services, 1991); compiling and analyzing available geohydrologic data from local, state, and Federal agencies; and analyzing data collected as part of this study. Wells used in the analysis and characterization of this region are shown on *Appendix figure 1* and listed in *Appendix table 1*.

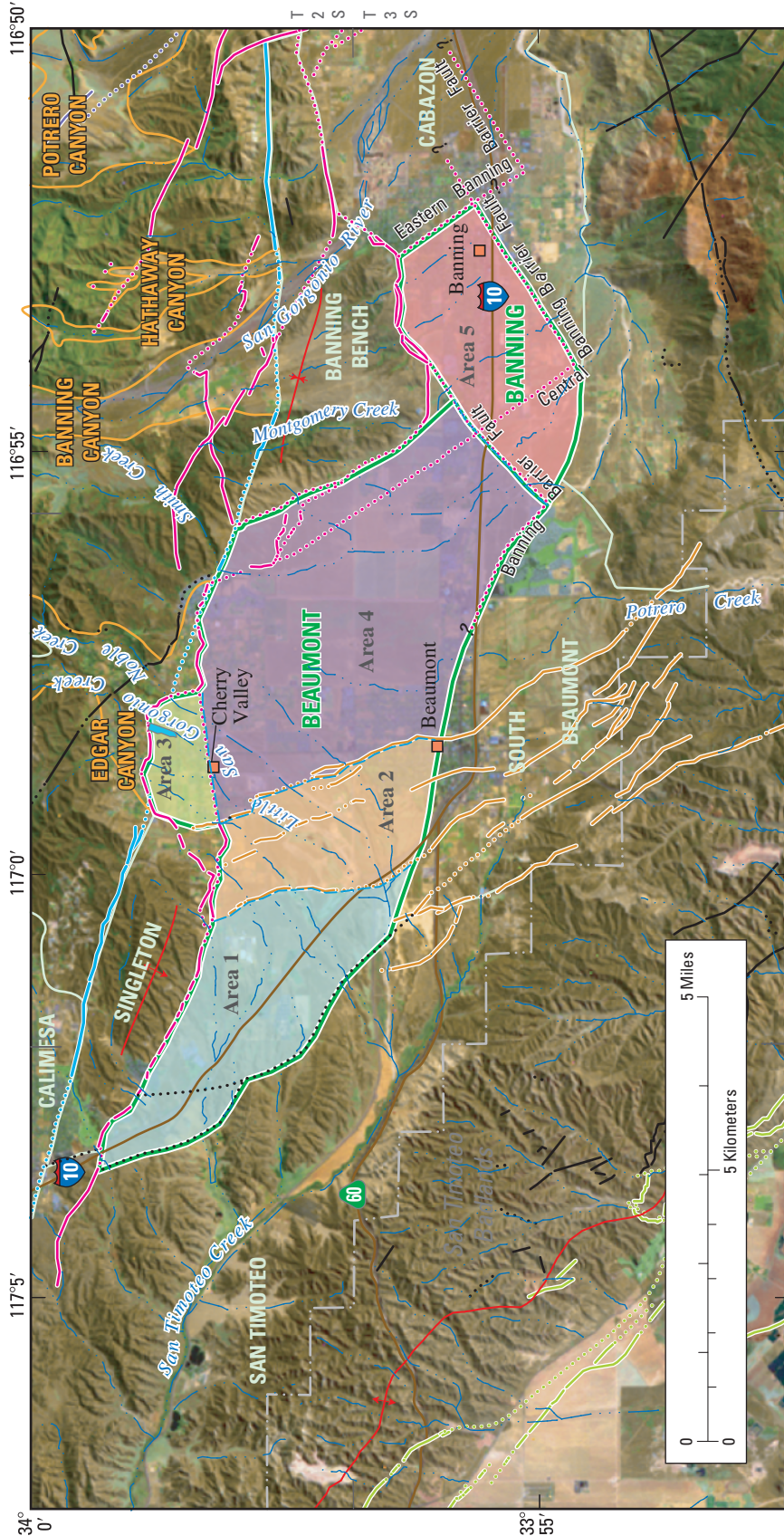
Storage Unit Characterization

The San Gorgonio Pass ground-water basin was defined by Bloyd (1971) as the water-bearing deposits within the SGPWA boundaries. Bloyd (1971) divided the San Gorgonio Pass ground-water basin into the Beaumont, Banning, Cabazon, Calimesa, San Timoteo, South Beaumont, Banning Bench, and Singleton storage units (*fig. 2*). The canyon storage

units (Edgar Canyon, Banning Canyon, Hathaway Canyon, Potrero Canyon, and Millard Canyon) were not considered part of the San Gorgonio Pass ground-water basin. The storage units were delineated on the basis of mapped or inferred faults. In most cases, the static ground-water levels are significantly different in adjacent storage units, or pumping effects are not observed across storage unit boundaries (Bloyd, 1971). The barrier effect of faults probably is caused by juxtaposition of non-water-bearing deposits opposite water-bearing deposits, by compaction and deformation of water-bearing deposits immediately adjacent to the faults, and by cementation of the fault zone by mineral deposits from ground water (Riley and Worts, 2001). An example of this barrier effect is evident in the approximately 600-ft water-level difference between monitoring wells 2S/1W-22G3 and 2S/1W-22Q3 (*fig. 6C*), located on opposite sides of the Banning Fault in the Cherry Valley area. Drilling and geophysical data gathered in the area by the USGS indicate a bedrock offset of greater than 800 ft across the fault (Christensen, 2000; Kevin Ellett, U.S. Geological Survey, written commun., 2000).

Geologic and hydrologic data, collected since Bloyd (1971) delineated the storage unit boundaries, were used in this study to refine the storage unit boundaries (*fig. 2*). The most significant changes were the southern and western boundaries of the Beaumont storage unit and the southern and eastern boundaries of the Banning storage unit (*fig. 2*). The current (2005) southern and western boundaries of the Beaumont storage unit are defined as the San Timoteo Canyon Fault west of the Beaumont Plan Fault Zone (*figs. 5 and 6A*), the contact of the water table with the older sedimentary deposits (QTso) in the southern part of the storage unit (*fig. 6C*), and the northwest-trending leg of the Banning Barrier Fault west of the Banning storage unit (*fig. 5*). The current (2005) southern boundary of the Banning storage unit is the contact with the water table and the older sedimentary deposits (QTso). The southern boundary is north of the surface exposure of unit QTso (*fig. 5*) because the unit dips gently to the north and the depth to the water table in the Banning Storage unit is in excess of 300 ft below land surface. The current (2005) eastern boundary of the Banning storage unit is the northeast-trending leg of the Central Banning Barrier Fault and the northwest-trending leg of the Eastern Banning Barrier Fault (*figs. 5 and 6A*).

The Beaumont, Banning, and Cabazon storage units are the most productive storage units within the San Gorgonio Pass ground-water basin. These storage units contain thick sections of saturated surficial and younger sedimentary deposits (*fig. 6*). Production wells in the Beaumont storage unit produce the greatest percentage of public water supply in the study area. For the purposes of this report, the Beaumont and Banning storage units were subdivided into five hydrologic areas to help describe the ground-water hydrology of the storage units (*fig. 8*). The Beaumont storage unit includes areas 1 through 4 and the Banning storage unit includes area 5 (*fig. 8*).



Faults modified from J. Matti; (USGS, written commun., 2003).

RTW R1E

R2W RTW

EXPLANATION

Hydrologic areas of the Beaumont and Banning storage units

- Area 1
- Area 2
- Area 3
- Area 4
- Area 5
- Hydrologic area boundary

Faults—Dotted where concealed. Queried where uncertain

- San Andreas Fault Zone
- San Jacinto Fault Zone
- Banning Fault
- San Gorgonio Pass Fault Zone
- Beaumont Plain Fault Zone
- Other faults
- Anticlinal fold
- Synclinal fold
- Recharge ponds

San Gorgonio Pass Water Agency boundary

- Storage unit boundary—In ground-water flow model
- Storage unit boundary—Outside ground-water flow model
- Canyon storage unit boundary
- Name of storage unit in ground-water flow model
- Name of storage unit outside ground-water flow model
- Name of canyon storage unit

Figure 8. Map showing the storage units and hydrologic areas of the San Gorgonio Pass area, Riverside County California.

The San Timoteo, Singleton, Banning Bench, and South Beaumont storage units provide only domestic water supplies. These storage units have older sedimentary deposits (QTso) at or near the water table (*figs. 5 and 6*). The older sedimentary deposits are considerably less permeable than the surficial and younger sedimentary deposits. Most of the supply wells in these storage units obtain their water from sediments deposited by streams that dissected the older sedimentary deposits. The water storage capacity of these stream deposits is limited owing to the limited lateral and vertical extent of these deposits.

The canyon storage units (Edgar Canyon, Banning Canyon, Hathaway Canyon, Potrero Canyon, and Millard Canyon) in San Bernardino are shallow alluvial-filled canyons surrounded by crystalline rocks of San Gabriel Mountains-type in the San Bernardino Mountains. The Banning Fault separates the canyon storage units from the Beaumont storage unit (*figs. 5 and 6*). Infiltration of precipitation and runoff from the canyon storage units contributes large volumes of water that recharge the canyon storage units. Surface runoff and ground-water discharge from the canyon storage units recharges the downstream ground-water storage units. The Edgar and Banning Canyons were the first of the canyon storage units to be developed for public and agricultural water supplies. The water supply in the canyon storage units is dependent on annual runoff owing to the limited storage capacity of the storage units. Local water agencies have developed diversion dams along the canyon streams to maximize the recharge to the canyon storage units. However, diversion of runoff and ground-water pumping in the canyon storage units reduce the quantity of runoff and ground-water discharge that formerly provided recharge to the downstream storage units.

Definition of Aquifers

The main water-bearing deposits in the San Gorgonio Pass ground-water basin are the saturated portions of the Quaternary surficial deposits (Qy, Ql, Qo, and Qvo) and the younger sedimentary deposits (Qsu and Qsl) (*figs. 5 and 6*). On the basis of lithologic and downhole geophysical logs, these deposits were divided into three aquifers: (1) the perched aquifer, (2) the upper aquifer, and (3) the lower aquifer.

The older sedimentary deposits (QTso) and the crystalline basement rocks (prb and trb) surround and underlie the surficial and younger sedimentary deposits (*figs. 5 and 6*). These deposits and rocks generally are impermeable, yielding only small quantities of water to wells (Bloyd, 1971). Although the older sedimentary deposits have considerable lithologic variability, the various lithologies are similar in terms of their greater degree of compaction, consolidation, and cementation relative to the younger sedimentary deposits, which greatly reduces the permeability of the older sedimentary deposits. For the purposes of this study, the crystalline

rocks and older sedimentary deposits are considered non-water bearing and form the base and, in many areas, the lateral boundaries of the ground-water basin.

A perched aquifer was identified in the surficial deposits north of the Cherry Valley Fault in the Beaumont storage unit above the contact between the older deposits (unit Qo) and very old deposits (unit Qvo) (*fig. 6C*). The surficial deposits are unsaturated throughout most of the remainder of the study area. The perched aquifer in the Cherry Valley area lies above a low permeability layer (silt and clay) present at the contact between units Qo and Qvo. This layer impedes the vertical flow of water from land surface to the regional aquifers. Downward percolating water forms a perched water body, or aquifer, on this silt and clay layer. Breaches in the silt and clay layer and interfingering sands and gravels allow water from the perched aquifer to move deeper through the unsaturated zone to the underlying upper aquifer.

The upper aquifer is the regional water-table aquifer and consists of the saturated part of the very old deposits (Qvo) and the upper part of the younger sedimentary deposits (Qsu). The thickness of this aquifer ranges from as much as 800 ft in the western part of the Beaumont storage unit to less than 400 ft in the Banning storage unit (*fig. 6*). The upper aquifer consists mainly of unconsolidated to slightly consolidated sand and gravel with interbedded silt and clay. Drillers' logs describe the upper aquifer as mostly medium- to coarse-grained sediments, and borehole geophysical logs show moderate to high resistivity values.

The lower aquifer is a confined aquifer and is contained within the lower part of the younger sedimentary deposits (Qsl). The thickness of this aquifer ranges from as much as 400 ft in the Banning storage unit to nonexistent in the south central part of the Beaumont storage unit (*fig. 6A*). The lower aquifer consists mainly of poorly consolidated to consolidated sand, silt, and clay. Drillers' logs describe the lower aquifer as containing hard, cemented layers of gravel, sand, silt and clay, and borehole geophysical logs indicate relatively low resistivity values.

The transmissivity of the upper and lower aquifers was estimated from specific-capacity data (*Appendix table 2*). Transmissivity is a measure of the ability of an aquifer to transmit water and specific capacity is the yield of a well per unit of drawdown. The specific capacity of a well is a function of the transmissivity of the aquifer and aspects of the well, such as efficiency and borehole storage. Thomasson and others (1960) reported that for unconfined valley-fill deposits in the Sacramento Valley of California, the specific capacity in units of gallon per minute per foot multiplied by 230 approximates the transmissivity in units of square feet per day. This relation between specific capacity and transmissivity was assumed representative of the alluvial deposits in the San Gorgonio Pass area.

A total of 44 specific capacity tests were compiled for 36 wells. Seven of the tests were considered unreliable because the reported drawdowns were unreasonably low. A possible explanation for the low drawdowns is that water levels in the wells were not allowed to fully recover prior to the start of the tests.

A total of 21 specific capacity tests were compiled for 13 wells perforated solely in the upper aquifer; however, one of the tests was considered unreliable. The estimated transmissivity values for the 20 specific capacity tests considered reliable ranged from 20 to 13,900 ft²/d and averaged about 6,000 ft²/d. The estimated transmissivity value for the one well perforated solely in the lower aquifer was about 2,000 ft²/d. A total of 19 specific capacity tests were compiled for 19 wells perforated in both the upper and lower aquifers; however, four of the tests were considered unreliable. The estimated transmissivity values for the 15 specific capacity tests considered reliable ranged from about 600 to 20,000 ft²/d and averaged about 5,500 ft²/d. The similarity of average transmissivity values for wells perforated solely in the upper aquifer and wells perforated in both aquifers suggests that the lower aquifer has a relatively low transmissivity compared with that for the upper aquifer.

Natural Ground-Water Recharge

Natural ground-water recharge of storage units in the San Geronio Pass area is defined in this study as areally distributed infiltration below the root zone that occurs in direct response to rain and snowmelt and infiltration of streamflow. A deterministic, distributed-parameter precipitation-runoff model, INFILv3 (Hevesi and others, 2003), was used to estimate the spatial and temporal distribution of natural ground-water recharge in the study area. A general description of the INFILv3 model, required input data, the calibration, and results are presented in this report.

INFILv3 was originally developed to estimate areally-distributed ground-water recharge for the numerical simulation of ground-water flow in the Death Valley Regional Flow System (Hevesi and others, 2003) and was subsequently applied to estimate recharge for the area near Joshua Tree, California (Nishikawa and others, 2004). For this study, the INFILv3 model was calibrated to measured daily mean streamflow of Little San Geronio Creek.

The INFILv3 model simulates daily net infiltration below the root zone, where the bottom of the root zone is the estimated maximum depth below ground surface affected by evapotranspiration, and net infiltration is defined as the percolation of rain, snow melt, and streamflow below the zone of evapotranspiration. Net infiltration in a ground-water basin is not necessarily equivalent to recharge in that basin because water that infiltrates past the root zone may not always reach the water table in that basin. The potential for differences between net infiltration and actual ground-water recharge tends to increase with increased unsaturated-zone thickness, increased travel time of the infiltrated water through the unsaturated zone, increased climate variability, and increased geologic heterogeneity in the unsaturated zone. For the purposes of this study, net infiltration was assumed to be the maximum potential ground-water recharge to the storage units in the San Geronio Pass area.

INFILv3 Model Description

The INFILv3 model uses a daily water-balance model of the root zone with a primarily deterministic representation of the processes controlling net infiltration. The daily water balance includes precipitation (as either rain or snow), snow accumulation, sublimation, snowmelt, infiltration into the root zone, evapotranspiration, drainage, water-content change throughout the root-zone profile, runoff (defined as excess rainfall and snowmelt), surface water run-on (defined as runoff that is routed downstream), and net infiltration (simulated as drainage from the bottom root-zone layer)(*fig. 9*). The INFILv3 model simulates precipitation occurring as snow based on daily air temperature data, where precipitation is assumed to occur as snow when the average daily air temperature is equal to or less than 32°F. The daily snowfall water-equivalent is added to a snow-pack storage term. When the average daily air temperature is greater than 32°F and the snow-pack storage term is greater than zero, snowmelt is simulated using a simple degree-day model (Hevesi and others 2003). The INFILv3 model does not account for interception storage and surface-retention storage processes. In addition, the model does not account for the processes of subsurface lateral flow and interflow or baseflow contributions to recharge. Detailed documentation of the INFILv3 model is presented in Hevesi and others (2003).

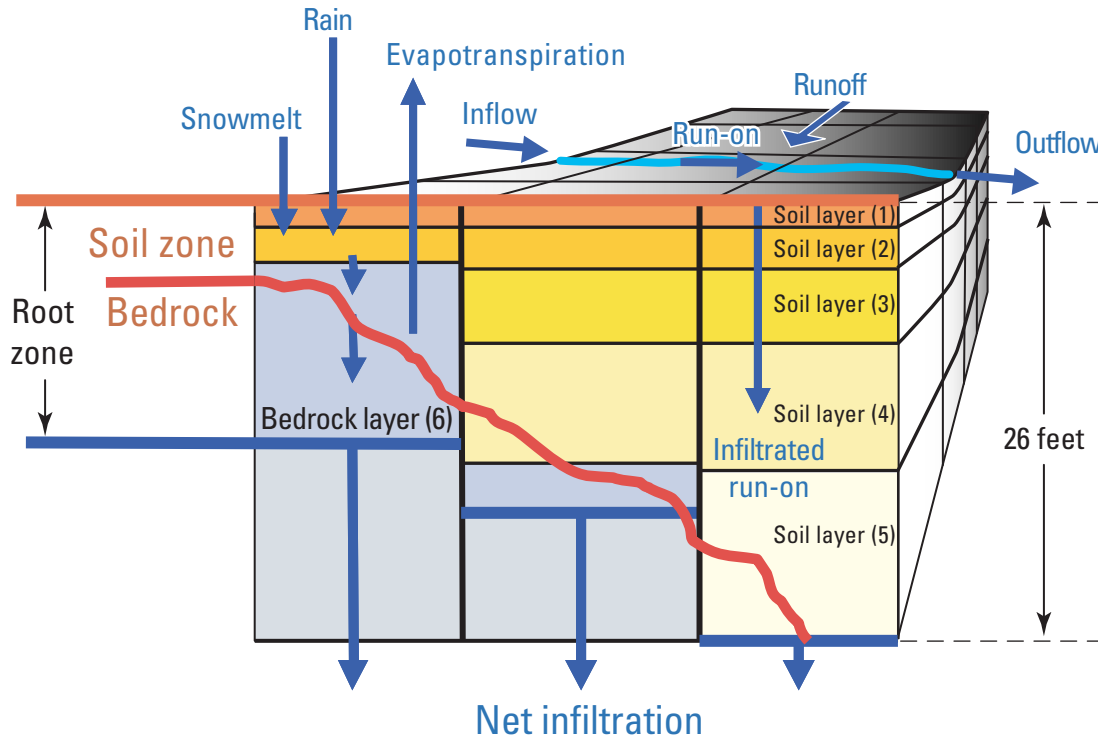


Figure 9. Schematic showing conceptual model of net infiltration illustrating the layered root-zone water-balance model for the San Gorgonio Pass area, Riverside County California.

INFILv3 Model Area and Discretization

The INFILv3 model area covers 117.5 square miles (mi^2) (about 75,200 acres) and includes three surface-water drainage basins: the San Timoteo Creek, Potrero Creek, and San Gorgonio River surface-water drainage basins (fig. 10, table 1). The San Timoteo Creek surface-water drainage basin is part of the Santa Ana watershed (USGS 8-digit HUC [hydrologic unit codes], <http://water.usgs.gov/GIS/metadata/usgswrd/XML/huc250k.xml> accessed March, 2006), the Potrero Creek drainage basin is part of the San Jacinto watershed, and the San Gorgonio River drainage basin is part of the Salton Sea watershed (fig. 10). The area of the surface-water drainage basins that are upstream of the Beaumont and Banning storage units were subdivided into 28 sub-drainage basins (fig. 11, table 1). The two largest sub-drainage basins upstream of the Beaumont and Banning storage units are sub-drainage basin 12 (Little San Gorgonio Creek) with an area of 6.9 mi^2 (about 4,420 acres) and sub-drainage basin 14 (Noble Creek) with an area of 5.1 mi^2 (about 3,230 acres). The total area covered by the 28 sub-drainage basins is 27.3 mi^2 (about 17,440 acres).

The INFILv3 model utilizes a rectangular grid to discretize the drainage basins being investigated into equal-area cells. For this study, the grid cells were 98.4 ft (30 m) on a side. Vertical discretization of the root zone is defined using one to five soil layers and one underlying bedrock layer, where the number and thickness of soil layers and the thickness of the bedrock layer are dependent on the estimated total soil and root-zone thickness at each grid cell location (fig. 9). The root

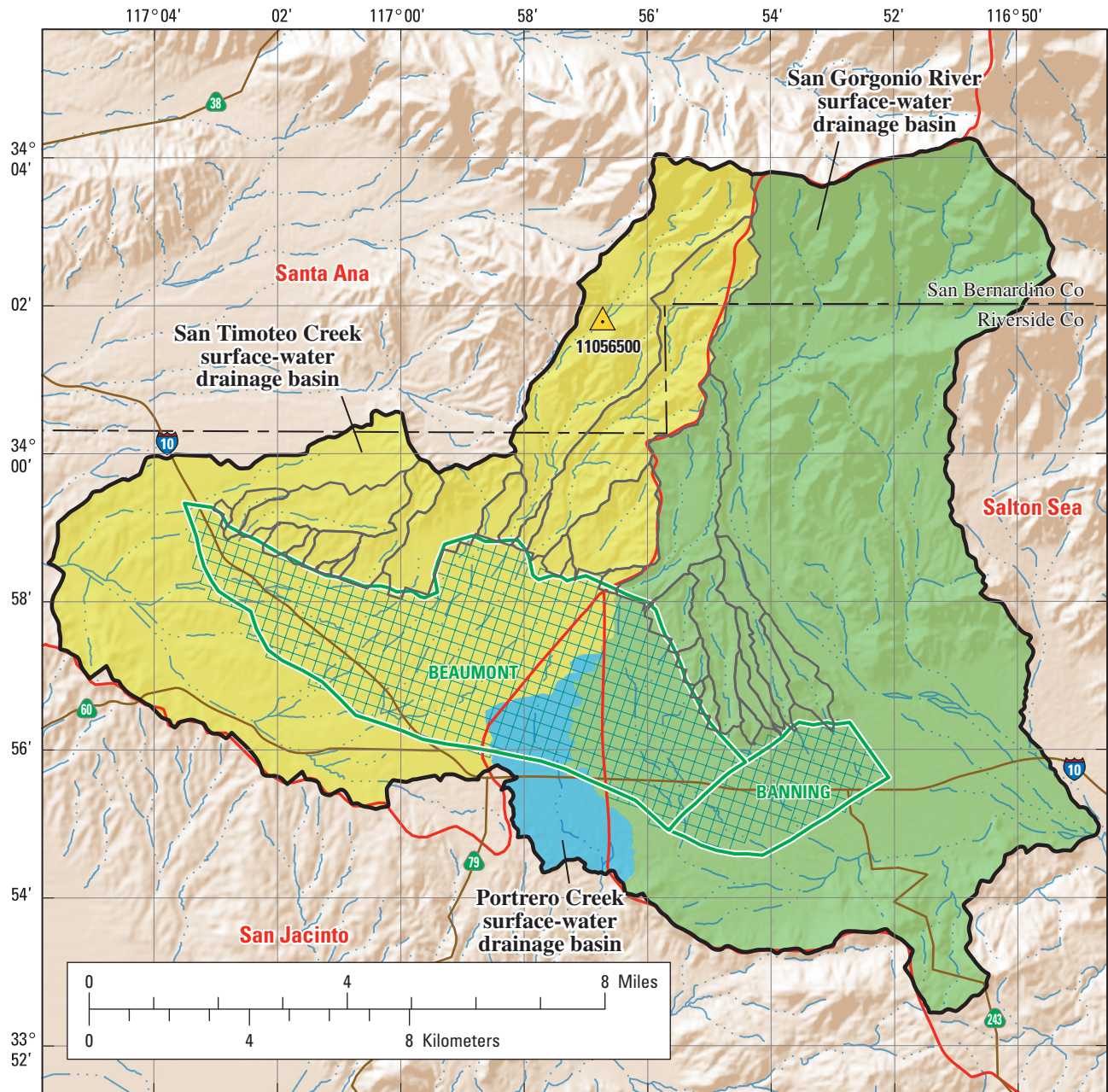
zone has multiple layers to account for differences in root density and root-zone water content as a function of depth. Calculations in the INFILv3 model use a water-balance approach for all root-zone layers and grid cells within the simulated drainage basins. The water-balance calculations are based on water volumes rather than water mass because it is assumed that temperature effects on water density are negligible. The calculations are performed using water-equivalent depths because all grid cells have equivalent areas [in this study $9,683 \text{ ft}^2$ (900 m^2)].

INFILv3 Model Inputs

Inputs to the INFILv3 model consist of three main input groups: (1) climate and meteorological data, (2) digital-map files and associated attribute tables, and (3) model coefficients, each of which is described in the following sections.

Climate and Meteorological Data

The daily-climate data (precipitation and air temperature) for water years 1927–2001 (a water year is defined by a starting date of October 1 and an ending date of September 30) were obtained from the National Climatic Data Center (NCDC) (EarthInfo, Inc., 2004) for a network of 102 climate stations in the Southern California region having records between October 1, 1926, and September 30, 2001 (fig. 12, table 2). Daily records consist of total daily precipitation and maximum and minimum air temperature. The selection of the



Base from U.S. Geological Survey digital data, 1:100,000, 1981-89; Universal Transverse Mercator Projection (NGVD 29), Zone 11.

EXPLANATION

- INFILv3 model boundary
- Watershed boundary and name
San Jacinto
- Ground-water storage unit and name
- INFILv3 modeled upstream sub-drainage basins
- USGS stream gage and identifier
11056500
- Ground-water flow model grid

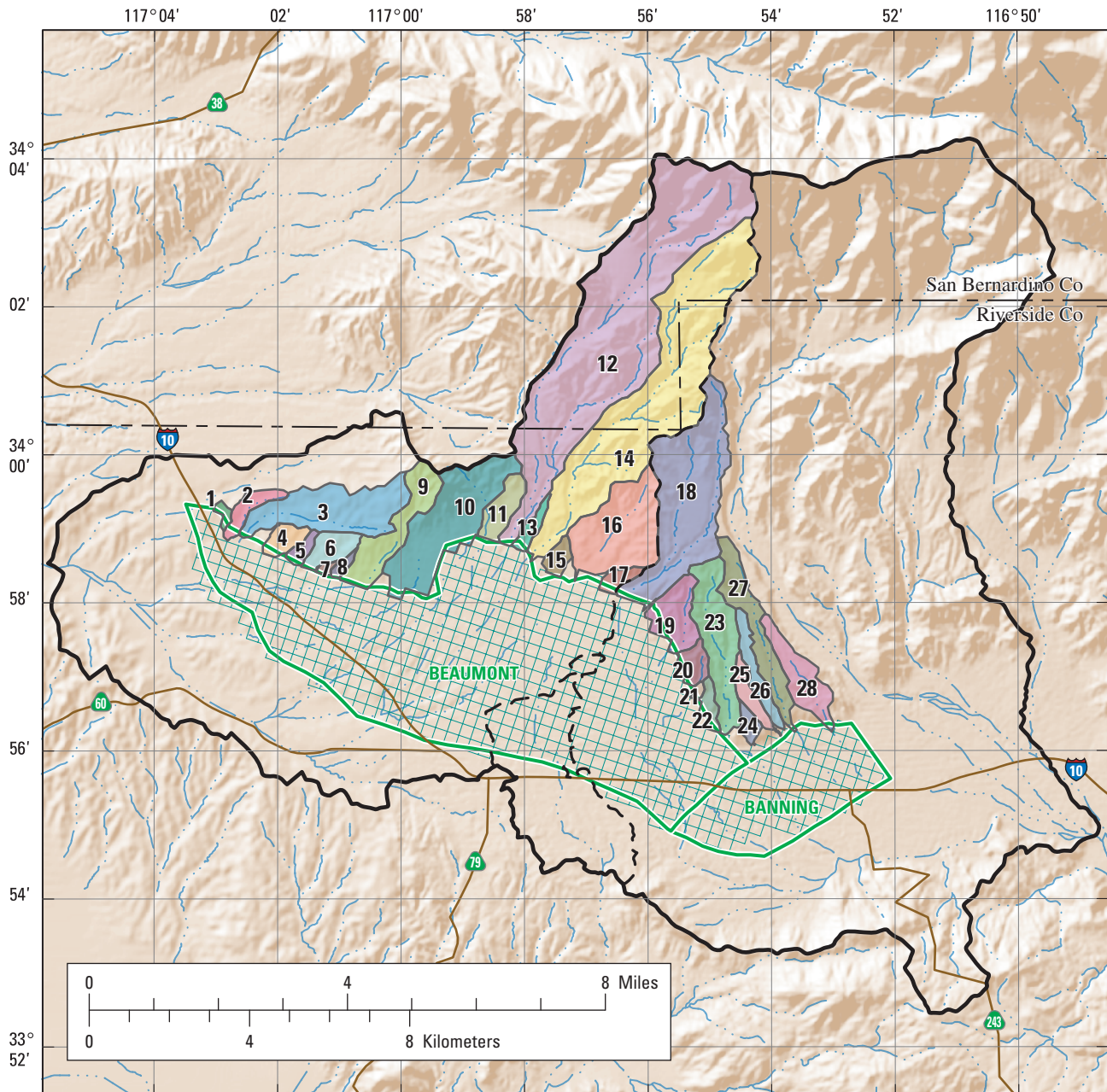
Figure 10. Map showing the San Timoteo Creek, Potrero Creek, and San Gorgonio River surface-water drainage basins used for the INFILv3 simulation, San Gorgonio Pass area, Riverside County, California.

24 Geology, Ground-Water Hydrology, Geochemistry, and Ground-Water Simulation, San Gorgonio Pass Area, California

Table 1. Area and altitude of surface-water drainage basins and surface-water sub-drainage basins upstream of and including the Beaumont and Banning storage units modeled using INFILv3 for the San Gorgonio Pass area, Riverside County, California.

[NGVD 29, National Geodetic Vertical Datum of 1929. ft, feet; mi², miles squared]

Area or map code (see fig. 11)	Number of INFILv3 grid cells	Area		Altitude (NGVD 1929)		
		(mi ²)	Acres	Average (ft)	Minimum (ft)	Maximum (ft)
Surface-water drainage basins						
San Gorgonio River	11,460	4.0	2,549	3,701	1,775	9,239
San Timoteo Creek	138,375	48.1	30,774	3,135	1,936	8,803
Potrero Creek	188,314	65.4	41,880	2,587	2,431	2,795
Total area	338,149	117.5	75,203	2,849	1,775	9,239
Surface-water sub-drainage basins upstream of Beaumont and Banning storage units						
1	186	0.06	41	2,423	2,330	2,530
2	736	0.26	164	2,474	2,316	2,618
3	4,351	1.51	968	2,792	2,349	3,488
4	706	0.25	157	2,548	2,352	2,759
5	346	0.12	77	2,575	2,412	2,799
6	969	0.34	216	2,706	2,474	2,907
7	119	0.04	26	2,550	2,471	2,677
8	211	0.07	47	2,647	2,533	2,871
9	2,611	0.91	581	3,044	2,539	3,911
10	5,482	1.90	1,219	3,071	2,622	3,914
11	1,147	0.40	255	3,151	2,933	3,616
12	19,855	6.90	4,416	5,001	2,936	8,803
13	478	0.17	106	3,096	2,930	3,294
14	14,527	5.05	3,231	4,457	2,943	7,671
15	482	0.17	107	3,029	2,914	3,238
16	4,634	1.61	1,031	3,375	2,930	4,157
17	441	0.15	98	3,149	2,943	3,557
18	7,965	2.77	1,771	3,799	2,982	4,935
19	1,793	0.62	399	3,194	2,877	3,701
20	680	0.24	151	2,987	2,759	3,232
21	111	0.04	25	2,819	2,743	2,982
22	467	0.16	104	2,814	2,635	3,074
23	3,518	1.22	782	3,163	2,661	3,704
24	372	0.13	83	2,862	2,592	2,989
25	726	0.25	161	2,982	2,631	3,215
26	1,037	0.36	231	3,059	2,648	3,419
27	2,558	0.89	569	3,227	2,592	3,750
28	1,914	0.67	426	2,934	2,484	3,274
Total upstream area	78,422	27.26	17,442	3,878	2,316	8,803
Beaumont and Banning storage units	64,872	22.54	14,427	2,584	2,202	3,091



Base from U.S. Geological Survey digital data, 1:100,000, 1981-89; Universal Transverse Mercator Projection (NGVD 29), Zone 11.

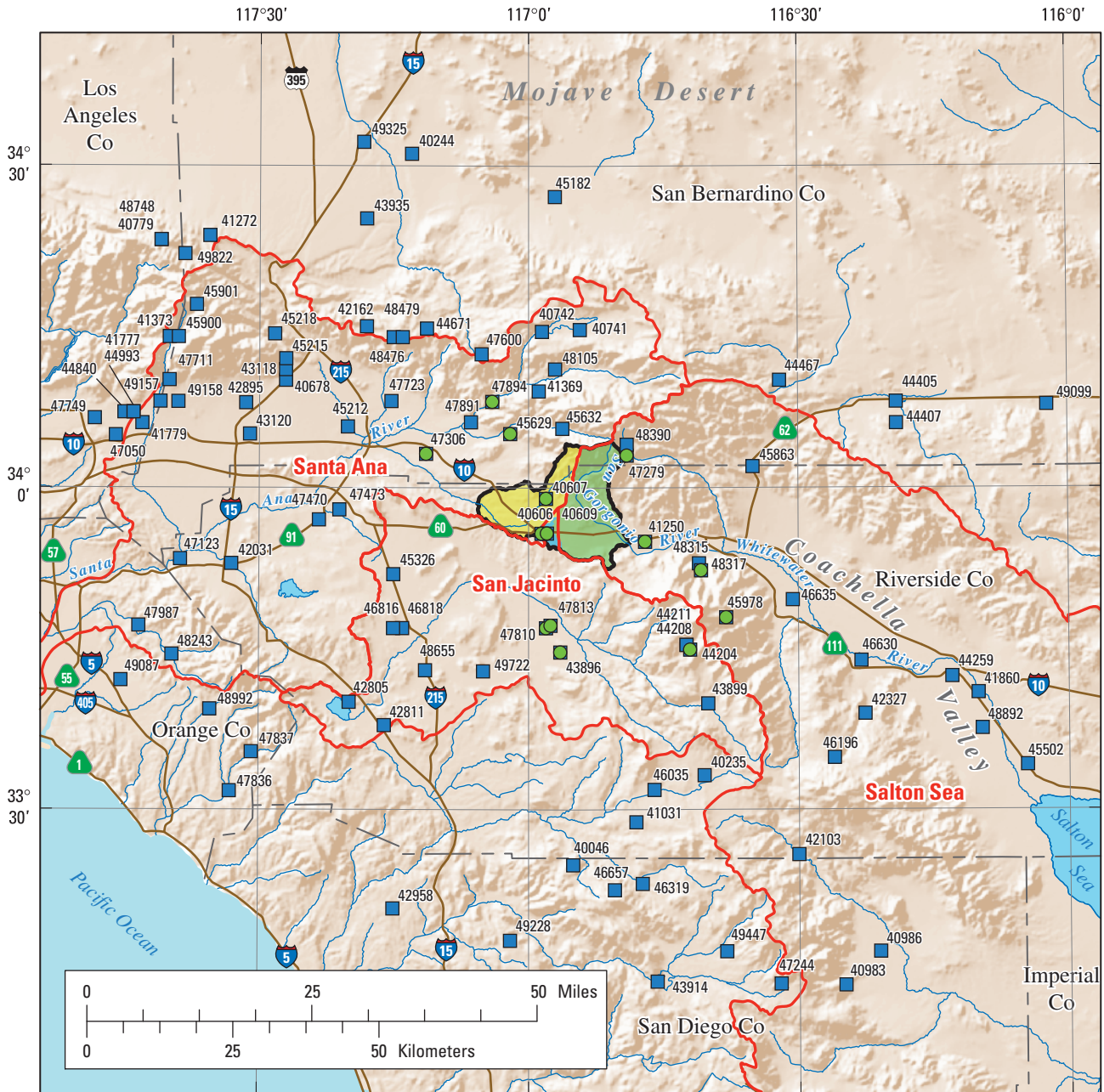
EXPLANATION

Surface-water sub-drainage basins simulated with INFILv3—Upstream of the Beaumont and Banning storage units

1	5	9	13	17	21	25
2	6	10	14	18	22	26
3	7	11	15	19	23	27
4	8	12	16	20	24	28

- Ground-water storage unit and name
- INFILv3 model boundary
- Surface-water drainage basins
- Ground-water flow model grid

Figure 11. Map showing surface-water sub-drainage basins upstream of the Beaumont and Banning storage units simulated using INFILv3, San Gorgonio Pass area, Riverside County, California.



Base from U.S. Geological Survey digital data, 1:100,000, 1981-89; Universal Transverse Mercator Projection (NGVD 29), Zone 11.

EXPLANATION

- | | | |
|-----------------------------------------------------------------------------------------------------------------------------------------------------------------------------------------------------------------------------------------------------------|-------------------------------------------------------------------------------------------------------------------------------------------------------------------------------------------------------------------------------------------------------------------------------------------------------------------------------------------------------------------------------------------------------------------------------------------------------------------------------------------------------------------------------------------------------------------|------------------------------------------------------------------------------------------------------------------------------------------------------------------------------------------------------------------------------------------------------------------------------------------------------------------------------------------------------------------|
| <ul style="list-style-type: none"> — San Jacinto INFILv3 model boundary - - - County boundary | <ul style="list-style-type: none"> Surface-water drainage basin areas San Timoteo Creek Potrero Creek San Gorgonio River | <ul style="list-style-type: none"> NCDC daily climate records used to develop INFILv3 daily climate inputs and monthly spatial distribution models 41031 ■ Climate stations used for daily climate input ● Climate stations used for monthly models |
|-----------------------------------------------------------------------------------------------------------------------------------------------------------------------------------------------------------------------------------------------------------|-------------------------------------------------------------------------------------------------------------------------------------------------------------------------------------------------------------------------------------------------------------------------------------------------------------------------------------------------------------------------------------------------------------------------------------------------------------------------------------------------------------------------------------------------------------------|------------------------------------------------------------------------------------------------------------------------------------------------------------------------------------------------------------------------------------------------------------------------------------------------------------------------------------------------------------------|

Figure 12. Map showing location of climate stations of the National Climatic Data Center (NCDC) in the Southern California region (EarthInfo, Inc., 2004).

Table 2. Climate stations in the Southern California Region with daily climate records maintained by the National Climatic Data Center (NCDC) and used to develop the INFILv3 model of the San Geronio Pass area, Riverside County, California.

[NGVD 29, National Geodetic Vertical Datum of 1929]

NCDC (climate station name)	NCDC station No. (see fig. 12)	Altitude of station in feet above NGVD 1929	NCDC (climate station name)	NCDC station No. (see fig. 12)	Altitude of station in feet above NGVD 1929
Aguanga Bergman Ranch	40046	3,104	La Verne Hts Fc 560 B	44840	1,211
Anza	40235	3,915	Live Oak Canyon	44993	1,250
Apple Valley	40244	2,934	Lucerne Valley 1 Wsw	45182	2,963
Beaumont ¹	40606	2,613			
Beaumont Pumping Plant ¹	40607	3,051	Lytle Creek Foothill B1	45212	1,160
			Lytle Creek Ph	45215	2,251
Beaumont 1 E ¹	40609	2,600	Lytle Creek R S	45218	2,730
Bennett Ranch	40678	1,850	March Field	45326	1,490
Big Bear Lake	40741	6,760	Mecca Fire Station	45502	-180
Big Bear Lake Dam	40742	6,815			
Big Pines Park Fc83b	40779	6,845	Mill Creek 2 ¹	45629	2,943
			Mill Creek Intake	45632	4,945
Borrego Desert Park	40983	805	Morongo Valley	45863	2,562
Borrego Springs 3 Nne	40986	630	Mt Baldy Fc85e	45900	4,281
Bradford Ranch	41031	3,353	Mount Baldy Notch	45901	7,746
Cabazon ¹	41250	1,801			
Cajon West Summit	41272	4,780	Mount San Jacinto Wsp ¹	45978	8,425
			Murcell Ranch	46035	3,714
Camp Angelus	41369	5,770	Nightingale	46196	4,032
Camp Baldy Fc 85 F	41373	4,304	Oak Grove R S	46319	2,750
Claremont Fc 230 D	41777	1,250	Palm Desert	46630	195
Claremont Pomona Col	41779	1,201			
Coachella Indio Caa	41860	-66	Palm Springs	46635	425
			Palomar Mountain Obs	46657	5,550
Corona	42031	610	Perris	46816	1,470
Coyote Canyon	42103	2,280	Perris 1 Wsw	46818	1,601
Crestline	42162	4,872	Pomona Fairplex	47050	1,040
Deep Canyon Lab	42327	1,200			
Elsinore	42805	1,285	Prado Dam	47123	560
			Ranchita	47244	4,114
Elsinore 4 Se	42811	1,450	Raywood Flats ¹	47279	7,073
Etiwanda	42895	1,390	Redlands ¹	47306	1,318
Fallbrook	42958	660	Riverside Fire Sta 3	47470	840
Fontana 5 N	43118	1,972			
Fontana Kaiser	43120	1,102	Riverside Citrus Exp St	47473	986
			Running Springs 1 E	47600	5,965
Hemet ¹	43896	1,655	San Antonio Cn Mouth	47711	2,392
Hemet Reservoir	43899	4,364	San Bernardino F S 226	47723	1,140
Henshaw Dam	43914	2,700	San Dimas Fire Fc95	47749	955
Hesperia	43935	3,202			
Idria	44204	2,651	San Jacinto ¹	47810	1,542
			San Jacinto R S ¹	47813	1,560
Idyllwild	44208	5,394	San Juan Canyon	47836	375
Idyllwild Fire Dept ²	44211	5,380	San Juan Guard Stn	47837	730
Indio Fire Station	44259	-21	Santa Ana River P H 3	47891	1,984
Joshua Tree	44405	2,723			
Joshua Tree 3 S	44407	3,491	Santa Ana River Ph 1 ²	47894	2,772
			Santiago Dam	47987	855
Kee Ranch	44467	4,334	Seven Oaks	48105	5,082
Lake Arrowhead	44671	5,205	Silverado Ranger Stn	48243	1,095

Table 2. Climate stations in the Southern California Region with daily climate records maintained by the National Climatic Data Center (NCDC) and used to develop the INFILv3 model of the San Gorgonio Pass area, Riverside County, California—Continued.

[NGVD 29, National Geodetic Vertical Datum of 1929]

NCDC (climate station name)	NCDC station No. (see fig. 12)	Altitude of station in feet above NGVD 1929
Snow Creek	48315	1,280
Snow Creek Upper ¹	48317	1,940
South Fork Cabin	48390	7,126
Squirrel Inn 1	48476	5,243
Squirrel Inn 2	48479	5,682
Sun City	48655	1,420
Table Mountain	48748	7,507
Thermal Fcwos	48892	-112
Trabuco Canyon	48992	970
Tustin Irvine Ranch	49087	235
Twenty-nine Palms	49099	1,975
Upland	49157	1,841
Upland 3 N	49158	1,611
Valley Center 6 N	49228	1,680
Victorville Pump Plant	49325	2,858
Warner Springs	49447	3,182
Winchester	49722	1,480
Wrightwood	49822	6,000

¹Station used for both daily climate input and for developing monthly regression coefficients.

²Station used only for developing monthly regression model coefficients.

102 climate stations was based on proximity to the study site, similarity of climate characteristics, and adequacy of record (only stations having 4 or more years of record were included in the network). Stations located outside of the study area were needed to ensure an adequate spatial and temporal coverage of the daily time series inputs for water years 1927–2001 (smaller networks tend to be more sensitive to gaps in the records) and to ensure that spatially-varying climate was well represented over an adequate range of altitudes. The daily data are compiled into a set of three time series input files (one file each for precipitation, maximum air temperature, and minimum air temperature), with each file containing the data for all 102 stations (all gaps in the record for each station are identified using a numeric flag).

Digital Map Files and Attribute Tables

Digital map files required for the INFILv3 model include a digital elevation model (DEM) of the study area, soil-type, surface geology, and vegetation type maps. These digital map files are used to define the drainage basin parameters for INFILv3, including (1) topographic parameters, (2) spatially distributed vegetation and root-zone parameters, (3) spatially distributed soil parameters, and (4) spatially distributed bedrock and deep-soil parameters. Attribute tables are used to define vegetation properties, soil properties, bedrock and deep alluvium properties representing the hydrologic characteristics of the root zone.

Topographic Parameters

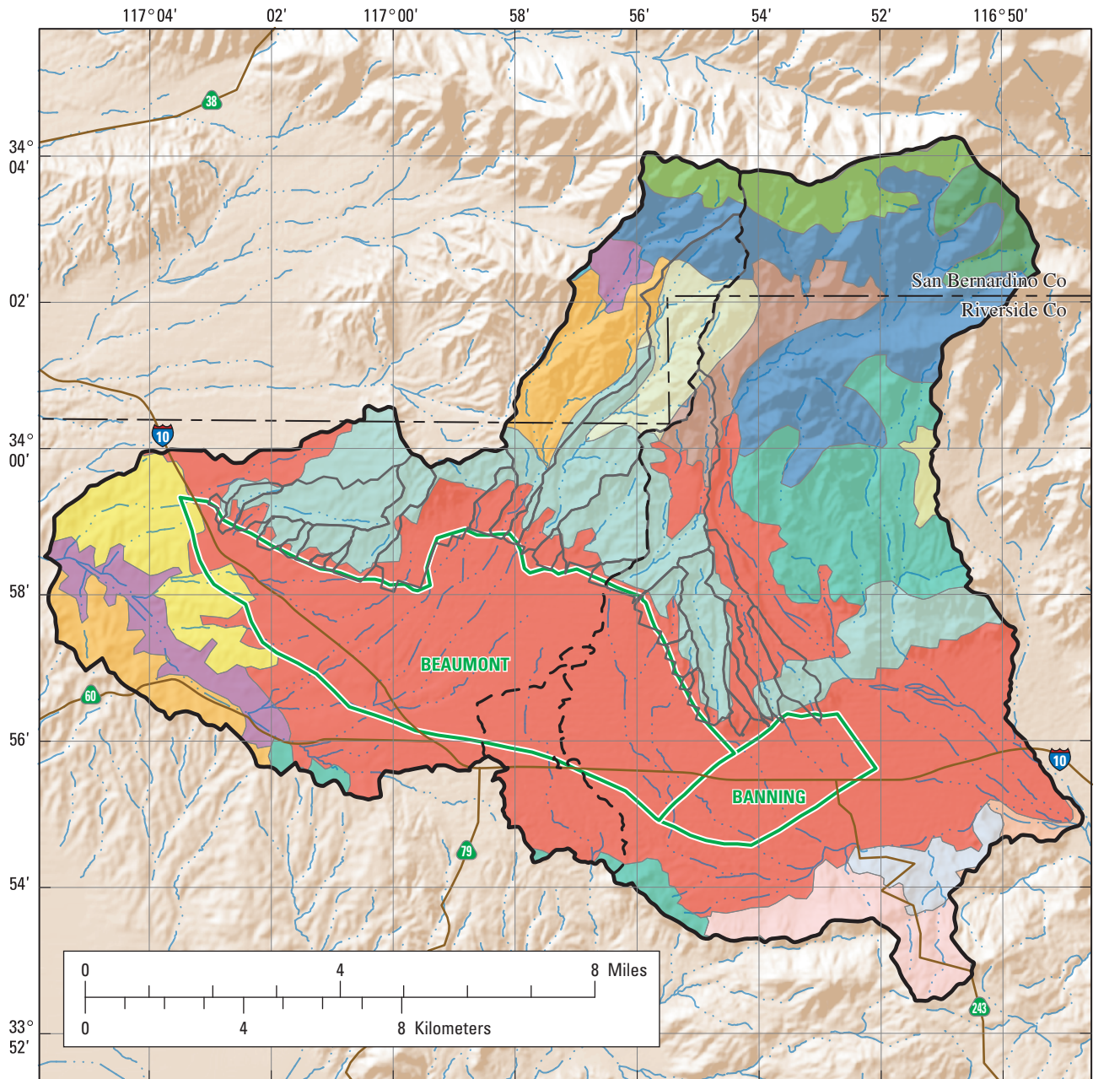
Topographic parameters are used to estimate potential evapotranspiration, spatially distribute the daily precipitation and temperature data over the drainage basin, and to route streamflow in the INFILv3 model. A 98.4 ft (30 m) resolution DEM of the study area was used to define the topographic parameters, which include location, altitude, aspect, slope, the skyview parameter (used to simulate incoming solar radiation), a set of 36 blocking ridge angles, and streamflow-routing data (location of upstream cell, location of downstream cell, and number of upstream cells) for each model cell (Hevesi and others, 2003).

Spatially Distributed Vegetation and Root-Zone Parameters

Spatially distributed vegetation parameters (vegetation type and cover) and root-zone parameters (maximum root-zone depth and root density as a function of depth) are presented in *table 3*. These values were estimated using the California Gap Analysis Program (GAP) digital map and an associated attribute table compiled by the U.S. Geological Survey (2000). For the model area, 17 different vegetation and land-use types were defined (*fig. 13*).

Spatially Distributed Soil Parameters

Soil parameters were estimated for each model cell using the State Soil Geographic Database (STATSGO) digital map and associated attribute tables compiled by the U.S. Department of Agriculture (1994). These spatially distributed parameters include root-zone thickness, soil-zone thickness, porosity, the wilting-point water content, a drainage-function coefficient, and saturated hydraulic conductivity. The INFILv3 model area included seven different STATSGO map unit identifiers (MUIDs), or soil codes (*fig. 14*), which were analyzed by methods described by Hevesi and others (2003) to develop initial model estimates of the soil parameters (*table 4*).



Base from U.S. Geological Survey digital data, 1:100,000, 1981-89; Universal Transverse Mercator Projection (NGVD 29), Zone 11.

EXPLANATION

GAP vegetation and land use units—

- | | | | |
|-----------------------------|--------------------------|-------------------------------|-----------------------------------------------------------------------------------------------------------------------------------------------|
| Semi-desert chaparral | Black oak forest | Bare rock | Ground-water storage unit and name
INFILv3 model boundary
INFILv3 modeled upstream sub-drainage basins
Surface-water drainage basins |
| Jeffrey pine-fir forest | Urban/built-up land | Sage scrub 2 | |
| Sierran mixed coniferous | Northern mixed chaparral | Montane manzanita chaparral | |
| Interior live oak chaparral | Sage scrub 1 | Arroyo willow riparian forest | |
| Ceanothus chaparral | Chamise chaparral | Mojave creosote bush scrub | |
| Scrub oak chaparral | Agriculture | | |
| | | | |

Figure 13. Map showing vegetation type and coverage used for the INFILv3 simulation of the San Gorgonio Pass area, Riverside County, California.

Table 3. Estimated vegetation cover and root densities used to define the root-zone parameters for the INFILv3 model of the San Geronimo Pass area, Riverside County, California.

[Vegetation types from U.S. Geological Survey, National Gap Analysis Program (GAP), 2000. Bedrock layer: for areas mapped as consolidated on figure 14. ft, feet]

Vegetation or land-use types	Estimated vegetation cover (percent)	Estimated root-densities (in percent)					
		Soil zone					Bedrock zone
		Layer 1	Layer 2	Layer 3	Layer 4	Layer 5	Layer 6
Semi-desert chaparral ¹	50	50	50	50	50	30	30
Jeffrey pine-fir forest ²	90	90	90	90	90	90	90
Sierran mixed coniferous ²	85	85	85	85	85	85	85
Interior live oak chaparral ²	60	60	60	60	60	60	60
Ceanothus chaparral ¹	50	50	50	50	50	30	20
Scrub oak chaparral ²	70	70	70	70	70	70	70
Black oak forest ¹	50	50	50	50	30	30	30
Urban/built-up land ¹	50	50	50	50	50	50	50
Northern mixed chaparral ¹	50	50	50	50	50	30	30
Sage scrub 1 ¹	40	40	40	40	30	20	10
Chamise chaparral ¹	50	50	50	50	50	30	20
Agriculture ²	80	80	80	80	80	30	30
Bare rock ¹	0	10	10	10	10	10	10
Sage scrub 2 ¹	40	40	40	30	30	20	10
Montane manzanita chaparral ¹	50	50	50	50	50	30	20
Arroyo Willow riparian forest ¹	40	40	40	40	30	20	15
Mojave creosote bush scrub ²	30	30	30	30	30	30	30

¹Layer 6 thickness equals 6.56 feet.

²Layer 6 thickness equals 9.84 feet.

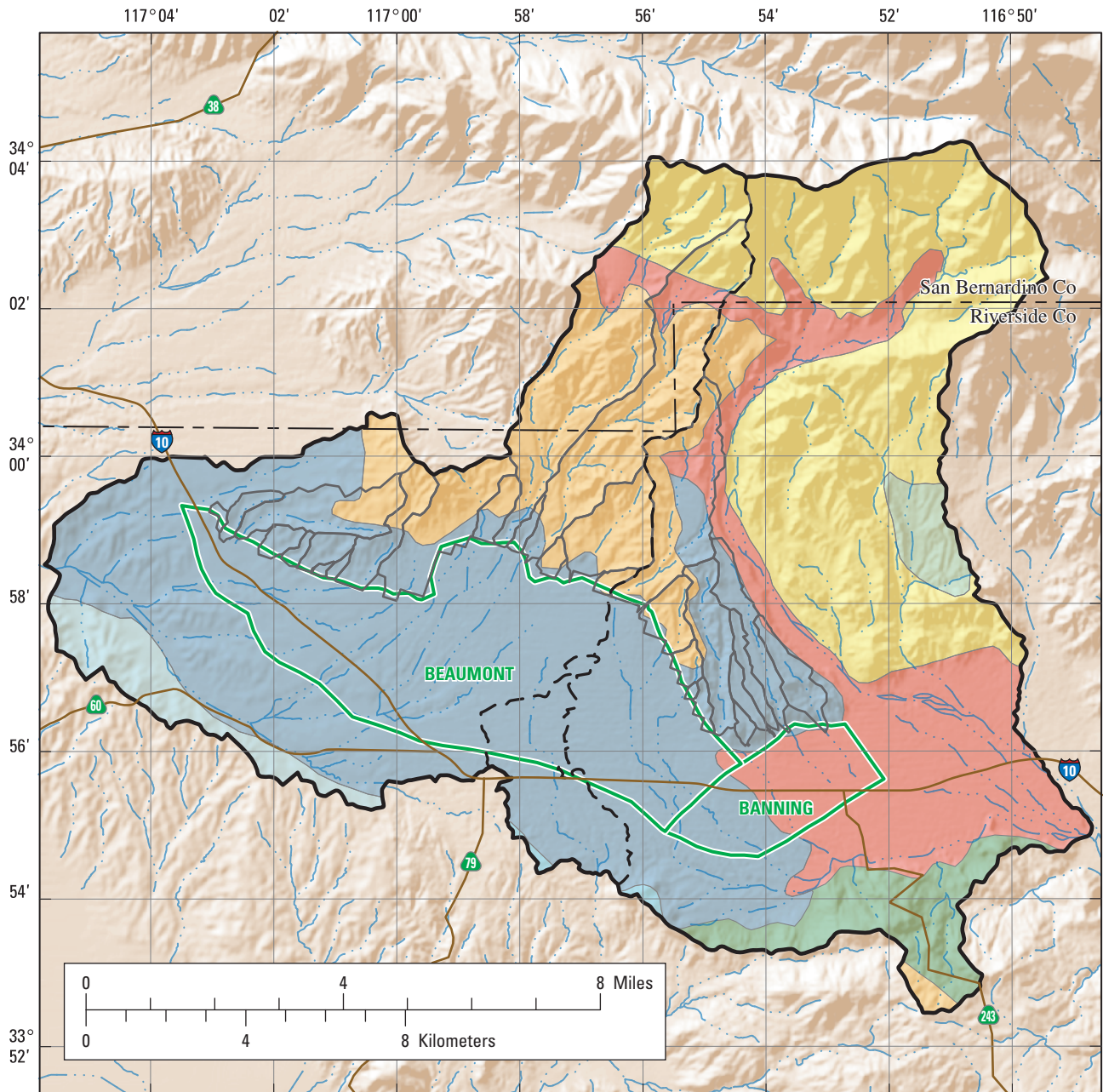
The root-zone thickness in the model area was defined using a surficial geologic map of the INFILv3 model area derived from the digital geologic map of California by Jennings (1977). This map was used because the geology includes the entire INFILv3 model area. A root-zone thickness of about 26 ft was assumed for all areas mapped as alluvium on figure 15 and about 7 or 10 ft for all areas mapped as consolidated rock, depending on vegetation type (table 3). The soil-zone thickness was assumed equal to the root-zone thickness in all areas mapped as alluvium, where the thickness of layer 1, the top soil layer, was 0.33 ft; layer 2 was 0.66 ft; layer 3 was 2.30 ft; layer 4 was 6.56 ft; and layer 5 was 16.41 ft. Layer 6, the bedrock zone, has a thickness of 0 ft for locations mapped as alluvium.

For locations mapped as consolidated rock, the soil-zone thickness was estimated from STATSGO data for each of the MUIDs, and range from 1.38 to 5.29 ft (table 4). These estimated soil-zone thicknesses were increased by 1.5 times during the model calibration. The soil zone in the consolidated rock areas were assumed to have the same thickness as the alluvium areas. However, because the initial and calibrated soil-zone thickness values for the consolidated rock areas are less than the soil-zone thickness values for the alluvium areas (about 26 ft), the thickness of the deeper layers are less than

the total thickness of the layer or in some cases 0 ft (table 4). Layer 6, the bedrock zone, has a thickness of either 7 ft or 10 ft (depending on vegetation type) minus the initial or calibrated soil-zone thickness for locations mapped as consolidated rock. Where calculated values were negative, layer 6 thickness was set to zero.

Spatially Distributed Bedrock and Deep-Soil Parameters

Spatially distributed bedrock and deep-soil parameters (soil layer 6 in the bedrock and alluvium areas, respectively) needed for the INFILv3 model are the root-zone porosity and hydraulic conductivity values (table 5). The geologic units identified on the surficial geologic map (fig. 15) were assigned an initial value of root-zone porosity and hydraulic conductivity consistent with those assigned to equivalent geologic units in the calibrated INFILv3 model of the Death Valley region (Hevesi and others, 2003) (table 5). The original estimates of root-zone porosity were not modified during the model calibration; however, the initial estimates of hydraulic conductivity were increased by a factor of about two during the model calibration (table 5).



Base from U.S. Geological Survey digital data, 1:100,000, 1981-89; Universal Transverse Mercator Projection (NGVD 29), Zone 11.

EXPLANATION

STATSGO MUIDs—

- | | | |
|-------------------------------------------------------------------------------------------|-------------------------------------------------------------------------------------------|-------------------------------------------------------------------------------------------|
|  CA671 |  CA609 |  CA625 |
|  CA639 |  CA614 |  CA648 |
| | |  CA624 |

 Ground-water storage units and name

-  INFILv3 model boundary
-  INFILv3 modeled upstream sub-drainage basins
-  Surface-water drainage basins

Figure 14. Map showing State Soil Geographic Database (STATSGO) soil units used for the INFILv3 simulation, San Geronimo Pass area, Riverside County, California.

Table 4. Initial and calibrated soil parameter values used as input to the INFILv3 model of the San Geronio Pass area, Riverside County, California.

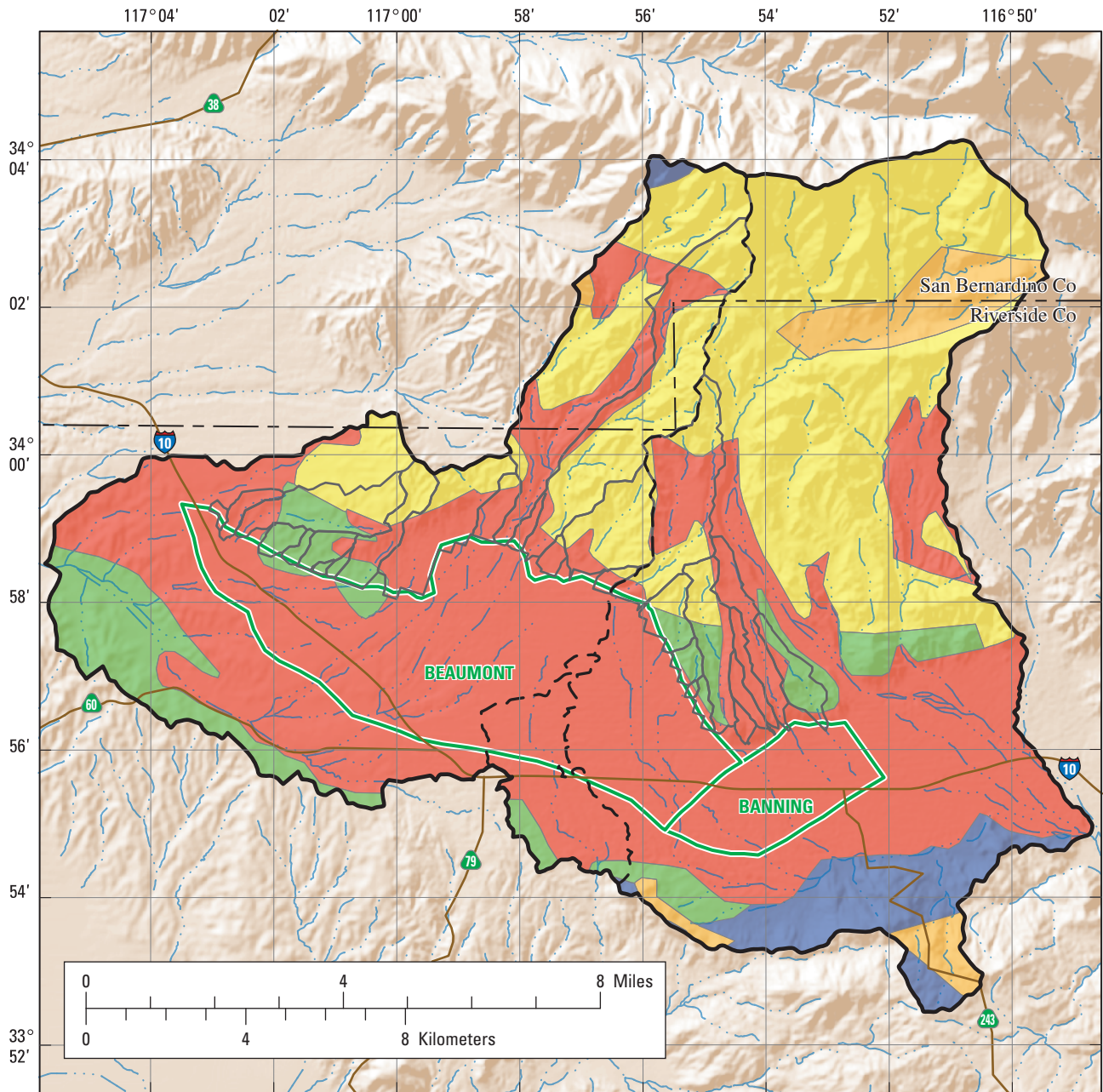
[STATSGO, State Soil Geographic database; MUID, a STATSGO map unit identifier. ft, feet; ft/s, feet per second]

STATSGO (MUID) (see fig. 13)	Soil parameter values									
	Estimated average soil zone thickness (ft)	Soil layer thickness for consolidated rock areas (ft)					Porosity	Wilting point	Drainage parameter	Saturated soil hydraulic conductivity (ft/s)
		Layer 1	Layer 2	Layer 3	Layer 4	Layer 5				
Initial										
CA671	1.79	0.33	0.66	0.81	0.00	0.00	0.41	0.016	3.757	3.32×10^{-4}
CA639	4.20	0.33	0.66	2.30	0.92	0.00	0.36	0.026	3.710	3.5×10^{-4}
CA614	4.93	0.33	0.66	2.30	1.65	0.00	0.36	0.053	4.978	1.96×10^{-4}
CA609	5.29	0.33	0.66	2.30	2.01	0.00	0.36	0.070	5.731	1.38×10^{-4}
CA625	1.74	0.33	0.66	0.75	0.00	0.00	0.37	0.031	3.888	3.56×10^{-4}
CA648	1.64	0.33	0.66	0.65	0.00	0.00	0.37	0.067	5.326	1.46×10^{-4}
CA624	1.38	0.33	0.66	0.40	0.00	0.00	0.38	0.103	7.181	6.82×10^{-4}
Calibrated										
CA671	2.69	0.33	0.66	1.70	0.00	0.00	0.41	0.016	3.757	3.32×10^{-4}
CA639	6.30	0.33	0.66	2.30	3.02	0.00	0.36	0.026	3.710	3.5×10^{-4}
CA614	7.40	0.33	0.66	2.30	4.12	0.00	0.36	0.053	4.978	1.96×10^{-4}
CA609	7.93	0.33	0.66	2.30	4.65	0.00	0.36	0.070	5.731	1.38×10^{-4}
CA625	2.60	0.33	0.66	1.62	0.00	0.00	0.37	0.031	3.888	3.56×10^{-4}
CA648	2.46	0.33	0.66	1.47	0.00	0.00	0.37	0.067	5.326	1.46×10^{-4}
CA624	2.80	0.33	0.66	1.09	0.00	0.00	0.38	0.103	7.181	6.82×10^{-5}

Table 5. Estimated root-zone porosity, initial, and final (calibrated) saturated hydraulic conductivity for bedrock and deep soil parameters used in the INFILv3 model of the San Geronio Pass area, Riverside County, California.

[See figure 14 for extent of geology. ft/s, feet per second]

Surface geologic unit	Estimated root-zone porosity	Initial saturated hydraulic conductivity (ft/s)	Calibrated saturated hydraulic conductivity (ft/s)
Alluvium	0.35	7.59×10^{-6}	1.52×10^{-5}
Continental sediments	0.25	1.90×10^{-7}	3.80×10^{-7}
Metamorphic rocks	0.05	3.80×10^{-9}	7.59×10^{-9}
Cretaceous granite	0.05	1.90×10^{-9}	3.80×10^{-9}
Quartzite	0.05	7.59×10^{-10}	1.52×10^{-9}



Base from U.S. Geological Survey digital data, 1:100,000, 1981-89; Universal Transverse Mercator Projection (NGVD 29), Zone 11.

Geology from Geologic Map of California, Charles W. Jennings, 1977.

EXPLANATION

Surface geology—

- | | | |
|-----------------------------------------------------------------------------------------------------------------------------|--------------------------------------------------------------------------------------------------------------------------------------------|-----------------------------------------------------------------------------------------------------------------------------------------|
| Alluvium | Consolidated rock | Quartzite |
| | Cretaceous granite | Metamorphic rocks |
| | Continental sediments | |

- Ground-water storage unit and name
- INFILv3 model boundary
- INFILv3 modeled upstream sub-drainage basins
- Surface-water drainage basins

Figure 15. Geologic map used for the INFILv3 simulation of the San Geronio Pass area, Riverside County, California. See *table 5* for estimated root-zone porosity and for initial and calibrated hydrologic conductivity for each map code area.

INFILv3 Model Coefficients

Model coefficients used in the INFILv3 model include average monthly linear regression coefficients for spatially distributing the daily precipitation and temperature data across all model grid cells, coefficients used to model sublimation and snowmelt, and coefficients defining stream-channel characteristics (Hevesi and others, 2003).

Fourteen climate stations (table 2) were selected from the regional network to define average monthly linear regression coefficients, which are used in INFILv3 to spatially distribute the daily precipitation and maximum and minimum daily air temperature data over the model area as a function of land-surface altitude. The results of the linear regression models, consisting of 12 sets of regression coefficients (slope and intercept) for each climate parameter (daily precipitation, maximum daily air temperature, and minimum daily air temperature) are presented in table 6. The correlation coefficient (*r*-squared) for each regression is also presented in table 6. The correlation coefficients indicate that precipitation is poorly correlated with land-surface altitude during the months of April through June (table 6).

The monthly climate-regression models spatially distribute the daily precipitation and temperature data from the 102 climate stations (fig. 12) using a modified inverse-distance-squared interpolation (Hevesi and others, 2003). The daily precipitation and temperature data are estimated for each grid cell as a weighted average of all available data collected at the 102 climate stations for a given date in the simulation period (only those stations having data for a given date are used for that date). The weighting factors are calculated by INFILv3

for each day of the simulation using a two-step procedure. In the first step, the inverse-distance-squared weighting factors are calculated using the distances between the model cell and all stations having data for that date. The second step of the procedure is an empirical method for incorporating orographic effects on precipitation and air temperature into the spatial interpolation. In the second step, the weighting factors for each station are adjusted using the ratio of the monthly regression model result (monthly precipitation, monthly maximum air temperature, or monthly minimum air temperature) at the model cell to the monthly regression result at the climate station, where the monthly regression results are calculated using the model cell altitude and the climate station altitude (table 6).

By utilizing a large number of climate stations in the spatial interpolation model, gaps in the record at any single station have a less significant impact on the estimated value. However, most of the data gaps tend to occur in the early part of the simulation period, when there were relatively few stations. For the simulation period used in this study, a minimum of two stations had data for a given date in the simulation. In general, the accuracy of the precipitation or air temperature estimate tends to decrease as the number of stations having data decreases (depending on the distance between the model cell and the nearest station having data).

Model coefficients for simulating snowmelt and sublimation were identical to those used by Hevesi and others (2003). Model coefficients used for simulating stream channel characteristics are dependent on the grid cell size and were adjusted during the model calibration process as described next.

Table 6. Average monthly precipitation and maximum and minimum regression model coefficients and statistics for spatially distributing daily climate inputs as a function of altitude and point measurements of average monthly precipitation in the INFILv3 model of the San Gorgonio Pass area, Riverside County, California.

[Average monthly maximum air temperature (in °F), and average monthly minimum air temperature (in °F); °F, degree Fahrenheit; ft, feet; in., inch]

Month	Average monthly precipitation regression model coefficients and statistics			Average monthly maximum air temperature regression model coefficients and statistics			Average monthly minimum air temperature regression model coefficients and statistics		
	Slope (in/ft)	Intercept (in.)	R-squared (unitless)	Slope (°F/ft)	Intercept (°F)	R-squared (unitless)	Slope (°F/ft)	Intercept (°F)	R-squared (unitless)
January	0.000504	1.98	0.88	-0.0034	70.2	0.89	-0.0029	43.1	0.72
February	0.000379	1.74	0.80	-0.0034	72.2	0.98	-0.0030	45.2	0.84
March	0.000376	1.58	0.62	-0.0034	74.7	0.94	-0.0030	46.7	0.84
April	0.000131	1.09	0.15	-0.0036	80.9	0.96	-0.0031	50.3	0.88
May	0.000448	1.44	0.18	-0.0033	86.5	0.86	-0.0029	54.6	0.88
June	0.000006	0.09	0.04	-0.0030	93.8	0.85	-0.0024	57.8	0.67
July	0.000064	0.05	0.55	-0.0034	102.6	0.92	-0.0021	63.5	0.57
August	0.000136	0.00	0.73	-0.0037	103.5	0.92	-0.0026	65.1	0.64
September	0.000115	0.19	0.60	-0.0037	98.9	0.95	-0.0029	62.7	0.65
October	0.000066	0.40	0.60	-0.0038	90.3	0.95	-0.0030	55.9	0.69
November	0.000167	1.17	0.48	-0.0033	79.0	0.92	-0.0026	47.8	0.68
December	0.000356	1.33	0.72	-0.0036	72.5	0.95	-0.0028	43.3	0.64

INFILv3 Model Calibration

Model calibration is the process of making adjustments, within justifiable ranges, to initial estimates of selected model parameters to obtain reasonable agreement between simulated and measured values. In this study, the model was calibrated to measured streamflow at the Little San Gorgonio Creek stream gaging site in the San Timoteo Creek drainage basin (gage 11056500; *fig. 10*) for the period of record (October 10, 1948, through September 30, 1985). The streamflow data can be retrieved from the USGS National Water Information System Web page (NWIS web) located at <http://waterdata.usgs.gov/ca/nwis/> using the USGS gaging station name or number.

The model calibration process used all daily mean discharge data for the complete period of record for the Little San Gorgonio Creek stream gage, with the exclusion of the daily mean discharge of 1,180 cubic feet per second (ft³/s) recorded on February 25, 1969. The streamflow on this date is considered to be associated with the occurrence of debris flows, which likely caused an overestimate of the stream discharge (Robert Meyer, U.S. Geological Survey, oral commun., 2002).

Calibration of the model was achieved by adjusting model parameters by trial and error for soil thickness, bedrock and deep soil (soil zone 6), saturated hydraulic conductivity, evapotranspiration coefficients, root-density coefficients, and coefficients defining stream channel characteristics. Initial estimates of these parameters resulted in greater simulated streamflow in Little San Gorgonio Creek than was measured. During the calibration process, the soil thickness was increased by 1.5 times and the saturated hydraulic conductivity of the bedrock and deep soil (soil zone 6) by 2 times to increase infiltration and thereby reducing simulated streamflow.

Measured and simulated total annual (water year), total monthly, and daily mean discharge at the Little San Gorgonio Creek stream gage are presented in figure 16 for the calibrated model. The simulated total annual streamflows are in good agreement with the measured streamflows with the exception of a few water years, especially 1969 (*fig. 16A*). Qualitatively, there was a better fit between measured and simulated total annual flows after water year 1970. Prior to water year 1970, both the measured and simulated results indicate very low flows for most water years resulting from lower than average precipitation during that period (*fig. 4*). In contrast, there was a better comparison between measured and simulated streamflow for the higher flows during water years 1978, 1980, and 1983 (*fig. 16A*). Results indicate a reasonable representation of the general character of observed record in terms of the timing and frequency of streamflow.

A quantitative analysis of the goodness-of-fit between the simulated and measured streamflow discharge for water years 1949–85 was completed for the total annual, total monthly, and daily mean discharges (*table 7*). The goodness-of-fit analysis also included a comparison of simulated and measured storm-event total discharge, where storm events were defined

as periods of measureable streamflow bounded by periods of no (zero) streamflow.

The goodness-of-fit statistics included the percent average estimation error, the correlation coefficient, and the slope and intercept of the regression line. The percent average estimation error provides an indication of model bias (values of plus or minus 10 percent or less were considered favorable in this study). The regression statistics (the correlation coefficient and the slope and intercept of the regression line) were calculated using measured discharge as the independent variable. The regression statistics were used to supplement the percent average estimation error: a favorable fit is indicated by a correlation coefficient greater than 0.5, a slope close to 1.0, and an intercept close to zero.

Annual and Seasonal Discharge

Simulated average annual discharge at the Little San Gorgonio Creek gage was 373 acre-ft, about 11 percent lower than the measured average annual discharge of about 420 acre-ft (*table 7*). Simulated average discharge for winter (October through June) was 342 acre-ft, about 8 percent lower than the measured average winter discharge of about 370 acre-ft. Simulated average discharge for summer (July through September) was 32 acre-ft, about 37 percent lower than the measured average summer discharge of about 50 acre-ft. These results indicate that the model underestimates the average winter and summer discharges; however, the underestimate is near the acceptable range for the average annual discharge and is acceptable for the winter discharge.

Based on 37 years of record (*table 7*), the correlation coefficient is 0.73 for the annual discharge, 0.75 for winter discharge, and 0.16 for summer discharge. Results indicate that the model fit for the annual and winter discharges are better than the fit for the summer discharge. Because the measured summer discharge is minimal in the study area, the error in the summer model fit does not significantly affect the model fit for the average annual discharge.

Monthly Discharge

Simulated average monthly discharge at the Little San Gorgonio Creek gage was about 30 acre-ft, about 11 percent lower than the measured average monthly discharge of about 34 acre-ft. Simulated average monthly discharge for winter was 40 acre-ft, about 7 percent higher than the measured average monthly winter discharge of about 37 acre-ft. Simulated average monthly discharge for summer was about 11 acre-ft, about 37 percent lower than the measured average monthly summer discharge of about 17 acre-ft. These results indicate that the model underestimates the average monthly winter and monthly summer discharges; however, the underestimate is near the acceptable range for average monthly discharge and is acceptable for the average monthly winter discharge. By definition, model bias is consistent between annual, monthly, and daily mean results.

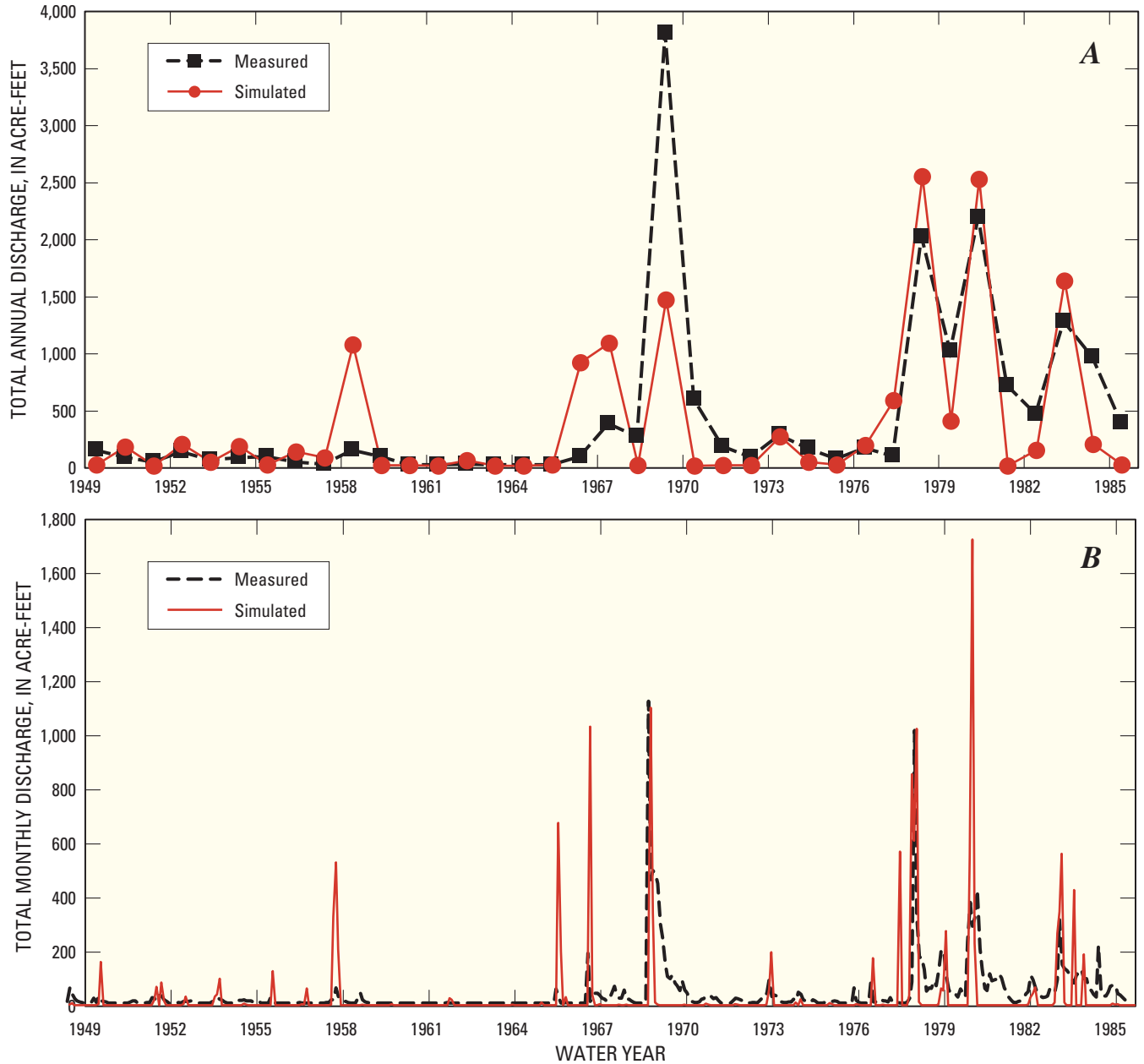


Figure 16. Graph showing measured and simulated streamflow at Little San Geronio Creek gage (11056500) for (A) total annual, (B) total monthly, and (C) daily mean discharge, San Geronio Pass area, Riverside County, California.

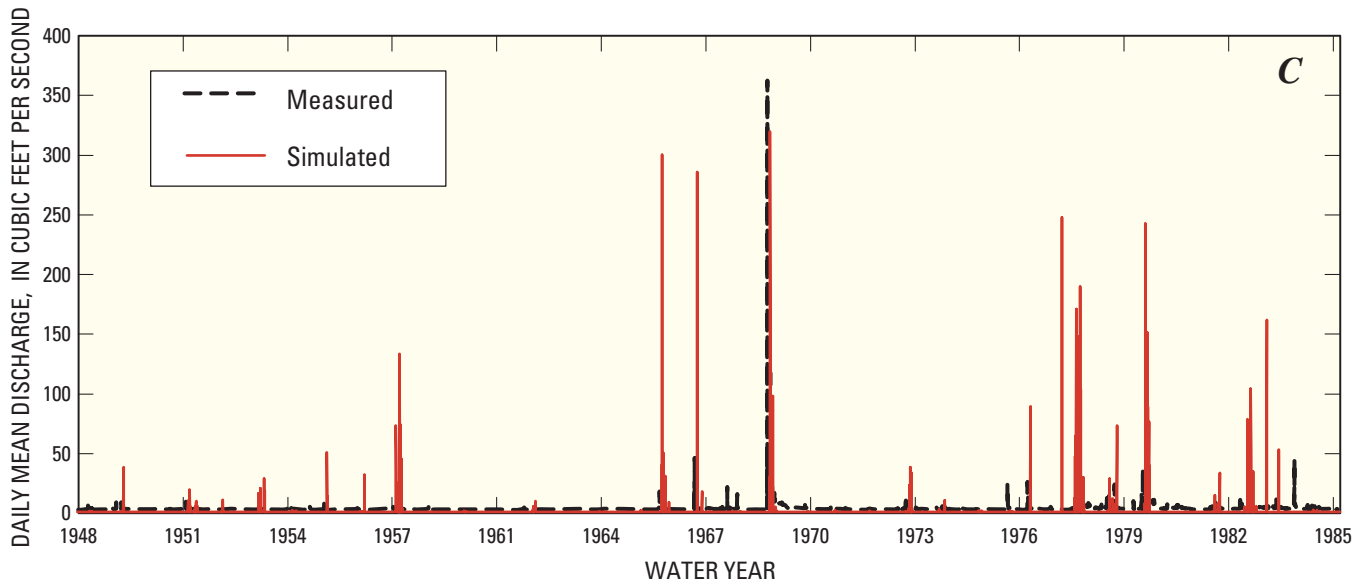


Figure 16. Continued.

The correlation coefficient is 0.54 for the monthly discharge, 0.56 for monthly winter discharge, and 0.11 for monthly summer discharge. These results indicate that the model fit for the monthly and monthly winter discharges are better than the fit for the monthly summer discharge. Because the measured summer discharge is minimal in the study area, the error in the summer model fit does not significantly affect the model fit for the monthly discharge. The simulated monthly discharge does not provide as good a fit to the measured data as does the annual discharge (*table 7*).

Daily Mean Discharge

Simulated daily mean discharge at the Little San Geronio Creek gage was 0.52 ft³/s, about 11 percent lower than the measured monthly discharge of 0.58 ft³/s. Simulated daily mean discharge for winter was 0.63 ft³/s, about 8 percent lower than the measured daily mean winter discharge of 0.68 ft³/s. Simulated daily mean discharge for summer was 0.17 ft³/s, about 37 percent lower than the measured daily mean summer discharge of 0.28 ft³/s.

The correlation coefficient is 0.49 for the daily mean discharge, 0.52 for daily mean winter discharge, and 0.09 for daily summer discharge. These results indicate that the model fit for the daily mean and daily mean winter discharges are better than the fit for the daily mean summer discharge. The simulated daily mean discharge does not provide as good a fit to the measured data as does the annual or monthly discharge (*table 7*). Simulated daily mean discharge results indicate that the INFILv3 model overestimates the measured daily mean discharge for major storms (*fig. 16C*); however, the timing and frequency of the higher magnitude simulated daily mean discharges are in good general agreement with the timing and

frequency of the observed higher daily mean discharges. The main reason for this over-estimation is all runoff and subsequent streamflow is simulated to occur during a 24-hour time step within the drainage area being modeled (the real-time downstream propagation of a flood wave is not physically modeled). This assumption results in an overestimation of daily mean discharge magnitudes during storms (days with precipitation) and an underestimation of daily mean discharge for the period immediately following storms.

Storm Event Total Discharge

For the period of record, a total of 191 storms were observed (*table 7*). Recall that storms were defined as periods of measureable streamflow bounded by periods of no streamflow. Simulated average storm discharge was 72 acre-ft per storm (acre-ft/storm), about 11 percent lower than the measured average storm discharge of 81 acre-ft/storm. Simulated average storm discharge for winter was 42 acre-ft/storm, about 93 percent greater than the measured average storm discharge of 22 acre-ft/storm. Simulated average storm discharge for summer was 212 acre-ft/storm, about 41 percent lower than the measured average storm discharge of 357 acre-ft/storm. These results indicate that the model underestimates the annual and summer storm discharges, and overestimates winter storm discharges.

The correlation coefficient is 0.93 for storm discharge, 0.75 for winter storm discharge, and 0.94 for summer storm discharge. These results indicate that the model fit for storms is good and indicate a much better goodness-of-fit compared with the annual, monthly, and daily mean discharge results.

Table 7. Measured and INFILv3-simulated total annual (water-year), total monthly, daily mean, and storm event total discharge, San Gorgonio Pass area, Riverside County, California.

Total annual discharge	Water years 1949–85		
	All records	Winter October–June	Summer July–September
Sample size (number of years)	37	37	37
Measured average (acre-feet/year)	420	370	50
Simulated average stream flow discharge (acre-feet/year)	373	342	32
Percent average estimated error	–11	–8	–37
Correlation coefficient	0.73	0.75	0.16
Slope of regression line	0.64	0.73	0.18
Intercept of regression line (acre-feet/year)	106	73	23

Total monthly discharge	Water years 1949–85		
	All records	Winter October–June	Summer July–September
Measured average (acre-feet/month)	34.0	39.8	16.8
Simulated average stream flow discharge (acre-feet/month)	30.4	37.0	10.6
Percent average estimated error	–11	–7	–37
Correlation coefficient	0.54	0.56	0.11
Slope of regression line	0.83	0.86	0.19
Intercept of regression line (acre-feet/month)	2.1	2.9	7.4

Daily mean discharge	Water years 1949–85		
	All records	Winter October–June	Summer July–September
Measured average (cubic-feet/second)	0.58	0.68	0.28
Simulated average stream flow discharge (cubic-feet/second)	0.52	0.63	0.17
Percent average error	–11	–8	–37
Correlation coefficient	0.49	0.52	0.09
Slope of regression line	1.05	1.06	0.43
Intercept of regression line (cubic feet/second)	–0.09	–0.09	0.1

Storm event total discharge	Water years 1949–85		
	All records	Winter October–June	Summer July–September
Measured average (acre-feet/storm)	81	22	357
Simulated average stream flow discharge (acre-feet/storm)	72	42	212
Percent average error	–11	93	–41
Correlation coefficient	0.93	0.75	0.94
Slope of regression line	0.67	0.95	0.67
Intercept of regression line (acre-feet/storm)	17.9	21.4	–25.7

INFILv3 Model Results

To develop estimates of natural ground-water recharge for the San Gorgonio Pass area, daily net infiltration was simulated using the INFILv3 model for water years 1927–2001. Initial conditions for the 1927–2001 simulation were defined using a root-zone water content of 1.5 times the wilting point for soil zone and zero for the bedrock zone or layer 6. To reduce the dependency of the results on the assumed initial water content, the first 3 water years of the simulation period (1927–29) were not included in the analysis of the daily time series results and the calculation of the average-annual water-balance terms. The average annual water balance terms were used to develop a simulated water budget for the San Timoteo Creek, Potrero Creek, and San Gorgonio River surface-water drainage basins, the Beaumont and Banning storage units, and the sub-drainage basins upstream of the Beaumont and Banning storage units.

Water Balance for San Timoteo Creek, Potrero Creek, and San Gorgonio River Surface-Water Drainage Basins

The INFILv3 simulation results for water years 1930–2001 for all components of the water balance for the San Timoteo Creek, Potrero Creek, and San Gorgonio River surface-water drainage basins are presented in *table 8A*. The simulated precipitation, snowfall, evapotranspiration, runoff, and net infiltration are presented in *figures 17–21*, respectively.

The simulated average annual precipitation (rainfall and snowfall) for all three basins is 19.7 in/yr (about 123,350 acre-ft/yr), with a maximum value of 34 in/yr for the highest altitude location in the northern part of the San Gorgonio River surface-water drainage basin and a minimum value of 14 in/yr in the eastern part of the San Gorgonio River surface-water drainage basin (*fig. 17* and *table 8A*). Simulated average snowfall is about 1.2 in/yr (about 7,440 acre-ft/yr) (*fig. 18* and *table 8A*). For most locations snowfall is not a critical component of the simulated water balance except for the higher altitude areas in the northern part of the model area where the simulated snowfall is 12 to 26 in/yr (*fig. 18*). There is no surface-water inflow into the surface-water drainage basins (*table 8*).

Most of the simulated precipitation and snowmelt is discharged from the model area by evapotranspiration. Total simulated evapotranspiration is 15.4 in/yr (about 96,410 acre-ft/yr), with a maximum value of about 24 in/yr for the highest altitude location in the northern part of the San Gorgonio River surface-water drainage basin and a minimum value of about 7 in/yr in the southern part of the San Gorgonio River surface-water drainage basin (*fig. 19* and *table 8A*). The simulated evapotranspiration is about 78 percent of the simulated precipitation (*table 8A*). In general, the spatial distribution of simulated evapotranspiration indicates an increase in evapotranspiration with an increase in altitude: available water is the limiting factor for evapotranspiration in the study area and precipitation generally increases with altitude (*figs. 17* and *19*). On a local scale, north facing slopes and locations

shaded from the south by blocking ridges have less simulated evapotranspiration than south facing slopes and locations not subjected to shading effects from surrounding terrain.

The average simulated surface-water outflow from the model area is about 0.6 in/yr (3,900 acre-ft/yr) with about 97 percent of the total simulated outflow occurring from the San Gorgonio River surface-water drainage basin (*table 8A*). The average simulated natural ground-water recharge (net infiltration) for the model area is about 3.4 in/yr (21,230 acre-ft/yr), about 17 percent of the simulated precipitation (*table 8A*). The simulated natural ground-water recharge exceeded 20 in/yr along stream channels having a high frequency and magnitude of simulated streamflow.

For the simulation period, the water-balance results indicate that the average change in stored water in the root zone is about 1,040 acre-ft/yr, indicating that the root zone became wetter during the simulation (*table 8A*). The simulated change in storage is relatively small, less than 1 percent of the simulated total inflow, indicating that the initial conditions were representative of the long-term average climate simulated using this model.

Water Balance for the Beaumont and Banning Storage Units

The Beaumont and Banning storage units of the San Gorgonio Pass ground-water basin include parts of the San Timoteo Creek, Potrero Creek, and San Gorgonio River surface-water drainage basins (*fig. 10*). The INFILv3 simulation results for water years 1930–2001 for all components of the water balance for the Beaumont and Banning storage units are presented in *table 8A*.

The simulated average annual precipitation rate for the Beaumont and Banning storage units is 17.8 in/yr (about 21,460 acre-ft/yr) (*table 8A*). Almost all the precipitation is simulated as rainfall (*table 8A*). The simulated average annual surface-water inflow rate from the upstream sub-drainage basins is about 0.9 in/yr (about 1,090 acre-ft/yr). Most of the simulated inflow (precipitation and surface-water inflow) is discharged from the storage units as evapotranspiration. The simulated average annual evapotranspiration rate is 15.2 in/yr (about 18,260 acre-ft/yr). Little water leaves the storage units as surface-water outflow. The average simulated surface-water outflow from the storage units is about 0.2 in/yr (about 230 acre-ft/yr). The simulated average annual natural ground-water recharge for the storage units is about 3.1 in/yr (about 3,710 acre-ft/yr) or about 17 percent of the simulated precipitation.

Spatial variability of simulated ground-water recharge (net infiltration) is high within the Beaumont and Banning storage units. A maximum recharge rate of about 31 in/yr was simulated along the Little San Gorgonio Creek channel and a minimum recharge rate of about 1 in/yr was simulated along the eastern and western parts of the storage units (*fig. 21A*). In contrast, simulated precipitation in the storage units varied from only 15 to 21 in/yr (*fig. 17*).

Table 8A. Summary of INFILv3 simulated water-balance results for natural conditions in the San Geronio Pass area, Riverside County, California, 1930–2001.

INFILv3 modeled area name or upstream sub-drainage basin identifier	INFILv3 simulation results of natural conditions (acre-feet/year)								
	Inflows				Outflows				Change in stored water
	Total precipitation	Rainfall	Snowfall	Surface-water inflow	Sublimation	Evapotranspiration	Surface-water outflow	Recharge	
Surface-water drainage basins									
Potrero Creek	3,806.73	3,797.71	9.02	0.00	0.69	3,188.33	1.48	559.58	56.64
San Timoteo Creek	49,705.01	48,059.68	1,645.33	0.00	168.15	39,321.23	133.24	9,610.71	471.68
San Geronio River	69,839.42	64,056.46	5,782.96	0.00	595.12	53,901.81	3,762.81	11,063.26	516.42
Totals	123,351.16	115,913.85	7,437.31	0.00	763.96	96,411.37	3,897.53	21,233.55	1,044.74
Surface-water sub-drainage basins upstream of the Beaumont and Banning storage units									
1	60.18	60.03	0.15	0.00	0.01	52.31	0.08	6.70	1.08
2	240.36	239.75	0.61	0.00	0.04	206.28	0.03	30.05	3.96
3	1,498.08	1,493.64	4.44	0.00	0.27	1,201.48	5.29	283.05	7.99
4	233.29	232.70	0.59	0.00	0.04	196.06	0.06	36.87	0.26
5	114.89	114.60	0.29	0.00	0.02	96.76	0.06	17.93	0.12
6	328.88	328.00	0.88	0.00	0.06	275.30	0.19	51.86	1.47
7	39.42	39.32	0.10	0.00	0.01	33.42	0.04	5.89	0.06
8	71.05	70.87	0.18	0.00	0.01	59.70	0.11	10.96	0.27
9	936.25	932.24	4.01	0.00	0.30	755.68	6.39	168.74	5.14
10	1,985.73	1,977.27	8.46	0.00	0.61	1,605.28	2.56	355.74	21.54
11	422.92	421.06	1.86	0.00	0.14	341.47	0.21	75.38	5.72
12	8,918.95	7,726.67	1,192.28	0.00	128.19	6,219.74	195.12	2,331.22	44.68
13	175.33	174.62	0.71	0.00	0.05	141.29	0.19	31.09	2.71
14	6,132.01	5,780.35	351.66	0.00	33.16	4,448.37	682.69	947.91	19.88
15	174.60	173.93	0.67	0.00	0.05	142.85	0.09	28.97	2.64
16	1,734.05	1,723.38	10.67	0.00	0.79	1,342.06	115.14	270.64	5.42
17	160.03	159.31	0.72	0.00	0.05	129.12	0.00	29.16	1.70
18	3,098.06	3,058.83	39.23	0.00	3.02	2,346.71	52.91	665.85	29.57
19	645.27	642.12	3.15	0.00	0.23	491.81	14.84	136.74	1.65
20	236.37	235.48	0.89	0.00	0.06	182.28	0.77	52.30	0.96
21	37.60	37.48	0.12	0.00	0.01	31.97	0.09	5.10	0.43
22	157.56	157.08	0.48	0.00	0.04	133.57	0.47	22.00	1.48
23	1,248.26	1,242.47	5.79	0.00	0.40	999.50	9.03	229.36	9.97
24	125.13	124.74	0.39	0.00	0.03	106.82	0.23	15.99	2.06
25	248.82	247.93	0.89	0.00	0.06	206.01	0.23	38.50	4.02

Table 8A. Summary of INFILv3 simulated water-balance results for natural conditions in the San Gorgonio Pass area, Riverside County, California, 1930–2001—Continued.

INFILv3 modeled area name or upstream sub-drainage basin identifier	INFILv3 simulation results of natural conditions (acre-feet/year)								
	Inflows				Outflows				Change in stored water
	Total precipitation	Rainfall	Snowfall	Surface-water inflow	Sublimation	Evapotranspiration	Surface-water outflow	Recharge	
26	359.21	357.82	1.39	0.00	0.09	294.75	0.29	58.30	5.78
27	908.55	904.22	4.33	0.00	0.30	732.52	1.19	160.20	14.34
28	644.51	642.43	2.08	0.00	0.14	527.34	1.32	112.52	3.19
Total for upstream area	30,935.36	29,298.34	1,637.02	0.00	168.18	23,300.45	1,089.62	6,179.02	198.09
Beaumont and Banning storage units	21,455.05	21,401.95	53.10	1,089.62	3.85	18,259.18	228.27	3,707.00	346.37
Total for area having potential to affect Beaumont and Banning storage units	52,390.41	50,700.29	1,690.12	0.00	172.03	41,559.63	228.27	9,886.02	544.46

For the simulation period, the water-balance results indicate that the average change in stored water in the root zone in the storage units is about 350 acre-ft/yr, indicating that the root zone became wetter during the simulation (*table 8A*). The simulated change in storage is relatively small, less than 2 percent of the simulated total inflow.

Water Balance for the Sub-Drainage Basins Upstream of the Beaumont and Banning Storage Units

The 28 sub-drainage basins upstream of the Beaumont and Banning storage units of the San Gorgonio Pass ground-water basin include parts of the San Timoteo Creek and San Gorgonio River surface-water drainage basins (*figs. 10 and 11*). The INFILv3 simulation results for water years 1930–2001 for all components of the water balance for the sub-drainage basins are presented in *table 8A*.

The simulated average annual precipitation rate in the sub-drainage basins is 21.3 in/yr (about 30,940 acre-ft/yr) with a maximum rate of 24.2 in/yr (about 8,920 acre-ft/yr) in the Little San Gorgonio Creek sub-drainage basin (sub-drainage basin 12) (*tables 1 and 8A*). There is no surface-water in-flow into the sub-drainage basins.

The simulated average annual evapotranspiration rate is 16.0 in/yr (about 23,300 acre-ft/yr) or about 75 percent of the simulated average annual precipitation rate. The simulated average annual surface-water outflow rate from the sub-drainage basins is about 0.7 in/yr (about 1,090 acre-ft/yr). The Noble Creek sub-drainage basin (sub-drainage basin 14), the second largest upstream sub-drainage, had the largest simulated surface-water outflow (about 680 acre-ft/yr) (*table 8A*). The simulated outflow is high because the fraction of area having thin soil underlain by low permeability bedrock was relatively high for this drainage basin. The simulated average annual natural recharge rate for all the sub-drainage basins is about 4.2 in/yr (about 6,180 acre-ft/yr), or about 20 percent of the total simulated precipitation in the sub-drainage basins (*table 8A*). Little San Gorgonio Creek (sub-drainage basin 12), the largest of the 28 upstream sub-drainage basins, had the largest simulated recharge of 6.3 in/yr (about 2,330 acre-ft/yr) (*table 8A*). This natural recharge in the sub-drainage basins upstream of the Beaumont and Banning storage units is a potential source of recharge to the storage units as ground-water underflow and baseflow.

Table 8B. Summary of INFILv3 simulated water-balance results for urban-area modified conditions in the San Gorgonio Pass area, Riverside County, California, 1930–2001.

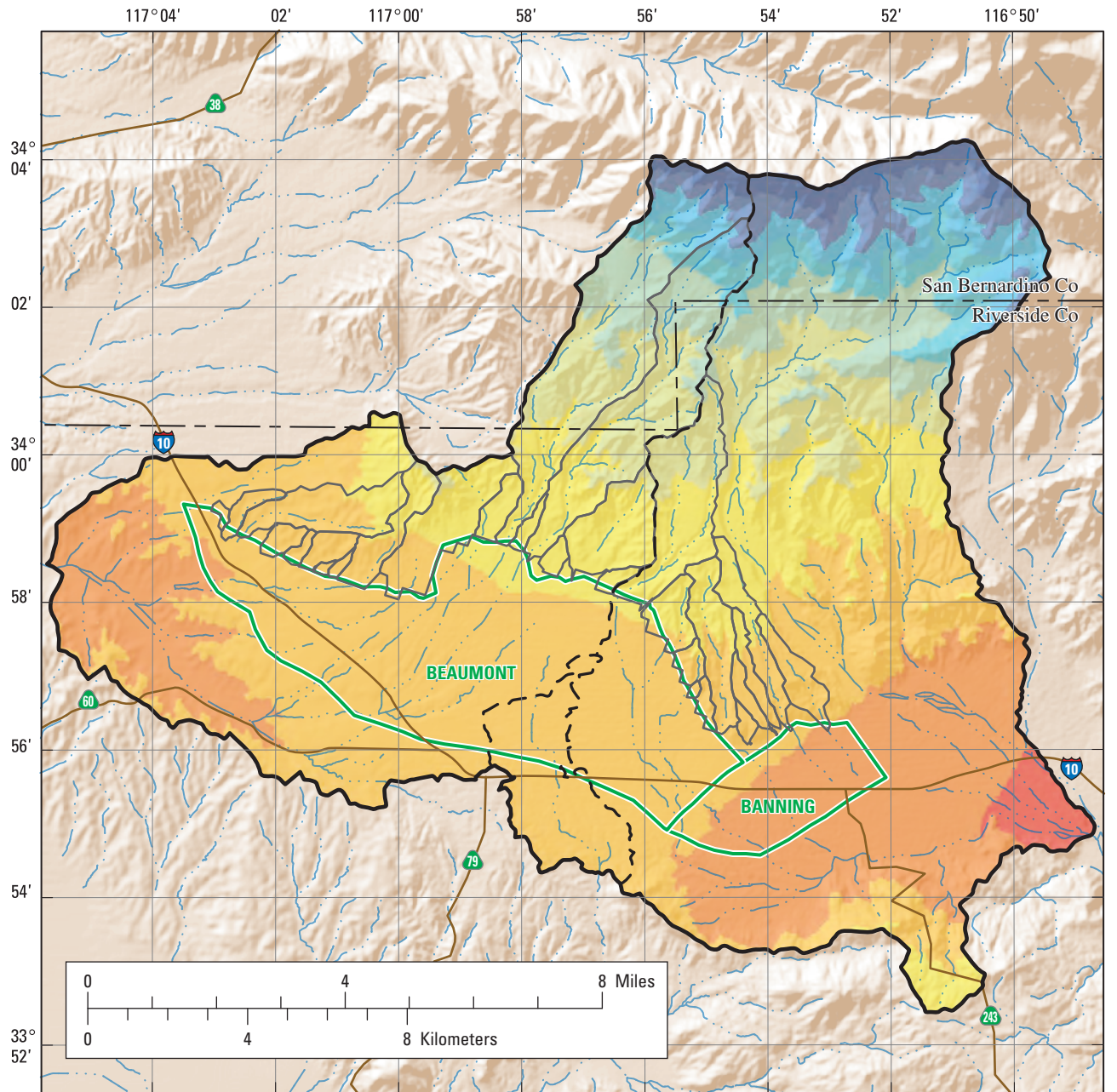
INFILv3 modeled area name or upstream sub-drainage basin identifier	Urban-area modified conditions (acre-feet/year)								Change in root-zone storage
	Inflows				Outflows				
	Total precipitation	Rainfall	Snowfall	Surface water inflow	Sublimation	Evapotranspiration	Surface water outflow	Recharge	
	Surface-water drainage basins								
Potrero Creek	3,806.73	3,797.71	9.02	0.00	0.69	3,033.82	23.98	707.17	41.07
San Timoteo Creek	49,705.01	48,059.68	1,645.33	0.00	168.15	38,839.18	284.50	9,993.95	419.23
San Gorgonio River	69,839.42	64,056.46	5,782.96	0.00	595.12	53,412.73	4,340.12	11,037.31	454.14
Totals	123,351.16	115,913.85	7,437.31	0.00	763.96	95,285.73	4,648.60	21,738.43	914.44
	Surface-water sub-drainage basins upstream of the Beaumont and Banning storage units								
1	60.18	60.03	0.15	0.00	0.01	50.82	1.23	7.26	0.86
2	240.35	239.74	0.61	0.00	0.04	205.15	0.06	31.36	3.74
3	1,498.00	1,493.56	4.44	0.00	0.27	1,195.26	19.49	275.61	7.37
4	233.28	232.69	0.59	0.00	0.04	195.66	0.06	37.26	0.26
5	114.89	114.60	0.29	0.00	0.02	96.72	0.13	17.90	0.12
6	328.87	327.99	0.88	0.00	0.06	274.94	0.31	52.08	1.48
7	39.42	39.32	0.10	0.00	0.01	33.21	0.53	5.60	0.07
8	71.05	70.87	0.18	0.00	0.01	59.64	0.12	11.01	0.27
9	936.20	932.19	4.01	0.00	0.30	753.56	11.57	165.76	5.01
10	1,985.63	1,977.17	8.46	0.00	0.61	1,596.48	8.41	359.24	20.89
11	422.90	421.04	1.86	0.00	0.14	337.37	5.22	74.60	5.57
12	8,918.51	7,726.29	1,192.22	0.00	128.19	6,220.33	217.77	2,306.06	46.16
13	175.32	174.61	0.71	0.00	0.05	137.99	1.16	33.80	2.32
14	6,131.71	5,780.06	351.65	0.00	33.16	4,447.07	732.32	898.91	20.25
15	174.59	173.93	0.66	0.00	0.05	142.32	3.09	26.44	2.69
16	1,733.95	1,723.28	10.67	0.00	0.79	1,337.19	182.76	208.01	5.20
17	160.03	159.31	0.72	0.00	0.05	128.69	3.83	25.55	1.91
18	3,097.89	3,058.66	39.23	0.00	3.02	2,346.68	58.51	659.65	30.03
19	645.24	642.09	3.15	0.00	0.23	491.61	15.17	136.60	1.63
20	236.36	235.47	0.89	0.00	0.06	182.27	0.77	52.30	0.96
21	37.60	37.48	0.12	0.00	0.01	31.73	0.42	5.04	0.40
22	157.55	157.07	0.48	0.00	0.04	132.74	1.42	22.00	1.35
23	1,248.21	1,242.42	5.79	0.00	0.40	997.31	10.89	230.01	9.60
24	125.12	124.73	0.39	0.00	0.03	106.71	0.24	16.08	2.06
25	248.81	247.92	0.89	0.00	0.06	205.52	0.41	38.87	3.95

Table 8B. Summary of INFILv3 simulated water-balance results for urban-area modified conditions in the San Gorgonio Pass area, Riverside County, California, 1930–2001—Continued.

INFILv3 modeled area name or upstream sub-drainage basin identifier	Urban-area modified conditions (acre-feet/year)								
	Inflows				Outflows				Change in root-zone storage
	Total preci- pitation	Rainfall	Snowfall	Surface water inflow	Subli- mation	Evapotrans- piration	Surface water outflow	Recharge	
26	359.19	357.80	1.39	0.00	0.09	293.58	0.51	59.46	5.55
27	908.50	904.17	4.33	0.00	0.30	728.62	2.18	163.57	13.83
28	644.47	642.39	2.08	0.00	0.14	524.75	2.55	113.90	3.13
Total upstream area	30,933.82	29,296.88	1,636.94	0.00	168.18	23,253.92	1,281.13	6,033.93	196.66
Beaumont and Banning Storage Units	21,453.97	21,400.87	53.10	1281.13	3.85	17,624.51	529.38	4,301.42	275.94
Total area hav- ing potential to affect Beaumont and Banning storage units	52,387.79	50,697.75	1,690.04	0.00	172.03	40,878.43	529.38	10,335.35	472.60

The simulated ground-water recharge in all the upstream sub-drainage basins is likely a high estimate of actual ground-water recharge because INFILv3 does not simulate ground-water discharge once the infiltrated water has percolated below the zone of evapotranspiration. In some areas, low-permeability layers may cause perched water table conditions where water could spread laterally and discharge to springs or move to areas that lie in the zone of evapotranspiration. This might be especially true for steep mountain drainage basins underlain by low-permeability bedrock, such as in the sub-drainage basins upstream of the ground-water storage units. In addition, INFILv3 does not simulate natural ground-water discharge from the saturated zone. In some basins, the recharged ground water will discharge to the surface as baseflow in stream channels or as spring flow. An unknown quantity of this baseflow and spring flow could be lost to evapotranspiration rather than contributing to recharge in the downstream ground-water storage units.

The annual simulation results for the Little San Gorgonio Creek sub-drainage basin (sub-drainage 12) for water years 1930–2001 are presented in *figure 22A*, and demonstrate the high degree of year-to-year variability typical in the simulated components of the water balance in the upstream sub-drainage basins. Simulated surface-water outflow had the highest degree of variability, with most years having no streamflow. The long-term 1930–2001 simulated average recharge was 6.3 in/yr (*fig. 22B*), with recharge rates for most years below the long-term average recharge rate. Only 21 of the 72 water years had simulated annual recharge rates greater than the long-term average recharge rate (*fig. 22B*). The 10-year moving average recharge rate indicates the simulation period is characterized by 3 periods of higher than average recharge (1940–50, 1978–88, and 1997–2001) and one period of prolonged below-average recharge (1951–74) (*fig. 22B*). Wetter-than-average years were less frequent than drier-than-average years, and wetter-than-average periods tended to have shorter durations than drier-than-average periods.



Base from U.S. Geological Survey digital data, 1:100,000, 1981-89; Universal Transverse Mercator Projection (NGVD 29), Zone 11.

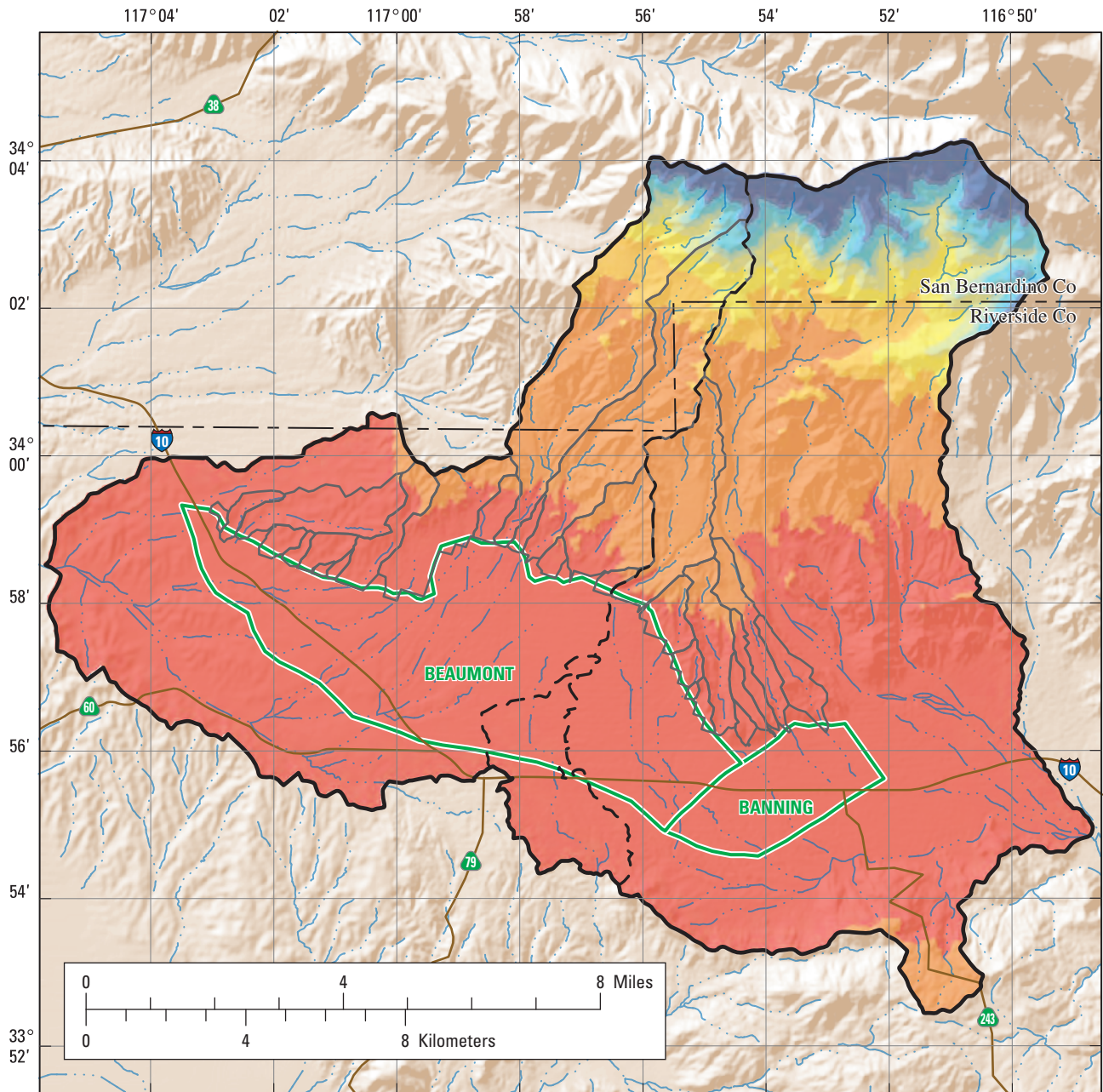
EXPLANATION

Precipitation simulated with INFILv3, in inches per year

14 to 14.99	19 to 20.99	25 to 26.99
15 to 16.99	21 to 22.99	27 to 28.99
17 to 18.99	23 to 24.99	29 to 30.99
		31 to 34

- Ground-water storage unit and name
- INFILv3 model boundary
- INFILv3 modeled upstream sub-drainage basins
- Surface-water drainage basins

Figure 17. Map showing average annual precipitation simulated by the INFILv3 model of the San Gorgonio Pass area, Riverside County, California.



Base from U.S. Geological Survey digital data, 1:100,000, 1981-89;
 Universal Transverse Mercator Projection (NGVD 29), Zone 11.

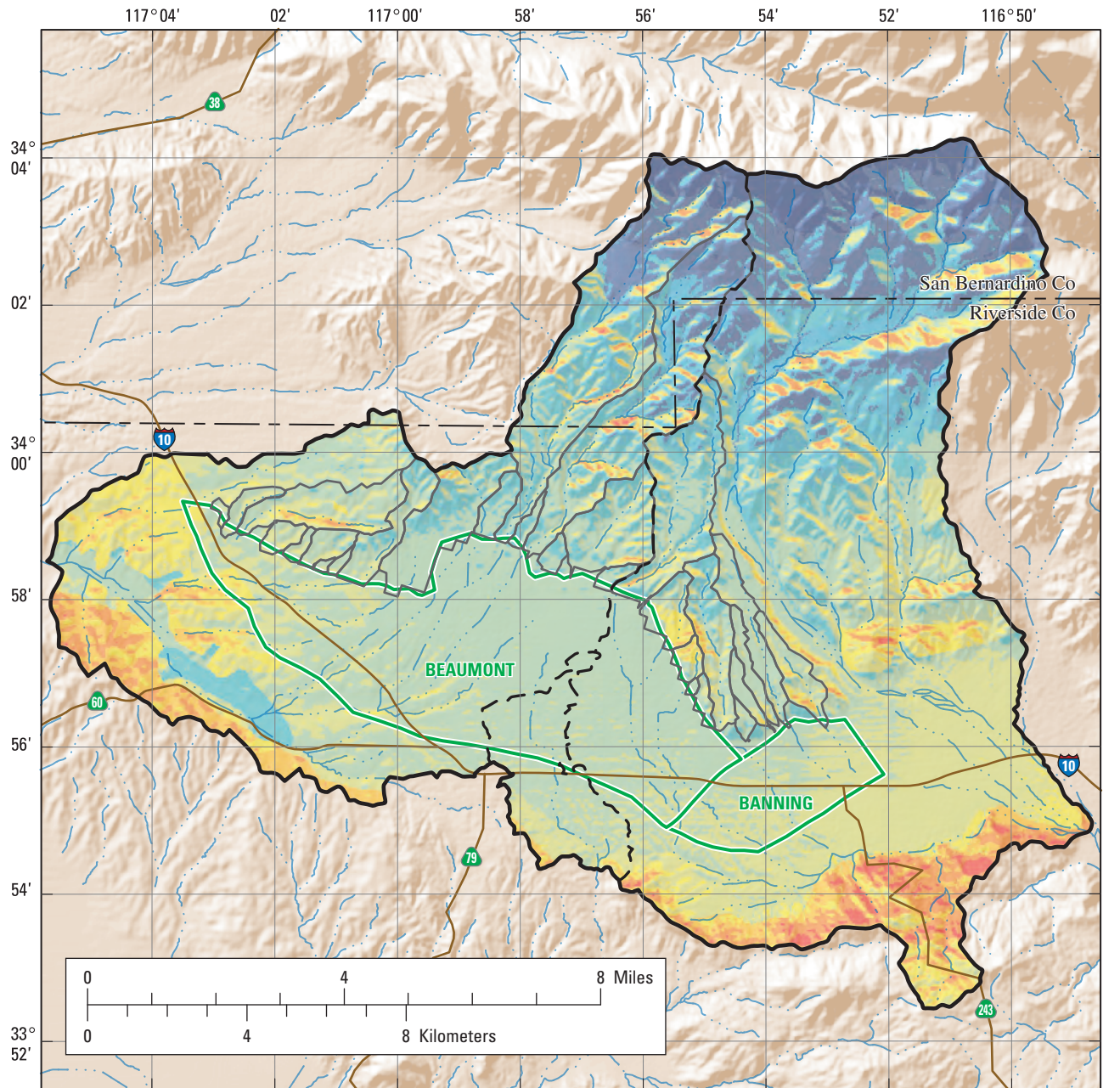
EXPLANATION

Snowfall simulated with INFILv3, in inches per year

<table border="0"> <tr> <td style="background-color: #e31a1c; width: 20px; height: 15px; display: inline-block;"></td> <td style="padding-left: 5px;">0.01 to 0.09</td> <td style="background-color: #ffff00; width: 20px; height: 15px; display: inline-block;"></td> <td style="padding-left: 5px;">2 to 3.99</td> <td style="background-color: #00b0f0; width: 20px; height: 15px; display: inline-block;"></td> <td style="padding-left: 5px;">8 to 9.99</td> </tr> <tr> <td style="background-color: #f4a460; width: 20px; height: 15px; display: inline-block;"></td> <td style="padding-left: 5px;">0.1 to 0.99</td> <td style="background-color: #c1e1c1; width: 20px; height: 15px; display: inline-block;"></td> <td style="padding-left: 5px;">4 to 5.99</td> <td style="background-color: #0099cc; width: 20px; height: 15px; display: inline-block;"></td> <td style="padding-left: 5px;">10 to 11.99</td> </tr> <tr> <td style="background-color: #fde725; width: 20px; height: 15px; display: inline-block;"></td> <td style="padding-left: 5px;">1 to 1.99</td> <td style="background-color: #8bc34a; width: 20px; height: 15px; display: inline-block;"></td> <td style="padding-left: 5px;">6 to 7.99</td> <td style="background-color: #3959ab; width: 20px; height: 15px; display: inline-block;"></td> <td style="padding-left: 5px;">12 to 13.99</td> </tr> <tr> <td></td> <td></td> <td></td> <td></td> <td style="background-color: #21468b; width: 20px; height: 15px; display: inline-block;"></td> <td style="padding-left: 5px;">14 to 26</td> </tr> </table>		0.01 to 0.09		2 to 3.99		8 to 9.99		0.1 to 0.99		4 to 5.99		10 to 11.99		1 to 1.99		6 to 7.99		12 to 13.99						14 to 26	
	0.01 to 0.09		2 to 3.99		8 to 9.99																				
	0.1 to 0.99		4 to 5.99		10 to 11.99																				
	1 to 1.99		6 to 7.99		12 to 13.99																				
					14 to 26																				

- ▭ Ground-water storage unit and name
- INFILv3 model boundary
- INFILv3 modeled upstream sub-drainage basins
- Surface-water drainage basins

Figure 18. Map showing average annual snowfall simulated by the INFILv3 model of the San Geronimo Pass area, Riverside County, California.



Base from U.S. Geological Survey digital data, 1:100,000, 1981-89; Universal Transverse Mercator Projection (NGVD 29), Zone 11.

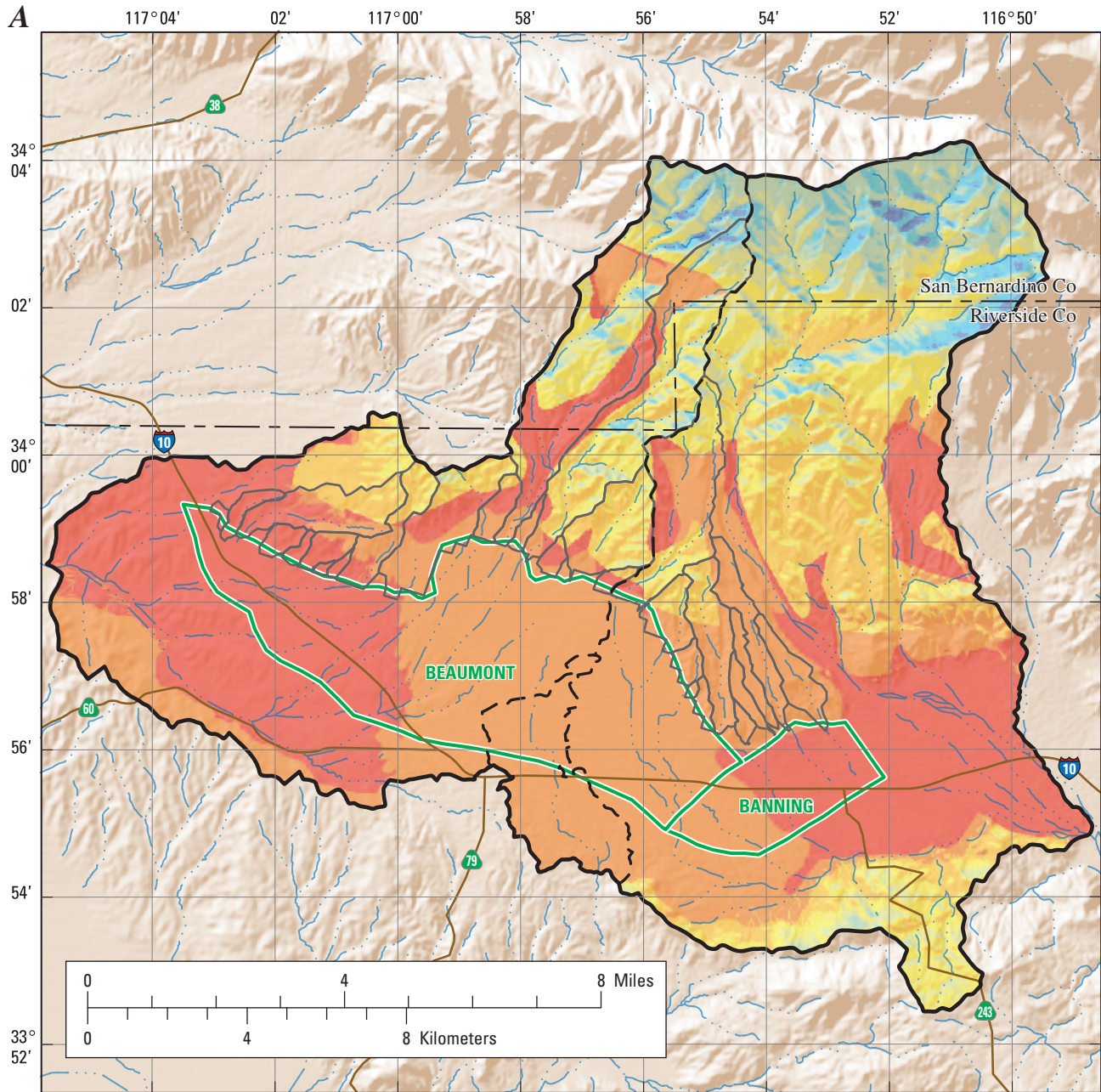
EXPLANATION

Evapotranspiration simulated with INFILv3, in inches per year

7 to 9.99	13 to 13.99	16 to 16.99
10 to 11.99	14 to 14.99	17 to 17.99
12 to 12.99	15 to 15.99	18 to 19.99
		20 to 24

- Ground-water storage unit and name
- INFILv3 model boundary
- INFILv3 modeled upstream sub-drainage basins
- Surface-water drainage basins

Figure 19. Map showing average annual evapotranspiration simulated by the INFILv3 model of the San Gorgonio Pass area, Riverside county, California.



Base from U.S. Geological Survey digital data, 1:100,000, 1981-89; Universal Transverse Mercator Projection (NGVD 29), Zone 11.

EXPLANATION

Runoff simulated with INFILv3, in inches per year

0 to 0.09	4 to 5.99	10 to 11.99
0.1 to 1.99	6 to 7.99	12 to 13.99
2 to 3.99	8 to 9.99	14 to 15.99
		16 to 18.5

- Ground-water storage unit and name
- INFILv3 model boundary
- INFILv3 modeled upstream sub-drainage basins
- Surface-water drainage basins

Figure 20. Map showing average annual runoff simulated by the INFILv3 model for (A) natural conditions and (B) the difference in simulated net runoff between urban-modified and natural conditions, San Gorgonio Pass area, Riverside County, California.

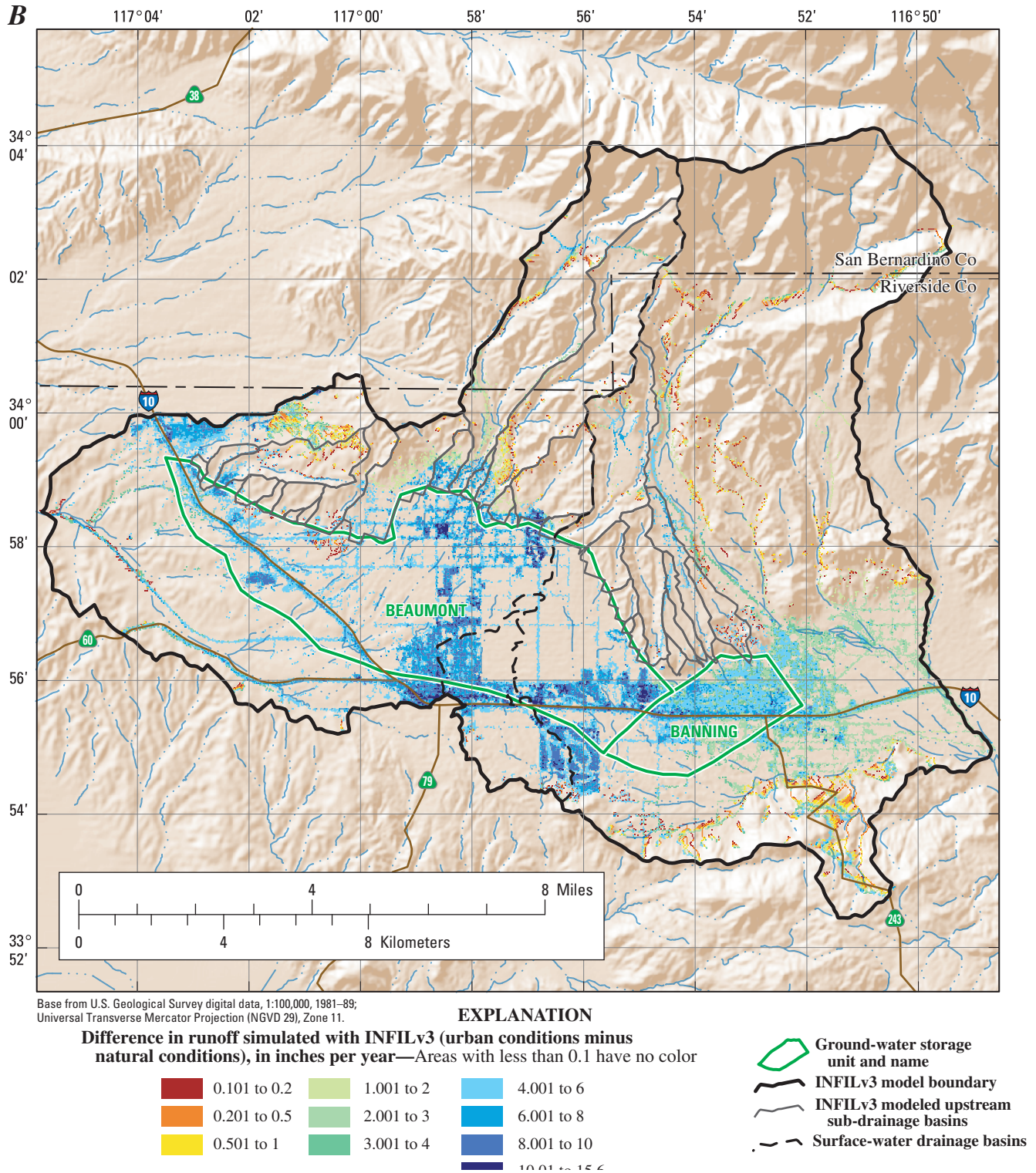
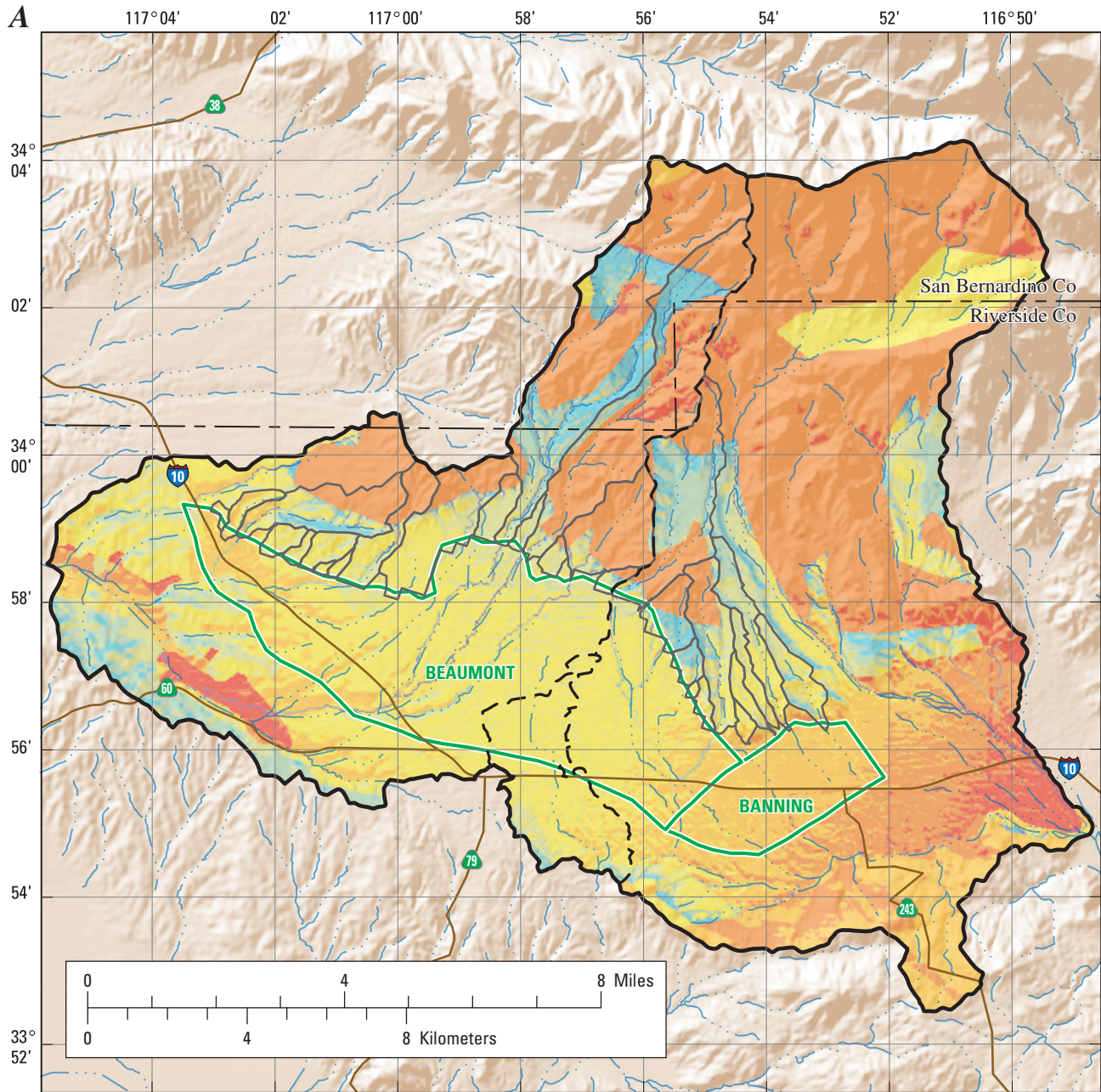


Figure 20. Continued.



Base from U.S. Geological Survey digital data, 1:100,000, 1981-89; Universal Transverse Mercator Projection (NGVD 29), Zone 11.

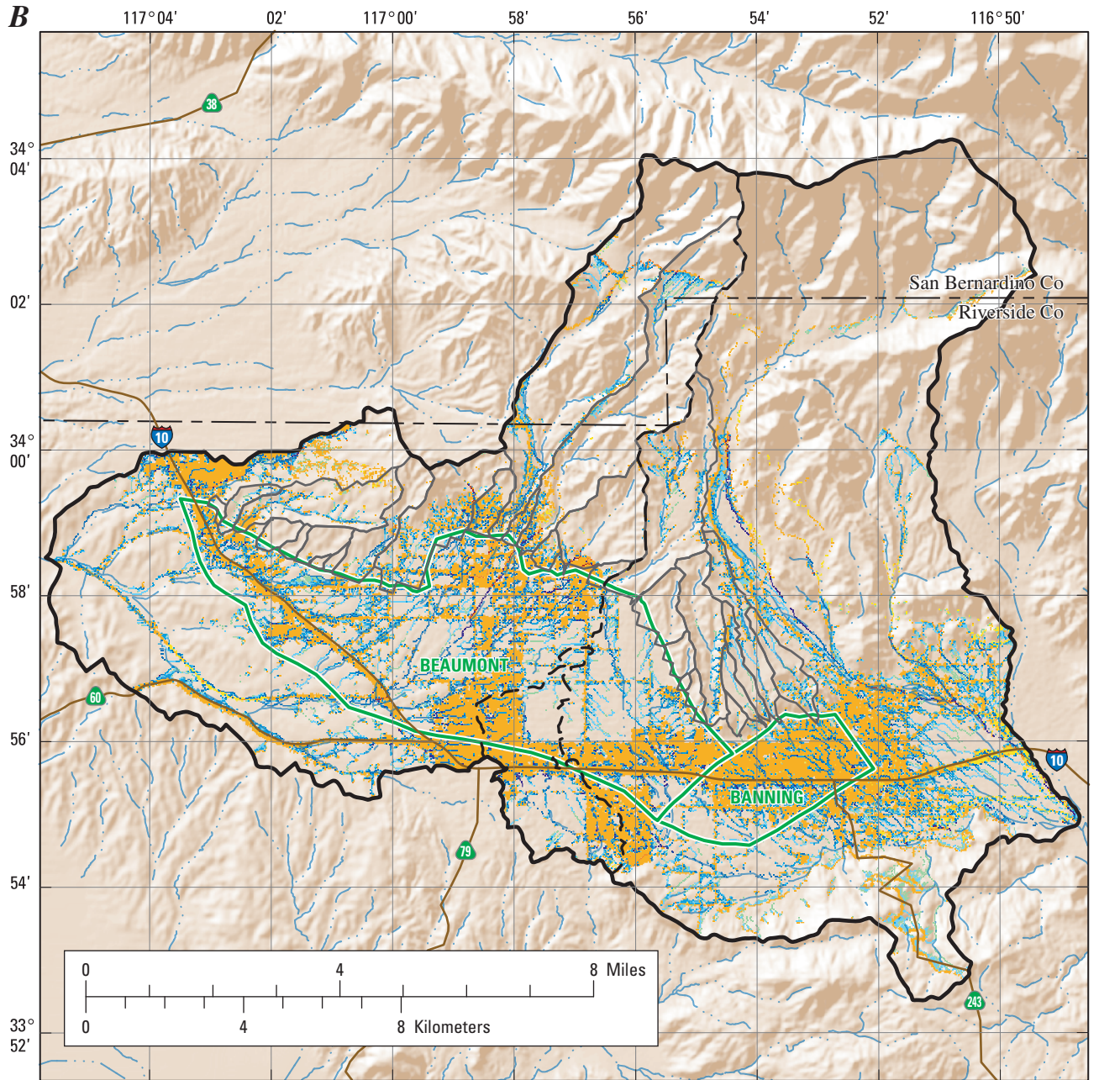
EXPLANATION

Net infiltration simulated with INFILv3, in inches per year

0 to 0.49	2 to 2.99	5 to 9.99
0.5 to 0.99	3 to 3.99	10 to 19.99
1 to 1.99	4 to 4.99	20 to 49.99
		50 to 2,878

- Ground-water storage unit and name
- INFILv3 model boundary
- INFILv3 modeled upstream sub-drainage basins
- Surface-water drainage basins

Figure 21. Map showing average annual net infiltration simulated by the INFILv3 model for (A) natural conditions and (B) the difference in simulated average annual net infiltration between urban-area modified and natural conditions, San Geronio Pass area, Riverside County, California.



Base from U.S. Geological Survey digital data, 1:100,000, 1981-89; Universal Transverse Mercator Projection (NGVD 29), Zone 11.

EXPLANATION

Difference in net infiltration simulated with INFILv3 (urban conditions minus natural conditions), in inches per year—Areas with values -0.009 to 0.01 have no color

Dark Red	-2,472 to -50	Yellow	-0.499 to -0.05	Light Green	0.011 to 0.05	Light Blue	0.501 to 5
Orange	-49 to -5	Light Yellow	-0.049 to -0.01	Medium Blue	0.051 to 0.5	Dark Blue	5.001 to 50
Dark Orange	-4.9 to -0.5			Dark Blue	50.001 to 442		

- Ground-water storage unit and name
- INFILv3 model boundary
- INFILv3 modeled upstream sub-drainage basins
- Surface-water drainage basins

Figure 21. Continued.

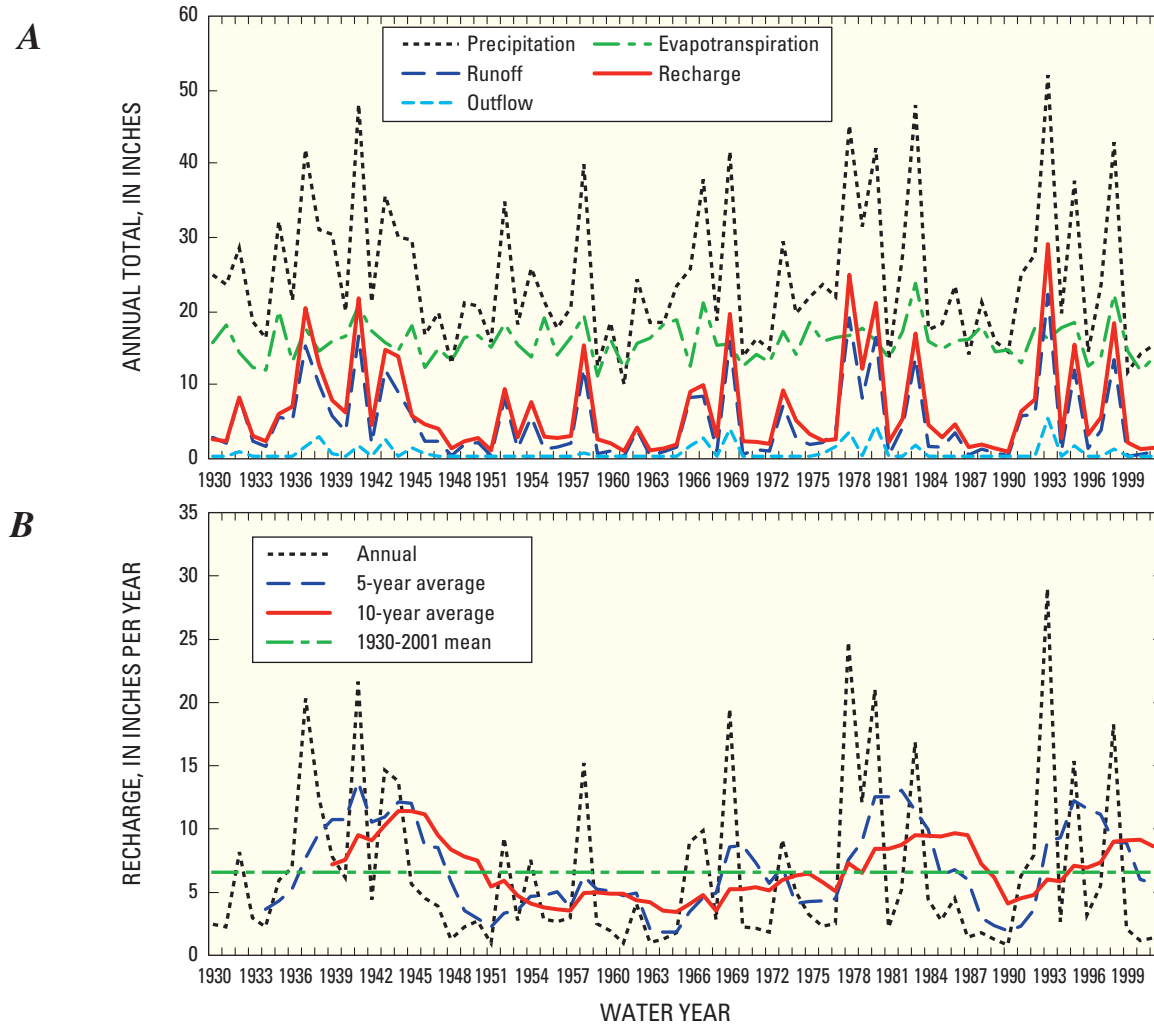


Figure 22. Graphs showing the annual precipitation, runoff, outflow, evapotranspiration, and recharge simulated by the INFILv3 model for Little San Gorgonio Creek sub-drainage basin, San Gorgonio Pass area, Riverside County,

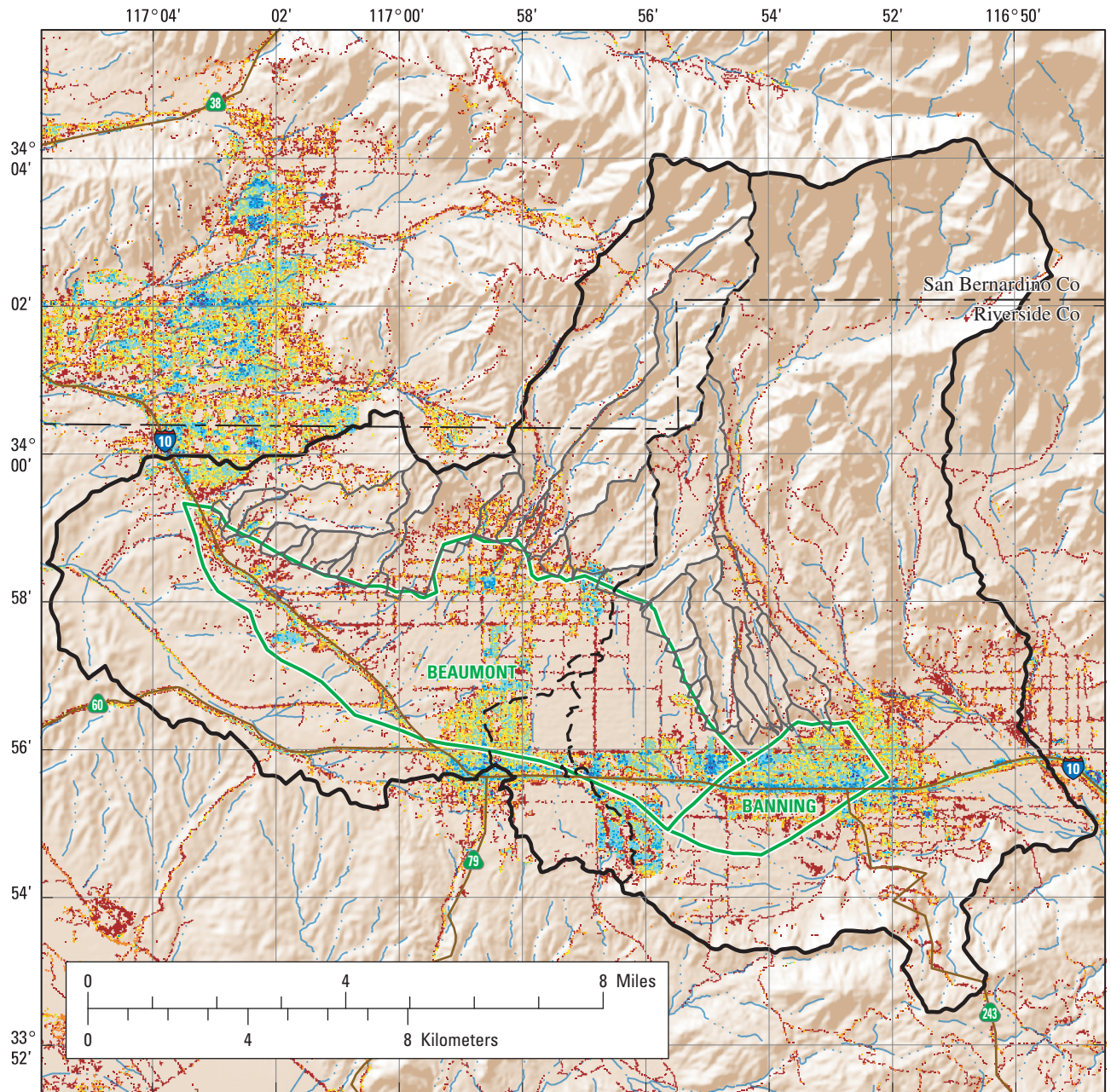
Effects of Urbanization on Simulated Average Annual Ground-Water Recharge and Surface-Water Outflow

A modified version of the INFILv3 model was developed to determine the effect of urbanization on simulated average annual ground-water recharge and surface-water outflow in the study area. The modified version of the model is referred to in this report as the urban-area model. The dominant change in model input parameters affected by urbanization is the reduction in the simulated soil hydraulic conductivity due to an increase in the percentage of the land surface area covered by relatively impervious engineered surfaces (mainly roads, buildings, and parking lots). The impervious surfaces can potentially increase runoff from rainfall and snowmelt. The effect of urbanization on recharge and surface-water outflow is dependent on the soil properties downstream of the locations where the increased runoff is generated. For example, if runoff from rooftops and parking lots is routed directly to street gutters and concrete-lined storm drains, recharge is likely to decrease; whereas, surface-water outflow is likely to increase.

If runoff is routed directly to permeable areas (lawns, recharge basins, natural stream beds), recharge is likely to increase; otherwise, surface-water outflow may decrease.

Data Required to Simulate Urbanization Affects Using INFILv3

The USGS National Land Cover Data (NLCD) 2001 impervious-area map (U.S. Geological Survey, accessed May 16, 2005) was used to define the INFILv3 model cells affected by urbanization. The 2001 impervious area map was projected to the INFILv3 98.4-ft base grid. Each cell of the INFILv3 model grid was assigned an integer value of 0 to 99, representing the percentage of urbanization in each cell (*fig. 23*). Impervious-area values of 1 or greater occur for about 16 percent of INFILv3 model cells (*table 9*). The Beaumont and Banning storage units have about 38 percent of their modeled area affected by urbanization; whereas, the upstream sub-drainage basin only have about 8 percent of their modeled area affected by urbanization (*table 9*).



Base from U.S. Geological Survey digital data, 1:100,000, 1981-89; Universal Transverse Mercator Projection (NGVD 29), Zone 11.

EXPLANATION

Impervious area estimates used as input for INFILv3, in percent

1 to 8	28 to 37	54 to 61
9 to 17	38 to 45	62 to 69
18 to 27	46 to 53	70 to 78
		79 to 99

- Ground-water storage unit and name
- INFILv3 model boundary
- INFILv3 modeled upstream sub-drainage basins
- Surface-water drainage basins

Figure 23. Map showing impervious area simulated in the urban-area INFILv3 model of the San Gorgonio Pass area, Riverside County, California. (Modified from USGS National Land Cover Database-Zone 60 Imperviousness layer, accessed May 16, 2005; <http://seamless.usgs.gov>).

Table 9. Urbanization parameters for drainage basins and sub-drainage basins upstream of and including the Beaumont and Banning storage units modeled using INFILv3 for the San Gorgonio Pass area, Riverside County, California.

UNFILv3 modeled area name or upstream sub-drainage basin identifier	Modeled area (acres)	Urban- affected area (acres)	Model cells affected by urbanization (percent)	Average impervious area (percent)	Average urbanization factor (unitless)
Surface-water drainage basins					
Potrero Creek	2,548.6	951.6	37.3	11.1	0.64
San Timoteo Creek	30,774.0	5,065.0	16.5	3.31	0.84
San Gorgonio River	41,880.2	6,137.7	14.7	3.40	0.86
Totals	75,202.8	12,154.3	16.2	3.62	0.85
Surface-water sub-drainage basins upstream of the Beaumont and Banning storage units					
1	41.4	11.3	27.4	6.16	0.74
2	163.7	10.2	6.3	0.47	0.94
3	967.6	107.4	11.1	1.99	0.89
4	157.0	5.3	3.4	0.10	0.97
5	76.9	1.1	1.4	0.05	0.99
6	215.5	3.8	1.8	0.06	0.98
7	26.5	2.4	9.2	0.33	0.91
8	46.9	0.7	1.4	0.07	0.99
9	580.7	37.8	6.5	0.49	0.94
10	1,219.2	222.4	18.2	1.64	0.83
11	255.1	107.6	42.2	6.30	0.60
12	4,415.6	233.5	5.3	0.52	0.95
13	106.3	45.1	42.5	3.05	0.60
14	3,230.7	139.9	4.3	0.35	0.96
15	107.2	37.1	34.6	3.66	0.67
16	1,030.6	58.5	5.7	1.30	0.95
17	98.1	33.1	33.8	11.81	0.67
18	1,771.4	84.3	4.8	0.19	0.96
19	398.8	2.9	0.7	0.02	0.99
20	151.2	0.0	0.0	0.00	1.00
21	24.7	0.9	3.6	1.16	0.96
22	103.9	6.7	6.4	0.16	0.94
23	782.4	29.8	3.8	0.25	0.96
24	82.7	0.9	1.1	0.05	0.99
25	161.5	6.9	4.3	0.20	0.96
26	230.6	18.0	7.8	0.49	0.93
27	568.9	63.2	11.1	0.92	0.90
28	425.7	40.3	9.5	0.98	0.91
Total for upstream area	17,440.8	1,311.1	7.5	0.83	0.93
Beaumont and Banning storage units	14,427.2	5,405.5	37.5	10.18	0.64
Total for area having potential to affect Beaumont and Banning storage units	31,868.0	6,716.6	21.1	5.06	0.80

The saturated hydraulic conductivity values of soil layer 1 in model cells with 1 to 99 percent impervious area were decreased by multiplying the previously calibrated saturated soil hydraulic conductivities (*table 3*) by an urbanization factor. The urbanization factor is defined for this study as

$$U = (100-IA)/1,000$$

where

- U is the urbanization factor and
- IA is an integer value representing the percentage of impervious area (*fig. 23*).

For IA values of 0, U was set to 1.0 (soil hydraulic conductivity was left unchanged). In defining U, an assumption was made to reduce the saturated soil hydraulic conductivity by at least one order of magnitude for all model grid cells affected by urbanization. For example, if a model cell in an area with a STATSGO soil code of CA609 (*fig. 13*) and a calibrated saturated soil hydraulic conductivity of 1.38×10^{-4} ft/s has an IA of 1 (1 percent impervious area), the U would equal 9.9×10^{-2} , resulting in a hydraulic conductivity of 1.37×10^{-5} ft/s for the urbanization simulation. If the same model cell has an IA of 99 (99 percent impervious area), the U would equal 1.0×10^{-3} , resulting in a hydraulic conductivity of 1.38×10^{-7} ft/s for the urbanization simulation. The hydraulic conductivity of concrete ranges from 2.73×10^{-11} to 8.56×10^{-13} ft/s (Cement Association of Canada, 2005), indicating that the lowest saturated soil hydraulic conductivity simulated is at least four orders of magnitude larger than the values reported for concrete.

Urban-Area INFILv3 Model Results

The urban-area INVILv3 model was used to simulate net infiltration (recharge) for water years 1927–2001 using the same initial conditions and simulation period (1930–2001) as the INVILv3 model developed assuming natural conditions. It was assumed that the urbanization represented by the 2001 impervious area map (*fig. 23*) is constant for the entire simulation period. Although the time-dependent urban-area impact during the simulation period is not represented by this simplifying assumption, the results are representative of a possible upper bound (or maximum impact) indicator for urban-area effects.

The simulated water budget for the urban-area INFILv3 model is presented in *table 8B*. Recharge and surface-water outflow simulated by the urban-area model for the Potrero Creek, San Tiomoteo Creek, and San Gorgonio River surface-water drainage basins are about 21,740 and 4,650 acre-ft/yr, respectively. The urban-area model simulated recharge and surface-water outflow are about 500 and 750 acre-ft/yr higher, respectively, compared with that simulated assuming natural conditions. Average annual simulated recharge increased by about 150 and 380 acre-ft/yr in the Potrero Creek and San Tiomoteo Creek surface-water drainage basins, respectively,

and decreased slightly, by about 30 acre-ft/yr, in the San Gorgonio River surface-water drainage basin. Recharge and surface-water outflow simulated for the Beaumont and Banning storage units by the urban-area model are about 4,300 and 530 acre-ft/yr, respectively. The urban-area model simulated recharge is about 600 acre-ft/yr higher and the simulated surface-water runoff is about 300 acre-ft/yr lower compared with that simulated assuming natural conditions. Recharge and surface-water outflow simulated for the upstream sub-drainage basins by the urban-area model are about 6,030 and 1,280 acre-ft/yr, respectively. The urban-area model simulated recharge is about 150 acre-ft/yr lower and the simulated surface-water outflow is about 190 acre-ft/yr higher compared with that simulated assuming natural conditions.

The urban-area model simulates an increase in the spatial variability of runoff and recharge. *Figure 20B* shows the difference in simulated runoff between the urban-area model and the natural conditions model. The results indicate that for all locations affected by urbanization and the corresponding impact of impervious areas, there is an increase in simulated runoff. Urbanization has resulted in localized areas with increased simulated runoff of as much as 10 to 15.6 in/yr (*fig. 20B*). For most areas within the Beaumont and Banning storage unit, increases in runoff due to urbanization range from 3 to 8 in/yr (*fig. 20B*).

Figure 21B shows the difference in simulated recharge between the urban-area model and the natural conditions model. The results indicate some areas have less simulated recharge while others have more. The areas with decreased recharge due to urbanization cover a greater percentage of the model area compared to areas with increased recharge due to urbanization (*fig. 21B*). The decrease in simulated recharge is the result of a decrease in direct recharge from infiltrating rain and snowmelt; the differences range from about 0 to more than 2,400 in/yr with the greatest frequency in the 0.5 to 4.9 in/yr (*fig. 21B*). The greatest decrease in recharge due to urbanization (50 to 2,472 in/yr) occurs over a very small area and is the result of impervious areas affecting major stream channels (Little San Gorgonio Creek and Noble Creek). Simulated recharge increases along most stream channels downstream of urban areas, which have the greatest runoff, with maximum increases ranging from 5 to 442 in/yr (*fig. 21B*).

INFILv3 Model Limitations

A primary limitation of the INFILv3 model applied in this study is the uncertainty in model calibration using simulated versus measured streamflow. Only a single stream gage record with adequate length of record was available for calibration, and the area upstream of the stream gage is only a small percentage of the total area modeled using INFILv3. In addition, the length of the streamflow record does not span the full simulation period.

The water-balance method used in the INFILv3 model has many simplifying assumptions concerning the physics of unsaturated ground-water flow. For example, the water-balance calculations assume that the process of vapor flow and the effects of temperature on water density are negligible. Constant water density allows the governing equations in the water-balance model to be applied as a volume balance rather than as a mass balance. In each grid cell of the model domain, water was assumed to move vertically downward through soil and bedrock; lateral flow in the subsurface between grid cells was assumed to be negligible. Recharge was assumed to occur as gravity drainage under a unit gradient. The effect of capillary forces on unsaturated flow in the root zone was not included in the model.

The INFILv3 model simulates the streamflow component originating as surface runoff, but it does not simulate the base flow component of streamflow. Base flow originates as ground-water discharge and (or) through-flow from perched zones. A major assumption applied in INFILv3 is that surface runoff, generated in response to rainfall or snowmelt, is the primary component of streamflow measured in the study area. In addition, simulation of daily streamflow is based on a daily routing algorithm that assumes episodic streamflows with durations less than 24 hours. Simulated streamflow either discharges from the drainage basin or infiltrates into the root zone at the end of each day. Temporary perched ground-water systems, which may be important sources of base flow and spring discharge at higher altitudes, are not represented by the INFILv3 model. In addition, dispersive streamflow (divergent as opposed to convergent streamflow), which can be an important characteristic of streamflow and overland flow across alluvial fans and basins with braided channels, is not directly represented in the surface-water flow-routing algorithm. All surface-water flow is simulated as convergent streamflow. These limitations in simulating surface-water flow may result in an overestimation of recharge in some parts of the study area, particularly in the higher-altitude sub-drainage basins.

Additional sources of model uncertainty include the values of model input parameters such as the hydraulic conductivity of bedrock, soil thickness, soil-hydrologic properties, parameters used to define stream-channel characteristics, root-zone depth, root density as a function of depth, and the assumed constant durations (in hours) for winter precipitation and streamflow, summer precipitation and streamflow, and snowmelt.

Summary of INFILv3 Results

The INFILv3 results indicate that, on average, the total potential ground-water recharge in the Beaumont and Banning storage units for natural conditions is 9,890 acre-ft/yr, which is the sum of recharge simulated in the Beaumont and Banning storage units (about 3,710 acre-ft/yr) and in the 28 upstream

sub-drainage basins (about 6,180 acre-ft/yr). This total potential ground-water recharge volume assumes that all recharge simulated in the upstream sub-drainage basins is available downstream (to the area of the Beaumont and Banning storage units) as ground-water underflow and baseflow. However, because INFILv3 does not simulate ground-water discharge once the infiltrated water has percolated below the zone of evapotranspiration, the estimated recharge in the upstream sub-drainage basins is probably too high due to the hydro-geologic conditions in those areas. Therefore, on the basis of the INFILv3 results, total potential ground-water recharge for the Beaumont and Banning storage units is estimated to range from 3,710 to 9,890 acre-ft/yr.

Incorporation of an assumed decrease in ground-surface (soil) permeability (saturated hydraulic conductivity) caused by urbanization into the INFILv3 model results in an increase in simulated runoff from the urbanized areas and an increase in simulated recharge in areas downstream of the urbanized areas. In the Beaumont and Banning storage units the increase in simulated average annual recharge is about 600 acre-ft/yr and the increase in surface-water outflow is about 300 acre-ft/yr. The urban-area model probably overestimates the effects of urbanization on average annual recharge and surface-water outflow because the urbanized area as represented by the 2001 impervious area map was assumed to represent the land-use conditions throughout the simulation period (1930–2001).

Natural Discharge

Prior to development of the ground water in the Beaumont and Banning storage units, ground water discharged from the Beaumont storage unit as baseflow into stream channels and ground-water underflow into the San Timoteo storage unit and as ground-water underflow from the Banning storage unit into the Cabazon storage unit. Bloyd (1971) reported that flowing wells and springs were present in the San Timoteo storage unit in 1926–27, prior to significant ground-water development. The flowing wells and springs were present along stream channels that flow across the San Timoteo Canyon Fault into the San Timoteo storage unit (*fig. 24*). Bloyd (1971) did not estimate the quantity of ground water discharged by the flowing wells and springs; however, he estimated that the steady-state ground-water underflow from the Beaumont storage unit to the Banning storage unit was 5,000 acre-ft/yr, and ground-water underflow from the San Timoteo Creek surface-water drainage basin (includes ground-water underflow from the Beaumont and San Timoteo storage units and ground-water underflow from the ground-water basins underlying the Yucaipa and Calimesa areas to the northwest) to downstream basins was 6,000 acre-ft/yr.

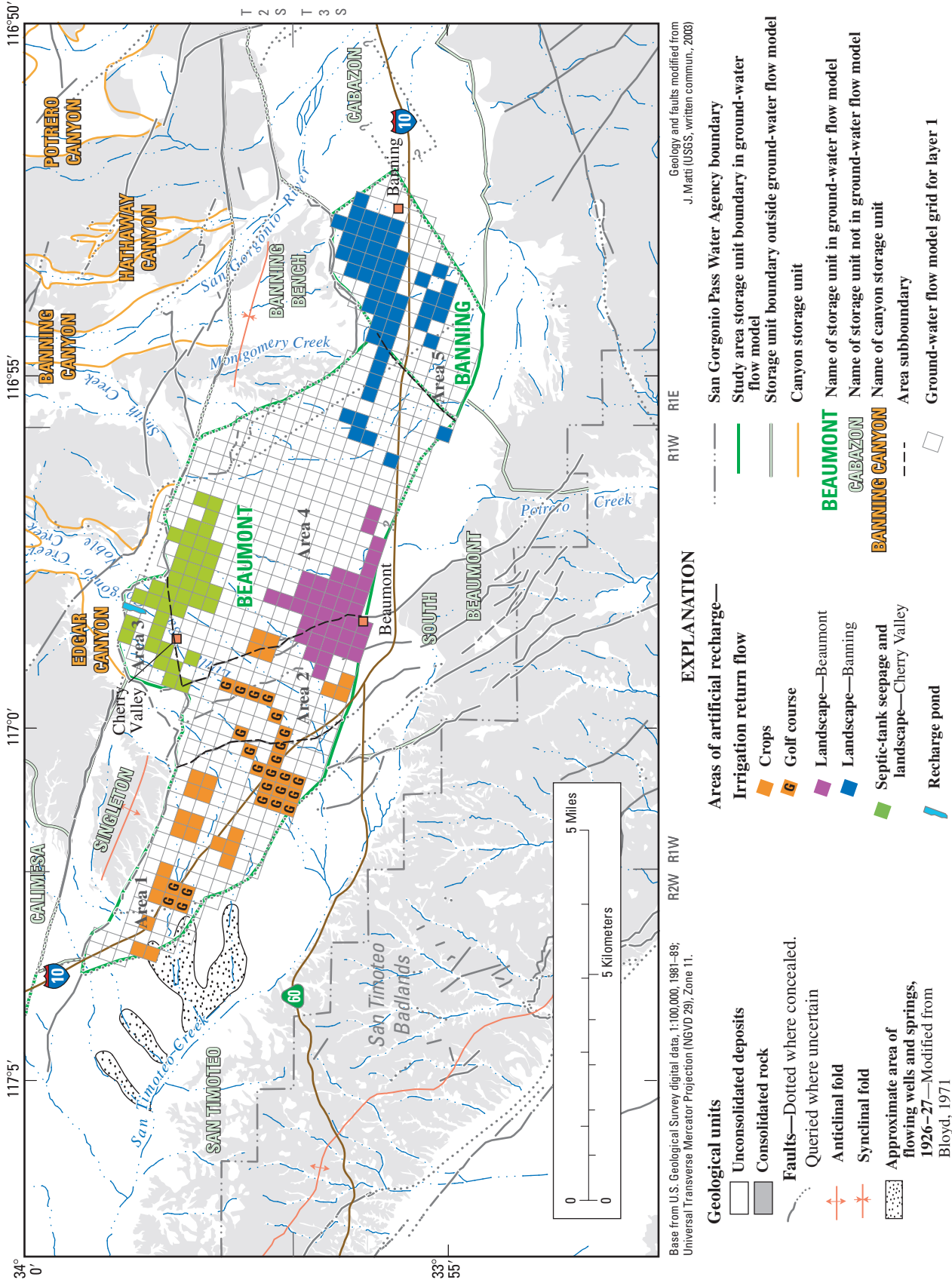


Figure 24. Map showing approximate areas of flowing springs and wells during 1926–27 and areas of artificial recharge from septic-tank seepage, irrigation return flow from the irrigation of crops, golf courses, and landscape in the San Gorgonio Pass area, Riverside County, California.

Boyle Engineering Corporation (1995) used a steady-state ground-water flow model to estimate ground-water underflow out of the Beaumont storage unit for three different estimates of ground-water recharge [low (9,110 acre-ft/yr), medium (10,610 acre-ft/yr), and high (11,610 acre-ft/yr)]. The model simulated that the quantity of ground-water underflow ranged from 3,000 to 5,500 acre-ft/yr with about 70 percent of the total ground-water underflow from the Beaumont storage unit discharging into the Banning storage unit and about 30 percent discharging into the San Timoteo storage unit.

Ground-Water Pumpage

The water supply for agricultural and municipal uses in the Beaumont and Banning storage units is supplied by pumping ground water from wells in the Canyon (Edgar and Banning Canyons), Banning Bench, Beaumont, and Banning storage units. Ground-water development in the study area probably started in the late 1800s but was not recorded until the late 1920s. Ground-water pumping in the Edgar and Banning Canyon storage units does not directly affect water levels in the Beaumont and Banning storage units; however, it does indirectly affect water levels by reducing the amount of ground-water underflow from the upstream canyon storage units that can recharge the downstream Beaumont and Banning storage units. Water delivered to the Beaumont and Banning storage units from the Canyon and Banning Bench storage units also can be a source of artificial recharge (return flow from applied water on crops, golf courses, and landscape and septic-tank seepage) to the Beaumont and Banning storage units.

Ground-water pumpage was compiled for 1927–2003 for this study (*Appendix table 3*). The total annual pumpage from the Beaumont and Banning storage units ranged from a low of about 1,630 acre-ft in 1936 to a high of about 20,000 acre-ft in 2003 (*Appendix table 3*). Sources of pumpage data included SGPWA; Beaumont-Cherry Valley Water District (BCVWD); City of Banning Water Company; Sunny Cal Egg and Poultry; California Department of Water Resources (CADWR); and the Water Resources Institute, California State University, San Bernardino, Archives [<http://wri.csusb.edu/web/pages/archives/index.htm>]. *Figure 25* shows the total pumpage by area for the Beaumont and Banning storage units. The figure also shows the pumpage by the BCVWD from the Beaumont (areas 3 and 4) and Edgar Canyon storage units and the pumpage by the City of Banning Water Company from the Beaumont (area 4) and Banning (area 5) storage units and the Banning Bench and Banning Canyon storage units.

From 1947 through 2003, pumpage by well was reported on an annual basis (*Appendix table 3*). Prior to 1947, only total pumpage was available by storage unit, except for the Beaumont storage unit, for which annual pumpage values were

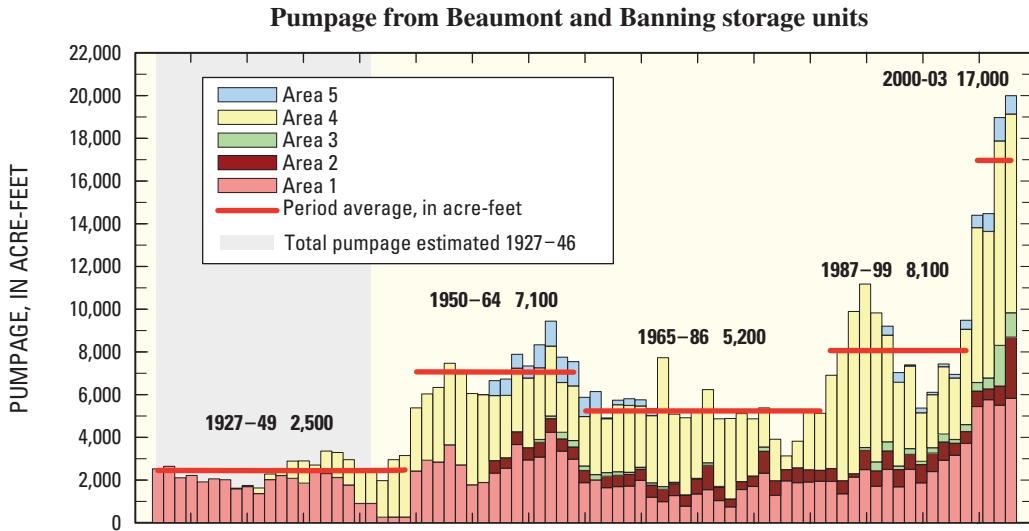
available for the Moreno Mutual Irrigation Company wells. The amount of ground water pumped from the Moreno Mutual Irrigation Company well field was reported by well (California Department of Water Resources, 1947) (*Appendix table 3*). All ground water pumped from this well field was exported from the Beaumont storage unit for agricultural use in San Jacinto (California Department of Water Resources, 1947). Pumpage by well for 1927 through 1946 was estimated for this study (*Appendix table 3*). If a well was drilled during this period and had reported pumpage in 1947, the pumpage reported for 1947 was assumed representative of pumpage from this well from the date it was drilled until 1947. Annual pumpage for the remaining wells was estimated by equally distributing the remaining reported annual pumpage to active wells. A production well was assumed active for a particular year if well records indicate that the well existed during that year.

Artificial Recharge

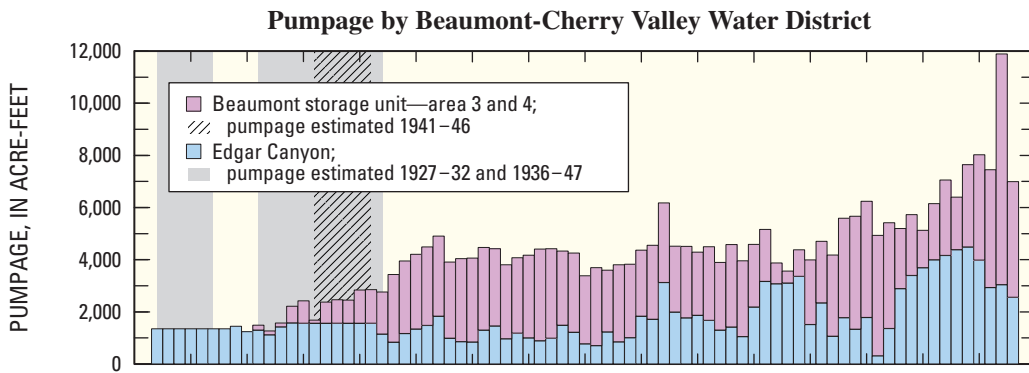
Since ground-water development began in the San Geronio Pass area, there have been several sources of artificial recharge to the basin, including return flow from water applied on crops, golf courses, and landscape; septic-tank seepage; infiltration of diverted storm runoff from Little San Geronio Creek; and imported SWP water into recharge ponds. The estimated annual rates of artificial recharge applied at land surface from 1927–2003 are shown in *figure 26* and range from about 420 acre-ft in 1927 to about 8,100 acre-ft in 2003.

Artificial recharge may require decades to reach the water table because of the thickness of the unsaturated zone in most of the study area (150 to 465 ft). A numerical model of the unsaturated zone in area 3 simulated that septic-tank seepage moved downward through the unsaturated zone at a rate of about 6.6 ft/yr (Flint and Ellet, 2004). Assuming that the simulated seepage rate is representative for the entire model domain and the thickness of the unsaturated zone averages about 150 ft in area 1; 265 ft in area 2; 470 ft in area 3; 365 ft in area 4; and 340 ft in area 5, the estimated travel time for artificial recharge to reach the water table is 23 years in area 1; 40 years in area 2; 71 years in area 3; 55 years in area 4; and 52 years in area 5. For example, the return flow of applied irrigation water to crops in area 1 in 1950 is estimated to recharge the underlying aquifer in 1973. Consequently, only about 37,000 acre-ft of the artificial recharge applied at land surface during 1927–2003 is estimated to reach the water table by 2003, significantly less than the estimated 224,000 acre-ft of artificial recharge that was applied at land surface during this period (*fig. 26 C and D*). Artificial recharge that was applied at land surface during 1927–2003 is estimated to finally all reach the water table by 2074 (*fig. 26 D*).

A



B



C

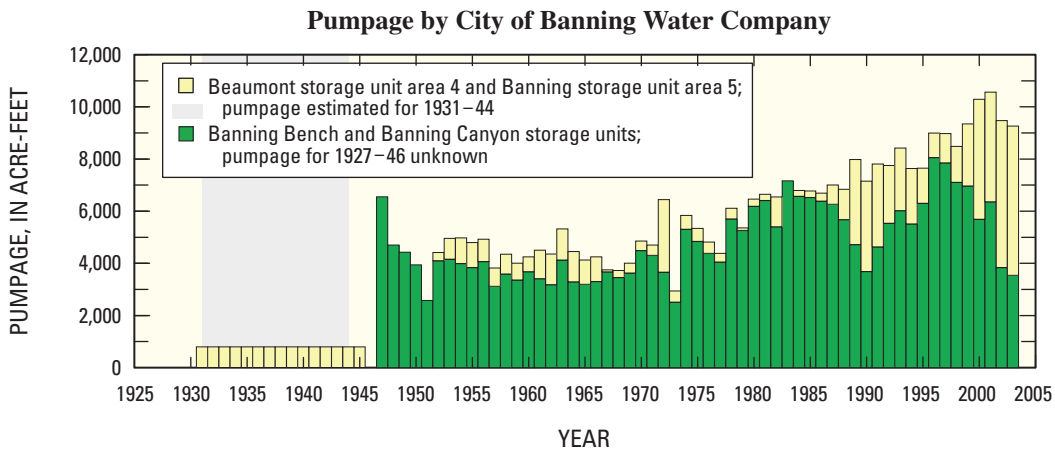


Figure 25. Graphs showing ground-water pumpage from the (A) Beaumont and Banning storage units by area, (B) Beaumont-Cherry Valley Water District, (C) City of Banning Water Company, and (D) cumulative ground-water pumpage from the Beaumont and Banning storage units for 1927-2003, San Gorgonio Pass area, Riverside County, California.

D

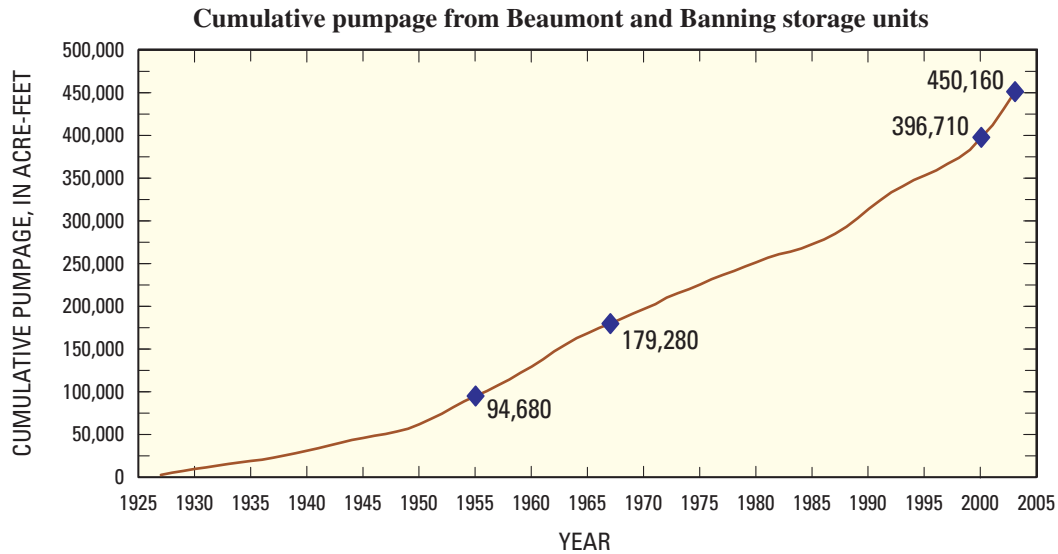


Figure 25. Continued.

Return Flow of Applied Water

Depending on irrigation practices and soil types, some of the water that is applied to crops, golf courses, and landscape infiltrates below the root zone of plants and returns to the underlying ground-water system. For this study, the consumptive use of applied water, or irrigation efficiency, was estimated to be 60 percent, indicating that 40 percent of the applied water returned to the ground-water system. The irrigation efficiency estimate of 60 percent is similar to that for other areas that use sprinkler irrigation techniques (Solomon, 1988). The return flow from the irrigation of crops in the Beaumont and Banning storage units was estimated by multiplying the annual pumpage for each well designated as an agricultural supply well in *Appendix table 3* by 40 percent. The estimated irrigation return flow from crops reached a maximum of about 1,690 acre-ft in 2003 (*fig. 26*).

Ground water was first used in the Beaumont and Banning storage units in 1974 to irrigate golf courses. For this study, it was assumed that 40 percent of the ground water pumped for irrigation of golf courses returns to the ground-water system. To estimate the return flow from the irrigation of golf courses, the annual pumpage for each well designated as a golf course supply well in *Appendix table 3* was multiplied by 40 percent. The estimated irrigation return flow from golf courses reached a maximum of about 890 acre-ft in 2000 (*fig. 26*).

The return flow from water applied for landscape irrigation in the Beaumont and Banning storage units was assumed to be 40 percent, similar to the return flow from the irrigation of crops and golf courses. The city of Beaumont reported that 31 percent of the water demand in the area is for indoor uses

(discharged to the sewage system) and 69 percent was for outdoor use (landscape irrigation) (Boyle Engineering Corporation., 1995). Assuming that this distribution between indoor and outdoor uses is representative for the entire study area and that 40 percent of applied water returns to the ground-water system, then about 28 percent of the water delivered for residential use returns to the ground-water system. The estimated irrigation return flow from landscape watering reached a maximum of about 5,480 acre-ft in 2002 (*fig. 26*).

Septic-Tank Seepage

The cities of Beaumont and Banning have centralized wastewater treatment plants that discharge treated wastewater outside of the Beaumont and Banning storage units; however, residences and businesses in the Cherry Valley area rely on onsite septic systems to discharge their wastewater. Boyle Engineering Corporation (1995) estimated that 95 percent of the indoor water use is discharged into septic systems. For this study, estimates of recharge from septic systems were based on an average septic-tank discharge of 70 gallon per day (gal/d) per person (Bookman-Edmonston Engineering, 1991) multiplied by the annual population of Cherry Valley. The population of Cherry Valley is available from 1970, 1980, 1990, 2000 census data, and the population for Beaumont is available for 1920 through 2000. For years with records for both areas, the population of Cherry Valley was about 64 percent of the population of Beaumont. This ratio was used to estimate the population for Cherry Valley for years without record (*fig. 3*). The estimated septic-tank seepage reached a maximum of about 600 acre-ft in 2003 (*fig. 26*).

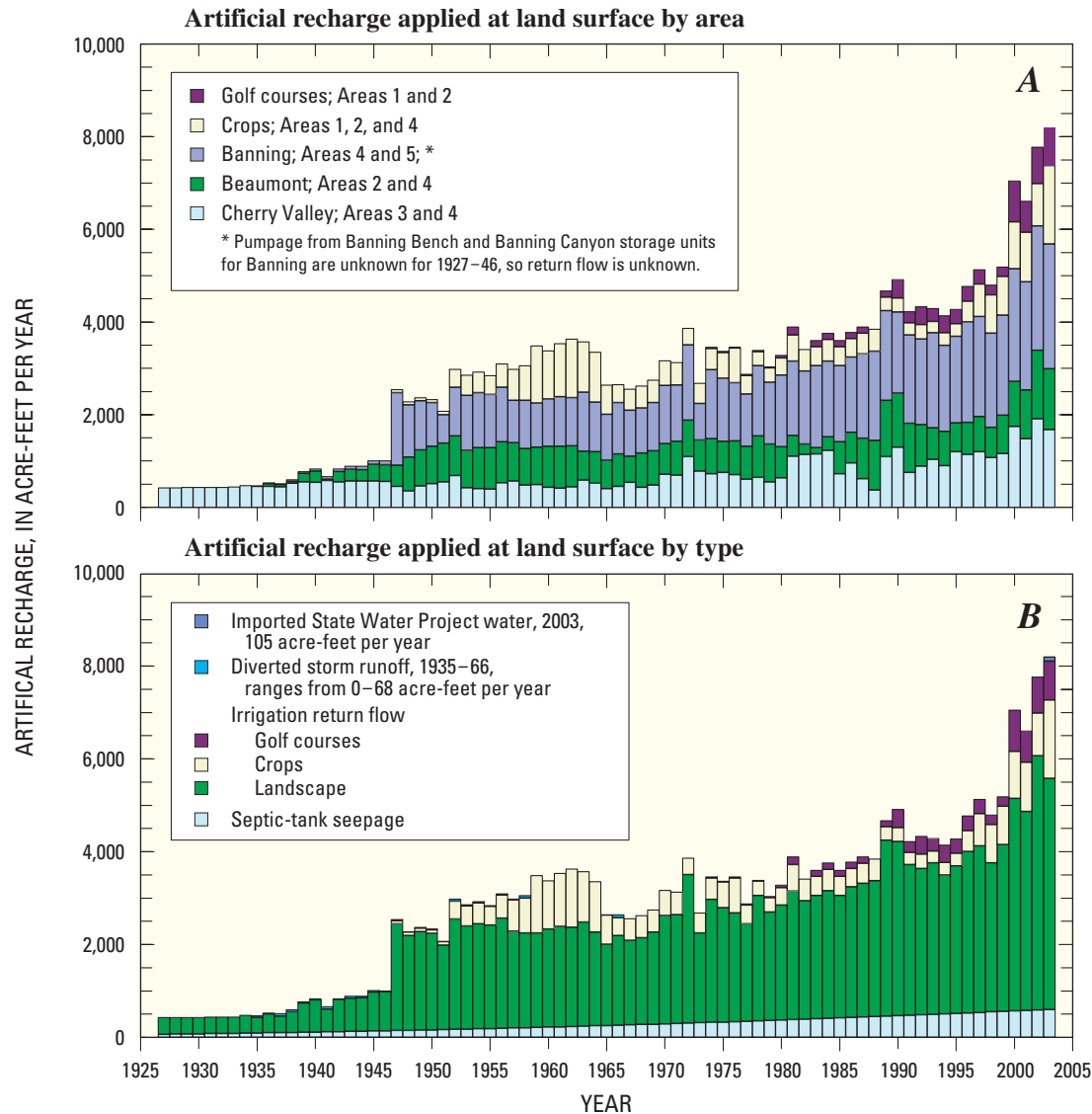


Figure 26. Estimated and reported annual rates of artificial recharge applied at land surface by (A) area, (B) type, 1927–2003, and the estimated annual totals and cumulative totals of artificial recharge (C) applied at land surface, and (D) reaching the water table, 1927–2074, San Gorgonio Pass area, Riverside County, California. See figure 8 for area locations.

Artificial Recharge Ponds

Artificial recharge ponds are located along the Little San Gorgonio Creek in the Cherry Valley area of the Beaumont storage unit (fig. 24). The Riverside County Flood Control and Water Conservation Districts diverted about 860 acre-ft of streamflow from Little San Gorgonio Creek into the recharge ponds in water years 1935–66 (Water Resources Institute, California State University, San Bernardino, Archives [http://wri.csusb.edu.web/pages/archives/index.htm]).

In 1961, the SGPWA entered into a contract with the California State Department of Water Resources to receive 17,300 acre-ft/yr of water to be delivered by the SWP to supplement natural recharge. However, until a pipeline was completed in 2003, SGPWA could not receive SWP water. In

2003, the SGPWA released about 100 acre-ft of SWP to the ponds and about 2,000 acre-ft in 2004.

Ground-Water Levels and Movement

Ground-water level maps presented by Boyd (1971) for 1926–27, 1955, and 1967 were used to describe the historical ground-water conditions in the Beaumont storage unit (fig. 27). Note that the areal extent of the Beaumont storage unit has been modified since Boyd’s (1971) work. Since 1997, the SGPWA has made semi-annual water-level measurements at approximately 70 wells within the SGPWA boundary and surrounding areas. A ground-water level map for 2000 was constructed from these data to show recent ground-water conditions in the Beaumont and Banning storage units

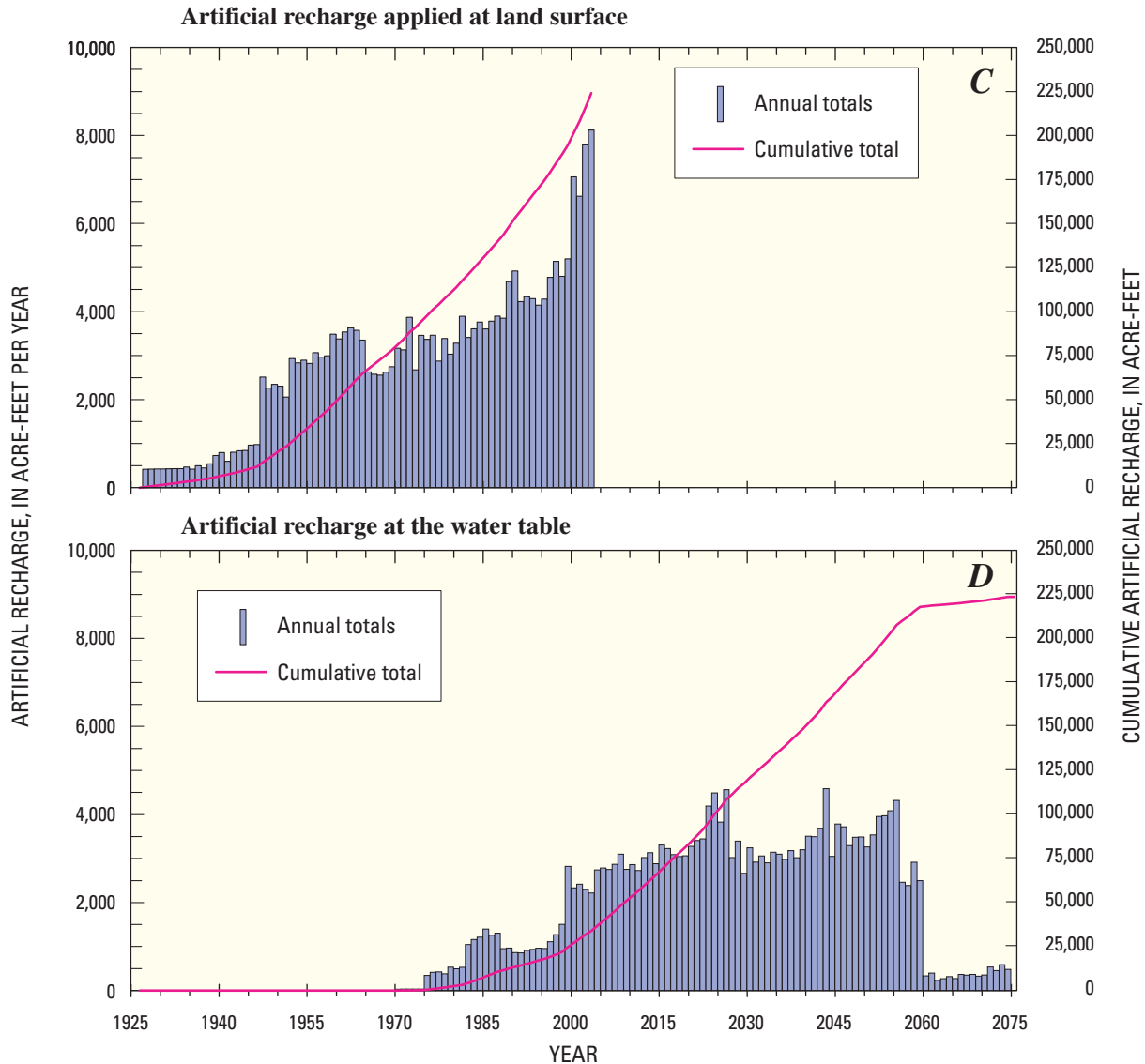


Figure 26. Continued.

(fig. 28). Water-level hydrographs were constructed for each of the five areas in the Beaumont and Banning storage units to show short-term and long-term changes in water levels (fig. 29). Most wells in the Beaumont and Banning storage units are perforated mainly in the upper aquifer, therefore, the ground-water level maps and hydrographs represent ground-water conditions in the upper aquifer, except where noted.

1926–27 Conditions

The 1926–27 water-level data were the oldest available in sufficient quantity to construct a water-level contour map for the Beaumont storage unit (Bloyd, 1971). For the purposes of this current study, it was assumed that the 1926–27 ground-water levels (fig. 27A) represent predevelopment or steady-

state conditions for the upper aquifer because ground-water pumpage was minimal and the 2 years prior to 1926 were not exceptionally wet or dry (Bloyd, 1971). In 1926–27, ground-water levels in the Beaumont storage unit, as defined for this study, ranged from greater than 2,350 ft above sea level (asl) in the Cherry Valley area to about 2,200 ft asl at the northwestern extent of the storage unit. In general, ground-water movement was from recharge areas in the Cherry Valley area toward discharge areas in the San Timoteo storage unit. Ground water discharged from the upper aquifer along the northwestern end of the Beaumont storage unit as baseflow into streams draining the San Timoteo storage unit and ground-water underflow in the alluvial deposits of the canyons of the San Timoteo storage unit.

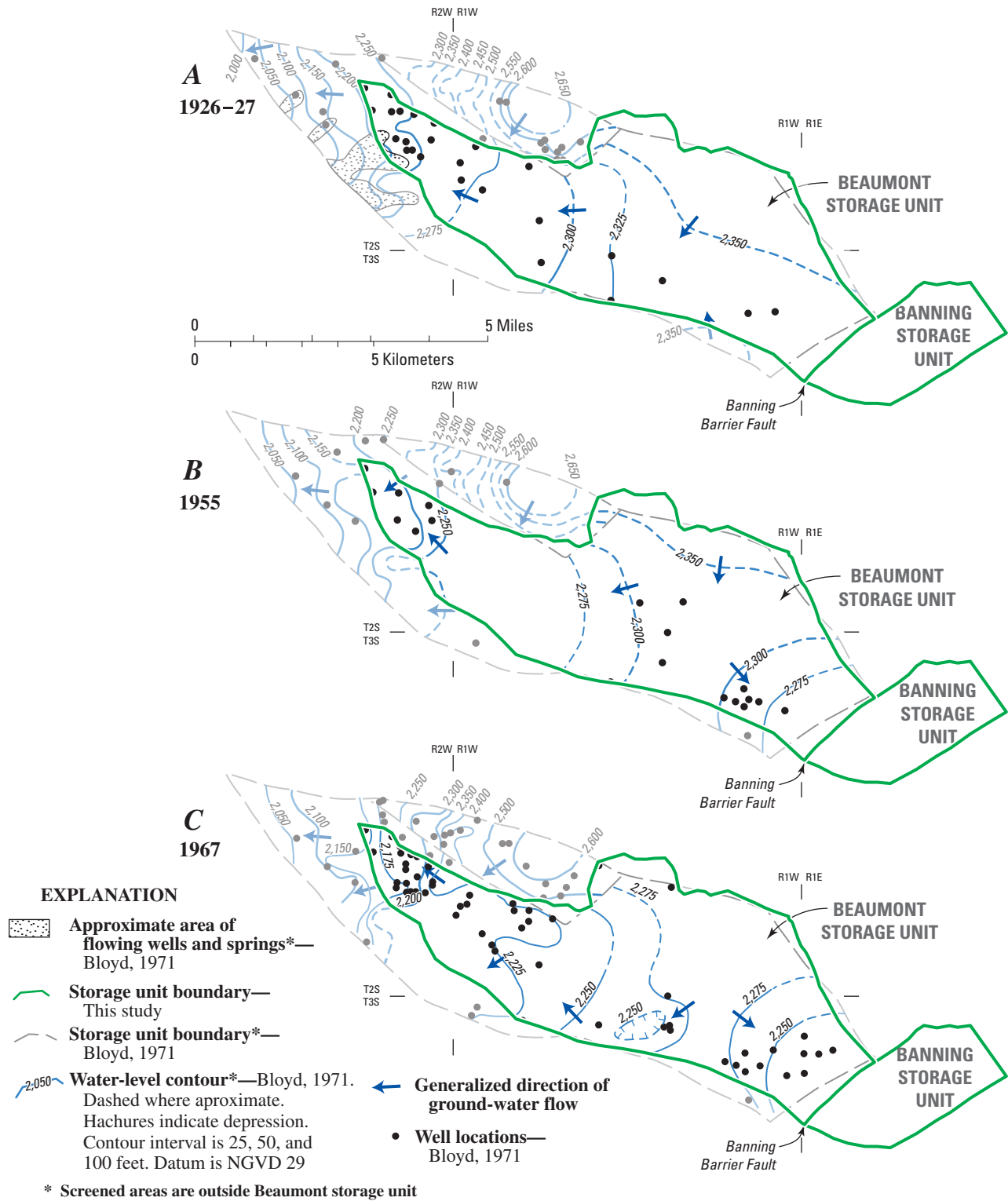


Figure 27. Maps showing ground water-level contours for (A) 1926-27, (B) 1955, and (C) 1967 for the Beaumont storage unit and surrounding area, San Geronio Pass area, Riverside County, California.

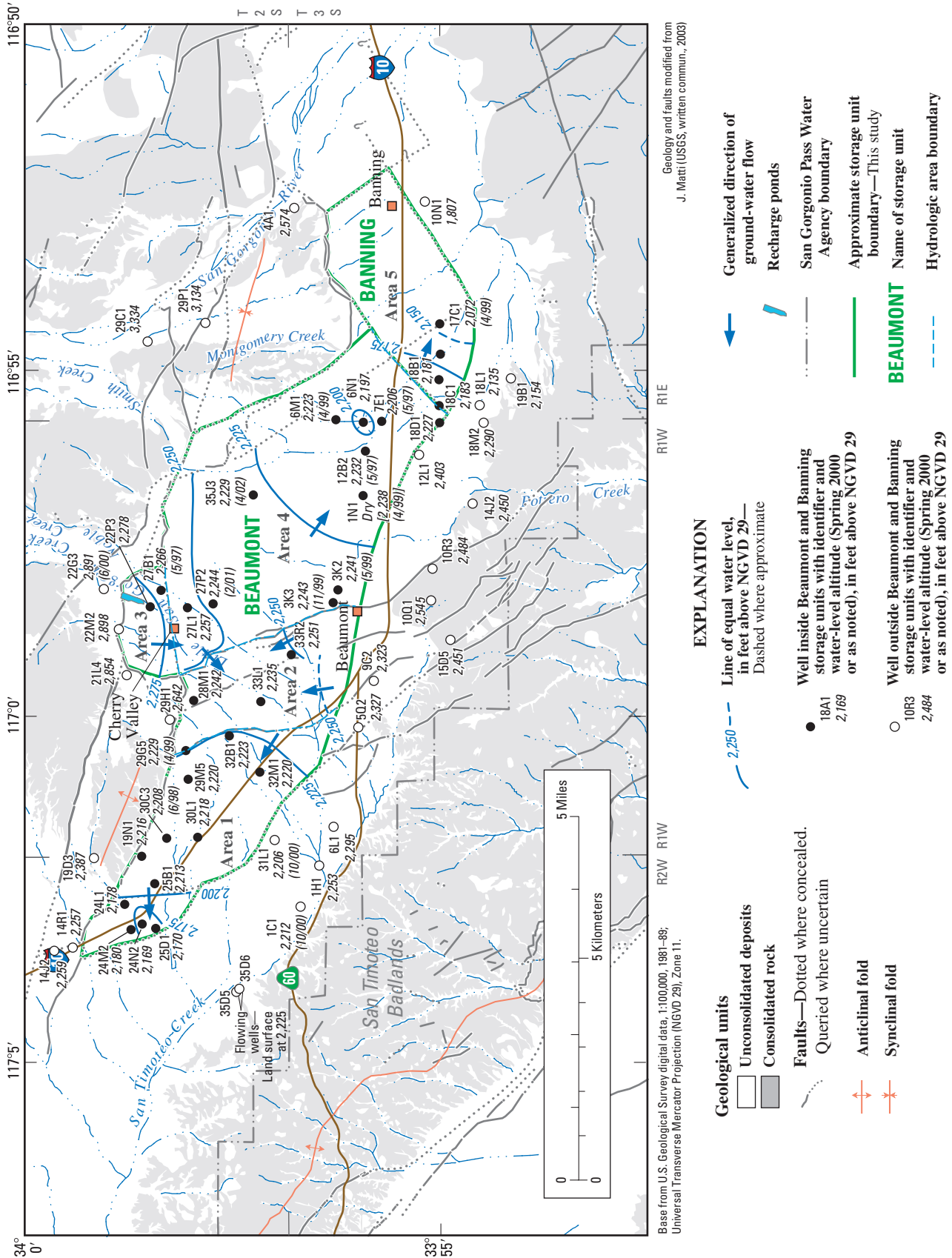
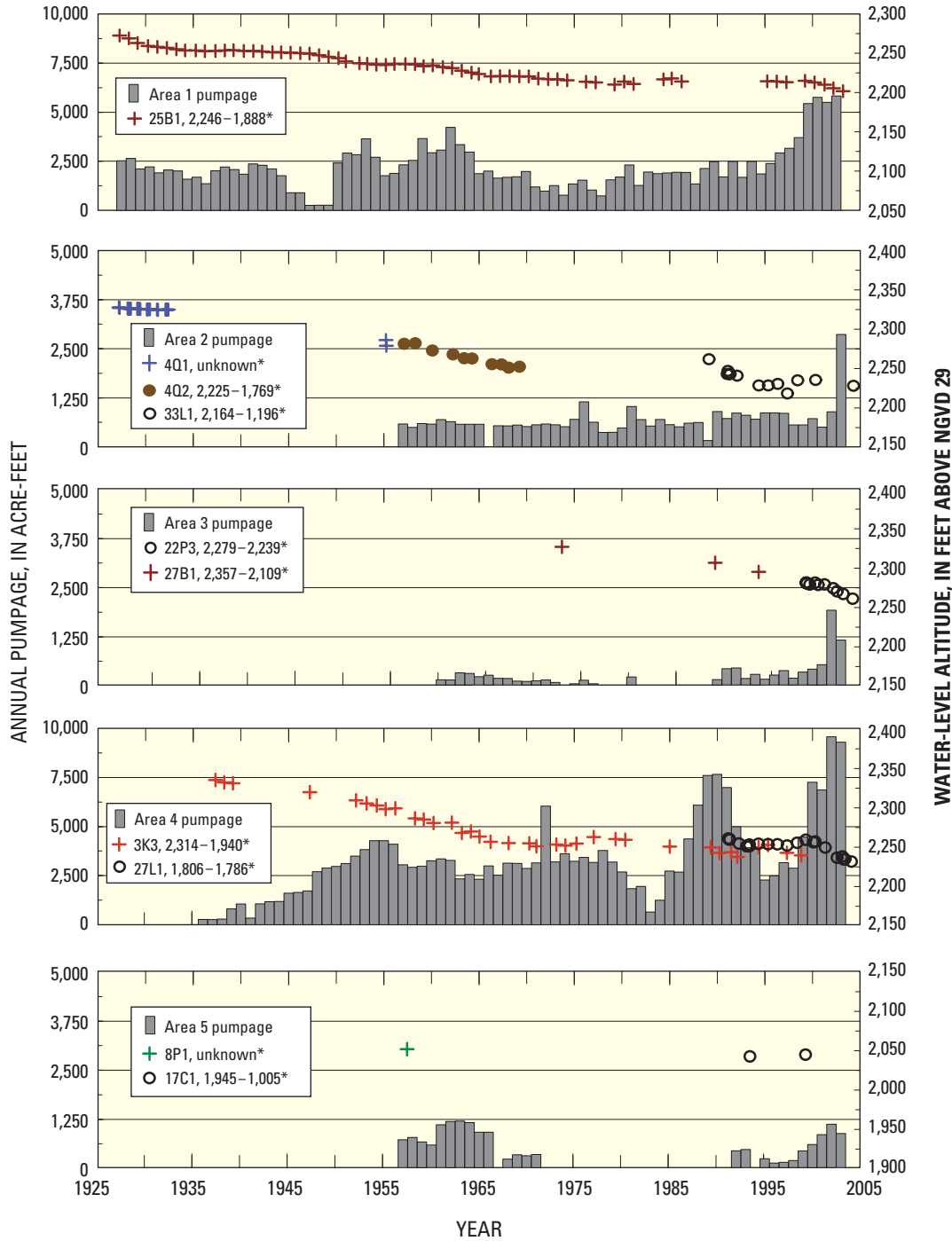


Figure 28. Map showing ground water-levels for Spring 2000 for the Beaumont and Banning storage units and surrounding area, San Gorgonio Pass area, Riverside County, California.



* WELL IDENTIFIER, PERFORATED INTERVAL IN FEET ABOVE NGVD 29

Figure 29. Graphs showing water-level hydrographs and pumpage by area for the Beaumont and Banning storage units, San Geronio Pass area, Riverside County, California.

1955 Conditions

The 1955 ground-water levels (*fig. 27B*) represent conditions in the upper aquifer after 29 years of ground-water pumping (a cumulative volume of about 94,680 acre-ft) in the Beaumont and Banning storage units (*fig. 25D*). Ground-water levels ranged from greater than 2,350 ft asl in the Cherry Valley area to about 2,150 ft asl at the northwestern end of the Beaumont storage unit. The 1955 water-level contour map shows significant water-level declines compared with the 1926–27 map. Water levels declined by more than 50 ft in the eastern part of the storage unit near the Banning Barrier Fault and in the extreme northwestern part of the storage unit. By 1955, water-level declines in the northwestern part of the storage unit caused many of the springs along the canyons in the San Timoteo storage unit to stop flowing. In fact, no areas of flowing wells and springs were indicated by Bloyd (1971) on the 1955 water-level map. A ground-water divide had been established in the eastern part of the storage unit. Bloyd (1971) reported that this divide was well established by 1941. Ground water east of the divide flowed toward the Banning storage unit to the east and ground water west of the divide flowed toward the San Timoteo storage unit to the west.

1967 Conditions

The 1967 ground-water levels (*fig. 27C*) represent conditions in the upper aquifer after 41 years of ground-water pumping (a cumulative volume of about 179,280 acre-ft) in the Beaumont and Banning storage units (*fig. 25D*). Ground-water levels ranged from greater than 2,275 ft asl in the Cherry Valley area to less than 2,150 ft asl at the northwestern extent of the Beaumont storage unit. The north–south ground-water divide continues to exist east of the city of Beaumont. From the divide, ground water flowed east toward the Banning storage unit and west toward a water-level depression created by pumping west of the city of Beaumont or toward the San Timoteo storage unit. The 1967 water-level contour map shows continued declines in water levels since 1955. Water levels declined a maximum of about 150 ft compared with water levels in 1926–27 in the southeastern part of the storage unit near the Banning Barrier Fault (Bloyd, 1971).

2000 Conditions

The 2000 ground-water levels (*fig. 28*) represent conditions in the upper aquifer after 74 years of ground-water pumping (a cumulative volume of about 396,710 acre-ft) in the Beaumont and Banning storage units (*fig. 25D*). Ground-water levels ranged from more than 2,275 ft asl north of the Cherry Valley Fault to less than 2,100 ft asl in the Banning Storage Unit and less than 2,175 ft asl in the northwestern extent of the Beaumont storage unit. The 2000 water-level data indicate

that the Cherry Valley Fault is a partial barrier to ground-water flow in the Beaumont storage unit. Water levels are about 20 ft higher on the north versus the south side of the fault (*fig. 28*). The north-south ground-water divide continues to be associated with the Beaumont Plain Fault Zone. From the divide, ground water flows southeast toward the Banning storage unit and west toward the San Timoteo storage unit.

A perched aquifer exists in the northern part of the Beaumont storage unit. Borehole geophysical logs for well 2S/1W-22P7 indicate a perching layer about 240 ft below land surface (2,670 ft asl) north of the Cherry Valley Fault, and water-level data for the well indicate that the hydraulic head of the perched aquifer was 2,678 ft asl in 2000.

Water-Level Change

A long-term hydrograph for the upper aquifer was constructed for each area of the Beaumont and Banning storage units to show long-term and short-term water-level changes in the study area (*fig. 29*). The hydrographs were constructed using spring water-level measurements from wells perforated mainly in the upper aquifer. For areas 2–5 a composite hydrograph was created from the periods of record of multiple wells to extend the overall period of record. In addition to water-level data, the hydrographs include total pumpage for each area of the Beaumont and Banning storage units to show the temporal effects of pumping on water levels.

The long-term hydrographs in areas 1–4 indicate a general decline in water levels throughout the Beaumont storage unit. The greatest water-level declines occurred in areas 2 and 4 with about 100 ft of drawdown for the period of record in each area (*fig. 29*). No water-level data are available for areas 3 and 5 prior to the 1950s so similar comparisons could not be made. In area 1, water-level measurements from well 2S/2W-25B1 indicate a water-level decline of about 70 ft from 1925 to 2003. In area 2, water-level measurements from wells 3S/1W-4Q1, 3S/1W-4Q2, and 2S/1W-33L1 indicate a water-level decline of about 100 ft from the 1927 to 2003. In area 3, water-level measurements from well 2S/1W-27B1 and 2S/1W-22P3 indicate a water-level decline of about 80 ft from the 1960s to 2004. In area 4, water-level measurements from well 3S/1W-3K3 and 3S/1W-27L1 indicate a water-level decline of about 100 ft from the late 1930s to 2004, with most of the decline occurring from the late 1930s to the early 1960s. The decrease in the rate of water-level decline since the early 1970s also is seen in area 2 but it does not correspond to a decrease in pumpage from these areas (*fig. 29*). The decrease in the rate of water-level decline is believed to be the result of artificial recharge from crop and landscape irrigation returns and septic-tank seepage (*fig. 26*) reaching the water table in the 1970s. In the Banning storage unit, water-level measurements from well 3S/1E-8P1 indicate a water-level decline of about 20 ft from the mid 1950s to 1980.

Geochemistry

The geochemistry of the ground water in the Beaumont, Banning, and surrounding storage units was defined by analyzing samples collected from 36 wells in the storage units and surrounding area (*fig. 30*) and one suction lysimeter installed in the perched aquifer in the Cherry Valley area. A suction lysimeter consists of a porous ceramic cup attached to a polyvinyl chloride pipe that is connected to land surface by two access tubes. Suction lysimeters are used to collect water samples from the unsaturated zone, however, water samples also can be collected from the saturated zone, as was done in this study. Water-quality samples also were collected from Little San Gorgonio Creek and Noble Creek in the Cherry Valley area. The samples were analyzed for concentrations of major ions, nutrients, and selected trace elements. Selected samples were analyzed for the stable isotopes of oxygen and hydrogen (oxygen-18 and deuterium, respectively); tritium, a naturally occurring radioactive isotope of hydrogen; and carbon-14 (^{14}C), a naturally occurring radioactive isotope of carbon. Some wells were sampled several times during the study period. Complete analyses for all the samples can be retrieved from the USGS National Water Information System database at <http://waterdata.usgs.gov/ca/nwis/> using the USGS State well numbers given in *Appendix table 1*.

The chemical character of ground water sampled during the study period for selected wells in the Beaumont, Banning, and surrounding storage units was determined using trilinear and Stiff diagrams (*figs. 31 and 32*). A trilinear diagram shows the relative contribution of major cations and anions, on a charge-equivalent basis, to the ionic content of the water (Piper, 1944). Percentage scales along the sides of the diagram indicate the relative concentration, in milliequivalents per liter (meq/L), of each major ion. Cations are shown in the left triangle, anions are shown in the right triangle, and the central diamond integrates the data (*fig. 31*). Trilinear diagrams are useful in determining if simple mixing between chemically different water is occurring (Hem, 1992). For wells with multiple samples, only the sample with the lowest dissolved-solids concentration is discussed in this report; no trends in major-ion composition were observed in water from wells having more than one analysis.

A Stiff diagram depicts the concentrations of major ions in meq/L and indicates relative proportions of major ions (Stiff, 1951). Analyses with similarly shaped diagrams represent ground water of similar chemical characteristics with respect to major ions. Changes in the width of the diagrams indicate differences in the concentration of dissolved constituents. Water that contains higher concentrations of major ions

has a wider diagram than the diagram for water with lower concentrations. All Stiff diagrams are shown at the same scale of +8 meq/L (*fig. 32*). The left side of the diagram shows the major cations: sodium plus potassium at the top, magnesium in the middle, and calcium at the bottom. The right side of the diagram shows major anions: chloride plus fluoride at the top, sulfate in the middle, and carbonate plus bicarbonate on the bottom.

General Water-Quality Characteristics

In general, ground water is of good quality in the Beaumont, Banning, and surrounding storage units as indicated by samples collected for this study (*figs. 30 and 32*). Dissolved-solids concentrations ranged from 177 mg/L in a sample from production well 3S/1E-18A1 in the Banning storage unit to 823 mg/L in a sample from monitoring well 2S/1W-22G3 located in Edgar Canyon. Dissolved-solids concentrations were 34 and 271 mg/L in samples collected from Little San Gorgonio Creek and Noble Creek, respectively.

Nitrate concentrations in samples collected from wells for this study, measured as nitrate plus nitrite, ranged from less than 1.0 to 11.3 mg/L as nitrogen (*fig. 30*). The highest concentration was analyzed in a sample from monitoring well 2S/1W-22G4, located in Edgar Canyon. The nitrate concentration in the sample from well 22G4 exceeded the U.S. Environmental Protection Agency (USEPA) Maximum Contaminant Level (MCL) of 10 mg/L for nitrate as nitrogen (U.S. Environmental Protection Agency, 2005). Well 22G4 is a shallow monitoring well that is perforated from 138 to 158 ft below land surface and is likely affected by an anthropogenic source of nitrogen that may include agricultural activity or septic-tank seepage.

Fluoride concentrations in samples collected from wells for this study ranged from less than 0.5 mg/L to 3.0 mg/L (*fig. 30*). The highest concentration analyzed was from monitoring well 2S/1W-22G3, which is located in Edgar Canyon. Well 22G3 is perforated from 300 to 320 ft below land surface in the fractured crystalline rocks of the San Gabriel Mountains-type. The high concentrations of fluoride may be explained by the dissolution of fluoride containing minerals present in igneous rocks. All samples contained fluoride concentrations below the USEPA MCL of 4 mg/L set by the U.S. Environmental Protection Agency (USEPA) for fluoride (U.S. Environmental Protection Agency, 2005).

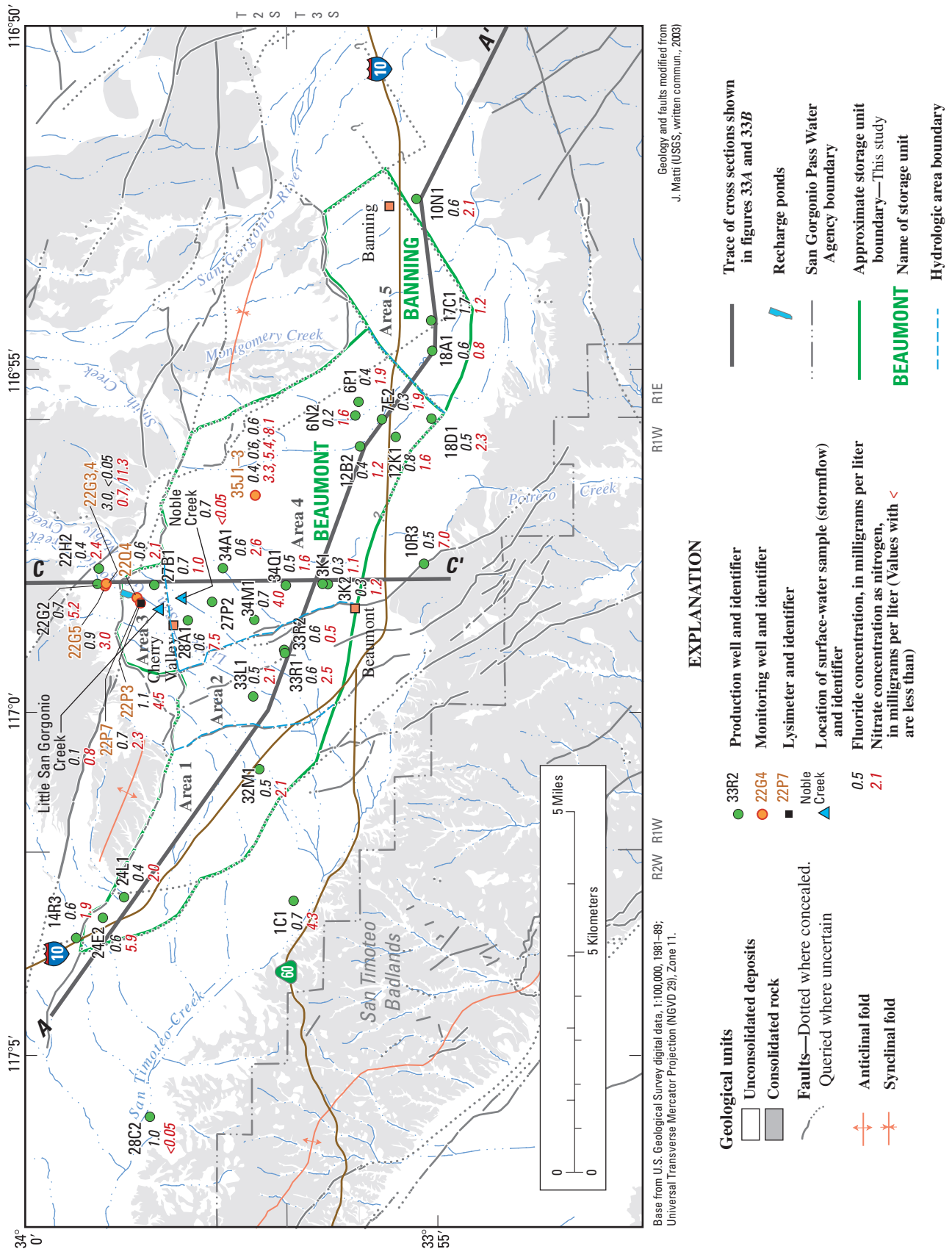


Figure 30. Map showing wells in the water-quality monitoring network and fluoride and nitrate concentrations as nitrogen in samples from selected production and monitoring wells, San Gorgonio Pass area, Riverside County, California.

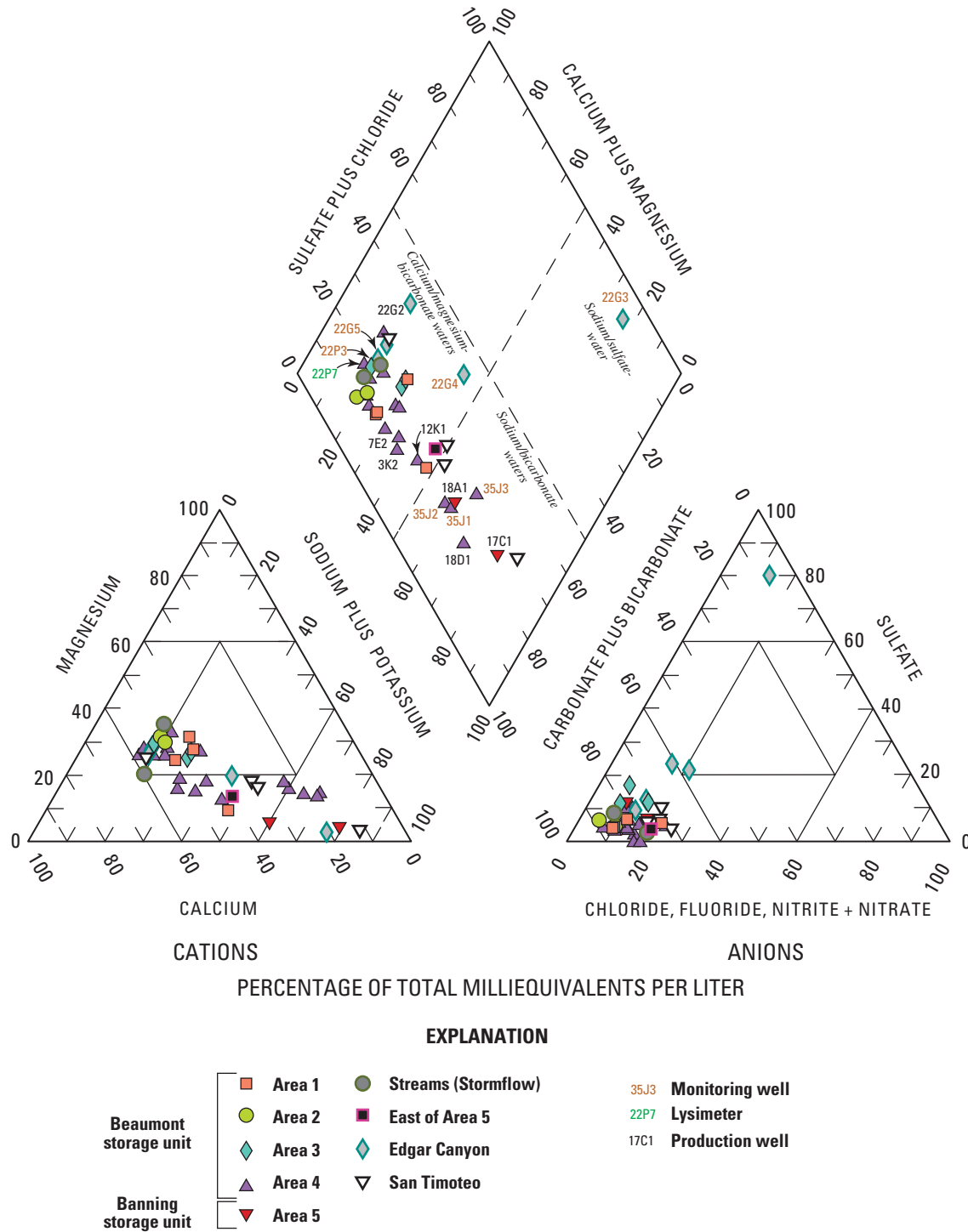


Figure 31. Graphs showing trilinear diagrams for samples from selected production and monitoring wells in the Beaumont and Banning storage units and surrounding area, San Gorgonio Pass area, Riverside County, California.

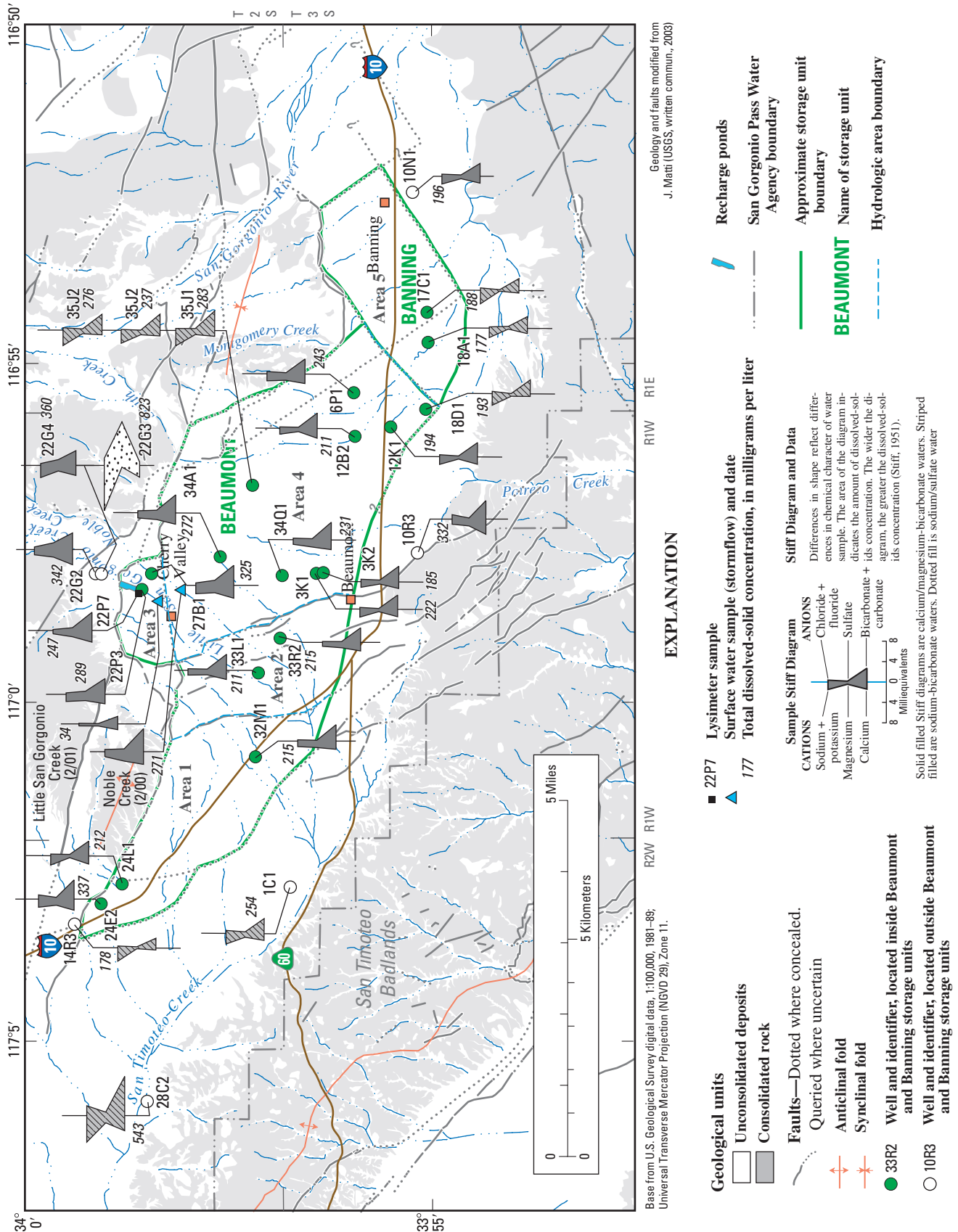


Figure 32. Map showing stiff diagrams and dissolved-solids concentrations for samples from selected production and monitoring wells in the Beaumont and Banning storage units and surrounding area, San Gorgonio Pass area, Riverside County, California.

Chemical Character of Ground Water

In this report, the dominant cation and anion species are used to describe the chemical character of a water sample. Where no one species exceeds 50 percent, the first and second most abundant ions are given for description purposes. The chemical character of ground water in the study area generally can be characterized as calcium/magnesium-bicarbonate type water or sodium-bicarbonate type water (*fig. 31*). Water-quality samples collected from Little San Gorgonio and Noble Creeks during stormflow are characterized as calcium/magnesium-bicarbonate type water (*fig. 32*). Few wells are perforated solely in the upper or lower aquifers (*fig. 33*). In general, wells in areas 1 through 4 of the Beaumont storage unit generally yielded calcium/magnesium-bicarbonate type water and wells in the Banning storage unit yield sodium-bicarbonate type water; however, wells 2S/1W-35J1-3 and 3S/1W-18D1, which are in the Beaumont storage unit, yield sodium-bicarbonate type water (*figs. 32 and 33*).

The sample from well 2S/1W-22G3 in Edgar Canyon, located upgradient of the Banning Fault, is sodium-sulfate type water (*figs. 31, 32, and 33B*). As stated previously, this well contains high concentrations of dissolved solids and fluoride compared with concentrations in wells in the Beaumont storage unit. Well 22G3 is perforated from 300 to 320 ft below land surface, opposite fractured crystalline rocks of the San Gabriel Mountains-type (*fig. 33B*). The differences in water type, dissolved-solids concentrations, and fluoride concentrations indicate that little if any of the ground water in the fractured crystalline rocks flows south across the Banning Fault into the Beaumont storage unit.

Determining the Source of Water to Wells

Depth-dependent samples were collected from temporary test wells constructed during the drilling of the pilot hole for well 2S/1W-27P2 in area 4 of the Beaumont storage unit (*fig. 34*). The test wells are temporary because they were removed as the pilot hole is deepened. Two samples were collected from the upper aquifer (810–830 and 996–1,016 ft below land surface) and one sample was collected from the lower aquifer (1,345–1,365 ft below land surface) (Thomas Harder, Geoscience Support Services, written commun., 2002). The two samples collected from the upper aquifer are calcium/magnesium-bicarbonate type water and plot at nearly the same position on the trilinear diagram (*fig. 34*). The sample collected from the lower aquifer is sodium-bicarbonate type water. If one assumes that the samples from the shallow

temporary wells at 27P2 represents the chemical character of water in the upper aquifer and that the sample from the deep temporary well at 27P2 represents the chemical character of water in the lower aquifer, then one can draw a mixing line between the two end members to determine the percentage of water contributed from the two aquifers to production wells perforated in both aquifers. Samples from wells that plot near the end members indicate that the well is pumping water from the aquifer represented by the end member. Samples that plot between the two end members are a composite of water from both aquifers and indicate that the well is pumping water from both aquifers. For example, the sample from production well 27P2, which is perforated in both the upper and lower aquifers, plots almost in the same position on the trilinear diagram as the samples collected from the shallow temporary wells (*fig. 34*), indicating that the lower aquifer contributes little or no water to well 27P2.

In general, the upper aquifer contributes more than 75 percent of the water pumped from most of the wells in areas 1 through 4 as indicated using the mixing line described above. However, the mixing line indicates that in area 4 the lower aquifer contributes about half of the water pumped from production wells 3S/1W-7E2, 3K2, and 12K1 and most of the water pumped from production well 3S/1E-18D1 (*figs. 31 and 34*).

In area 5, the sample from well 3S/1E-18A1 (*fig. 31*) plots near the lower aquifer end member represented by the sample from the deep temporary well at 27P2 (*fig. 34*) indicating that the lower aquifer contributes most of the water pumped from this well. However, the sample from 3S/1E-17C1 plots below the lower aquifer end member indicating a different source of water (*fig. 34*). Recall well 17C1 is perforated in the older sedimentary deposits (QTso) as well as in the upper and lower aquifers (*fig. 33A*); therefore, the QTso deposits may be the different source of water.

In order to define the chemical character of ground water from the QTso deposits, depth-dependent samples were collected from well 3S/1E-17C1 while it was pumping using a small-diameter sampling hose following the techniques described by Izbicki and others (1999). Using these techniques, the sampling hose is pressurized to greater than the hydrostatic pressure of water at the sample depth and then lowered into the well. When the sample depth is reached, the hose is vented at land surface and water from the well enters the hose at the sample depth. The hose is retrieved and the sample is expelled from the hose using nitrogen gas.

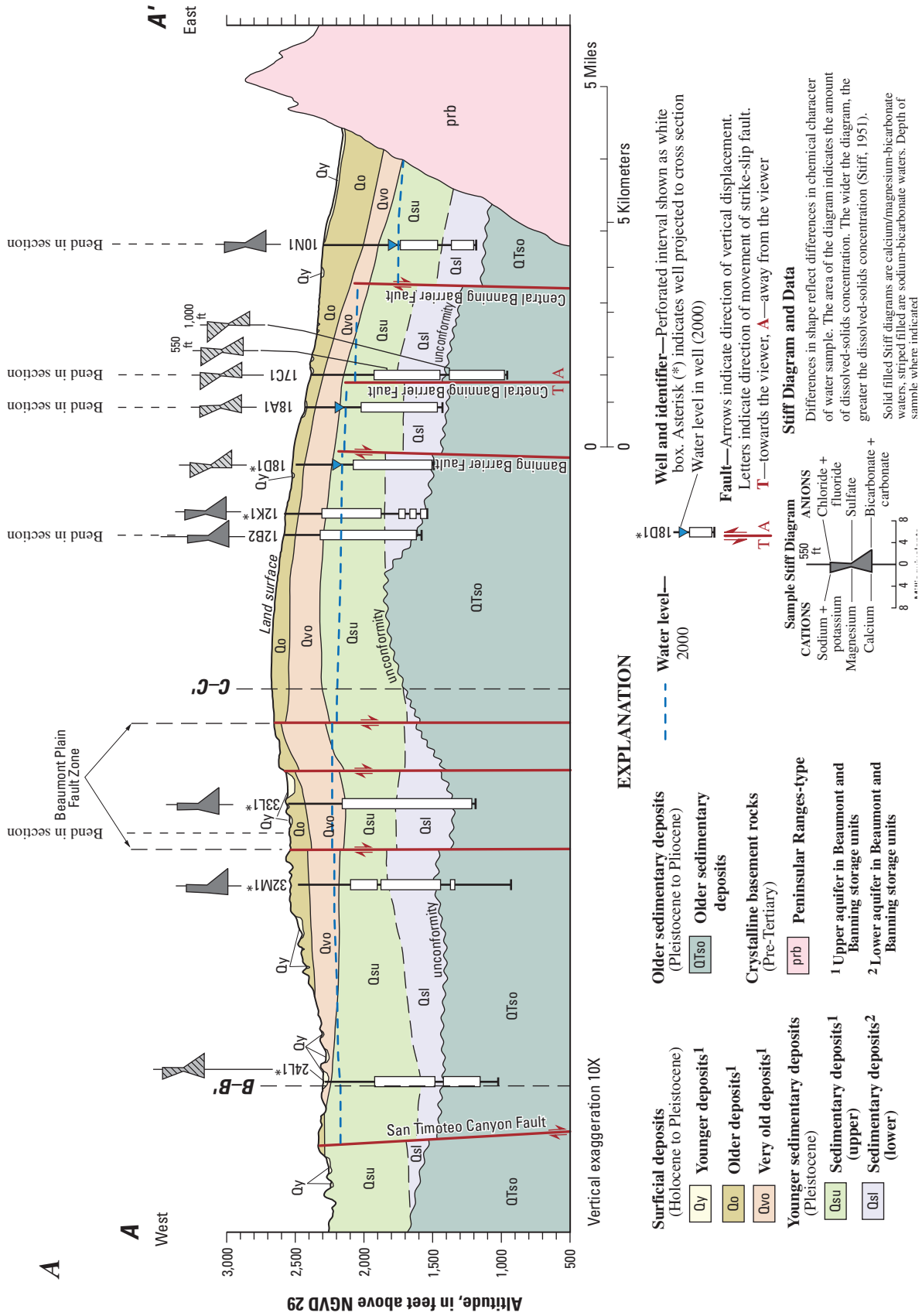


Figure 33. Geologic cross sections (A) A–A' and (B) C–C' showing Stiff diagrams and perforated intervals for selected wells, San Gorgonio Pass area, Riverside County, California.

B

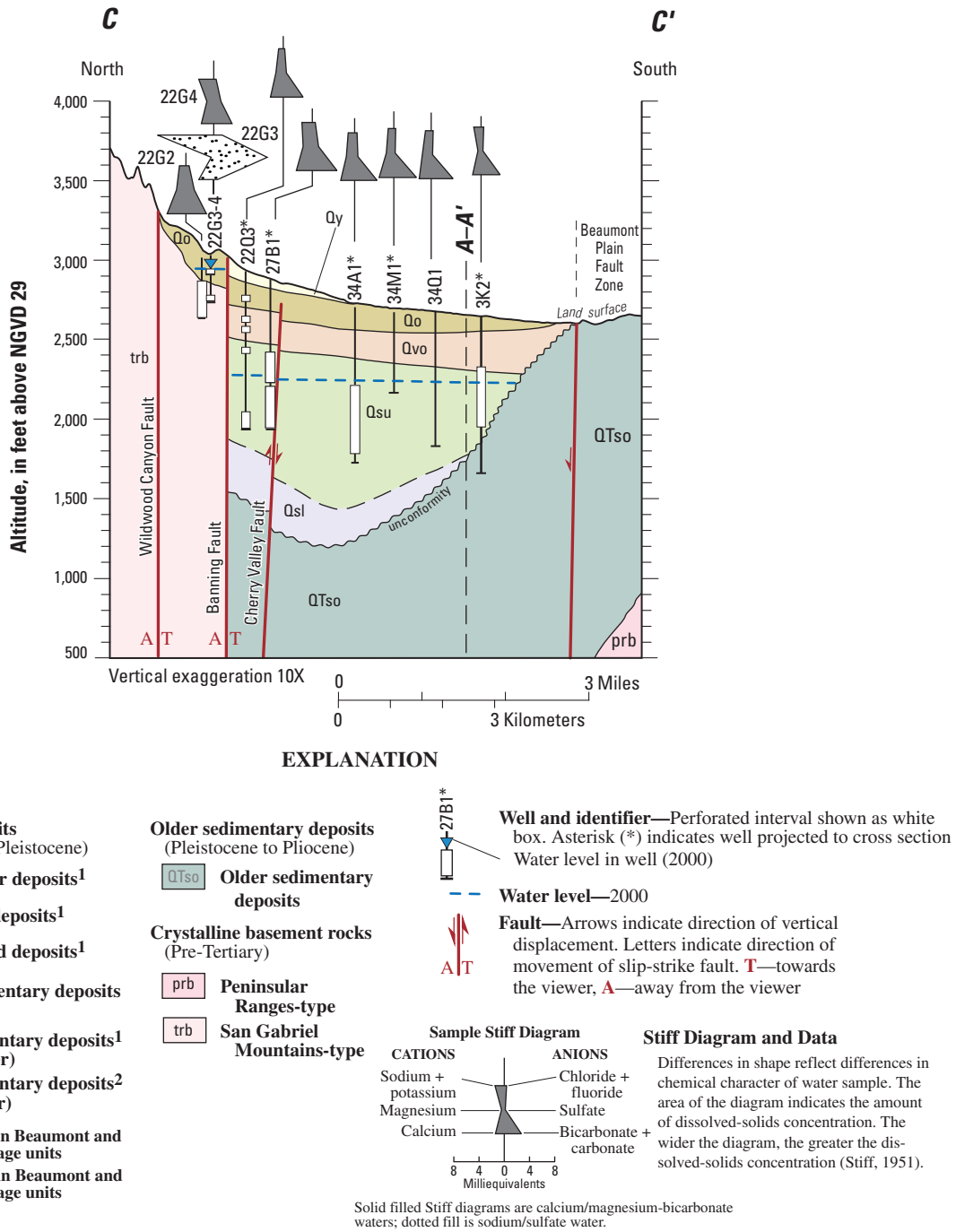
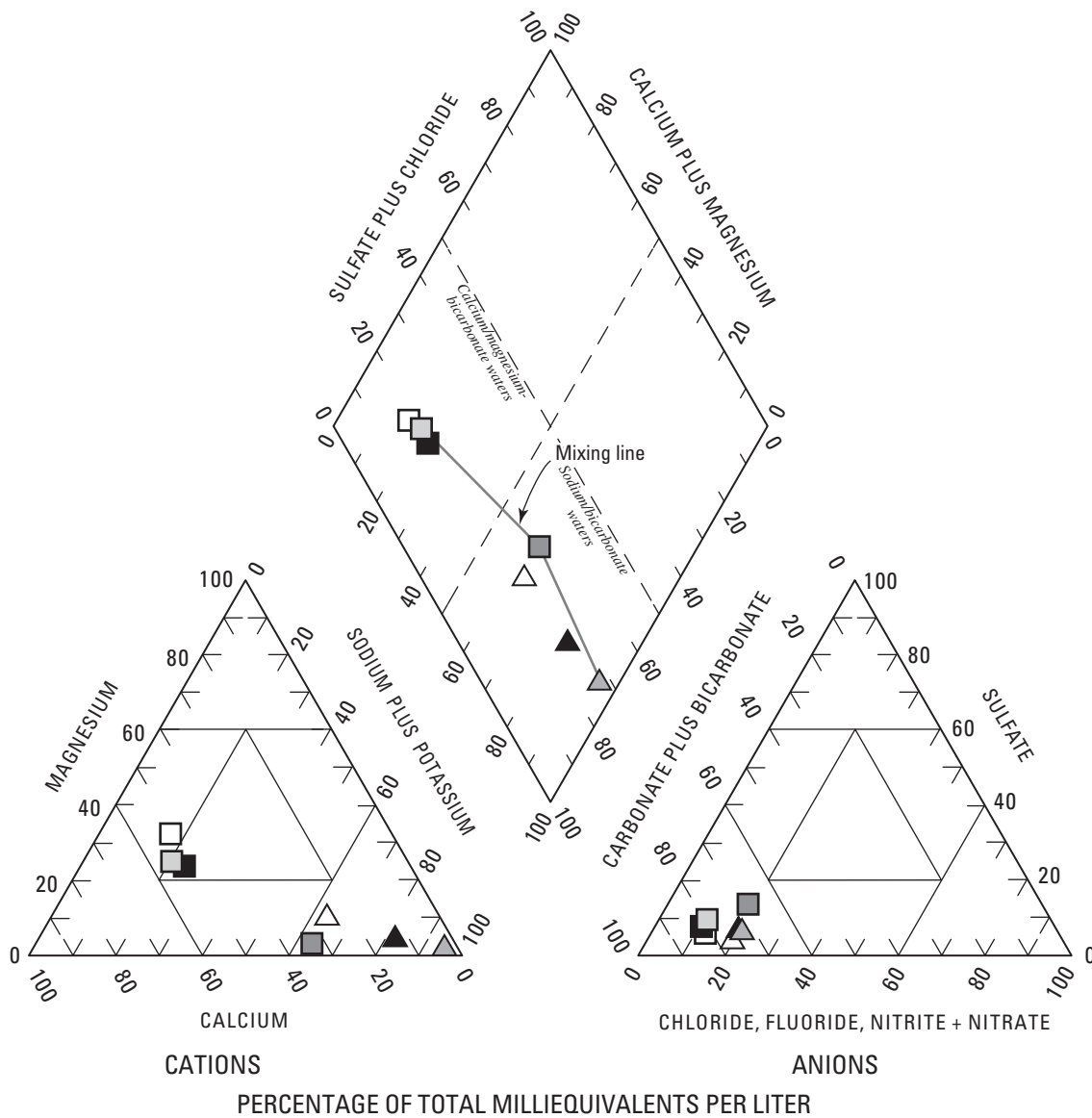


Figure 33. Continued.



EXPLANATION

Depth-dependent samples,
in feet below land surface

17C1

- △ 550'
- ▲ 1,000'
- ▲ Well

Perforated interval of temporary well samples,
in feet below land surface

27P2

- 810–830'
- ◻ 996–1,016'
- 1,345–1,365'
- Completed well

Figure 34. Graphs showing trilinear diagrams for samples collected from temporary wells installed during the construction of well 2S/1W-27P2, from well 2S/1W-27P2 after construction, from well 3S/1E-17C1, and from 550 feet and 1,000 feet below land surface in well 3S/1E-17C1, San Geronio Pass area, Riverside County, California.

The perforated intervals of well 3S/1E-17C1 are 460 to 930 and 1,000 to 1,400 ft below land surface (*fig. 33A* and *Appendix table 1*) and the pump intake is about 600 ft below land surface. For well 17C1, two samples were collected from the well—a shallow sample was collected above the pump intake at a depth of 550 ft below land surface and a deep sample was collected below the pump intake at a depth of 1,000 ft below land surface. The shallow sample is a composite of water that has entered the well from the perforated interval above the sample-collection depth (460–550 ft below land surface) and is representative of water in the upper aquifer at the well. The deep sample is a composite of water that has entered the well from the perforated interval below the sample collection depth (1,000–1,400 ft below land surface) and is representative of water in the QTso deposits at the well. Both samples are sodium-bicarbonate type water with the QTso sample having a higher percentage of sodium (93 percent) than any other sample collected for this study in the Banning and Beaumont storage units (*figs. 31* and *34*). If one assumes that the sample from the QTso deposits represents the chemical character of water in those deposits, then one can draw a mixing line between the lower-aquifer end member and the QTso-deposits end member to determine the percentage of water contributed from the QTso deposits to production wells perforated in both the lower aquifer and the QTso deposits. A sample collected from the discharge, which is a composite of water pumped from all screened intervals of well 17C1, indicates that the source of about 50 percent of the water pumped from this well is the QTso deposits (*fig. 34*). Unlike the chemical character of samples from other wells that are perforated in the upper aquifer, the chemical character of the shallow sample from well 17C1 is similar to the chemical character of the lower aquifer; this may be the result of water from the QTso deposits migrating upward along the inferred fault adjacent to the well (*fig. 33A*) and mixing with water from the upper aquifer.

Samples from wells 2S/1W-22G2 and 22G4 in Edgar Canyon plot away from the mixing line indicating mixing with waters of a different source than that represented by the samples collected from the temporary wells constructed during the drilling of well 2S/1W-27P2 (*fig. 31* and *34*). The samples from wells 2S/1W-22G2 and 22G4 probably reflect mixing of infiltrated Little San Geronio Creek streamflow with water from the fractured crystalline rocks as indicated by the sample from well 2S/1W-22G3 (*fig. 33B*).

Source and Age of Ground Water

Samples collected from 36 wells and one suction lysimeter in the study area were analyzed for the stable isotopes of oxygen (oxygen-18) and hydrogen (hydrogen-2, or deuterium) to determine the source of water to wells and to evaluate the movement of water through the study area. Selected samples also were analyzed for the radioactive isotopes of hydrogen (hydrogen-3, or tritium) and carbon (carbon-14, or ^{14}C) to determine the age, or time since recharge, of the ground water; 22 samples were analyzed for tritium and 21 samples were analyzed for ^{14}C .

Stable Isotopes of Oxygen and Hydrogen

Oxygen-18 (^{18}O) and deuterium (D) are naturally occurring stable isotopes of oxygen and hydrogen. The isotopic ratios are expressed in delta notation (δ) as per mil (parts per thousand) differences relative to the standard known as Vienna Standard Mean Ocean Water (VSMOW) (Gonfiantini, 1978). The $\delta^{18}\text{O}$ and δD composition of precipitation throughout the world is linearly correlated because most of the world's precipitation is derived originally from the evaporation of seawater. This linear relationship is known as the meteoric water line (Craig, 1961). Differences in isotopic composition can be used to help determine general atmospheric conditions at the time of precipitation and the effects of evaporation before water entered the ground-water system. The $\delta^{18}\text{O}$ and δD of ground water relative to the global meteoric water line provides evidence of the source of the water and fractionation processes that have affected stable-isotope values. For example, water from a given air mass that condensed at higher altitudes and cooler temperatures contains a greater amount of the lighter isotopes of oxygen and hydrogen and, therefore, has lighter $\delta^{18}\text{O}$ and δD values (more negative) than water that condensed from the same air mass at lower altitudes and warmer temperatures. In some areas, fractionation during atmospheric condensation and precipitation, or during evaporation prior to ground-water recharge, may result in recharge waters with different $\delta^{18}\text{O}$ and δD values. Information about the source and evaporative history of water can be used to evaluate the movement of water between aquifers. Because ground water moves slowly, isotopic data collected near the end of long flow lines typically preserve a record of ground-water recharge and movement under predevelopment conditions. This is especially useful in areas where traditional hydrologic data (such as water levels) have been altered by pumping, by changes in recharge and discharge, or as a result of human activities.

The $\delta^{18}\text{O}$ and δD composition of ground-water samples collected from the Beaumont, Banning, and surrounding storage units ranged from -6.35 to -10.93 and -47.30 to -75.80 per mil, respectively (*fig. 35*). The isotopic range of δD in ground water sampled in the Beaumont and Banning storage units was significantly heavier than the volume-weighted average of precipitation (-77 per mil) collected near Big Bear, California (Friedman and others, 1992) indicating that the source of ground-water recharge in the study area is precipitation from storms passing through the San Gorgonio Pass as opposed to runoff from the higher altitudes of the San Bernardino Mountains (*fig. 2*). The δD in the ground-water sample from well 2S/1W-22G3 is significantly lighter (-75.80 per mil) than any of the other ground-water samples (*fig. 35*). As described previously, this well is located upgradient from the Banning Fault (*fig. 33B*) and is perforated in the fractured crystalline rocks. These isotopic values offer additional support that little if any of the ground water in the fractured crystalline rocks flows across the Banning Fault into the Beaumont storage unit.

Most of the ground-water samples plot near the meteoric water line indicating that ground-water recharge was not subjected to evaporation before infiltrating (*fig. 35*). Partial evaporation of precipitation or runoff before it infiltrates causes fractionation of $\delta^{18}\text{O}$ and δD that results in a shift in isotopic values to the right of the meteoric water line. Samples from wells 3S/1W-10R3 (in the South Beaumont storage unit) and 2S/2W-28C2 (in the San Timoteo storage unit) indicate that water pumped from these wells was subject to partial evaporation (*fig. 35*).

Tritium

Tritium is a naturally occurring radioactive isotope of hydrogen that has a half-life of 12.4 years. The concentration of tritium is measured in tritium units (TU); each TU equals 1 atom of tritium in 10^{18} atoms of hydrogen. Approximately 800 kilograms of tritium was released into the atmosphere as a result of the atmospheric testing of nuclear weapons between 1952 and 1962 (Michel, 1976). As a result, tritium concentrations in precipitation and ground-water recharge increased during that time. Tritium concentrations are not affected significantly by chemical reactions other than radioactive decay because tritium is part of the water molecule. Therefore, tritium is an excellent tracer of the movement and relative age of water on timescales ranging from recent to about 50 years before present (post 1952). In this report, ground water that has detectable tritium (greater than 0.2 TU) is interpreted to be water recharged after 1952, or recent recharge.

Tritium concentrations in samples from wells in areas 1, 2, 4, and 5 were less than or equal to 0.2 TU, with the exception of samples from four wells (2S/2W-24E2, 2S/1W-28A1, 3S/1E-7E2, and 3S/1W-12K1), indicating that the water pumped from most of the wells in these areas was recharged prior to 1952 (*fig. 36*). These concentrations were not unexpected because the thick unsaturated zone in these areas (greater than 300 ft in most areas) results in long travel times for infiltrated water to reach the water table. A numerical model of the unsaturated zone in area 3 (where the unsaturated zone is about 640 ft thick) simulated that the travel time for stream infiltration to reach the water table was about 50 years directly beneath the Little San Gorgonio Creek channel and about 250 years for areas away from the stream channel (Flint and Ellett, 2004). Samples collected from the four wells in the Beaumont storage unit had tritium concentrations in excess of 0.2 TU, ranging from 0.5 to 1.9 TU indicating that these wells have received recharge within the past 50 years. Wells 24E2, 28A1, 7E2, and 12K1 are adjacent to stream channels (*fig. 36*); infiltration along these stream channels probably is the source of the recent recharge to these wells.

The tritium concentrations in samples from well 2S/1W-22P3 (screened opposite the upper aquifer) and suction lysimeter 2S/1W-22P7 (sampled from the perched aquifer) in area 3 were 0.7 and 2.9 TU, respectively (*fig. 35*). These sampling sites are adjacent to the recharge ponds along Little San Gorgonio Creek (*fig. 36*), which explains the relatively high tritium concentrations. The difference in tritium concentrations between the perched and upper aquifers indicate a travel time of about 25 years, which was based on the decay rate of tritium and an assumption that the perched aquifer is the sole source of water for the upper aquifer.

The tritium concentrations in samples from wells located in the San Timoteo, South Beaumont, and Edgar Canyon storage units ranged from 1.0 to 2.4 TU indicating recharge within the past 50 years. These wells are located along stream channels, and, therefore, the tritium concentrations are likely the result of local recharge from stream infiltration (*fig. 36*).

Carbon-14

Carbon-14 is a naturally occurring radioactive isotope of carbon that has a half-life of about 5,730 years (Mook, 1980). Carbon-14 data are expressed as percent modern carbon (pmc) by comparing ^{14}C activities to the specific activity of National Bureau of Standards oxalic acid: 13.56 disintegrations per minute per gram of carbon in the year 1950 equals 100 pmc (Kalin, 2000). Carbon-14 was produced, as was tritium, by the atmospheric testing of nuclear weapons (Mook, 1980).

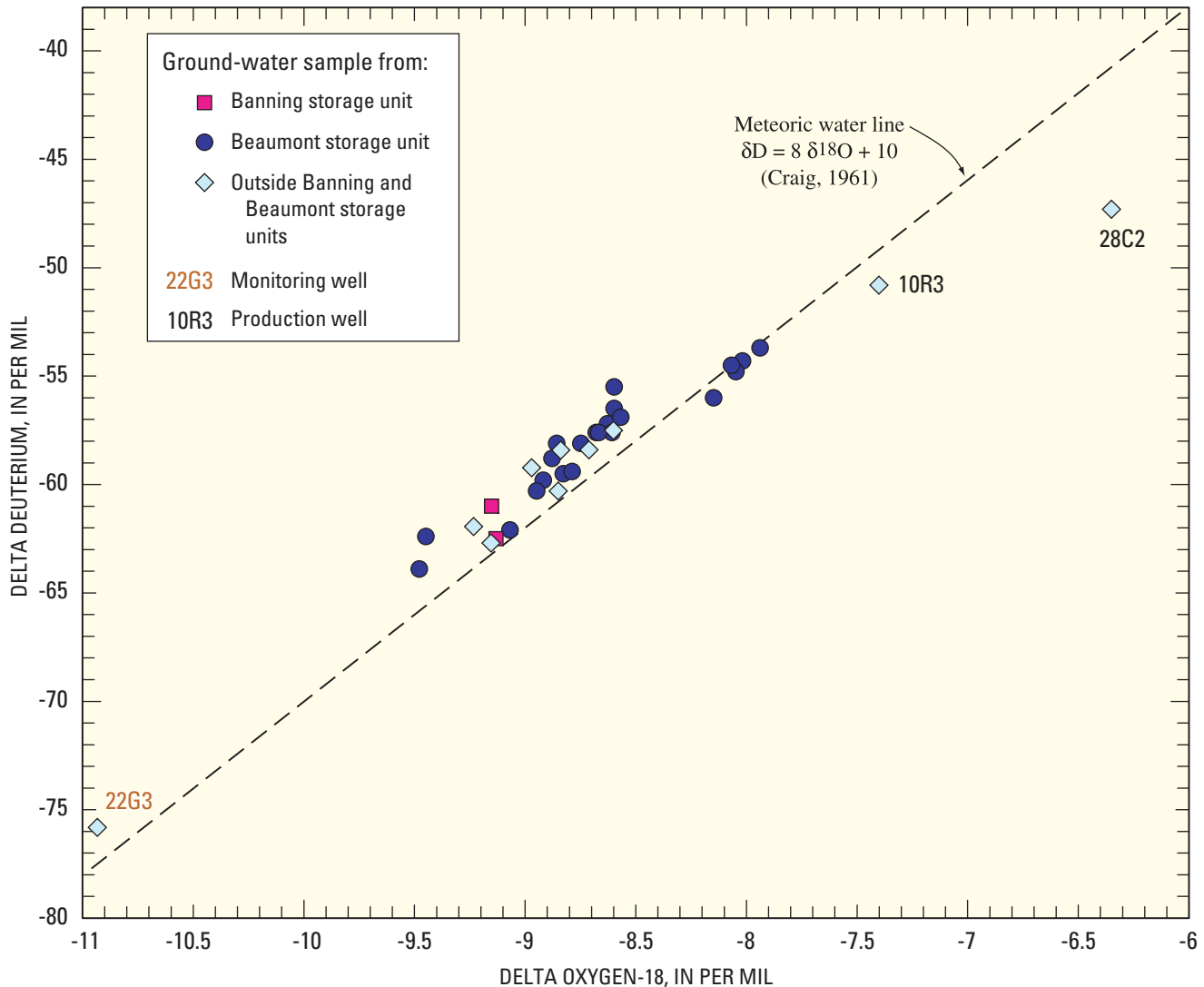


Figure 35. Graph showing stable isotope data for selected wells in the Beaumont and Banning storage units and surrounding area, San Gorgonio Pass area, Riverside County, California.

As a result, ^{14}C activities may exceed 100 pmc in areas where ground water contains tritium. Carbon-14 activities are used to determine the age of a ground-water sample on timescales ranging from recent to more than 20,000 years before present. Carbon-14 is not part of the water molecule and, therefore, ^{14}C activities may be affected by chemical reactions that remove or add carbon to solution. In addition, ^{14}C activities are affected by the mixing of younger water that has high ^{14}C activity with older water that has low ^{14}C activity. Carbon-14 ages presented in this report do not account for changes in ^{14}C activity resulting from chemical reactions or mixing and, therefore, are considered uncorrected ages. In general, uncorrected ^{14}C ages are older than the actual age of the associated water. Izbicki and others (1995) estimated that uncorrected ^{14}C ages were as much as 30 percent older than actual ages for ground water in the regional aquifer in the Mojave River ground-water basin (not shown), about 40 mi northwest of the study area.

Carbon-14 activities in ground water sampled from wells in the Beaumont, Banning, and surrounding storage units ranged from about 12 to 95 pmc. These ^{14}C activities correspond to uncorrected ^{14}C ground-water ages ranging from about 17,500 to 400 years before present (fig. 36). Excluding the samples from wells in the southeastern part of area 4 and in area 5, the ^{14}C activities ranged from 82 to 95 pmc with uncorrected ^{14}C ages of about 1,800 to 400 years before present. The chemical character of samples from the wells with high ^{14}C activities indicates that the upper aquifer contributes most of the water pumped from these wells; whereas, the chemical character of samples from the wells with low ^{14}C activities indicates that the lower aquifer contributes most of the water pumped from these wells. One would expect that water in the lower aquifer should have greater age than water in the upper aquifer because of longer vertical flow paths and lower permeability in the lower aquifer.

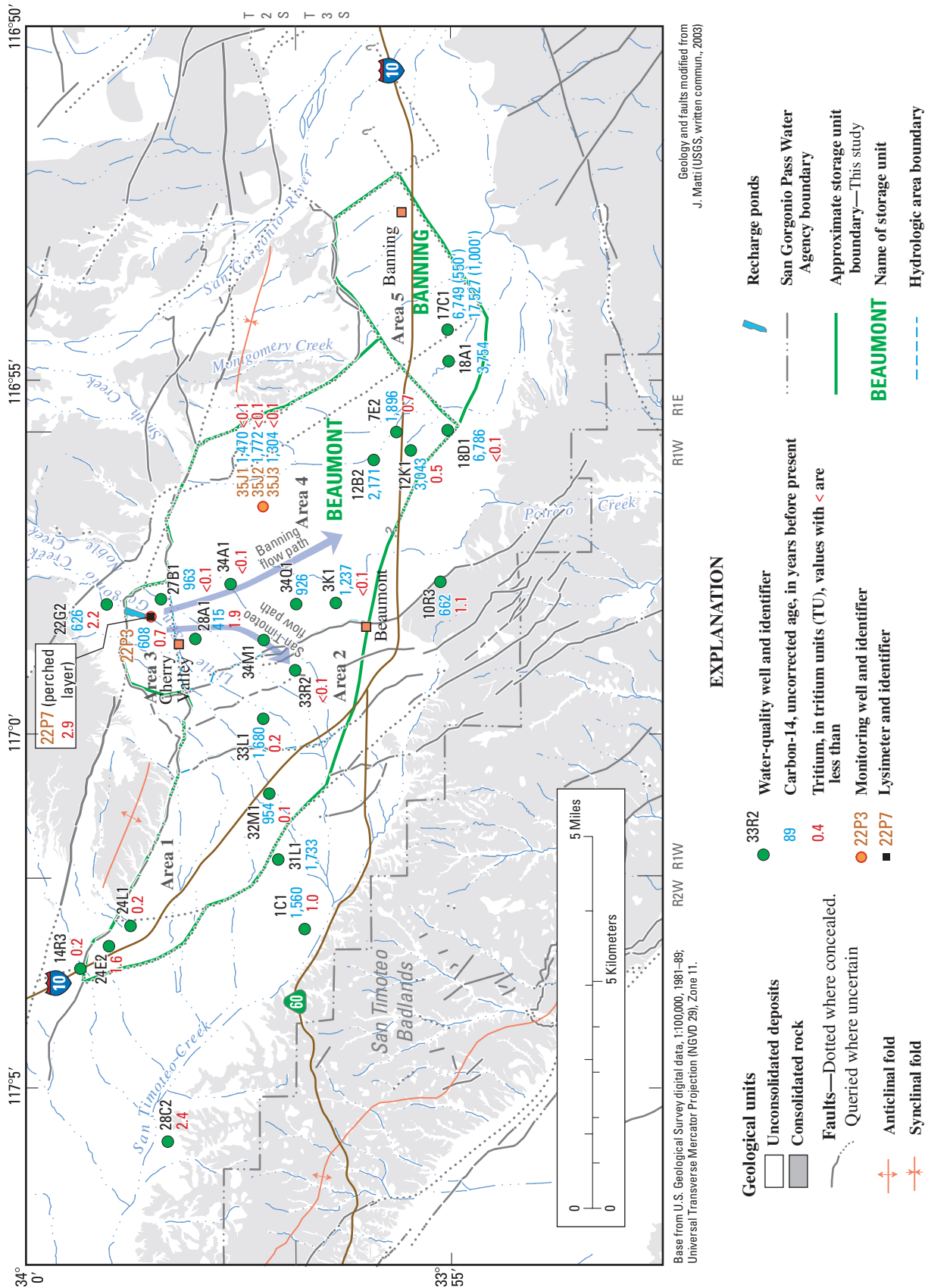


Figure 36. Map showing carbon-14 and tritium data for selected wells in the Beaumont and Banning storage units and surrounding area, San Geronimo Pass area, Riverside County, California.

The samples from wells in the eastern part of area 4 (3S/1W-12B2 and 12K1; 3S/1E-7E2 and 18D1) and in area 5 (3S/1E-17C1 and 18A1) had ^{14}C activities that ranged from 12 to 79 pmc which correspond to uncorrected ^{14}C ground-water ages ranging from about 17,500 to about 1,900 years before present. As previously stated, the lower aquifer contributes 50 percent or more of the water pumped from these wells. Pumping in the eastern part of area 4 near the Banning Barrier Fault has resulted in the dewatering of the upper aquifer (*fig. 33A*), causing a higher percentage of the pumped water to come from the lower aquifer.

The samples from 3S/1E-17C1, 18A1, and 18D1 have the lowest ^{14}C activities (12 to 64 pmc). Well 17C1 is perforated in the upper aquifer, the lower aquifer, and the underlying QTso deposits; whereas, wells 18A1 and 18D1 only are perforated in the upper and lower aquifers (*fig. 33A*). The samples from well 17C1 were collected at 550 and 1,000 ft below land surface, representing water from the upper aquifer and from the QTso deposits, respectively. The 550-ft sample had 44 pmc (uncorrected age of about 6,750 years before present) and the 1,000 ft sample had 12 pmc (uncorrected age of about 17,500 years before present). The low carbon activities in samples from these three wells probably indicate some mixing with ground water from the QTso deposits. Water from the QTso deposits can mix with the water pumped from a well by (1) entering the well directly if the well is perforated in these deposits (as is the case for well 17C1), (2) direct upward migration from the QTso deposits to the overlying lower aquifer, or (3) upward migration along fault zones to the upper and lower aquifers. In addition, the barrier effect of the Banning Barrier Fault and the inferred central Banning Barrier Fault restricts ground-water flow across the faults and increases the travel time for water to move from the Beaumont storage unit to wells 18A1 and 17C1 in the Banning storage unit.

Some samples contain tritium in excess of 0.2 TU, indicating recharge after 1952, and low ^{14}C activities, indicating older water (*fig. 36*). This indicates that the wells are pumping water from different zones or aquifers that contain different age ground water. For example, the sample from well 3S/1W-12K1 [perforated in the upper and lower aquifers (*fig. 33A*)] has 0.5 TU and has an uncorrected ^{14}C age of about 3,000 years before present (*fig. 36*).

Ground-Water Simulation Model

Model Objectives and Assumptions

To better understand the dynamics of ground-water flow and the potential effects of water-level changes resulting from the artificial recharge of imported SWP water, and for use as a tool to help manage ground-water resources in the San Gorgonio Pass area, a regional-scale, numerical ground-water flow model was developed for the Banning and Beaumont

storage units. The ground-water flow model was developed using MODFLOW-96 (McDonald and Harbaugh, 1996). MODFLOW-96 is a finite-difference model that simulates ground-water flow in a three-dimensional heterogeneous and anisotropic medium provided that the principal axes of hydraulic conductivity are aligned with the coordinate directions and that the fluid has constant density. For additional information regarding MODFLOW-96, the reader is referred to McDonald and Harbaugh (1996). The MODFLOW-96 packages used in this model included Basic (BAS), Block-Centered Flow (BCF3), Drain (DRN), Horizontal-Flow-Barrier (HFB), Recharge (RCH), General Head (GHB), and Well (WEL) (McDonald and Harbaugh, 1988, 1996; Hsieh and Freckleton, 1993). The Preconditioned Conjugate-Gradient (PCG2) solver was used for both steady state and transient simulations (McDonald and Harbaugh, 1988; Hill, 1990). In addition, the Wet/Dry option was used to allow model cells to dry and rewet as heads fluctuated in response to changes in pumping stresses (McDonald and others, 1992).

A numerical ground-water flow model is a simplified representation of the actual ground-water flow system. The model is based on simplifying assumptions and approximations and, therefore, it cannot simulate exactly the inherent complexity of the geohydrologic framework. The results of model simulation are only an approximation or an expectation of actual conditions and are only as accurate or realistic as the assumptions and data used in its development. Limitations of the model are discussed later in this report.

Input data were provided by the SGPWA, various water agencies in the area, the California Department of Water Resources; the Water Resources Institute; California State University, San Bernardino, Archives; and the USGS National Water Information System database. The extent and vertical geometry of the active model domain were defined on the basis of interpretations of surface and subsurface geology as described earlier in this report.

Assumptions used to develop the model in this study include

- the ground-water flow system of the Banning and Beaumont storage units can be conceptualized as two aquifers and each aquifer can be represented by a separate model layer;
- ground-water flow within each aquifer is primarily horizontal and flow between aquifers is vertical;
- the aquifers are horizontally homogeneous and isotropic and vertically anisotropic;
- historical ground-water pumping did not cause aquifer deformation or compaction;
- tectonism did not affect the ground-water flow system during the simulated time period (1926–2003); and
- the older sedimentary deposits and crystalline basement rocks that underlie the Beaumont and Banning storage units do not contribute ground water to the flow system.

Model Discretization

Spatial Discretization

To numerically solve for the distribution of hydraulic heads within the continuous aquifer system, it is necessary to spatially and temporally discretize the system. The aquifer system was discretized areally into 1,000- by 1,000-foot cells in a 50-row by 130-column grid (*fig. 37*). The model grid extends eastward to include the Cabazon storage unit to allow future expansion of the model. The active model domain includes the Beaumont and Banning storage units. For modeling purposes, the Beaumont and Banning storage units were subdivided into five areas on the basis of faults that are partial barriers to ground-water flow (*fig. 38*). The model domain initially was based on geohydrologic data collected by previous investigators and for this study. Estimates of average aquifer properties (such as hydraulic conductivity and storage coefficient) were assigned to the representative cell, and average hydraulic head was calculated at the center, or node, of each cell.

The aquifer system was vertically discretized into two layers to simulate vertical flow through the ground-water system. The vertical layering is shown with the relative thicknesses and altitudes of the model layers in *figure 39*. Model layer 1 represents the upper aquifer (*fig. 38A*), which consists of the saturated part of the very old deposits (Qvo) and the upper part of the younger sedimentary deposits (Qsu). Model layer 1 was simulated as an unconfined aquifer. Model layer 2 represents the lower aquifer (*fig. 38B*), which consists of the lower part of the younger sedimentary deposits (Qsl). Model layer 2 was simulated as a convertible aquifer (either confined or unconfined), that is, cells in layer 2 convert from confined to unconfined conditions when an overlying cell is simulated as being unsaturated. Conversely, cells in layer 2 convert from unconfined to confined conditions when an overlying cell in layer 1 is simulated as being saturated. When the model layer represents confined conditions, hydraulic conductivity and storage coefficient are used in the flow equation; when the model layer represents unconfined conditions, hydraulic conductivity and specific yield are used in the flow equation.

The top altitude of model layer 1 represents the water table. The bottom altitude of model layer 1, or the top altitude of model layer 2, is the contact between the upper and lower parts of the younger sedimentary deposits (*figs. 6 and 39*). The bottom altitude of model layer 2 is the contact between the lower part of the younger sedimentary deposits and the older sedimentary deposits or the crystalline basement rocks. The top and bottom altitudes of the model layers were spatially variable, and were determined using the geological cross sections developed for this study (*fig. 6*). The bottom altitudes of

model layers 1 and 2 are presented on *figure 40*. During model simulations, the water-table altitude may rise to land surface and drop to the bottom of layer 2. As a result, both layer 1 and layer 2 can have variable saturated thickness.

Temporal Discretization

The model was used to simulate both steady-state and transient conditions. The steady-state simulation represented pre-1927 conditions, which are assumed to represent predevelopment conditions in the Beaumont and Banning storage units. These simulated predevelopment conditions were used as initial conditions for the transient simulation that represented conditions from 1926 through 2003.

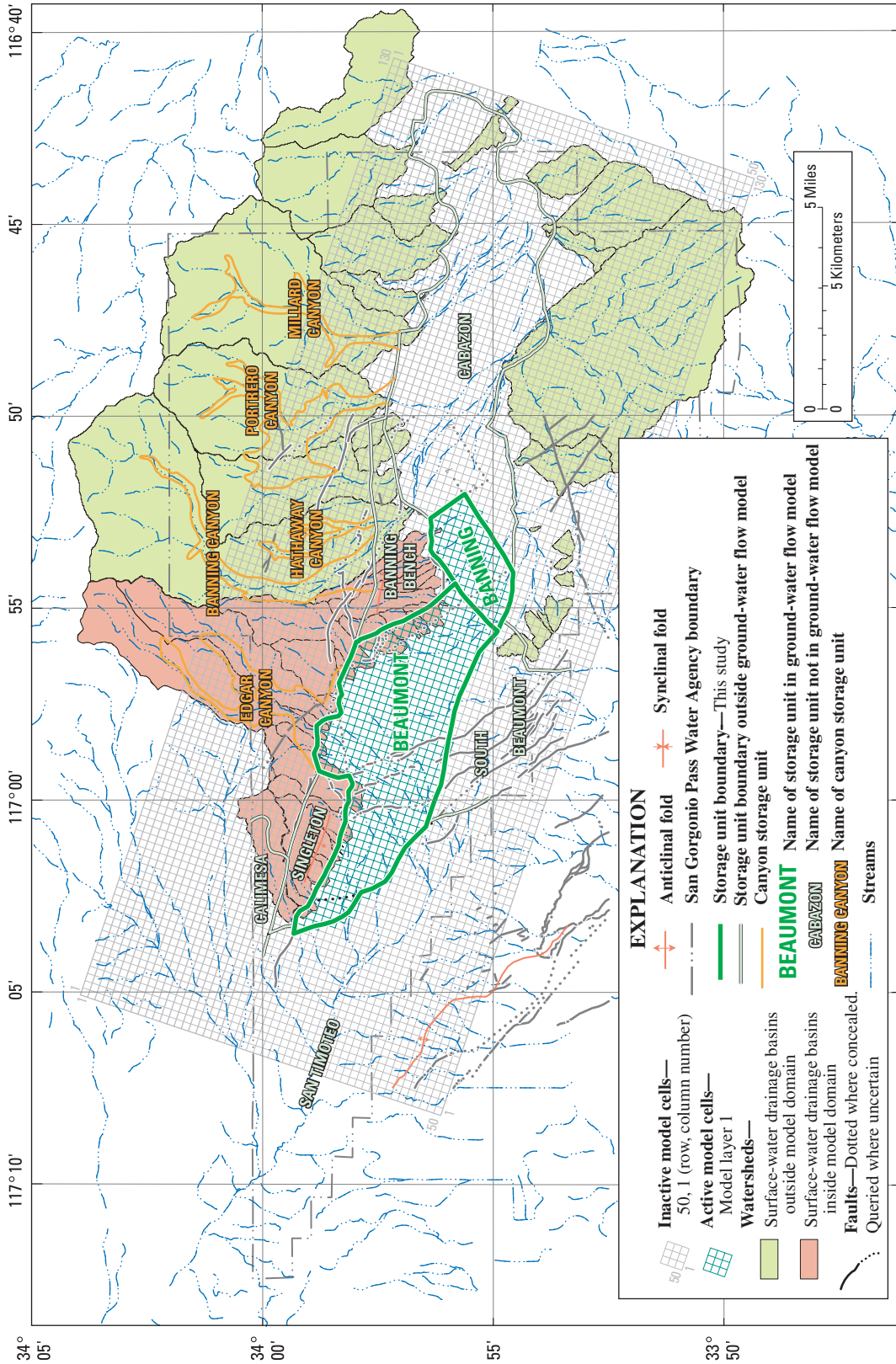
For the transient simulation, the temporal discretization consisted of seventy-eight 1-year stress periods, each simulated using 1-month time steps. A stress period is a time interval during which all external stresses are constant (McDonald and Harbaugh, 1988). One-year stress periods were selected to be able to adequately represent the reported change in annual pumpage rates in the Beaumont and Banning storage units.

The adequacy of the transient temporal discretization was verified by analyzing the time-varying mass-balance and the cumulative mass-balance errors. In general, the time-varying mass-balance errors did not fluctuate in an unstable manner, and the cumulative mass-balance errors were small (*fig. 41*).

Boundary Conditions

For the ground-water flow model in this study, two general types of boundary conditions were used: specified flux and head-dependent flux boundaries. Specified-flux boundary conditions are used to simulate water flowing into or out of the model domain at a specified rate that remains constant for the entire stress period. Head-dependent flux boundaries are used to simulate water flowing into or out of the model domain at a rate that is the product of a specified factor and the difference between the simulated head at the boundary and a specified head of an external source/sink.

Specified-flux boundary conditions were assigned to the top of model layer 1 to simulate natural recharge from stream-flow infiltration and the direct infiltration of precipitation; all active cells in model layer 1 were assigned a specified-flux boundary (*fig. 38*). Specified-flux cells also were assigned to selected cells along the northern boundary of the Beaumont and Banning storage units to simulate mountain-front recharge (*fig. 38*).



Base from U.S. Geological Survey digital data, 1:24,000, 1927 North American Datum; Universal Transverse Mercator Projection, Zone 11.

Figure 37. Map showing the ground-water flow model grid for the Beaumont and Banning storage units, San Gorgonio Pass area, Riverside County, California.

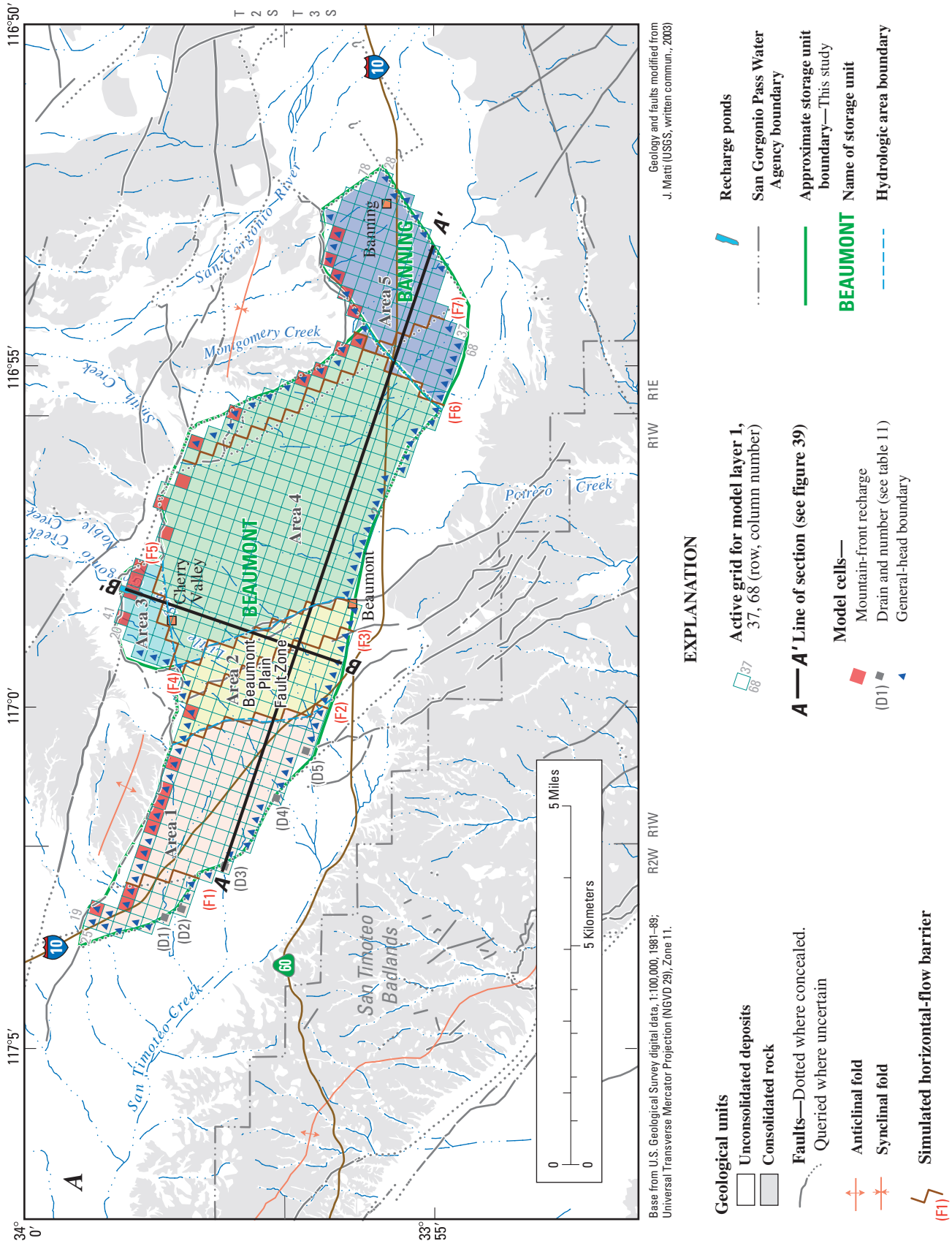


Figure 38. Map showing the active model grid and boundary conditions for the ground-water model for (A) model layer 1 and (B) model layer 2, San Gorgonio Pass area, Riverside County, California.

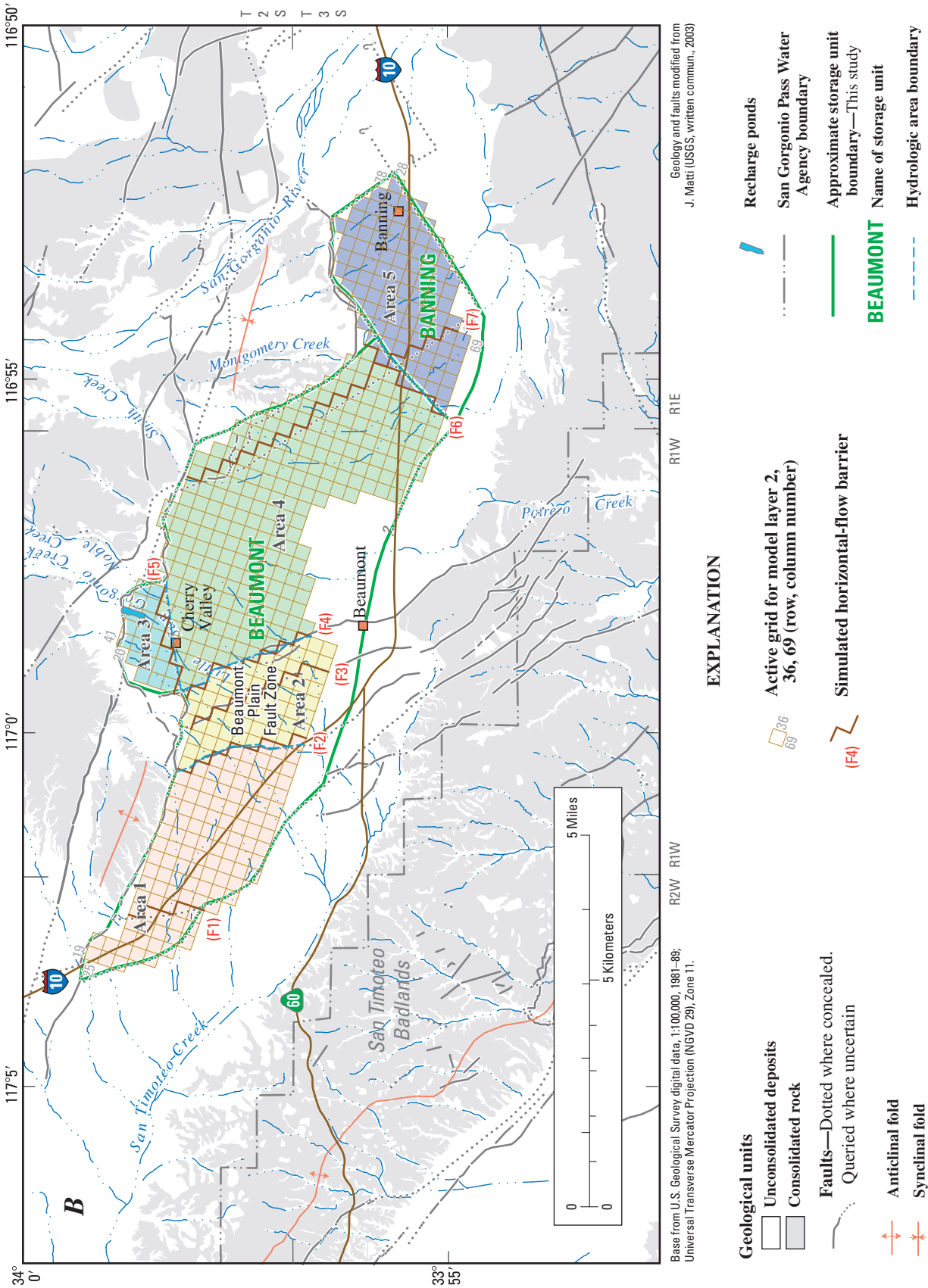


Figure 38. Continued.

Geology and faults modified from J. Matti (USGS, written commun., 2003)

Base from U.S. Geological Survey digital data, 1:100,000, 1981-89; Universal Transverse Mercator Projection (NAD 83), Zone 11.

EXPLANATION

- Geological units
 - Unconsolidated deposits
 - Consolidated rock
- Faults—Dotted where concealed. Queried where uncertain
 - Anticlinal fold
 - Synclinal fold
- Recharge ponds
- San Geronio Pass Water Agency boundary
- Approximate storage unit boundary—This study
- Name of storage unit
- Hydrologic area boundary
- Active grid for model layer 2, 36, 69 (row, column number)
- Simulated horizontal-flow barrier

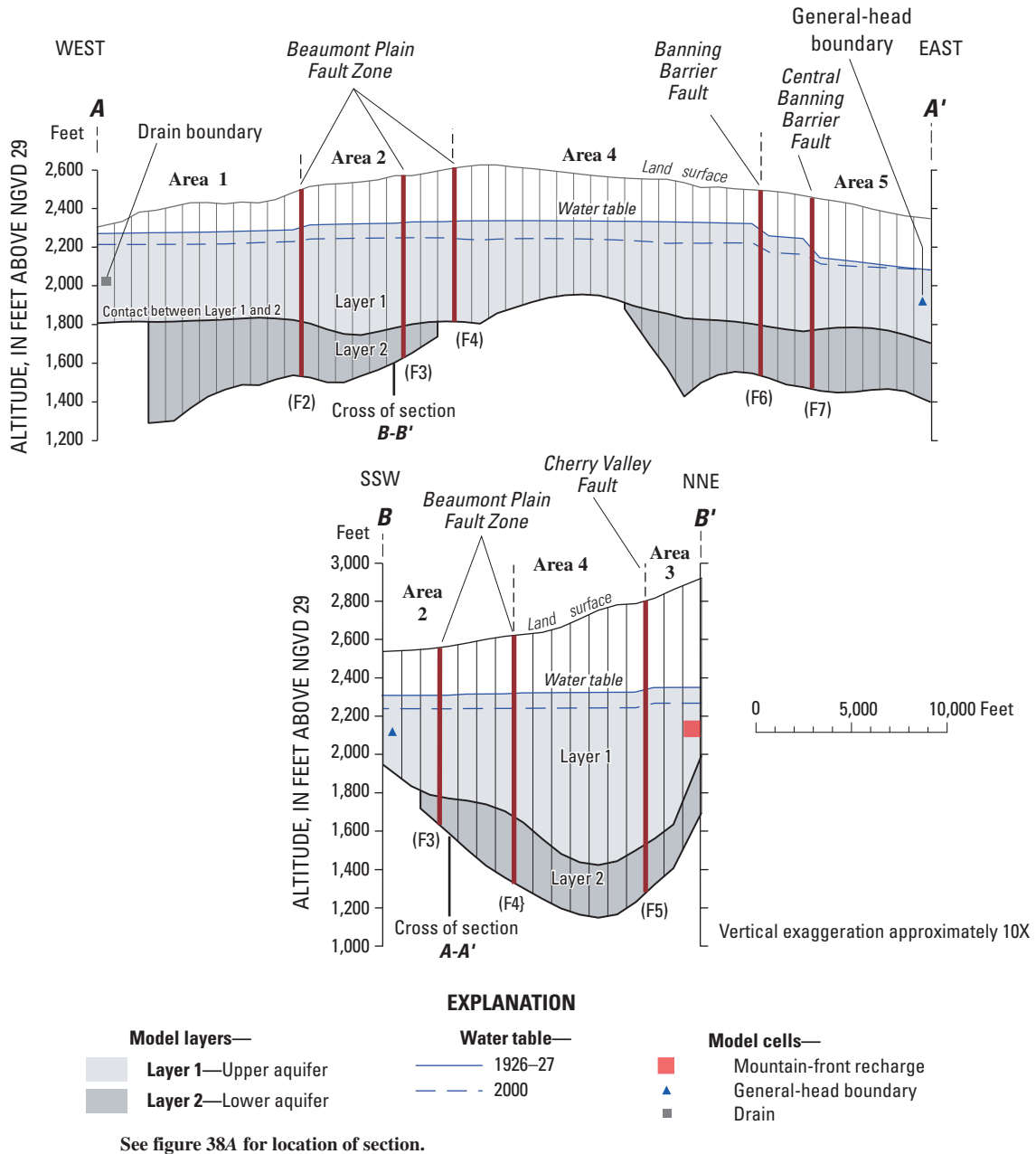


Figure 39. Generalized model cross sections A–A’ and B–B’ showing vertical discretization of the ground-water flow model, San Geronio Pass area, Riverside County, California.

No-flow boundary conditions were assigned to model layer 1 along the northern boundary of area 3 and part of the southern boundary of area 5 (fig. 38A), and were assigned to model layer 2 along all lateral boundaries (fig. 38B). A no-flow boundary is a special case of a specified flux boundary where zero flux conditions exist. A no-flow boundary indicates that there is no exchange of water between the model cell and the domain outside of the model. For the most part, these no-flow boundaries correspond to locations where low-

permeability crystalline basement rocks and the upper and lower aquifers are juxtaposed or where the older sedimentary deposits (QTso) and lower aquifer are juxtaposed (fig. 6). The bottom of the model also was assigned a no-flow boundary because it corresponds to the top of the older sedimentary deposits (QTso) or crystalline basement rocks, which were assumed to yield little to no water to the ground-water flow system.

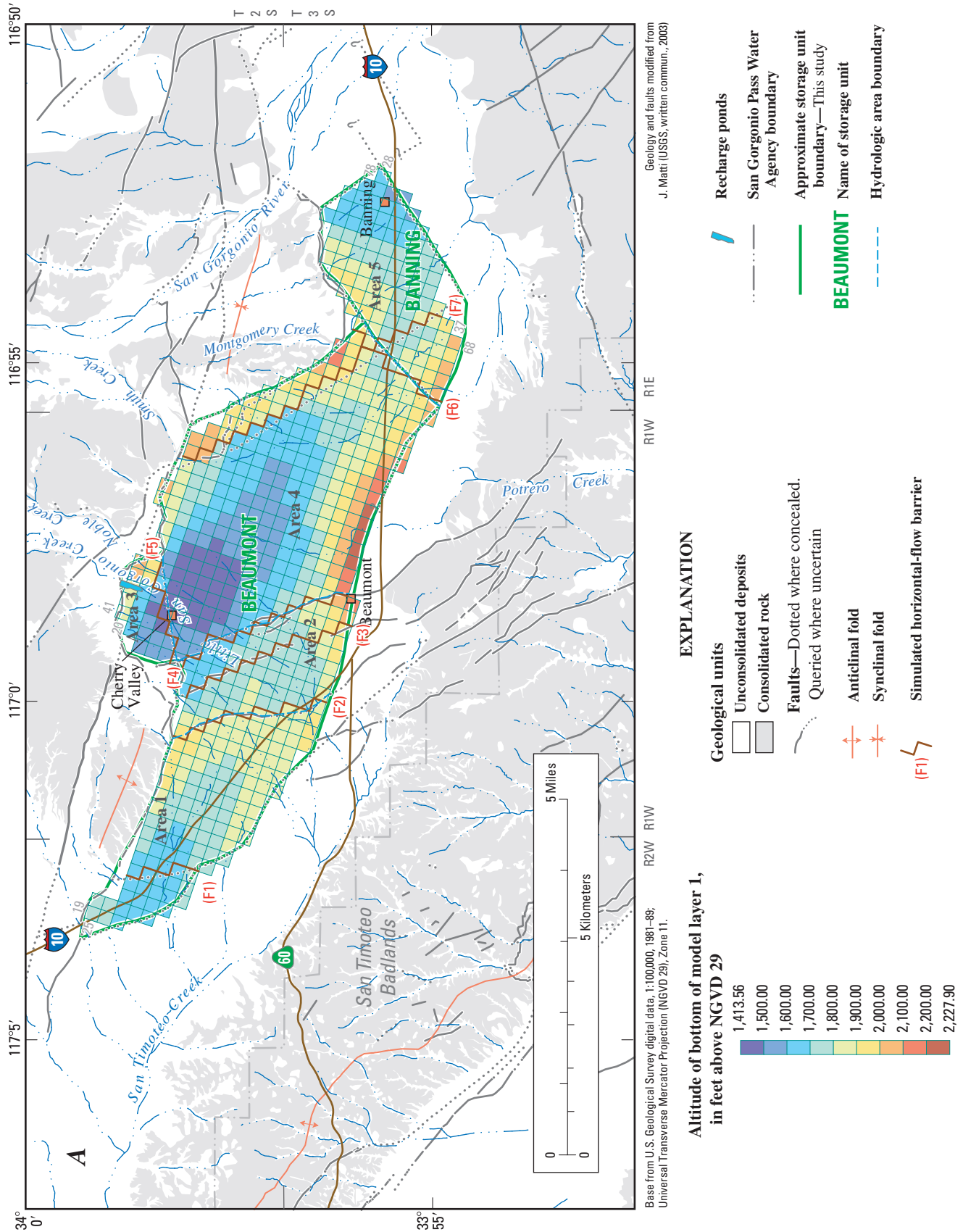


Figure 40. Map showing the bottom altitudes for (A) model layer 1 and (B) model layer 2, San Gorgonio Pass area, Riverside County, California.

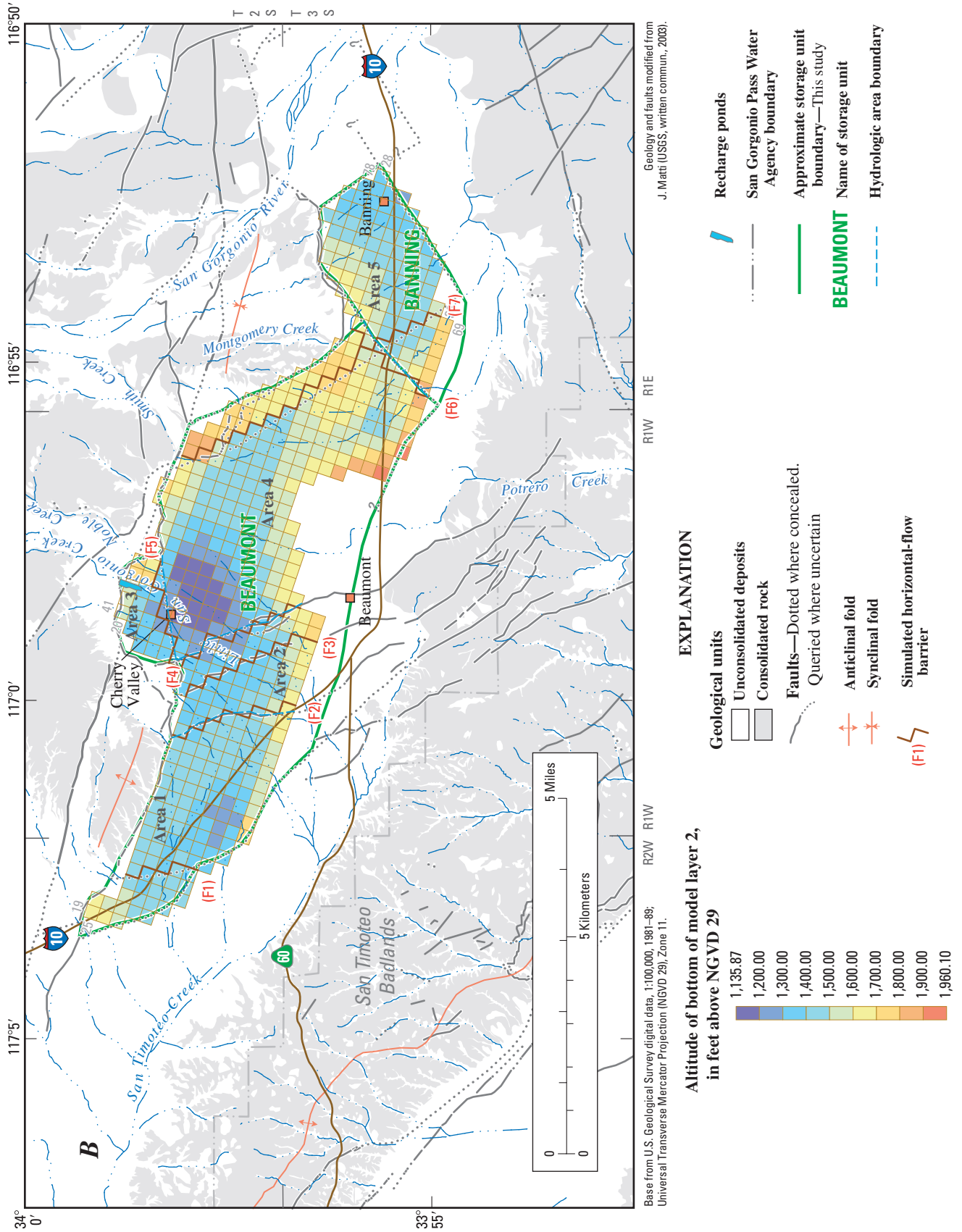


Figure 40. Continued.

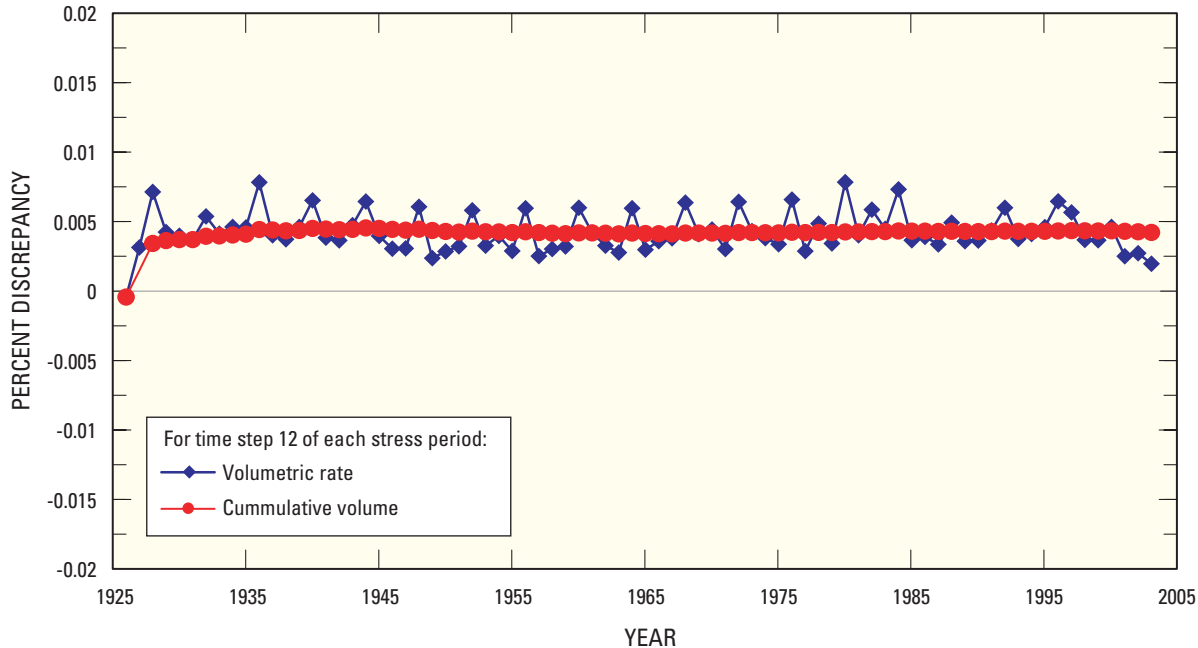


Figure 41. Time-varying and cumulative mass-balance errors simulated by the ground-water flow model, San Geronio Pass area, Riverside County, California.

Drain boundary conditions were assigned to model layer 1 along parts of the southwestern boundary of the Beaumont storage unit to simulate the natural ground-water discharge from the Beaumont storage unit to stream channels draining the San Timoteo storage unit (fig. 38A). A drain is a head-dependent flux boundary condition which removes water from the model domain at a rate proportional to the difference between the simulated head in the drain cell and some specified head or elevation, as long as the simulated head is above the specified elevation; a drain cell reverts to a variable-head cell if the simulated head falls below that specified elevation (McDonald and Harbaugh, 1988). The variable-head cell reverts back to the drain cell if the simulated head rises above the specified elevation. Drain elevations were set to 50 ft below the average land-surface elevation of the stream channel (the estimated depth of the stream deposits). The constant of proportionality is termed the drain conductance (L^2T^{-1}). Drain conductance values were determined during the calibration process (table 10).

General-head boundaries were assigned to model layer 1 along most of its lateral boundaries (fig. 38A) to simulate ground-water movement between the upper aquifer and the surrounding older sedimentary deposits (QTso), except in parts of areas 3 and 5 where crystalline rocks and the upper aquifer are juxtaposed. Although the permeability of the QTso unit is low, there is probably limited ground-water movement between the shallow less consolidated part of these deposits and the upper aquifer. A general-head boundary is a head-dependent flux boundary used to simulate a source of water outside the model area that either supplies water to, or receives

water from, the general-head cells at a rate proportional to the hydraulic-head differences between the source and the model cell (McDonald and Harbaugh, 1988). The head assigned to the general-head boundary was estimated from available water-level data and was assumed constant with time (figs. 27 and 28, table 10). The constant of proportionality is termed the conductance (L^2T^{-1}). General-head conductance values were determined during the calibration process (table 10). For this study, the general-head conductance values were low because the boundary generally is associated with a low permeability fault zone.

Aquifer Properties

Aquifer properties assigned to model layers, such as horizontal and vertical hydraulic conductivity, vertical conductance, specific yield, specific storage, hydraulic characteristics of flow barriers, and boundary conditions, affect the rate at which ground water moves through an aquifer, the volume of water in storage, and the rate and areal extent of ground-water-level declines caused by pumping. Initial estimates of horizontal and vertical hydraulic conductivity, vertical conductance, specific yield, and specific storage used by this model were estimated using previous modeling studies, aquifer tests, interpreted geologic data, or published values (Freeze and Cherry, 1979; Fetter, 1994). The final estimates of these aquifer properties were determined during the model-calibration process using a trial-and-error approach under steady-state and transient conditions.

Table 10. Summary of initial and calibrated parameter estimates used in the ground-water flow model of the San Geronio Pass area, Riverside County, California.

[See figure 38 for area distribution. Altitude in feet above National Geodetic Vertical Datum of 1929. ft, feet; ft/d; feet per day; ft⁻¹, per foot; ft²/d, square foot per day; d⁻¹, per day]

Hydraulic properties		Affected layer	Area					Applicable units
			1	2	3	4	5	
Horizontal hydraulic conductivity	Initial	1	20.0	20.0	20.0	20.0	20.0	ft/d
		2	1.0	1.0	1.0	1.0	1.0	
	Calibrated	1	30.0	30.0	30.0	30.0	10.0	
		2	2.0	2.0	2.0	2.0	2.0	
Vertical hydraulic conductivity ¹	Initial	1	0.20	0.20	0.20	0.20	0.20	ft/d
		2	0.01	0.01	0.01	0.01	0.01	
	Calibrated	1	0.30	0.30	0.30	0.30	0.10	
		2	0.02	0.02	0.02	0.02	0.02	
Specific yield ²	Initial	1	0.10	0.10	0.10	0.10	0.10	ft ⁻¹
	Calibrated	1	0.18	0.18	0.14	0.18	0.05	
Specific storage ²	Initial	1	1.0 × 10 ⁻⁶	ft ⁻¹				
	Calibrated	1	1.0 × 10 ⁻⁶					

General-head property ranges for layer 1 along Beaumont and Banning storage unit boundaries with other storage units

Storage units	Affected area	Initial		Calibrated	
		Altitude of source hydraulic head (ft)	Conductance (ft ² /d)	Source hydraulic head (ft)	Conductance (ft ² /d)
San Timoteo	1	2,175–2,205	1.0 × 10 ⁴	2,175–2,205	1.0–125.0
Singleton	1–4	2,300–2,500	1.0 × 10 ⁴	2,300–2,500	2.0
South Beaumont	2,4,5	2,240–2,250	1.0 × 10 ⁴	2,240–2,250	2.5–40.0
Banning Bench	4,5	2,500–3,100	1.0 × 10 ⁴	2,500–3,100	2.0
Cabazon	5	1,805	1.0 × 10 ⁴	1,805	185.0

Drain properties

Drain number	Affected layer	Initial		Calibrated	
		Altitude (ft)	Conductance (ft ² /d)	Altitude (ft)	Conductance (ft ² /d)
D1	1	2,200	1.0 × 10 ⁴	2,170	2.5 × 10 ⁻³
D2	1	2,300	1.0 × 10 ⁴	2,270	5.0 × 10 ⁻³
D3	1	2,400	1.0 × 10 ⁴	2,350	4.0 × 10 ⁻³
D4	1	2,420	1.0 × 10 ⁴	2,370	4.0 × 10 ⁻³

Horizontal-flow barrier hydraulic characteristic

Horizontal-flow barrier number	Affected area	Initial		Calibrated	
		Layer 1 (d ⁻¹)	Layer 2 (ft/d)	Layer 1 (d ⁻¹)	Layer 2 (ft/d)
F1	1	20.0	700	1.5 × 10 ⁻³	1.5 × 10 ⁻³
F2	1, 2	20.0	1,100	1.2 × 10 ⁻³	1.2 × 10 ⁻³
F3	2	20.0	850	2.0 × 10 ⁻³	2.0 × 10 ⁻³
F4	2, 4	20.0	800	2.0 × 10 ⁻³	2.0 × 10 ⁻³
F5	3, 4	20.0	550	3.0 × 10 ⁻⁴	3.0 × 10 ⁻⁴
F6	4, 5	20.0	600	7.0 × 10 ⁻⁴	7.0 × 10 ⁻⁴
F7	5	20.0	600	6.0 × 10 ⁻⁴	3.0 × 10 ⁻⁵

¹Vertical anisotropy assumed 100:1.

²Transient state only.

Hydraulic Conductivity and Transmissivity

The transmissivity of model layers 1 and 2 is calculated by the model and is the product of the horizontal hydraulic conductivity (K_h) and the saturated thickness for each model cell. Initial values of K_h for both model layers were estimated by dividing the transmissivity values estimated from specific capacity tests (*Appendix table 2*) by the perforated interval of the tested well. The initial values were modified during the steady-state calibration process. Final calibrated K_h values are presented in *table 10*.

The saturated thickness of model layer 1, for a particular stress period, is calculated in the model by subtracting the altitude of the bottom of layer 1 (fig. 40A) from the simulated water-table altitude. The saturated thickness of model layer 2, for a particular stress period, is calculated in the model by subtracting the altitude of the bottom of layer 2 (fig. 40B) from the altitude of the bottom of layer 1 if the simulated water table is above the altitude of the bottom of layer 1 or by subtracting the altitude of the bottom of layer 2 from the simulated water table if the simulated water table is below the altitude of the bottom of layer 1. The transmissivity distribution calculated by the model for layers 1 and 2 for steady-state conditions is shown on *figure 42*.

Vertical Conductance

Vertical leakage of water between model layers 1 and 2 occurs whenever there is a difference in hydraulic head between those layers. The rate at which this leakage occurs is described by the equation:

$$Q = \frac{K_v A (H_1 - H_2)}{B}$$

where:

- Q is the vertical leakage [L^3T^{-1}],
- K_v is the effective value of vertical hydraulic conductivity between the center of cells [LT^{-1}],
- A is the area of the cell [L^2],
- H_2 is the hydraulic head in layer 2 [L],
- H_1 is the hydraulic head in layer 1 [L], and
- B is the length of the vertical flow path [L].

The quantity K_v/B in the above equation is referred to as the vertical leakage term and is known in the MODFLOW

model as VCONT (McDonald and Harbaugh, 1988). MODFLOW-96 requires that the user specifies VCONT as input data. VCONT is calculated using the following equation:

$$VCONT = \frac{2}{\left(\frac{b_i}{K_{vi}}\right) + \left(\frac{b_{i+1}}{K_{vi+1}}\right)},$$

where

- b_i is the saturated thickness of model layer i [L] and,
- K_{vi} is the vertical hydraulic conductivity of model layer i [LT^{-1}].

The values of K_v for model layers 1 and 2 were assumed to be equal to one-hundredth the K_h of the model layers. The K_v of the model layers was assumed to be smaller than the K_h of the model layers because the K_v of an aquifer is controlled by the K_v values of fine-grained interbedded layers present in the upper and lower aquifers. It is not uncommon for layered heterogeneity to lead to regional anisotropy on the order of 100:1 or even larger (Freeze and Cherry, 1979). The values of saturated thickness used in the above equation were those that existed during steady-state conditions. VCONT values were varied only to reflect calibration changes in K_v . *Figure 43* shows the areal distribution of the calibrated VCONT values.

Specific Yield and Storage Coefficient

Model layer 1 was modeled as an unconfined layer; therefore, the input for the storage term was specific yield (S_y). S_y is defined as the volume of water released from storage in an unconfined aquifer per unit surface area of the aquifer per unit decline in head (Lohman, 1972). Model layer 2 was modeled as a convertible layer; therefore, the inputs for the storage term were S_y and storage coefficient (S). The S of an aquifer is the volume of water released from or taken into storage per unit of surface area per unit change in head (Lohman, 1972).

Initially S_y was assumed to equal 0.10 for the entire model area and the S of model layer 2 was estimated by multiplying the thickness of model layer 2 by a specific storage

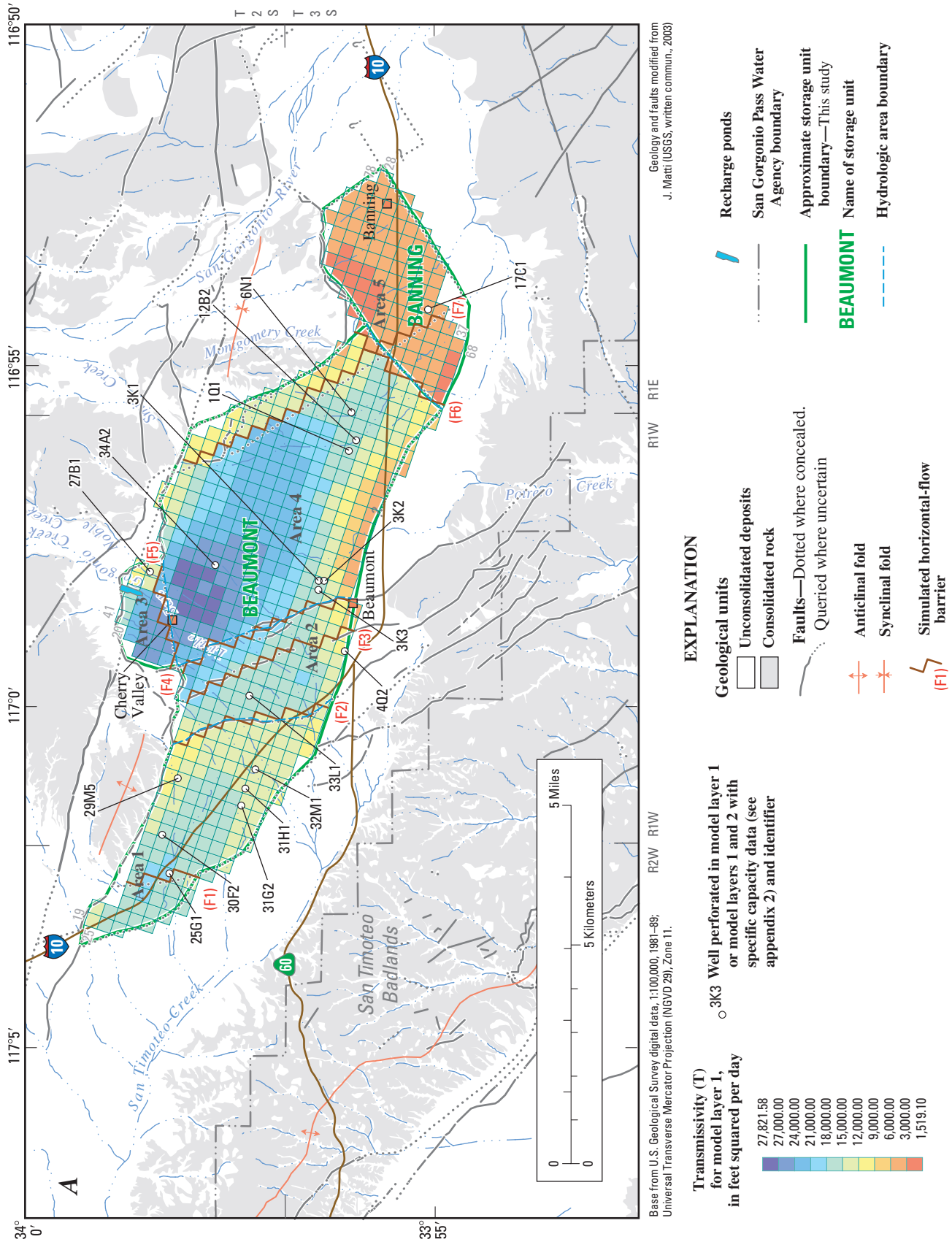


Figure 42. Map showing distribution of transmissivity values for (A) model layer 1, and (B) model layer 2 for the steady-state ground-water flow model, and (C) the percent decrease in transmissivity between the steady state and year-2003 for model layer 1.

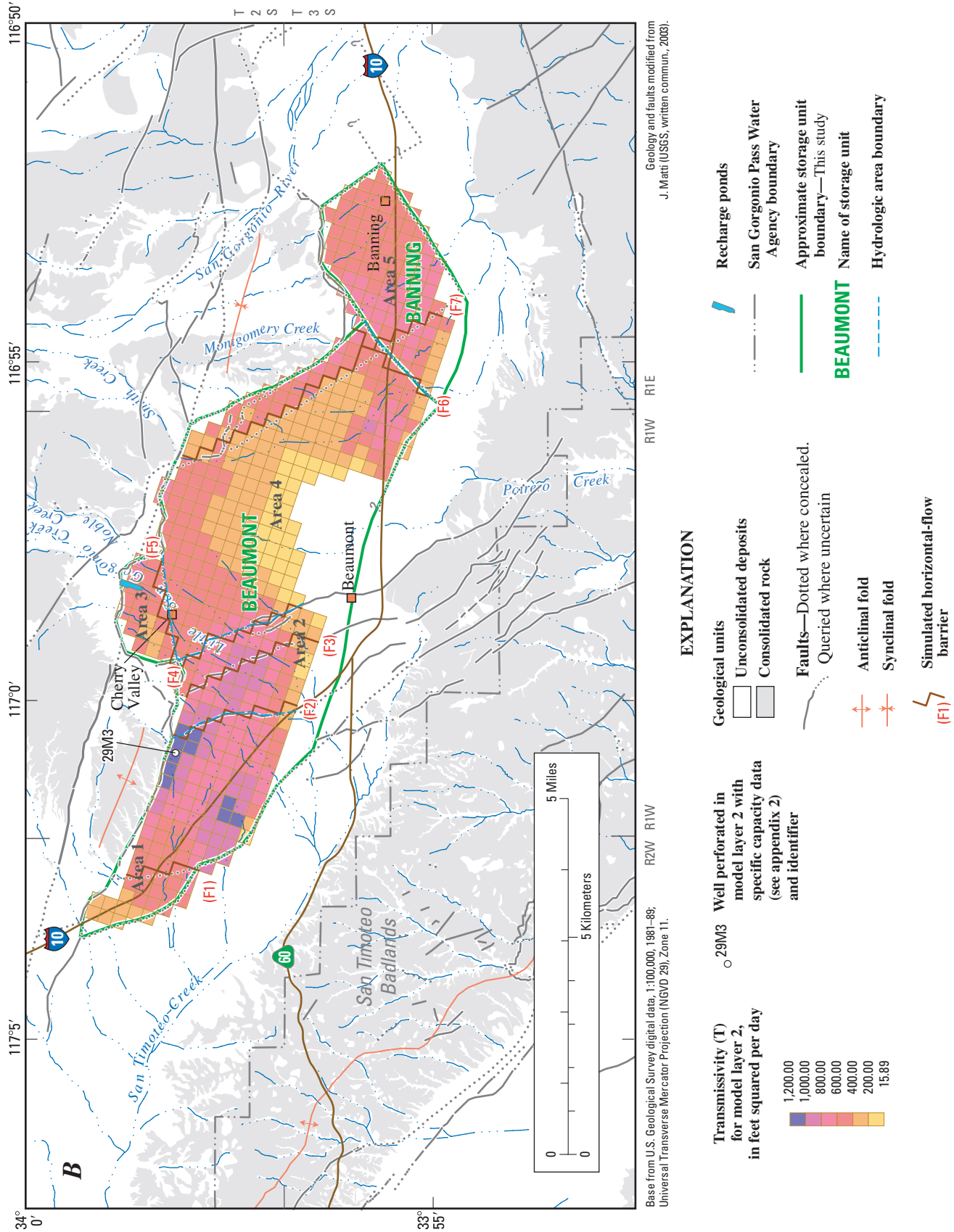


Figure 42. Continued.

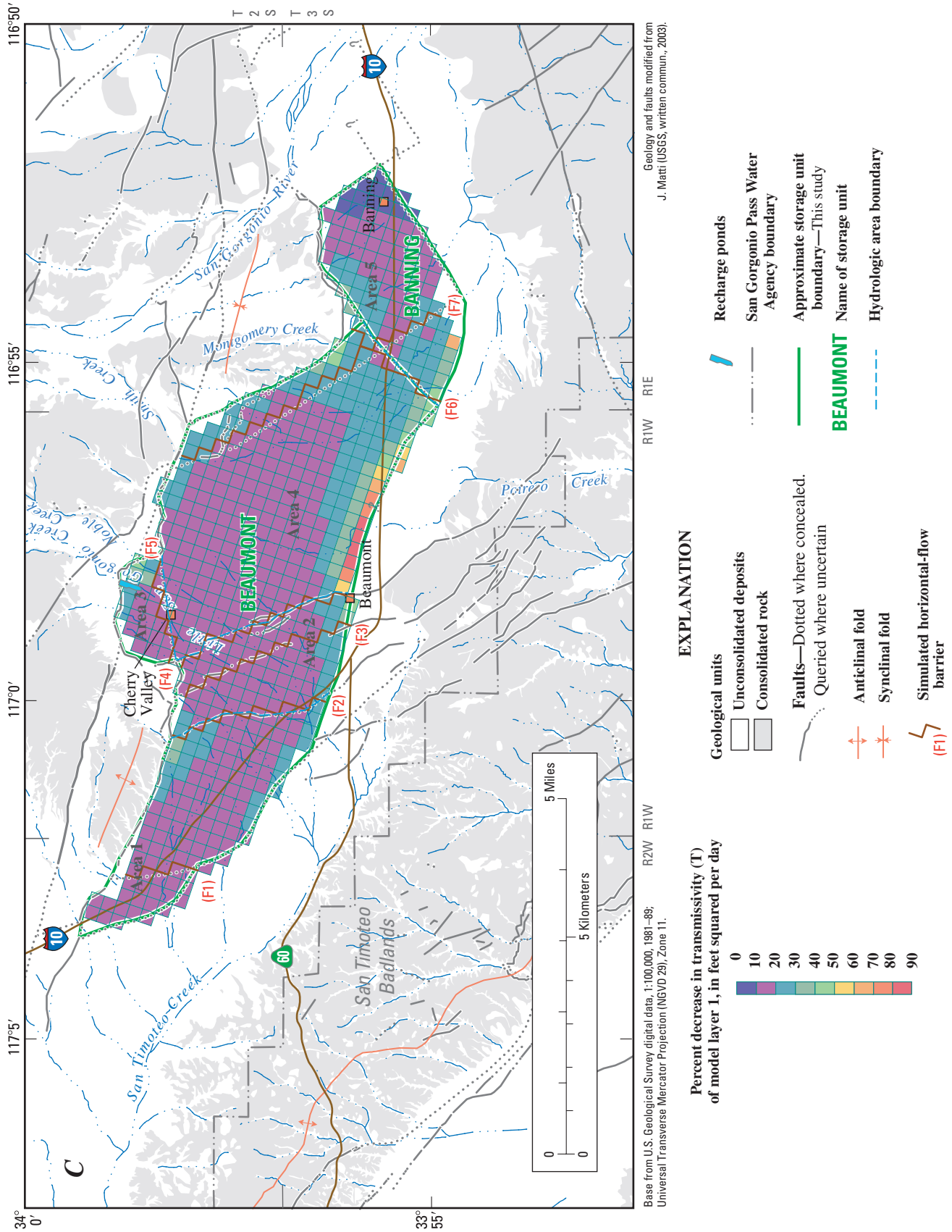


Figure 42. Continued.

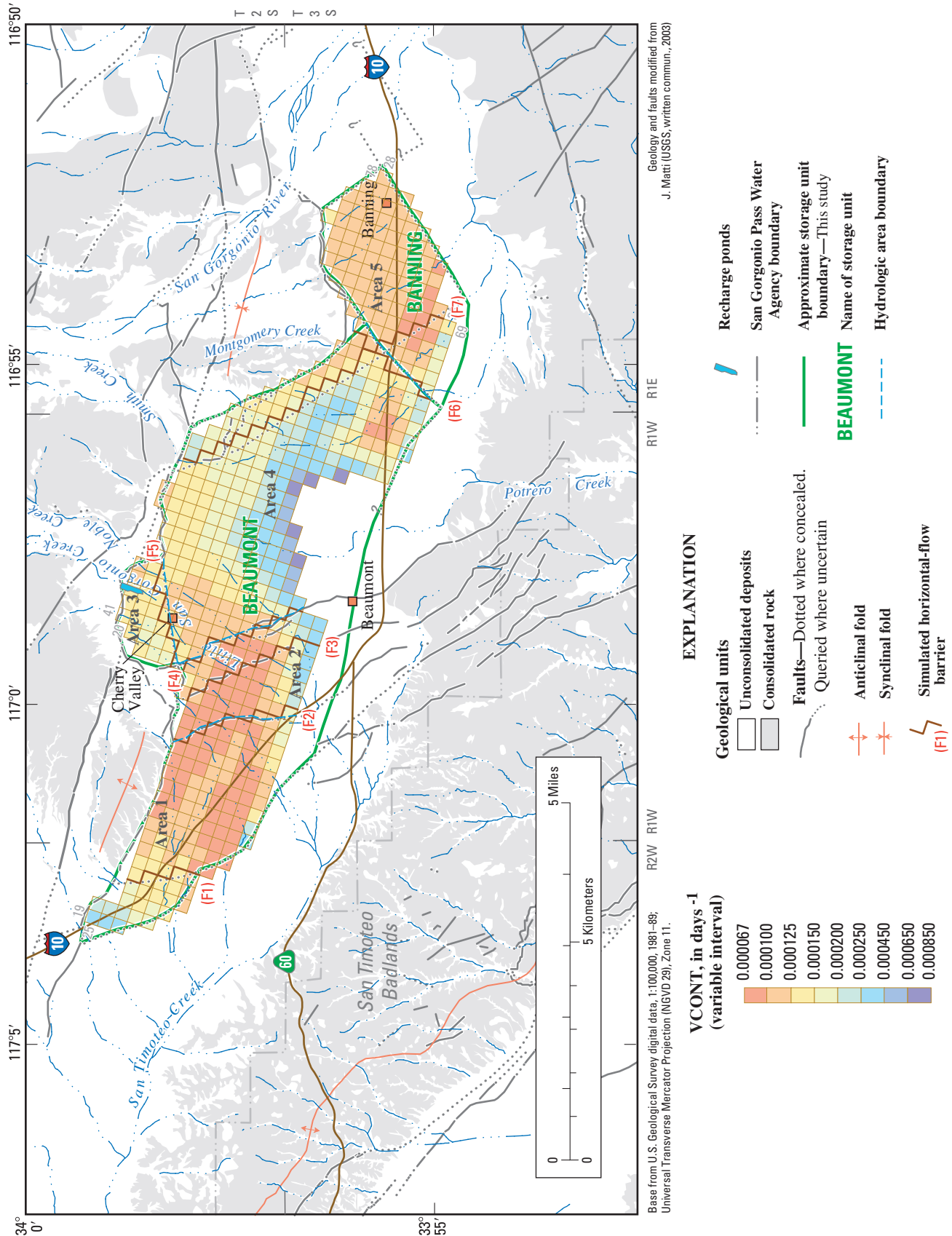


Figure 43. Map showing distribution of vertical conductance (VCONT) for the ground-water flow model between model layers 1 and 2, San Geronio Pass area, Riverside County, California.

coefficient (S_y) value of $1.0 \times 10^{-6} \text{ ft}^{-1}$ (Lohman, 1972). The S_s of a saturated confined aquifer is the volume of water that an aquifer releases from storage per volume of aquifer per unit decline in the component of hydraulic head normal to that surface (Freeze and Cherry, 1979). These initial estimates were adjusted during the model calibration process. The calibrated S_y values ranged from 0.05 in area 5 to 0.18 in areas 2 through 4. The calibrated S values for model layer 2 are presented on *figure 44*.

Faults

For this study, the MODFLOW-96 Horizontal Flow Barrier (HFB) Package (Hsieh and Freckleton, 1993) was used to simulate flow barriers, or faults, that affect ground-water flow within the model domain. The HFB package simulates faults as thin, vertical, low-permeability geologic features that impede the horizontal flow of ground water. Faults are approximated as a series of horizontal-flow barriers conceptually situated between pairs of adjacent cells in the finite-difference grid (Hsieh and Freckleton, 1993). Flow across a simulated fault is proportional to the hydraulic-head difference between adjacent cells where the constant of proportionality is the hydraulic characteristic whose value was determined during the calibration process. For unconfined aquifers, such as the upper aquifer simulated with model layer 1, the hydraulic characteristic equals the hydraulic conductivity of the flow barrier divided by the width of the barrier. For confined aquifers, such as the lower aquifer simulated as model layer 2, the hydraulic characteristic equals the transmissivity of the flow barrier divided by the width of the barrier.

The locations and areal extents of faults and flow barriers were identified from geologic information (as described in the geology section) or inferred from localized steep hydraulic-head (water-level) gradients. The faults simulated by the model were the inferred splay of the San Timoteo Canyon Fault (F1), faults in the Beaumont Plains Fault Zone (F2–4), the Cherry Valley Fault (F5), the Banning Barrier Fault (F6), and the Central Banning Barrier Fault (F7) (*fig. 38*). The calibrated hydraulic characteristic values are shown in *table 10*. Hydraulic characteristic values for individual faults and barriers were calibrated to simulate head gradients and drawdown throughout the transient simulation period.

Simulated Model Recharge

Ground-water recharge in the study occurs in direct response to rain and snowmelt and infiltration of streamflow in the Beaumont and Banning storage units, ground-water underflow from the canyon storage units, and artificial recharge. For

the purposes of this report, recharge in the model domain that occurs in direct response to rain and snowmelt and infiltration of streamflow that falls or flows over the model domain is termed areal recharge and recharge contributed by ground-water underflow from the canyon storage units is termed mountain-front recharge. Artificial recharge consists of return flow from applied water on crops, golf courses, and landscape; septic-tank seepage; infiltration of diverted storm runoff from Little San Gorgonio Creek; and imported SWP water into recharge ponds.

Areal recharge

Areal recharge was estimated for water years 1927 through 2001 using a deterministic, distributed-parameter precipitation-runoff model, INFILv3, described earlier in this report. The INFILv3 simulation results for natural conditions (prior to urbanization) indicated that the simulated average annual recharge for the Beaumont and Banning storage units is about 3,710 acre-ft/yr. This is equivalent to about 3.3 in/yr or about 17 percent of the precipitation rate. This simulated areal recharge represents in-place recharge in direct response to precipitation that falls on the storage units and also recharge resulting from infiltration of water in stream channels that originated as surface runoff in the Beaumont and Banning storage units and surface-water runoff from the canyon storage units.

The INFILv3 simulated average annual recharge was used as input to the ground-water flow model and was simulated in the ground-water flow model using the RCH package (McDonald and Harbaugh, 1988). The simulated areal recharge was applied to the top face of the cells in model layer 1; if a cell in model layer 1 went dry (that is, the water table dropped below the bottom of the cell) then the recharge was applied to the top of the cell in model layer 2 (*fig. 45*).

Areal recharge was assumed constant for the duration of the simulation period (1926–2003). This assumption is supported by results from a study by Bouwer (1980) that indicate that seasonal and annual fluctuations in infiltration are attenuated as a function of sediment particle size in the unsaturated zone and vertical distance to the water table. Bouwer (1980) found that downward velocities in the unsaturated zone decrease with decreasing particle size of the materials and that deep percolation reaches virtually a steady uniform flow at a depth of about 50 to 100 ft below land surface. Because the depth to water throughout most of the study area is in excess of 300 ft, using a constant recharge rate is reasonable.

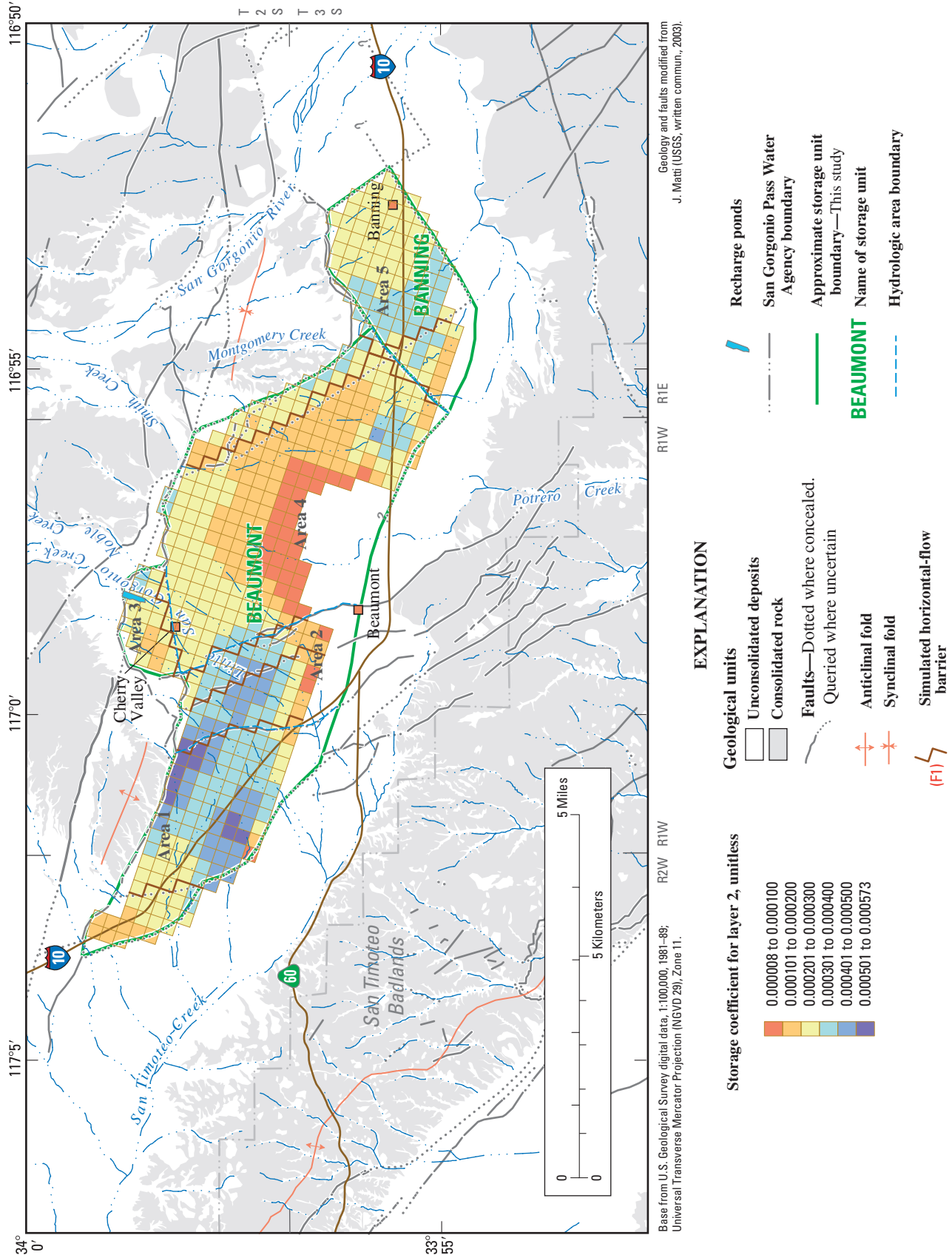


Figure 44. Map showing distribution of storage coefficient values for model layer 2 in the transient ground-water flow model, San Gorgonio Pass area, Riverside County, California.

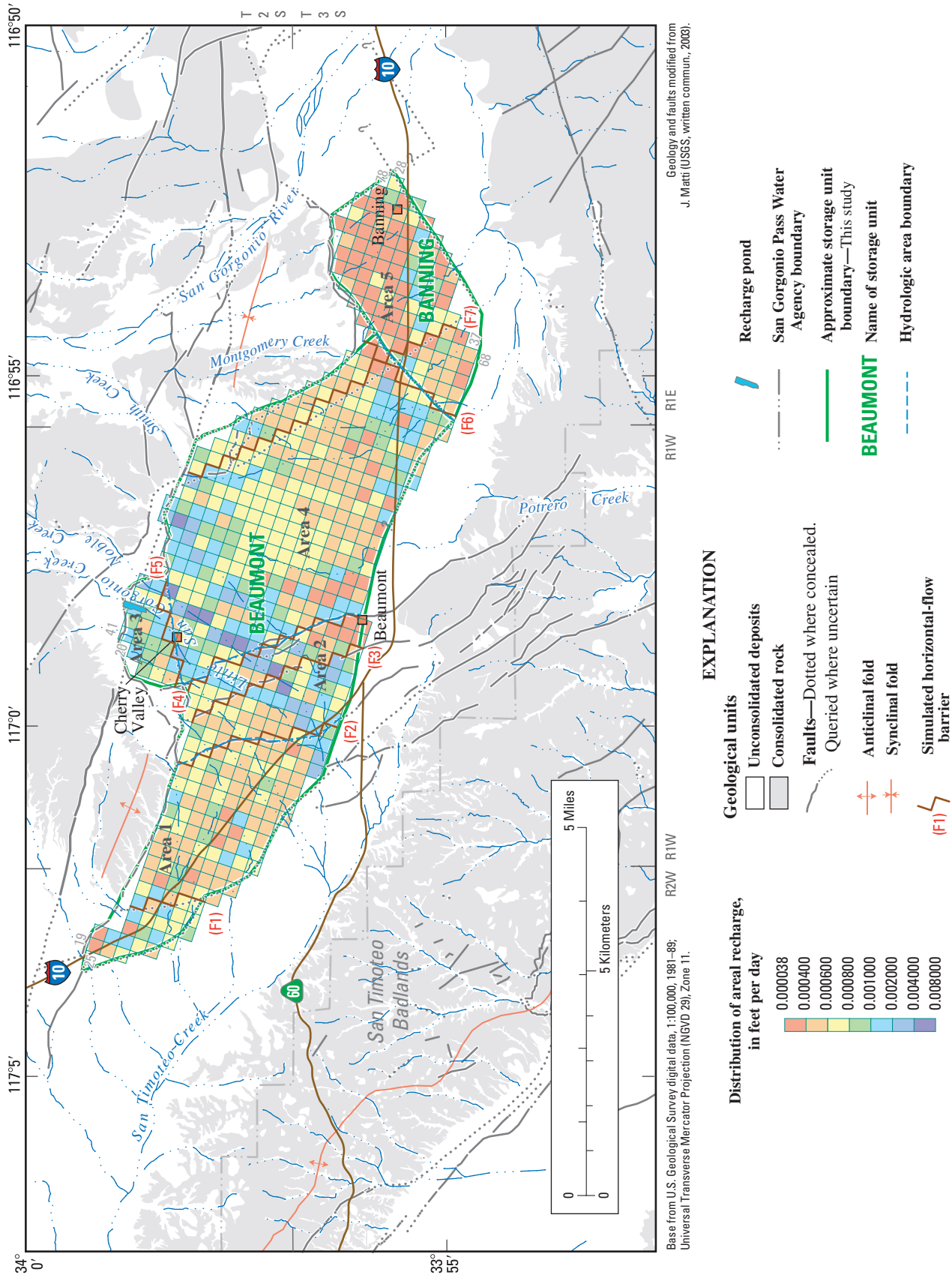


Figure 45. Map showing the distribution of areal recharge cells for the ground-water flow model, San Gorgonio Pass area, Riverside County, California.

Natural recharge may require decades to reach the water table because of the great thickness of the unsaturated zone in most of the study area. A numerical model of the unsaturated zone near the recharge ponds in area 3 simulated that the time required for natural recharge to move from the ground surface to the water table ranged from about 50 years for locations directly beneath stream channels to more than 250 years for locations away from the stream channels (Flint and Ellet, 2004). In the area of the recharge ponds, the unsaturated zone is about 600 ft thick; therefore, the simulated flux ranges from about 2.4 to 12 ft/yr. Assuming that the simulated natural recharge rates are representative of natural recharge in the entire model area and the thickness of the unsaturated zone ranges from about 150 to 600 ft, the estimated travel time for natural recharge ranges from about 60 to 250 years for the 2.4 ft/yr flux and from about 12 to 50 years for the 12 ft/yr flux.

The 75-year climatic period used to estimate the average annual recharge rate for this study (water years 1927–2001) may not be representative of the climatic period that was the source of the recharge because of the large travel times for natural recharge to reach the water table. Inspection of the cumulative departure of tree-ring indices for southern California compiled by the National Atmospheric and Oceanic Administration (1994) for 1458 through 1966 indicates that the climatic patterns observed for 1927–2001 are similar to those of the climatic period recorded in the tree-ring indices since the early 1700s (*fig. 46*). Since the early 1700s, the climate has been dominated by wet and dry periods of similar frequency and amplitude (Hanson and others, 2003). Wet climatic periods are determined using the rising limb of the cumulative departure curve, and dry climatic periods are determined using the falling limb of the cumulative departure curve. Prior to the early 1700s, wet and dry periods were about 20 to more than 60 years long; whereas after the early 1700s, wet and dry periods were about 5 to 20 years long. The climatic period simulated for this study is representative of the average climatic period since the early 1700s because it extends over five wet periods and five dry periods.

Incorporation of urbanization into the INFILv3 model resulted in an increase in simulated runoff from the urbanized areas and an increase in simulated recharge in areas downstream of the urbanized areas. In the Beaumont and Banning storage units the increase in simulated average annual natural recharge is about 600 acre-ft/yr for a total of about 4,300 acre-ft/yr. Recharge due to urbanization was not incorporated into the transient model (1926–2003) because urbanization did not affect the model area until about the 1950s (*fig. 3*) and the estimated time for natural recharge to travel through the unsaturated zone in most of the study area exceeded 50 years.

Mountain-Front Recharge

For the purposes of this report, ground-water recharge that occurs in the sub-drainage basins of the canyon storage units upstream of the Beaumont and Banning storage units is referred to as mountain-front recharge. The total INFILv3-simulated recharge rate for the 28 sub-drainage basins upstream of the Beaumont and Banning storage units is about 6,180 acre-ft/yr (*table 8A*). As previously discussed in sections “Ground-Water Levels and Movement” and “Geochemistry,” water-level and water-quality data indicate that the Banning Fault (*fig. 5*) restricts ground-water underflow from the upstream sub-drainage basins into the Beaumont and Banning storage units. The fault is a barrier to ground-water flow and forces some of the ground water to discharge to stream channels that cross the fault. Where the fault has been eroded by streamflow, ground water can leave the upstream sub-drainage basins as ground-water underflow. The ground-water discharge that becomes streamflow and the ground-water underflow are potential sources of recharge for the Beaumont and Banning storage units. However, an unknown quantity of this ground-water discharge is lost to evapotranspiration and is not available as potential recharge in the downstream ground-water storage units.

The quantity of mountain-front recharge contributed to the Beaumont and Banning storage units from the upstream sub-drainage basins was determined during the steady-state calibration. Initially, all of the ground-water recharge estimated by INFILv3 for each upstream sub-drainage basin was assumed to recharge the Beaumont and Banning storage units. The mountain-front recharge was simulated using the WEL package (McDonald and Harbaugh, 1988), which simulates constant rates of well discharge or recharge per stress period at user-selected model cells. Mountain-front recharge was simulated in the active model cell in layer 1 directly downgradient of the stream channel that drains each of the upstream sub-drainage basins (*fig. 38A*). If a mountain-front recharge cell in layer 1 were to become dry, the WEL package would not simulate recharge to that cell. None of the mountain-front recharge cells became dry during the simulation period.

The INFILv3 estimates of mountain-front recharge were modified during the steady-state calibration of the ground-water flow model. During the calibration, some of the initial estimates of mountain-front recharge were reduced (*table 11*). The calibrated steady-state mountain-front recharge rate was about 2,670 acre-ft/yr, about 43 percent of the water estimated by INFILv3 to be recharged in the sub-drainage basins upstream of the Beaumont and Banning storage (*table 11*). Smith Creek, (sub-drainage basin 18), contributed the greatest quantity of mountain-front recharge (about 360 acre-ft/yr), followed by Little San Gorgonio Creek (sub-drainage basin 12; about 350 acre-ft/yr), and Noble Creek (sub-drainage basin 14; about 330 acre-ft/yr).

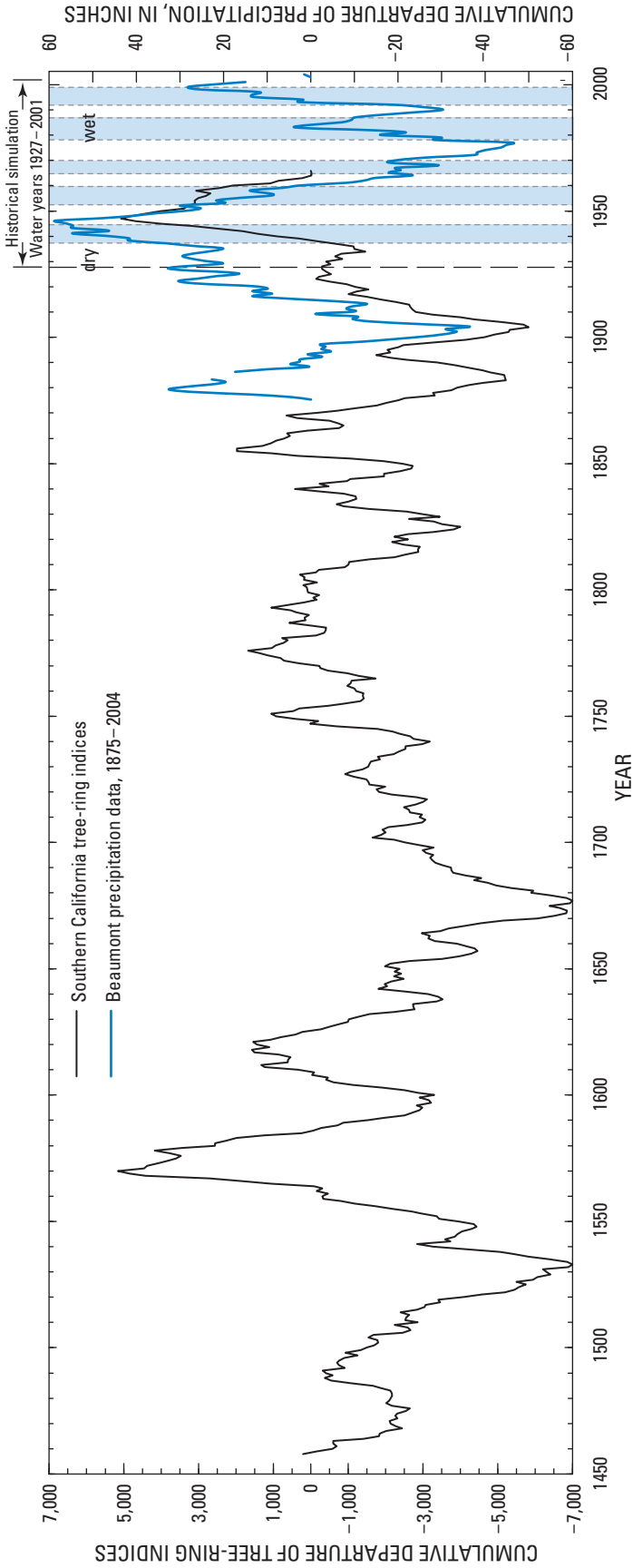


Figure 46. Graph showing departure of tree-ring indices for southern California (1458–1966), cumulative departure of precipitation at Beaumont (1875–2003), and wet and dry climatic periods for the INFILv3 simulation period (water years 1926–2003), San Gorgonio Pass area, Riverside County, California.

With the exception of mountain-front recharge originating from the Little San Geronio Creek sub-drainage basin, the steady-state calibrated mountain-front recharge was assumed constant throughout the simulation period (1926–2003). Ground-water pumpage from the Little San Geronio Creek sub-drainage basin would undoubtedly reduce the quantity of water available to recharge the Beaumont storage unit. For modeling purposes, the available water for mountain-front recharge in the Little San Geronio Creek sub-drainage basin was assumed to decrease if the amount of reported pumpage in Edgar Canyon exceeded the INFILv3 estimated recharge in the sub-drainage basin (about 2,330 acre-ft/yr) (*table 11*). The first year with reported pumpage in excess of 2,330 acre-ft/yr was 1972. As stated previously, it is estimated to take about 50 years for water to move through the thick unsaturated zone beneath the Little San Geronio Creek channel near the recharge ponds to the water table. Assuming that it also would take 50 years for pumpage in Edgar Canyon to affect the water available for recharge in the model area, then the affect of pumpage in 1972 would not be observed until 2022. Therefore, for the transient simulation period (1926–2003), mountain-front recharge originating from the Little San Geronio Creek sub-drainage basin was assumed constant.

Simulated Artificial Recharge

Since ground-water development began in the San Geronio Pass area, there have been several sources of artificial recharge to the basin, including return flow from applied water on crops, golf courses, and landscape; septic-tank seepage; and infiltration of diverted storm runoff from Little San Geronio Creek and imported SWP water into recharge ponds. Potential artificial recharge was estimated for 1926–2003 for this study (*fig. 26*). Artificial recharge was estimated to reach the water table from about 23, 40, 71, 56, and 52 years after the artificial recharge was applied at land surface in areas 1–5, respectively, because of the great thickness (150–465 ft) of the unsaturated zone in these areas. The methods and assumptions used to make these estimates are presented in the “Artificial Recharge” section of this report.

Return Flow of Crop and Golf-Course Irrigation

Recharge from the return flow of ground water pumped for crop and golf-course irrigation was simulated in model layer 1 using injection wells in the same general location where the pumping occurred (*fig. 47*). The quantity of return flow from irrigation of crops was estimated by multiplying the

annual pumpage for each well designated as an agricultural supply well in *Appendix table 3* by 40 percent. The quantity of return flow from golf-course irrigation was estimated by multiplying the annual pumpage for each well designated as a golf-course supply well in *Appendix table 3* by 40 percent.

Return Flow of Landscape Irrigation in Banning and Beaumont

Recharge from the return flow of water applied for landscape irrigation in the sewerred areas of the cities of Banning and Beaumont was simulated in model layer 1 using injection wells in the model cells that corresponded to residential land use (*fig. 47*). The quantity of return flow for the Banning area (*fig. 47*) was estimated by multiplying the combined pumpage from the City of Banning Water Company wells (*Appendix table 3*) by 28 percent. The quantity of return flow for the Beaumont area (*fig. 47*) was estimated by multiplying the quantity of water pumped from model area 3 in the Beaumont storage unit obtained from the Beaumont-Cherry Valley Water District (BCVWD) (*Appendix table 3*) by 28 percent.

Septic-Tank Seepage and Return Flow of Landscape Irrigation in the Cherry Valley Area

Residences and businesses in the Cherry Valley area rely on onsite septic systems to treat their wastewater. Recharge from septic-tank seepage was simulated in model layer 1 using injection wells in the model cells that corresponded to residential land use in the Cherry Valley area (*fig. 47*). The quantity of septic-tank seepage was estimated by multiplying an average septic-tank discharge of 70 gal/d per person (Bookman-Edmonston Engineering, 1991) by the reported and estimated annual population of Cherry Valley (*fig. 3*). Return flow of landscape irrigation in Cherry Valley was estimated by subtracting the estimate of septic-tank seepage for a particular year from the quantity of water delivered to the Cherry Valley area for that year and then multiplying this value by 40 percent. It was assumed that the water pumped from Edgar Canyon and from model area 3 of the Beaumont storage unit by the BCVWD was delivered to the Cherry Valley area (*fig. 25B*). The combined quantity of estimated annual septic-tank seepage and return flow of landscape irrigation was distributed evenly between the model cells designated as residential land use in Cherry Valley (*fig. 47*).

Table 11. Mountain-front recharge simulated in the ground-water flow model of the San Geronio Pass area, Riverside County, California.

[acre-ft/yr, acre-feet per year]

Upstream sub-drainage basin	Model area affected	Upstream watershed area (acres)	Percent of watershed area	INFILv3 model	Ground-water model		Volume of INFILv3 recharge not simulated as mountain-front recharge (acre-ft/yr)
				Estimated recharge in upstream watershed (acre-ft/yr)	Estimated net mountain front recharge (acre-ft/yr)	Percent net infiltration (recharge) from total watershed runoff	
1	1	41	0.2	6.7	6.7	100	0
2	1	164	0.9	30.0	30.0	100	0
3	1	968	5.5	283.0	60.3	21.3	222.7
4	1	157	0.9	36.9	36.9	100	0
5	1	77	0.4	17.9	17.9	100	0
6	1	216	1.2	51.9	35.9	69.2	16.0
7	1	26	0.1	5.9	5.9	100	0
8	1	47	0.3	11.0	11.0	100	0
9	1	581	3.3	168.7	168.7	100	0
10	2	1,219	7.0	355.7	173.6	48.8	182.1
11	3	255	1.5	75.4	75.4	100	0
12 Little San Geronio Creek							
	3	4,416	25.3	2,331.2	352.7	15.1	1,978.5
13	3	106	0.6	31.1	31.1	100	0
14 Noble Creek							
	3	3,231	18.5	947.9	327.8	34.6	620.1
15	4	107	0.6	29.0	29.0	100	0
16	4	1,031	5.9	270.6	270.6	100	0
17	4	98	0.6	29.2	29.2	100	0
18 Smith Creek							
	4	1,771	10.2	665.8	361.5	54.3	304.3
19	4	399	2.3	136.7	136.7	100	0
20	4	151	0.9	52.3	52.3	100	0
21	4	25	0.1	5.1	5.1	100	0
22	4	104	0.6	22.0	22.0	100	0
23	5	782	4.5	229.4	109.0	47.5	120.4
24	5	83	0.5	16.0	16.0	100	0
25	5	161	0.9	38.5	38.5	100	0
26	5	231	1.3	58.3	58.3	100	1
27	5	569	3.3	160.2	115.9	72.3	44.3
28	5	426	2.4	112.5	96.4	85.7	16.1
Totals		17,442	100	6,178.9	2,674.4	43.3	3,504.5

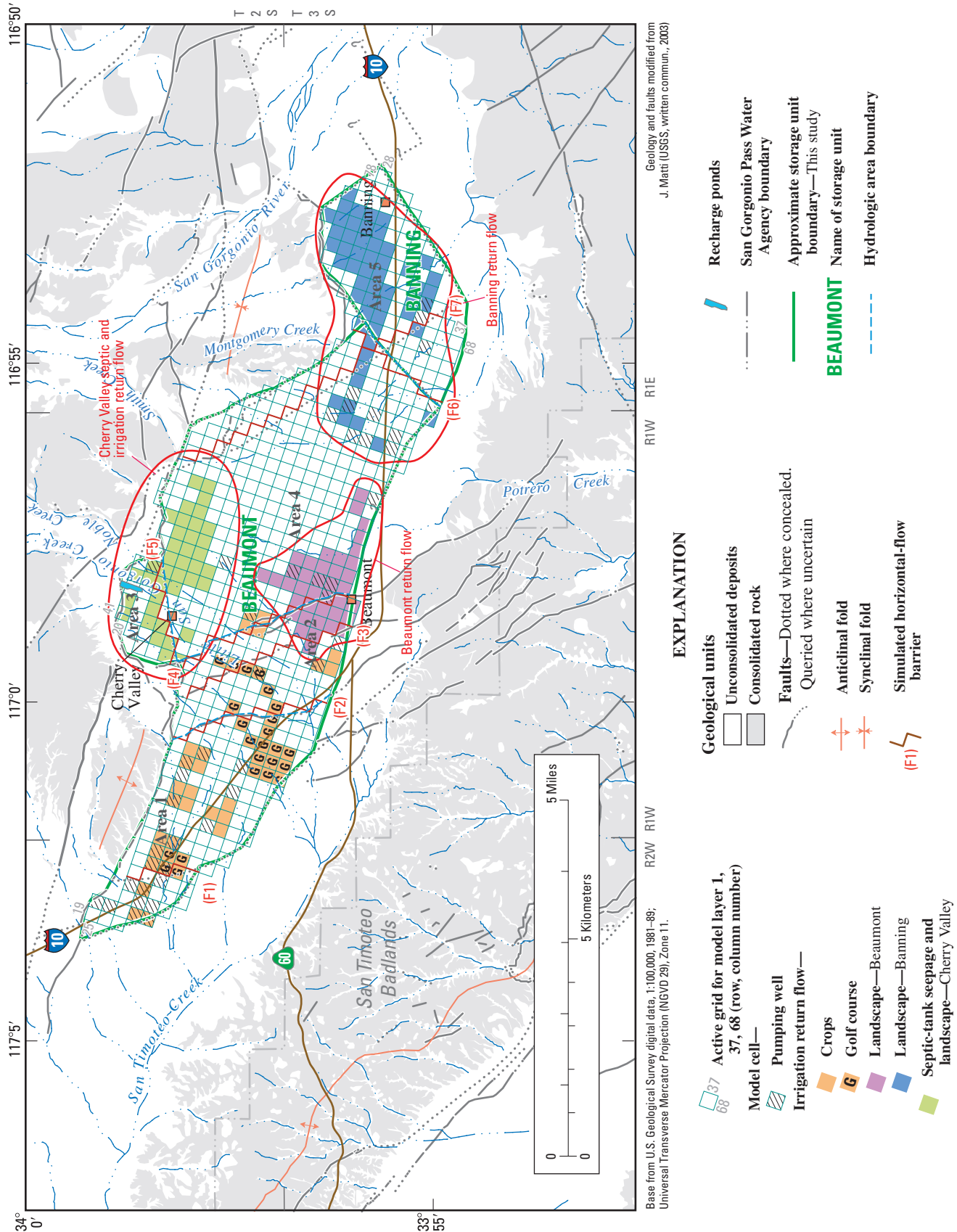


Figure 47. Map showing the distribution of pumpage and return flow cells in the ground-water flow model, San Gorgonio Pass area, Riverside County, California.

Model Discharge

Ground water is discharged from the study area either by pumping or as natural ground-water discharge along the southwest boundary of the Beaumont storage unit and across the unnamed inferred fault that forms the southeastern boundary of the Banning storage unit. The natural ground-water discharge was simulated using drains and general-head boundaries as described earlier in the “Boundary Conditions” section of this report.

Annual pumpage compiled and estimated for this study for 1927–2003 (*fig. 25; Appendix table 3*) was assigned to the active cell that contained the well or wells with pumpage data (*fig. 47*). All pumpage was assumed to come from model layers 1 or 2, even for wells screened beneath the base of the model domain. Pumpage was distributed to the different model layers as a function of screen interval and horizontal hydraulic conductivity, using the following equation:

$$Q_i = \left(\frac{K_i \times si_i}{\sum (K_i \times si_i)} \right) \times Q,$$

where

- Q is the total pumpage from a well (L^3T^{-1});
- Q_i is the pumpage assigned to layer i (L^3T^{-1});
- K_i is the horizontal hydraulic conductivity of layer i (LT^{-1});
- si_i is the screen interval in layer i (L); and
- i is the model layer number.

The percentage of pumpage by model layer for each well simulated in the model is shown in *Appendix table 3*.

Model Calibration

The ground-water flow model of the Beaumont and Banning storage units was calibrated using a trial-and-error process in which the initial estimates of the aquifer properties and the distribution and quantity of recharge were iteratively adjusted to improve the match between simulated hydraulic heads and measured ground-water levels. Measured ground-water levels for the period 1926–2003 were used to calibrate the ground-water flow model. The locations of the wells used for model calibration are shown in *figures 48 and 49*.

The calibration process involved (1) calibrating the model for steady-state or predevelopment conditions by adjusting model parameters until simulated hydraulic heads matched measured water levels; (2) calibrating the model for transient (1926–2003) conditions by using the simulated steady-state hydraulic heads as initial conditions and adjusting the specific yield and storage coefficient values and other model parameters until simulated hydraulic heads matched measured water levels; and (3) updating model parameters in the steady-state model adjusted during the transient calibration and rerunning the steady-state simulation to ensure that the changes made during the transient calibration produced reasonable steady-

state results. This process was repeated until a satisfactory match between measured and simulated results was obtained for both steady-state and transient conditions.

Steady-State Calibration

Measured ground-water levels collected prior to 1927 were used to calibrate the ground-water flow model to predevelopment or steady-state conditions. Pre-1927 ground-water conditions were assumed to represent steady-state conditions because few wells had been drilled prior to 1927 and the few available water levels show little change (*fig. 29*). The steady-state calibration consisted of adjusting initial estimates of mountain-front recharge, horizontal and vertical hydraulic conductivity, the hydraulic characteristic of simulated faults, and drain and general-head boundary conductance values. The quantity and distribution of areal recharge simulated for this study using INFILv3 were not adjusted during the model calibration.

During the calibration process the original INFILv3 estimate of mountain-front recharge was reduced by about 40 percent (*table 11*). The original estimate of mountain-front recharge required unreasonably high values of transmissivity in order for simulated steady-state hydraulic heads to match measured water levels. The model calculated steady-state transmissivity values generally are higher than values estimated from specific-capacity and aquifer-test data (*fig. 42; Appendix table 2*). During the steady-state calibration process, more weight was given to the transmissivity data than to the mountain-front recharge estimates. As stated in the “Natural Ground-Water Recharge” section of this report, INFILv3 does not simulate ground-water discharge once the infiltrated water has percolated below the zone of evapotranspiration; therefore, the estimated mountain-front recharge originating from the upstream sub-drainage basins is probably high.

The horizontal hydraulic conductivity values in model layers 1 and 2 were modified by area. Initially, all areas of model layer 1 and 2 were assigned horizontal hydraulic conductivity values of 20 ft/d and 1 ft/d, respectively. During the calibration process the horizontal hydraulic conductivity values of model layer 1 were increased to 30 ft/d in areas 1–4 and decreased to 10 ft/d in area 5. All areas of model layer 2 were increased to 2 ft/d. The vertical hydraulic conductivity values for model layers 1 and 2 were assumed equal to one-hundredth the horizontal hydraulic conductivity values of the model layers. The ratio between vertical and horizontal hydraulic conductivity was not adjusted during the steady-state calibration process.

The steady-state model was relatively insensitive to hydraulic characteristic values of simulated faults. Therefore, initial estimates of this parameter were adjusted during the transient calibration. A subsequent steady-state simulation was run to verify that the changes made during the transient simulation to this parameter resulted in a reasonable steady-state simulation.

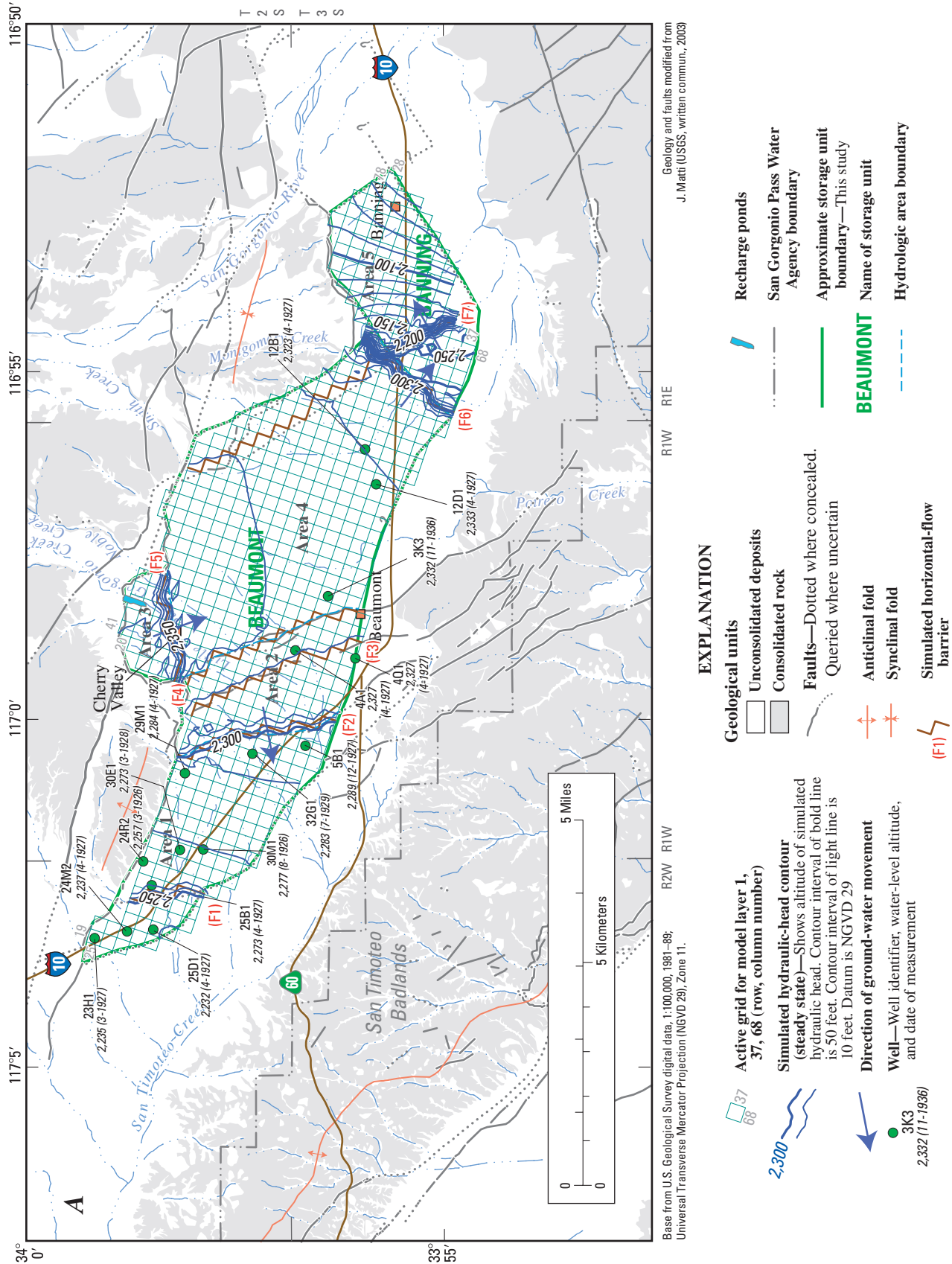


Figure 48. Map showing the measured water levels for 1926–27 and simulated hydraulic-head contours for the calibrated steady-state ground-water flow model for (A) model layer 1 and (B) model layer 2, San Gorgonio Pass area, Riverside County, California.

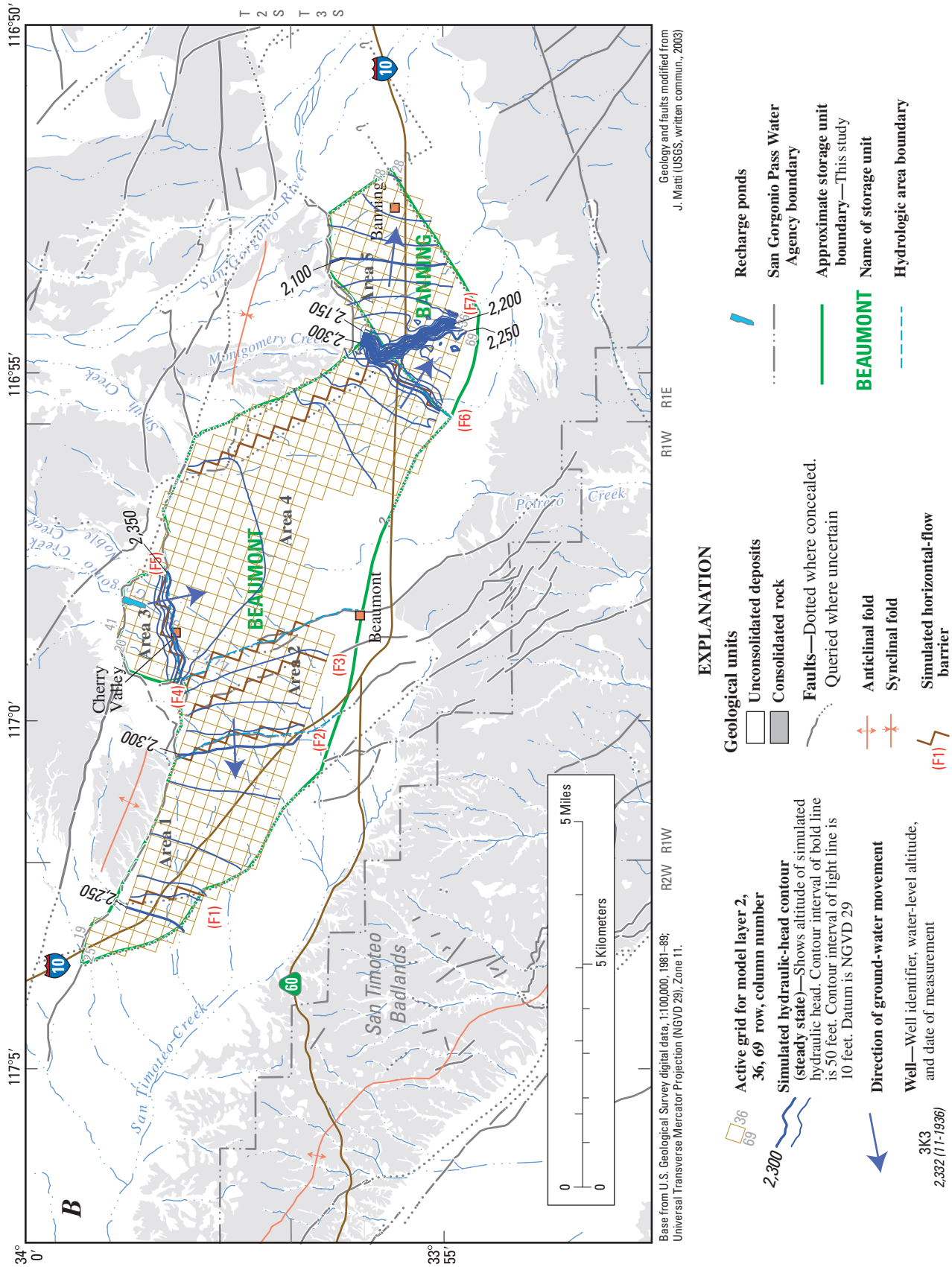


Figure 48. Continued.

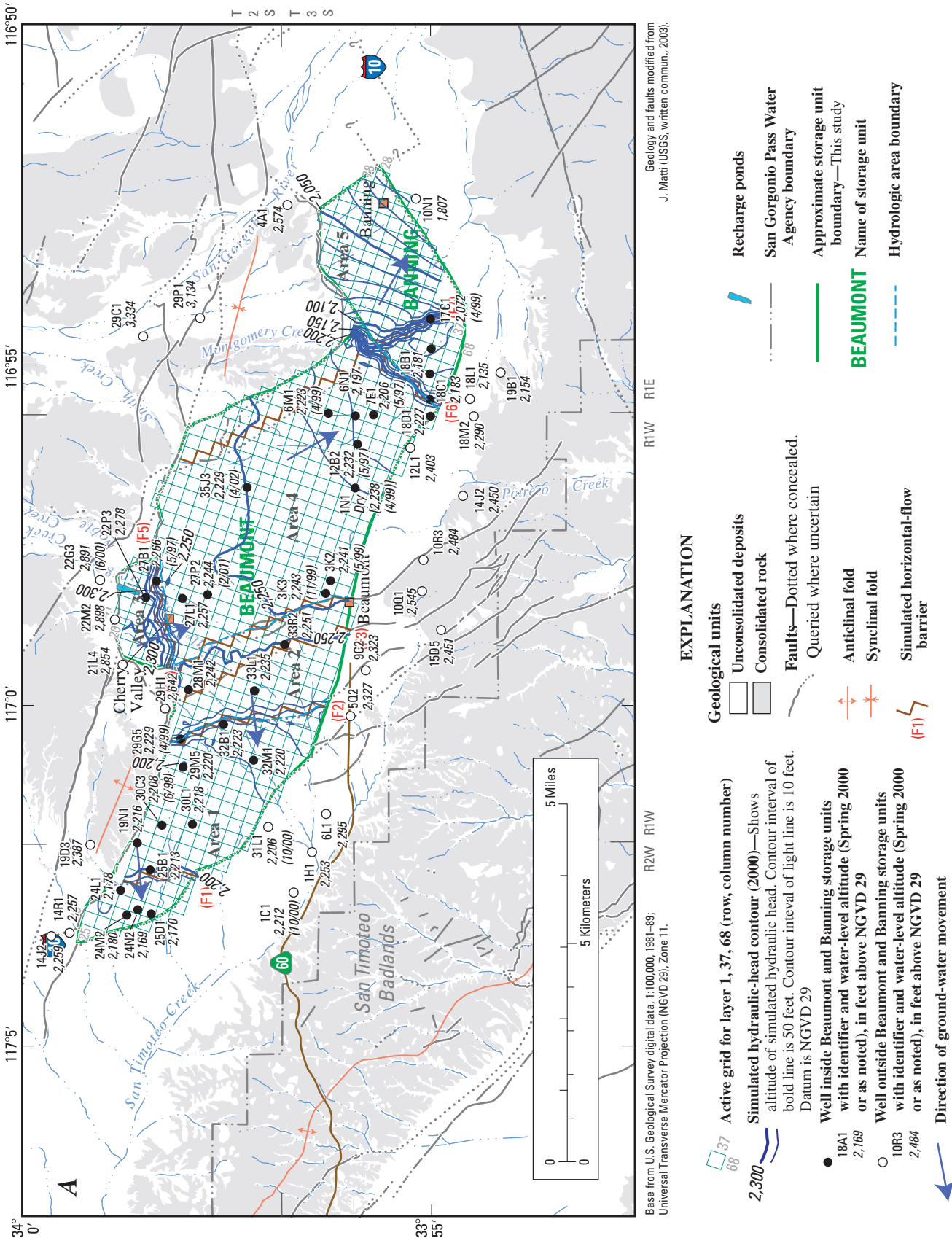
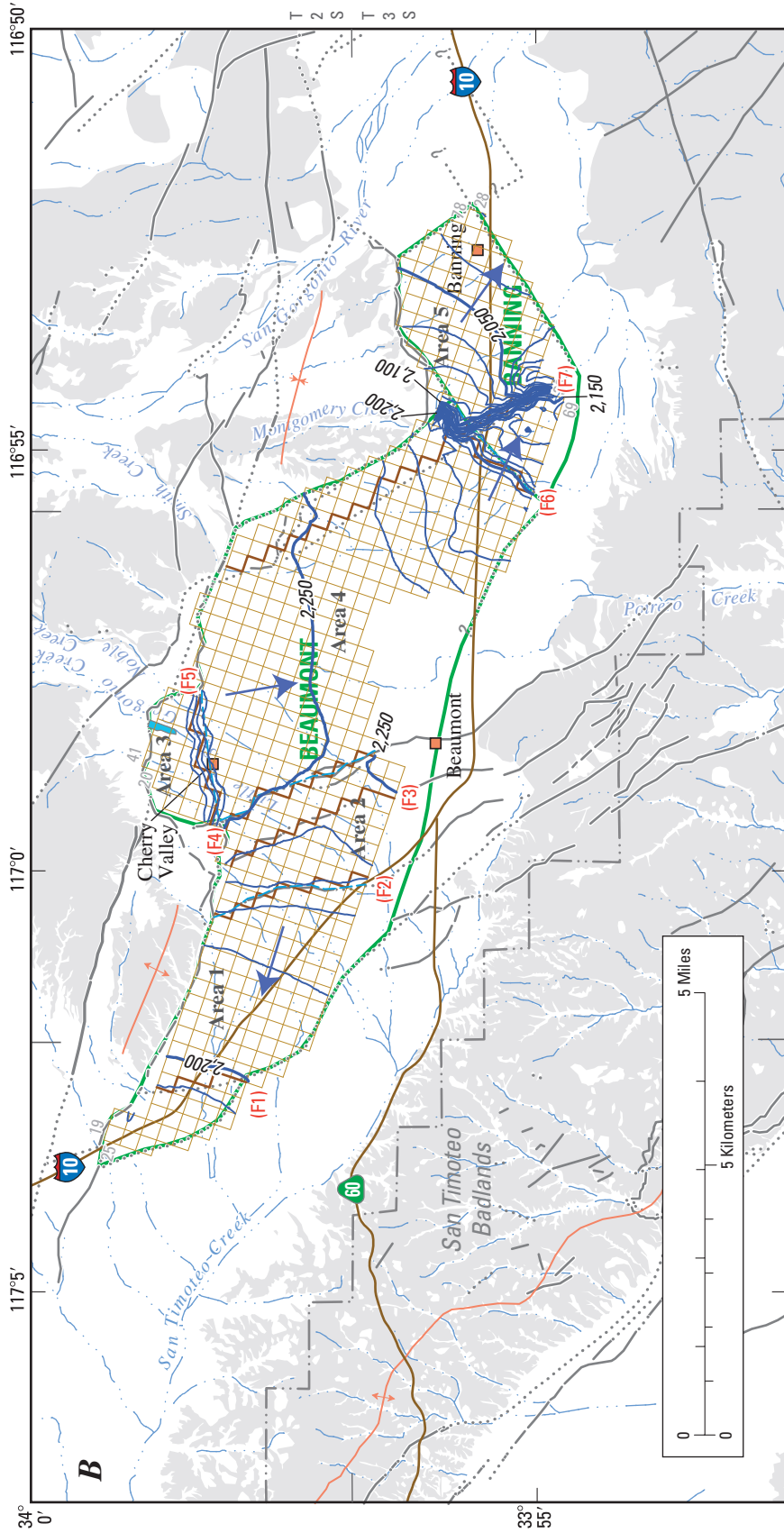


Figure 49. Maps showing measured Spring 2000 water levels and simulated hydraulic-head contours for the calibrated transient-state ground-water flow model for (A) model layer 1 and (B) model layer 2, San Gorgonio Pass area, Riverside County, California.



Geology and faults modified from J. Matti (USGS, written commun., 2003)

RTW RIE

R2W RTW

EXPLANATION

- Active grid for layer 2, 36, 69 (row, column number)
- Simulated hydraulic-head contour (2000)—Shows altitude of simulated hydraulic head. Contour interval of bold line is 50 feet. Contour interval of light line is 10 feet. Datum is NGVD 29
- Direction of ground-water movement
- Unconsolidated deposits
- Consolidated rock
- Faults—Dotted where concealed. Queried where uncertain
- Anticlinal fold
- Synclinal fold
- Simulated horizontal-flow barrier (F1)
- Recharge ponds
- San Geronimo Pass Water Agency boundary
- Approximate storage unit boundary—This study
- BEAUMONT** Name of storage unit
- Hydrologic area boundary

Figure 49. Continued.

The simulated steady-state hydraulic head distribution was very sensitive to the simulated drain and general-head boundary conductance values. The original estimates of the conductance values were large to allow unrestricted flow through the drain and general-head boundaries. During the calibration process the drain conductance was reduced by as much as 75 percent and general-head conductance was reduced by as much as four orders of magnitude (*table 10*). The general-head conductance values were low because the boundaries generally are associated with low permeability fault zones.

Transient Calibration

Measured ground-water levels from 1926 to 2003 were used to calibrate the ground-water flow model for transient conditions caused by hydraulic stresses within the storage units. The transient calibration used the steady-state hydraulic heads as initial conditions. Transient conditions exist when an aquifer system is subject to stresses that change over time, such as recharge and discharge, and may result in an increase or decrease in the quantity of water stored in the aquifer. Seasonal and long-term climate changes also can influence hydrologic conditions but they are not addressed in this study. The magnitude of simulated changes in hydraulic head is dependent on ground-water pumpage from the storage units, natural and artificial recharge to the storage units, the horizontal and vertical hydraulic conductivity of the aquifer system, the storage properties of the aquifer system, the hydraulic characteristic values of simulated faults, and the drain and general-head boundary conductance. The calibrated parameter values used in the transient simulation are presented in *table 10*.

Reported and estimated annual pumpage data (*Appendix table 3*) were entered into the model by layer on the basis of the hydraulic conductivity of the model layer as described in the "Model Discharge" section of the report. The pumpage values were not modified as part of the transient calibration. The quantity and distribution of areal and mountain-front recharge simulated in the steady-state calibration were simulated as average annual values in the transient calibration. The natural recharge was assumed constant through the transient simulation period.

The quantity of artificial recharge estimated for this study (*fig. 26*) was simulated in the transient simulation without modification. The estimated vertical travel times for artificial recharge to reach the water table ranged from about 23, 40, 71, 56, and 52 years in areas 1–5, respectively. The methods and assumptions used to make these estimates are presented in the "Artificial Recharge" section of this report.

The horizontal hydraulic conductivities estimated in the steady-state calibration were used in the transient simulation without modification. The vertical hydraulic conductivities for model layers 1 and 2 were assumed equal to one-hundredth

of the horizontal hydraulic conductivity values. Other ratios between horizontal and vertical hydraulic conductivity were tested during the calibration process; however, the model results showed no improvement.

During the transient calibration it was determined that the results were most sensitive to changes in the specific yield of model layer 1. Specific yield in layer 1 was varied by area. Initially, all areas were assigned a specific yield of 0.10. During the calibration process the specific yield in areas 1, 2, and 4 were increased to 0.18, the specific yield in area 3 were increased to 0.14, and the specific yield in area 5 was decreased to 0.05. In general, the calibrated specific yields correspond with the sediment present in the model areas. Inspection of geologic logs from wells in the model area indicated that areas 1–4 contained coarser grained sediments in the upper aquifer and area 5 contained finer grained sediments.

The storage coefficient of model layer 2 was estimated by multiplying the thickness of model layer 2 by a specific storage coefficient of $1.0 \times 10^{-6} \text{ ft}^{-1}$. The model was insensitive to reasonable changes in the specific storage of model layer 2; therefore, the initial estimates of storage coefficient of model layer 2 were not changed during the calibration process.

The initial hydraulic-characteristic values for all faults in model layer 1 were set equal to the hydraulic conductivity of the model area divided by the assumed thickness of the fault (1 ft), and the initial hydraulic-characteristic values for all faults in model layer 2 were set equal to the maximum transmissivity value of each model area divided by the assumed thickness of the fault (1 ft), allowing unrestricted hydraulic connection across the faults. To reproduce the measured water levels, it was necessary to reduce the initial estimates of the hydraulic characteristic by as much as eight orders of magnitude (fault F7 layer 2; *table 10*).

The drain and general-head conductance values were the same as those simulated in the steady-state calibration.

Model Calibration Results

A total of 345 water levels measured in the model area from 1926 through 2003 were compared to simulated hydraulic heads to help calibrate the model (*table 12*). The water levels used for calibration purposes were all measured in spring (April–June) because, in the model area, spring water levels were least affected by ground-water pumping. *Figure 50A* shows that the measured water levels and corresponding simulated hydraulic heads closely follow a 1:1 correlation line with most residuals within ± 20 ft. If the model simulated the measured data perfectly, all the data would plot on the 1:1 correlation line. The root-mean-square error (RMSE) for these data is 14.4 ft, and the relative error of the residuals (standard deviation of the residuals divided by the observed range) is 4.3 percent (*table 12*). The distribution of the RMSE by model area ranges from 11.9 ft in area 1 to 21.7 ft in area 5,

and the relative error of the residuals ranges from 6.0 percent in area 4 to 18.7 percent in area 5 (*table 12*). The time varying sum of the model residuals is shown by pumping period on *figure 50B*. As shown on the figure, the sum of the residuals is greatest during the 1950–65 and the 1966–86 pumping periods. The maximum RMSE for 1966–86 pumping period is 19.8 ft (*table 12*).

Simulated hydraulic heads and measured water levels for selected wells are shown in *figure 51* with the total annual pumpage by model area for 1926–2003. In general, the simulated hydraulic heads match the measured water levels. However in model-area 1, the simulated hydraulic heads at well 2S/2W-23H1 are higher than measured water levels during the period 1972–80 (*fig. 51A*). This overestimation may be caused by underestimating the pumpage during this period or overestimating the quantity of simulated return-flow recharge. In model-area 4 the simulated hydraulic heads are 10 to 25 ft higher than measured water levels in wells 2S/1W-34M1, 3S/1W-03K3, 01N1, and 12E2 between 1960 and 1980 (*fig. 51C*). Similar to model area 1, this overestimation may be caused by underestimating the pumpage or overestimating the quantity of simulated return-flow recharge. In model-area 5 the simulated hydraulic heads are as much as 100 ft higher than measured water levels at wells 3S/1E-8P1 and 17C1 (*fig. 51D*). These wells are active production wells; therefore, a possible explanation for these differences may be that the water-level data probably were collected under non-static conditions.

By the end of the transient period (2003), hydraulic heads in model layer 1 were simulated to decline by as much as 100 ft compared to steady-state conditions (*fig. 51*). These declines in simulated hydraulic head result in a decrease in the simulated transmissivity of model layer 1 compared to steady-state conditions (*fig. 42C*). The greatest decreases in transmissivity (70 to 90 percent) are simulated in the southern margins of model layer 1, where the altitudes for the bottom of the model layer are the highest (*fig. 40A* and *42C*) and the thickness of the model layer for steady-state conditions was the least. Most of model layer 1 has a 10 to 20 percent decrease in simulated transmissivity; with a 20 to 30 percent decrease in the southwestern part of area 4 and the western part of area 5. Because there is a direct relation between transmissivity and well yield, decreases in transmissivity will result in similar decreases in well yield.

The simulated hydraulic-head contours for model layer 1 compare reasonably well with measured water levels for 1926–27 and 2000 (*figs. 48* and *49*). These results, and the hydrograph results, indicate that the model reasonably represents historical ground-water conditions in the Beaumont and Banning storage units.

Water Budgets

Water budgets for the calibrated steady-state model and selected stress periods of the transient-state model are presented in *table 13*. The flux and cumulative volume of each budget term is shown in *figure 52*. The flow budget for each model area for steady state and year 2003 are shown in *figure 53*. The total steady-state inflow rate, or recharge, was about 6,590 acre-ft/yr with about 3,710 acre-ft/yr from areal recharge, about 2,670 acre-ft/yr from mountain-front recharge, and about 210 acre-ft/yr from general-head boundaries (the surrounding older sedimentary deposits) (*fig. 53A* and *table 13*). Note that the values shown in *figure 53* are net fluxes for a specific component of the hydrologic budget; therefore, the values shown in *figure 53* and *table 13* may not be directly comparable. The total steady-state outflow rate, or discharge, was about 6,590 acre-ft/yr with about 2,865 acre-ft/yr as ground-water underflow from the Banning storage unit to the Cabazon storage unit, about 2,035 acre-ft/yr as ground-water underflow to the surrounding older sedimentary deposits along the southern boundary of the model, and about 1,690 acre-ft/yr to drain boundaries that simulate the discharge to stream channels draining the San Timoteo storage unit (*fig. 53A* and *table 13*). The total discharge is similar to estimates by Bloyd (1971) and Boyle Engineering Corporation (1995); however, the model results indicate that more water is discharged along the southern boundary and less along the southeastern boundary than estimated by either Bloyd (1971) or Boyle Engineering Corporation (1995).

The year-2003 water budget indicates that the total recharge was about 9,920 acre-ft/yr with about 3,710 acre-ft/yr from areal recharge, about 2,740 acre-ft/yr from return flow and septic-tank seepage, about 2,670 acre-ft/yr from mountain-front recharge, and about 720 acre-ft/yr from ground-water underflow from the surrounding older sedimentary deposits (general-head boundary) (*fig. 53A* and *table 13*). The total year-2003 discharge was about 22,310 acre-ft/yr with about 20,000 acre-ft/yr as pumpage, and about 2,270 acre-ft/yr as ground-water underflow from the Banning storage unit to the Cabazon storage unit (*fig. 53B* and *table 13*). The model simulates about 12,420 acre-ft/yr, or about 62 percent of the pumpage, from aquifer storage. In addition, the pumpage reduced the quantity of ground-water outflow to the Cabazon storage unit (general-head boundary) from about 2,870 acre-ft/yr during steady-state conditions to about 2,270 acre-ft/yr in 2003 (*fig. 53*). Pumpage also reduced the quantity of ground-water outflow to the stream channels draining the San Timoteo storage unit (drain boundary) from about 1,690 acre-ft/yr during steady-state conditions to about 0 acre-ft/yr in 2003 (*fig. 53B*). The pumpage also reversed the flux from the surrounding older sedimentary deposits along the southern boundary of the model domain (*fig. 53*).

Table 12. Comparisons of measured spring water levels and simulated hydraulic heads for (A) steady-state and transient conditions (1926–2003), (B) areas, (C) pumping periods, and (D) decade for the San Geronio Pass area, Riverside County, California.

[See figure 8 for area location; see figure 25 for pumping period average. Mean errors and residuals are in feet]

A. Steady-state and transient conditions (1926–2003)

	Number of data points	Sum of the residuals	Root mean square error	Mean error	Absolute mean error	Residuals			Percent standard deviation/range
						Minimum	Maximum	Median	
Steady-state condition	13	443.4	5.8	-3.0	4.8	-12.0	4.0	-4.7	6.2
Transient state condition	345	3,284.1	14.4	9.5	11.8	-24.9	49.0	9.6	4.3

B. Comparison by area for transient state condition

Area	Number of data points	Sum of the residuals	Root mean square error	Mean error	Absolute mean error	Residuals			Percent standard deviation/range
						Minimum	Maximum	Median	
1	149	992.1	11.9	6.7	9.5	-16.7	34.6	6.6	8.1
2	42	614.6	16.0	14.6	14.7	-1.9	24.1	16.0	6.7
3	8	124.9	17.5	15.6	15.6	3.4	24.3	21.7	13.9
4	133	1,527.9	15.4	11.6	12.8	-19.0	39.5	11.1	6.0
5	13	24.6	21.7	1.9	18.4	-24.9	49.0	0.0	18.7

C. Comparison by pumping periods

Stress periods	Years	Number of data points	Sum of the residuals	Root mean square error	Mean error	Absolute mean error	Residuals			Percent standard deviation/range
							Minimum	Maximum	Median	
1–24	1926–49	111	756.0	11.1	6.8	9.2	-16.7	22.2	6.6	6.9
25–40	1950–65	68	665.7	14.6	9.8	12.3	-13.7	49.0	12.6	4.6
41–61	1966–86	70	1,196.5	19.8	17.1	17.7	-3.8	34.6	19.4	6.1
62–74	1987–99	64	381.2	11.6	6.0	9.7	-24.9	24.2	7.2	7.4
75–78	2000–03	32	284.8	15.5	8.9	12.3	-19.0	39.5	7.2	9.7

D. Comparison by decade

Stress periods	Years	Number of data points	Sum of the residuals	Root mean square error	Mean error	Absolute mean error	Residuals			Percent standard deviation/range
							Minimum	Maximum	Median	
2–5	1927–30	18	59.4	5.5	3.3	4.4	-5.7	9.9	2.3	3.9
6–15	1931–40	51	380.7	10.5	7.5	8.6	-10.5	21.7	6.5	5.8
16–25	1941–50	44	348.9	13.6	7.9	12.0	-16.7	22.2	13.2	9.0
26–35	1951–60	39	352.6	14.1	9.0	11.6	-12.0	49.0	8.6	4.6
36–45	1961–70	53	683.4	17.2	12.9	28.5	-13.7	31.5	15.5	10.2
46–55	1971–80	39	730.6	20.8	18.7	19.1	-0.3	34.6	19.6	5.6
56–65	1981–90	12	129.8	12.4	10.8	10.5	-1.9	21.6	9.6	5.2
66–75	1991–00	65	377.7	11.7	5.8	9.7	-24.9	24.3	7.0	8.3
76–78	2001–03	24	221.0	16.4	9.2	13.3	-19.0	39.5	7.6	10.4

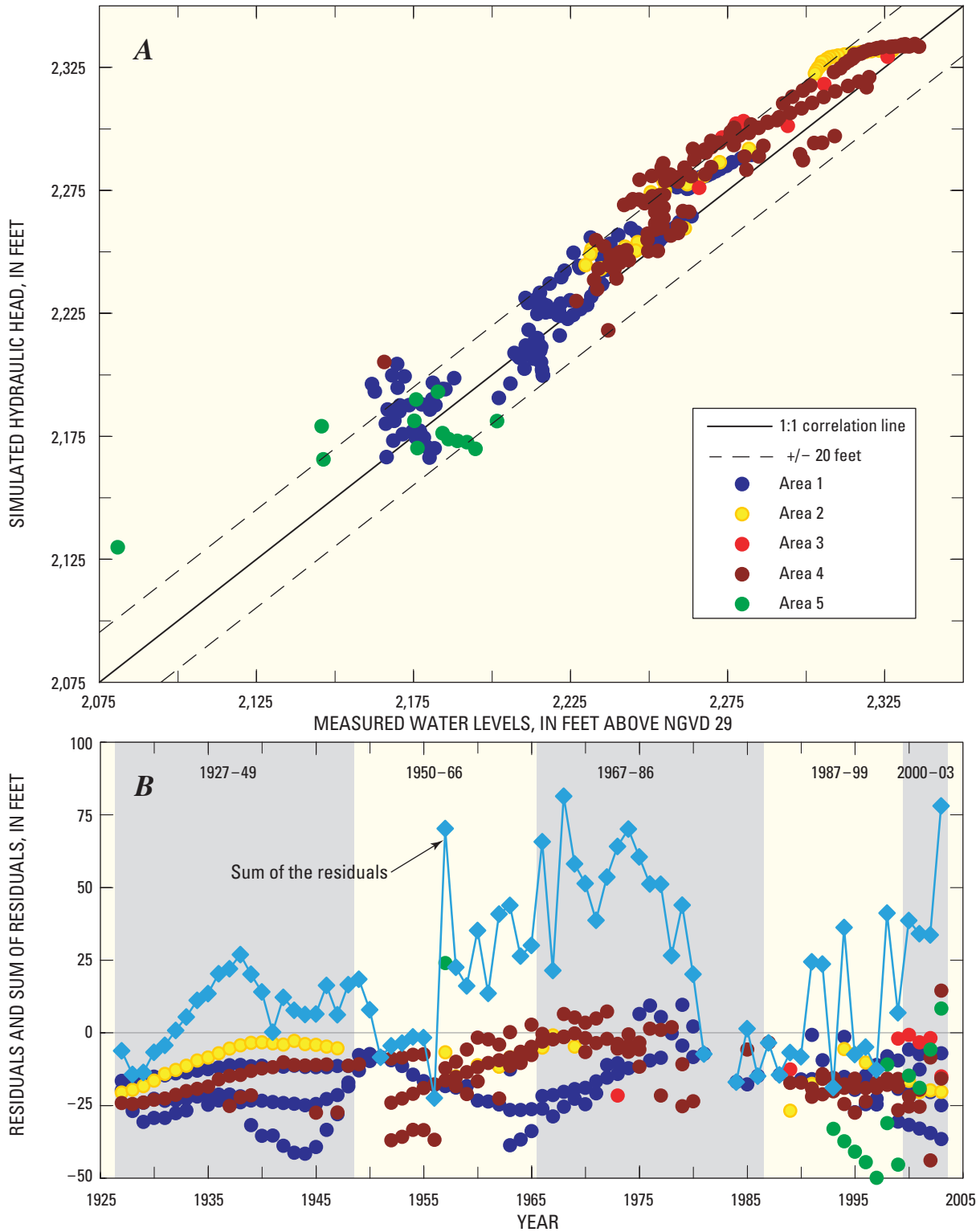


Figure 50. Graphs showing (A) measured water levels and simulated hydraulic heads and (B) residuals and sum of residuals for the calibrated ground-water flow model, 1926–2003, San Gorgonio Pass area, Riverside County, California.

A

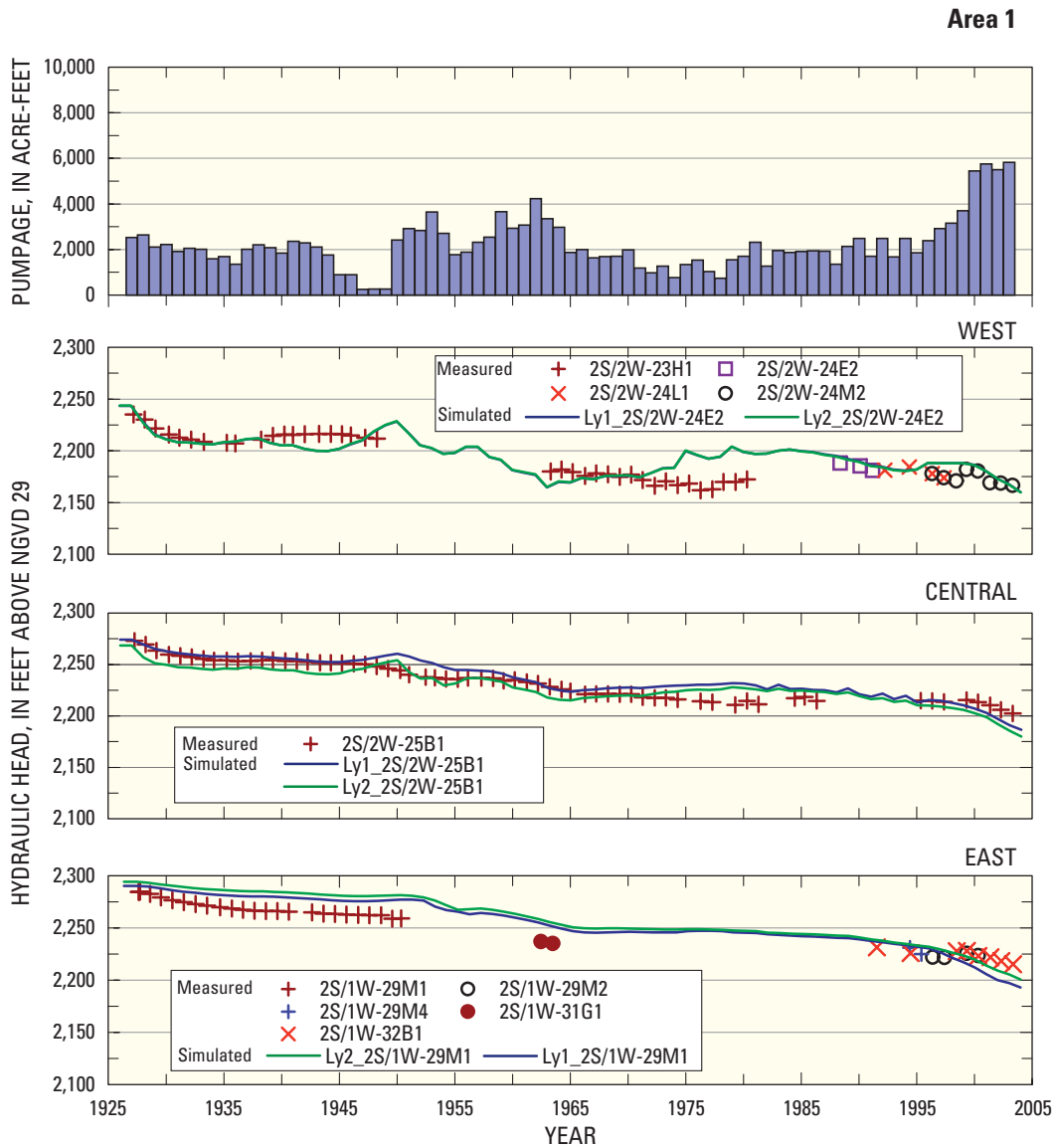


Figure 51. Graphs showing measured and simulated hydraulic heads for selected wells, and pumpage by model area, for (A) Area 1, (B) Areas 2 and 3, (C) Area 4, and (D) Area 5, San Gorgonio Pass area, Riverside County, California.

The cumulative storage depletion from 1926–2003 was about 222,660 acre-ft (*fig. 52D* and *table 13*). The declines in measured water levels (*fig. 51*) are directly related to the storage depletion (*fig. 52D*). The simulated water budget for 1926–2003 indicates that of the total simulated volume of water pumped from the aquifer (450,160 acre-ft), about 50 percent was derived from depletion of ground-water storage (222,660 acre-ft), about 21 percent was derived from the reduction of underflow to the Cabazon and San Timoteo storage units (about 96,280 acre-ft), about 19 percent was derived from a reduction of ground-water outflow to the stream channels draining the San Timoteo storage unit (about 86,030 acre-ft), about 8 percent was derived from irrigation return flows and septic-tank seepage (about 36,780 acre-ft), and about 2 percent was derived from an increase in ground-water underflow from the surrounding older sedimentary deposits (about 8,410 acre-ft).

Sensitivity Analysis

A sensitivity analysis evaluates the sensitivity of a model to variations in its input parameters. The analysis involves keeping all input parameters and model stresses constant except the one being analyzed, varying that parameter or model stress through a range that includes the uncertainties in that parameter or stress. The parameter or stress being tested was changed in both the steady-state and transient-state models. Simulated hydraulic heads from year-2000 of the calibrated model were compared with simulated hydraulic heads from year-2000 of the sensitivity simulation to evaluate the sensitivity of the model. Model sensitivity was evaluated using RMSE and mean error (ME) for each of the tested parameters and model stresses (*fig. 54*).

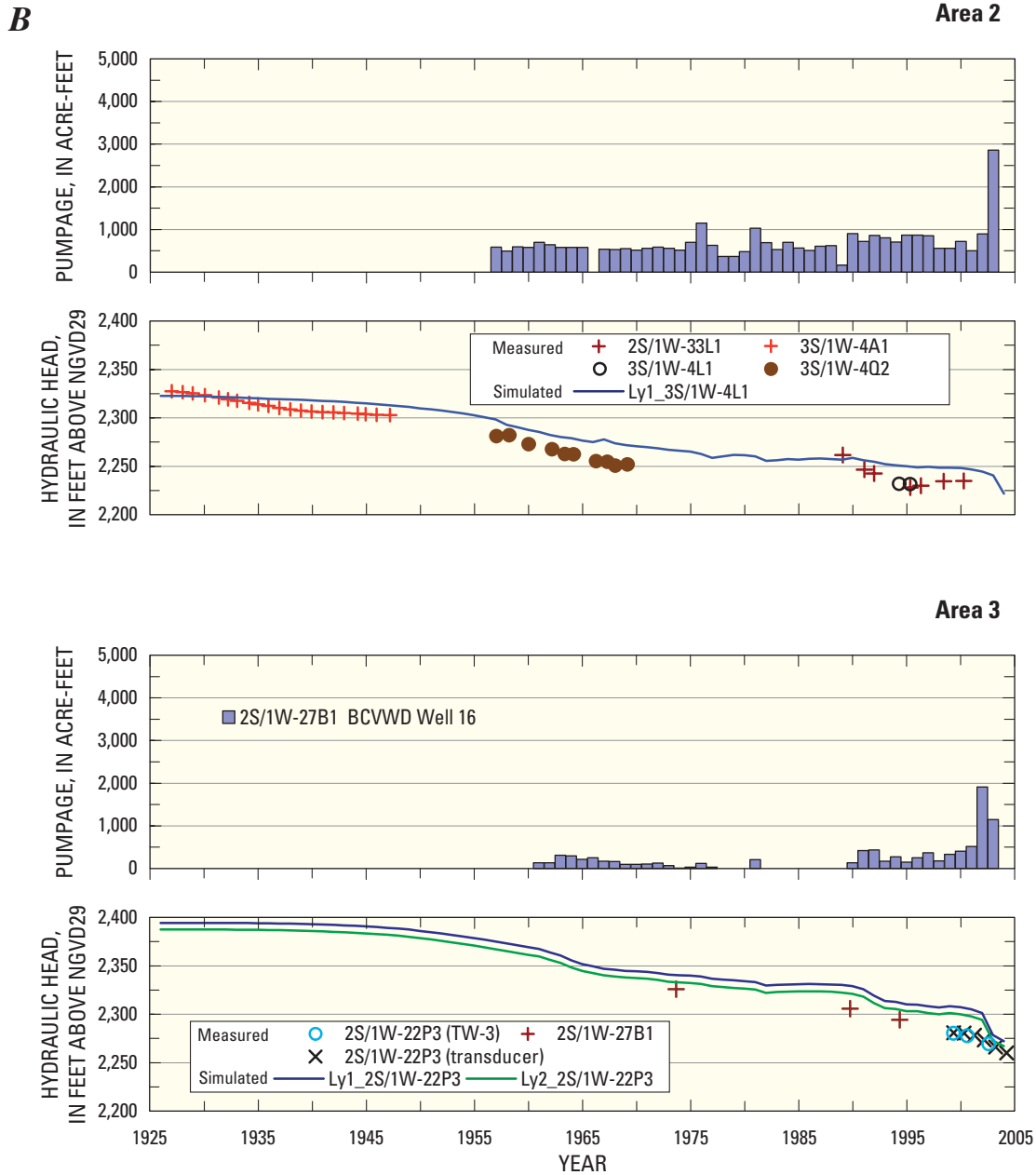


Figure 51. Continued.

The sensitivity analysis varied vertical hydraulic conductivity (K_v) by 0.01, 0.1, 10, and 100 times the calibrated value for both model layers separately. The sensitivity of horizontal hydraulic conductivity (K_h), specific yield (S_y), storage coefficient (S), general-head boundary (GHB) conductance, drain conductance, and hydraulic characteristic (hc) of simulated faults F1–7 (fig. 38) was tested by varying the calibrated value of an individual parameter by 0.5 and 2.0 times for both layers simultaneously. In addition, the sensitivity of the calibrated model to changes in areal recharge, mountain-front recharge, artificial recharge, and pumpage fluxes was tested by varying the calibrated flux by plus or minus 10 percent.

The simulated hydraulic heads in model layer 1 were relatively insensitive to varying the K_v of model layer 1; however, the simulated hydraulic heads in model layer 2 were very sensitive to decreasing the K_v of model layer 1 by two orders of magnitude (fig. 54). The simulated hydraulic heads in model layer 1 were relatively insensitive to changes in the K_v of model layer 2; although, they were more sensitive than to changes in K_v of model layer 1 (fig. 54). The simulated hydraulic heads in model layer 2 are very sensitive to decreases in the K_v of model layer 2 (fig. 54). Decreasing the K_v of model layers 1 and 2 by two orders of magnitude resulted in simulated hydraulic heads in model layer 2 being significantly higher than the calibrated values as indicated by the ME (fig. 54).

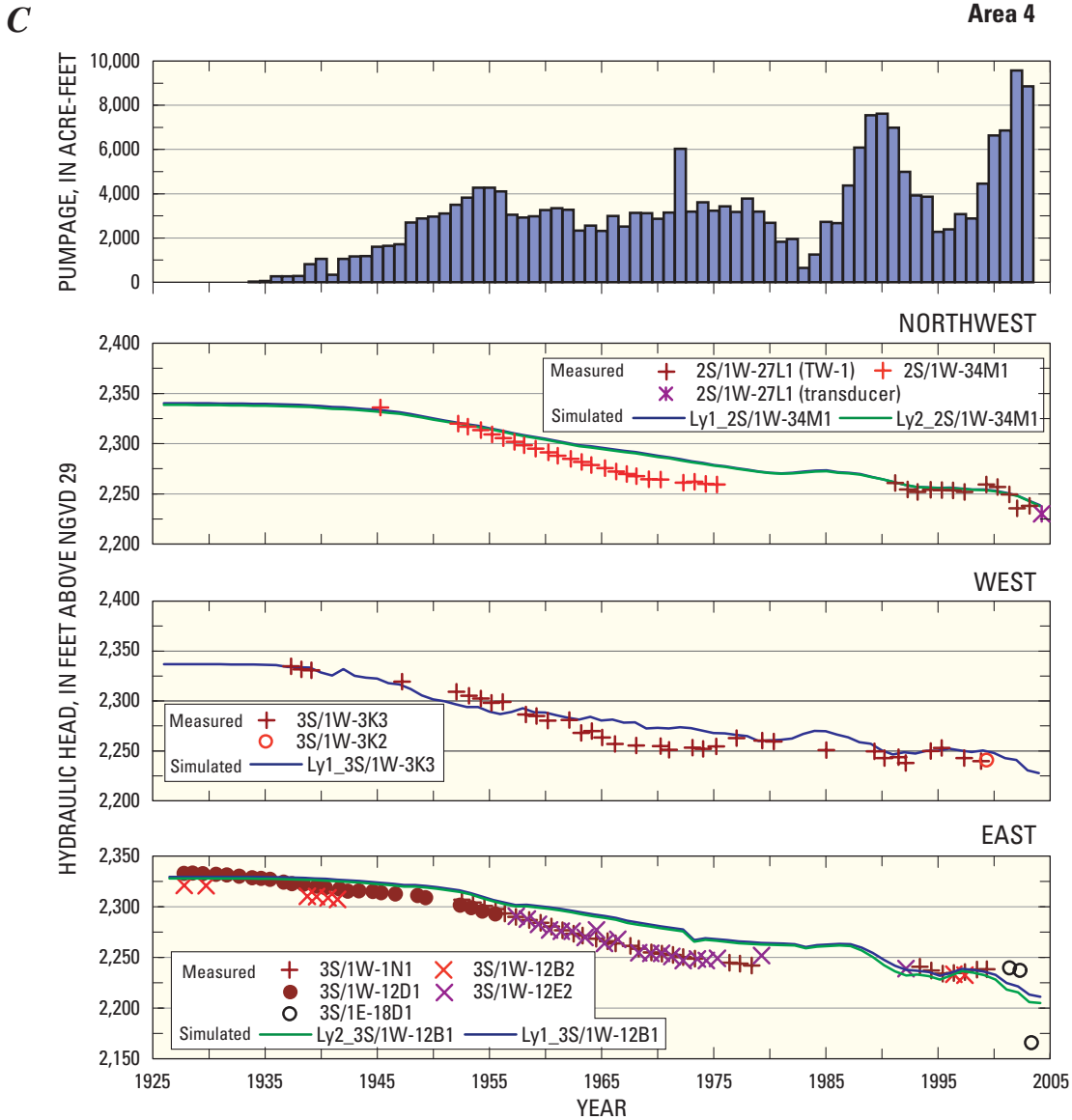


Figure 51. Continued.

The simulated hydraulic heads in model layers 1 and 2 were very sensitive to increases and decreases in the K_h and S_y of model layer 1 and the GHB conductance; however, the simulated hydraulic heads in model layers 1 and 2 were relatively insensitive to changes in the K_h of model layer 2, S of model layer 2, and drain conductance (fig. 54).

The simulated hydraulic heads for model layers 1 and 2 were relatively sensitive to changes in recharge and pumpage. The degree of sensitivity is directly related to the magnitude of the flux, that is, the higher the flux the higher the model sensitivity. The simulated hydraulic heads of both model layers also were relatively sensitive to changes in the hc value of

all of the faults. The simulated hydraulic heads were most sensitive to changes in the hc value of faults F6 and F7 and least sensitive to changes in the hc value of faults F1 and F5 (fig. 54). Although, the simulated hydraulic heads were relatively insensitive to the hc value of fault F5 when the entire model is evaluated, the simulated hydraulic heads in area 3, upgradient of the Cherry Valley Fault (fault F5), were very sensitive to changes in this parameter.

D

Area 5

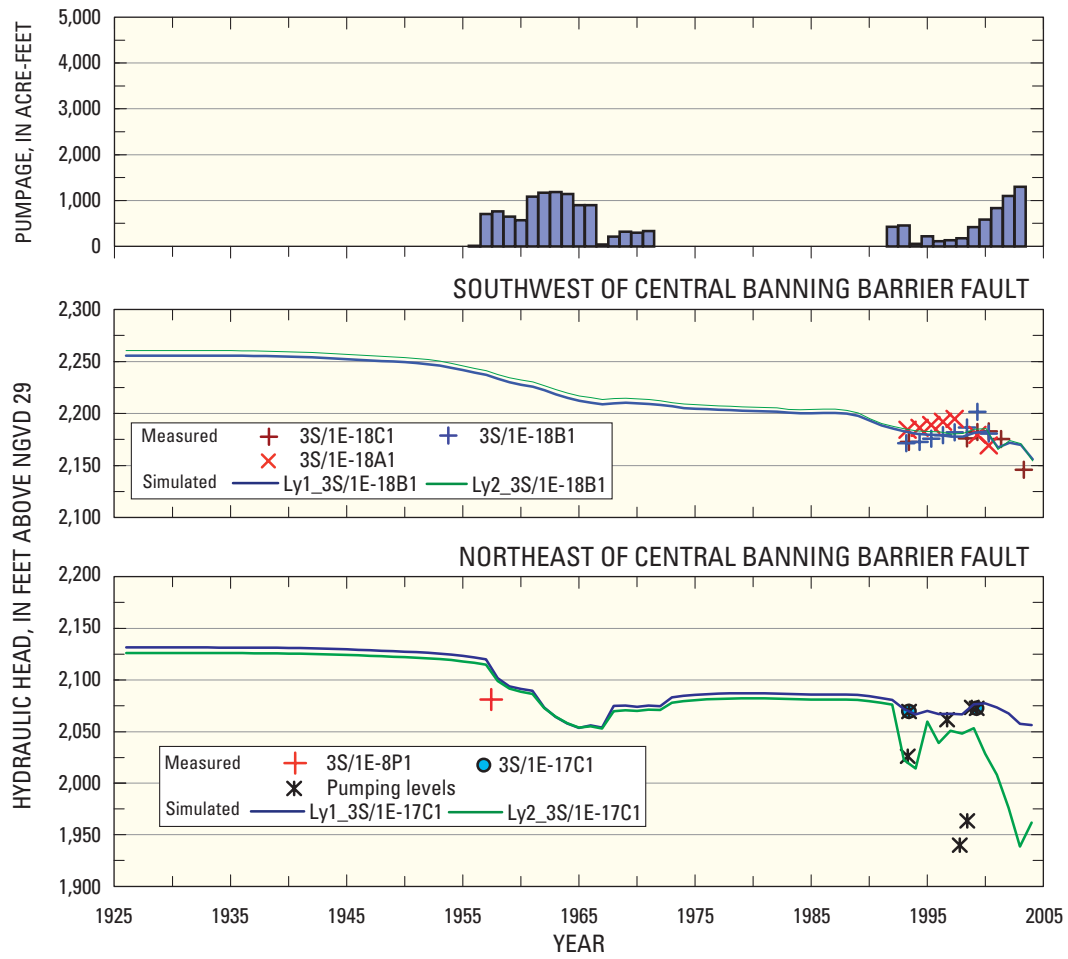


Figure 51. Continued.

Table 13. Water budget for the calibrated steady-state model and for selected periods of the transient-state model of the San Geronio Pass area, Riverside County, California.

[Values are in acre-feet per year; —, no storage data for steady-state conditions]

Water-budget components	Steady-state (predevelopment)	Transient-state stress period										Cumulative 1-78 (1926-2003)
		1 (1926)	5 (1930)	15 (1940)	25 (1950)	35 (1960)	45 (1970)	55 (1980)	65 (1990)	75 (2000)	78 (2003)	
Inflow												
Storage	—	0.1	1,016.7	1,502.7	4,026.9	4,602.0	2,543.7	1,492.4	7,046.9	7,994.6	12,416.1	245,420.9
General head boundary ¹	210.5	210.5	215.3	220.7	223.8	349.7	387.3	323.3	381.8	497.3	776.8	24,829.2
Return flow	0.0	0.0	0.0	0.0	0.0	0.0	32.0	528.7	854.9	2,415.6	2,740.9	36,776.4
Mountain-front recharge	2,674.0	2,674.0	2,674.0	2,674.0	2,674.0	2,674.0	2,674.0	2,674.0	2,674.0	2,674.0	2,674.0	208,574.0
Areal recharge	3,707.2	3,707.2	3,707.2	3,707.2	3,707.2	3,707.2	3,707.2	3,707.2	3,707.2	3,707.2	3,707.2	289,156.3
Total	6,591.7	7,613.1	8,104.7	10,631.9	11,333.0	9,344.2	8,725.7	14,664.7	17,288.7	22,315.1	22,315.1	804,756.9
Outflow												
Storage	—	0.0	0.0	18.5	0.0	0.0	82.2	1.2	0.0	4.8	0.0	22,757.0
General head boundary ¹	4,902.0	4,654.3	4,530.8	4,431.0	3,660.3	3,176.8	3,189.5	2,963.2	2,628.6	2,318.5	2,318.5	286,065.3
Drains ²	1,689.9	1,689.0	744.2	656.2	327.9	325.2	668.8	526.7	253.4	0.0	0.0	45,707.8
Pumpage	0.0	0.0	2,214.0	2,898.0	7,343.5	5,759.3	4,865.0	11,174.0	14,400.7	19,996.0	19,996.0	450,155.2
Total	6,591.9	7,612.5	8,103.5	10,631.4	11,331.7	9,343.5	8,724.5	14,664.0	17,287.5	22,314.5	22,314.5	804,685.3
Difference: inflow-outflow	-0.2	-0.1	0.6	1.2	0.5	1.3	0.7	1.2	0.7	1.2	0.6	71.6

¹Ground-water underflow.²Ground-water outflow to stream channels draining the San Timoteo storage unit.

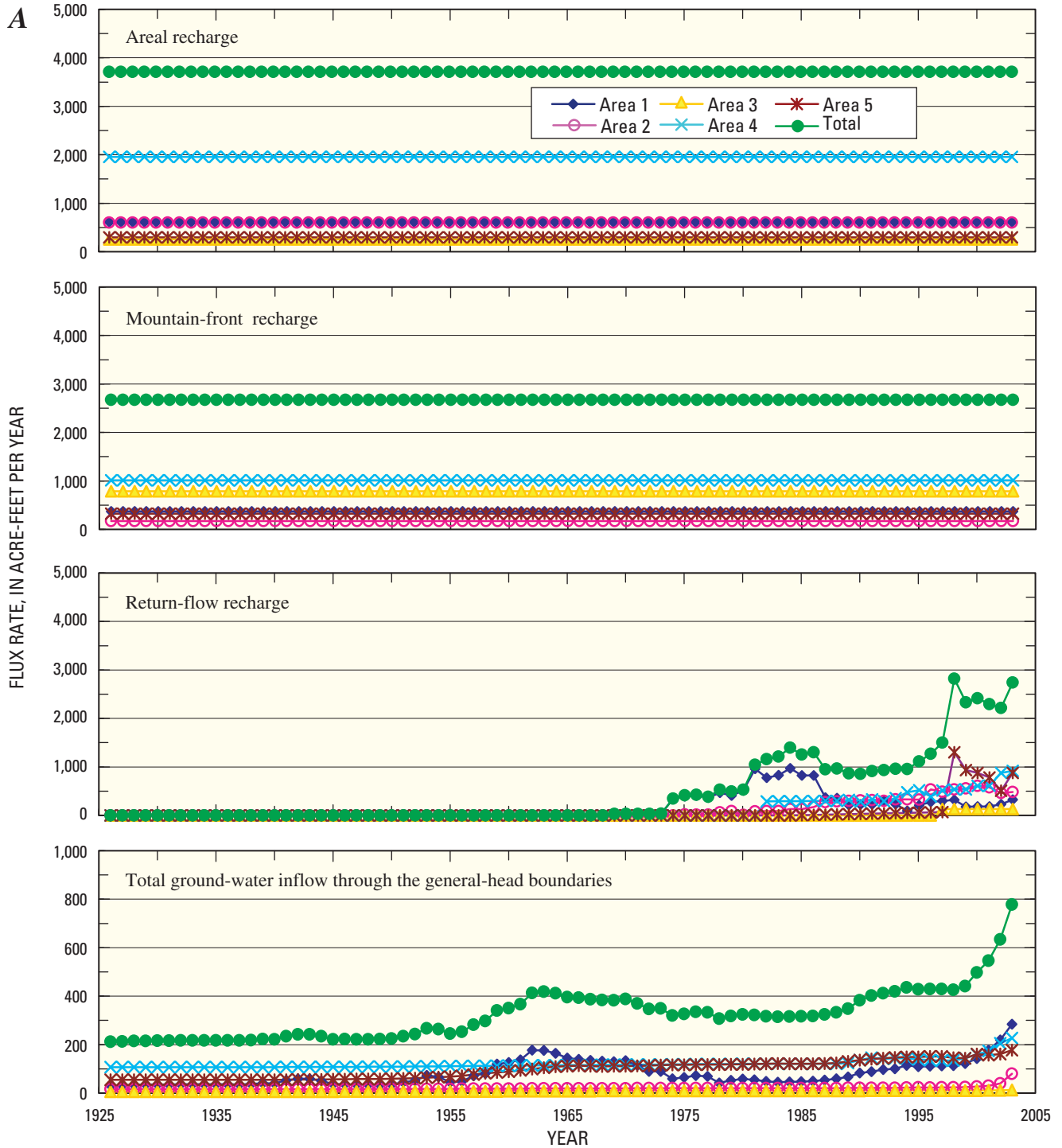


Figure 52. Graphs showing the simulated (A) recharge flux, (B) discharge flux, (C) cumulative recharge, and (D) cumulative discharge, 1926–2003, San Geronigo Pass area, Riverside County, California.

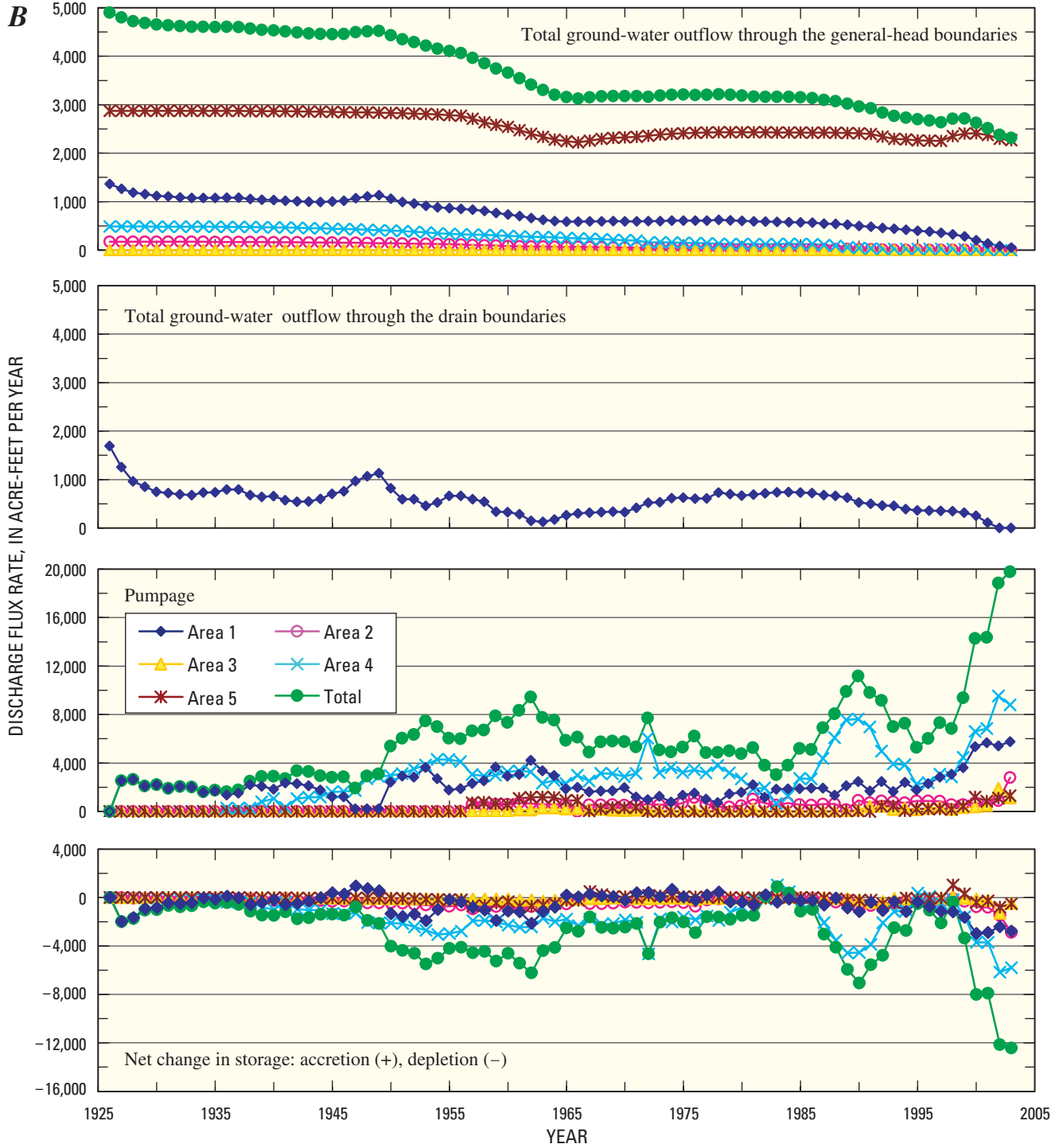


Figure 52. Continued.

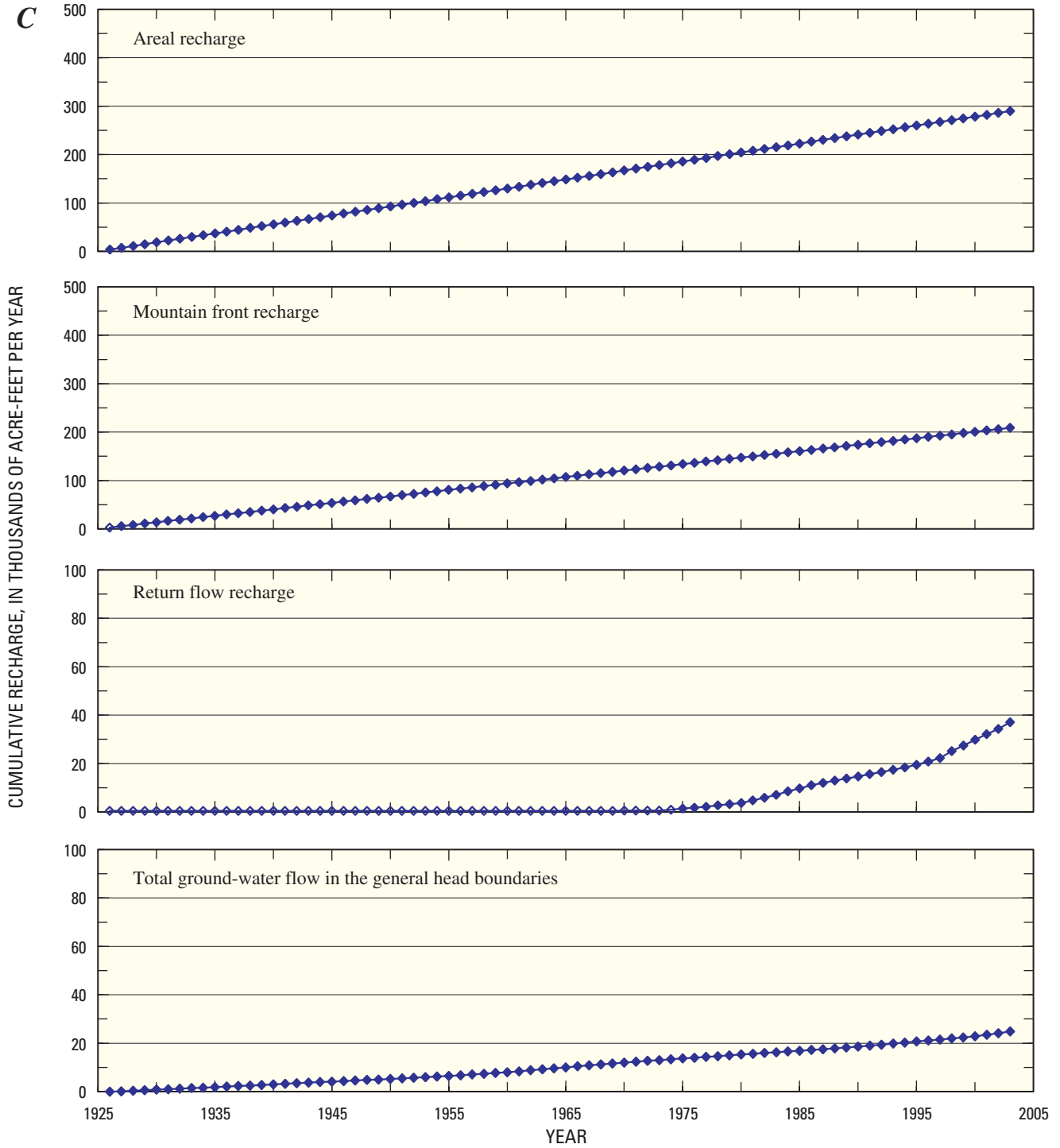


Figure 52. Continued.

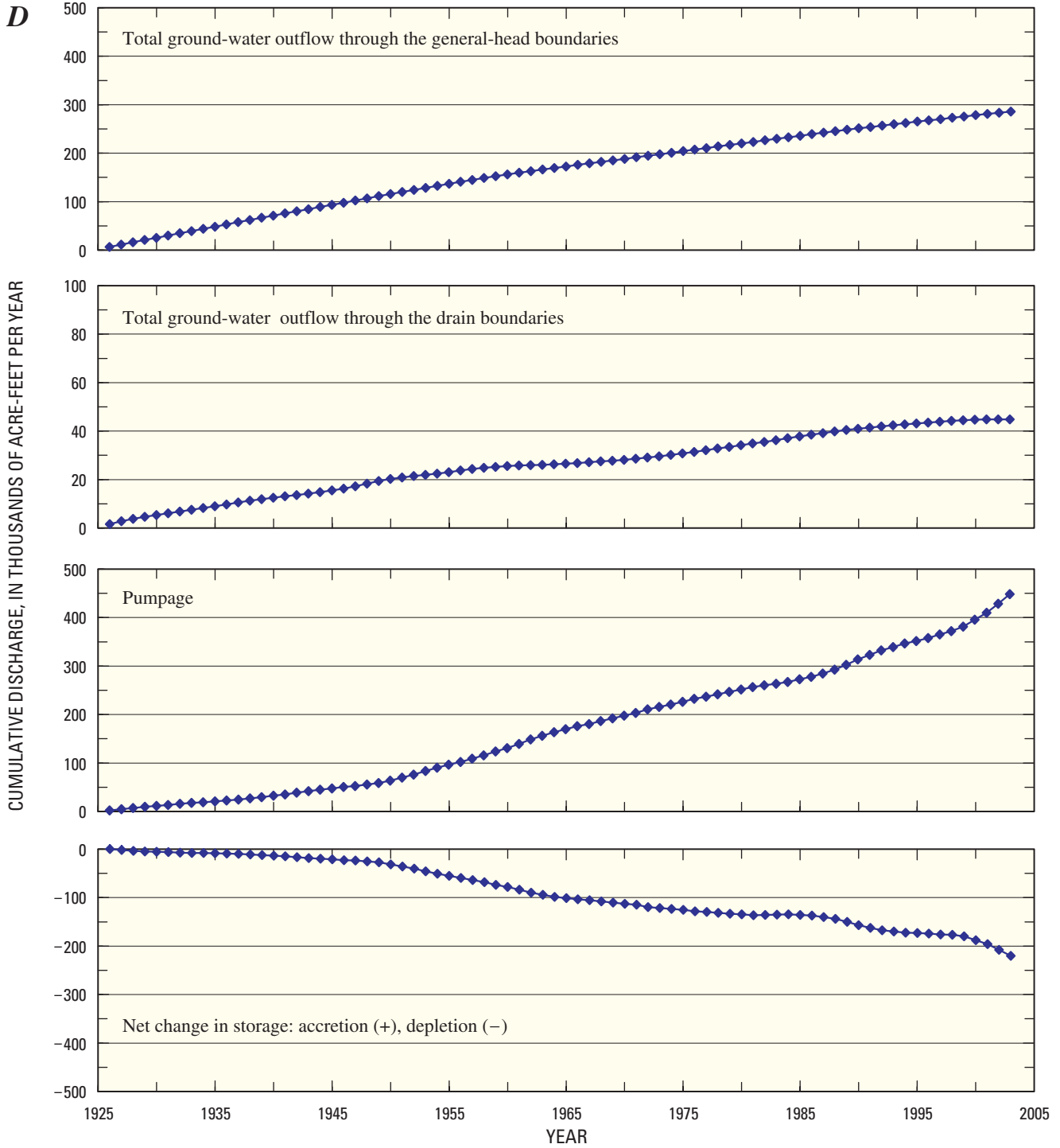


Figure 52. Continued.

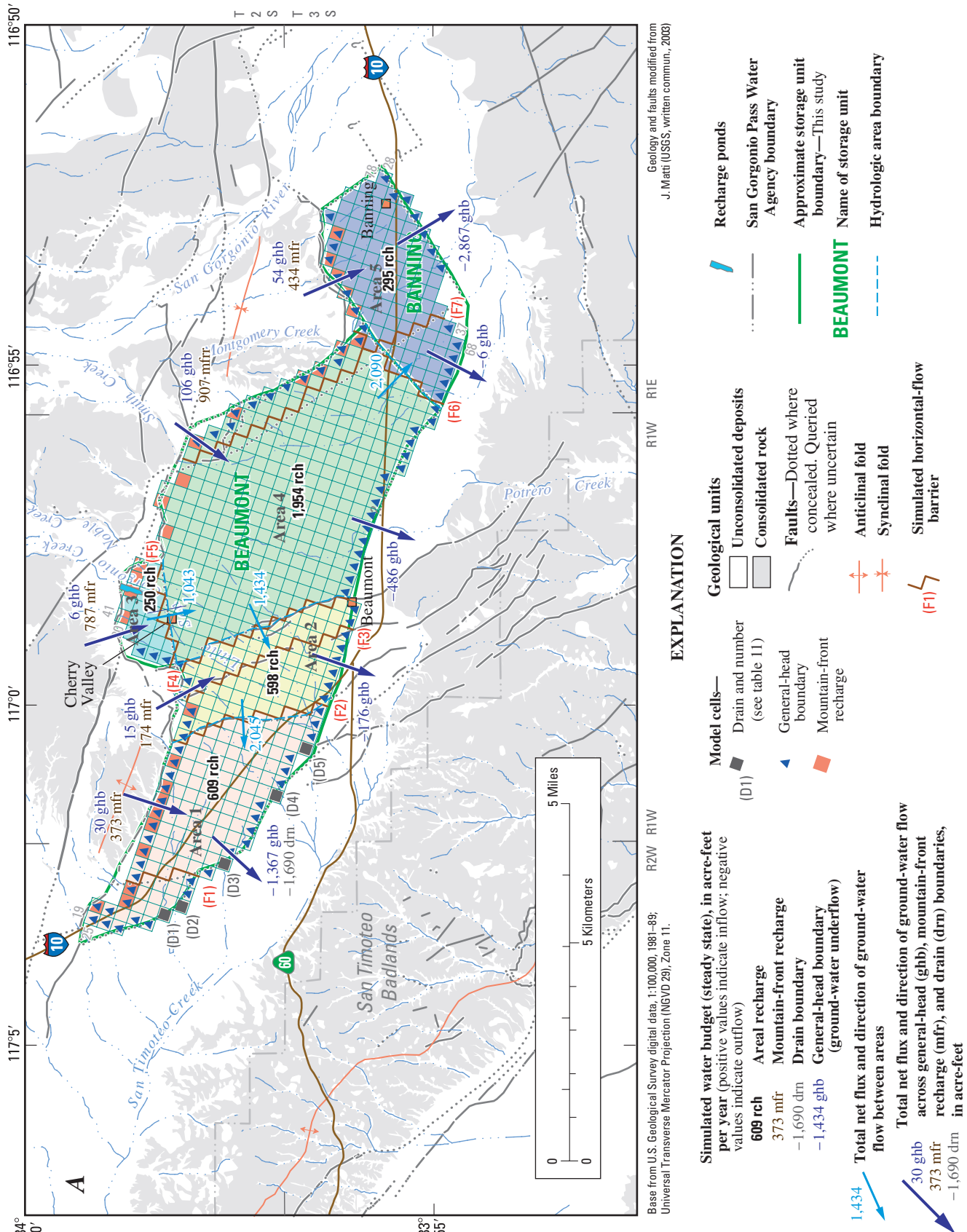


Figure 53. Maps showing the simulated water budget for simulated (A) steady-state conditions and (B) year-2003 conditions, San Gorgonio Pass area, Riverside County, California.

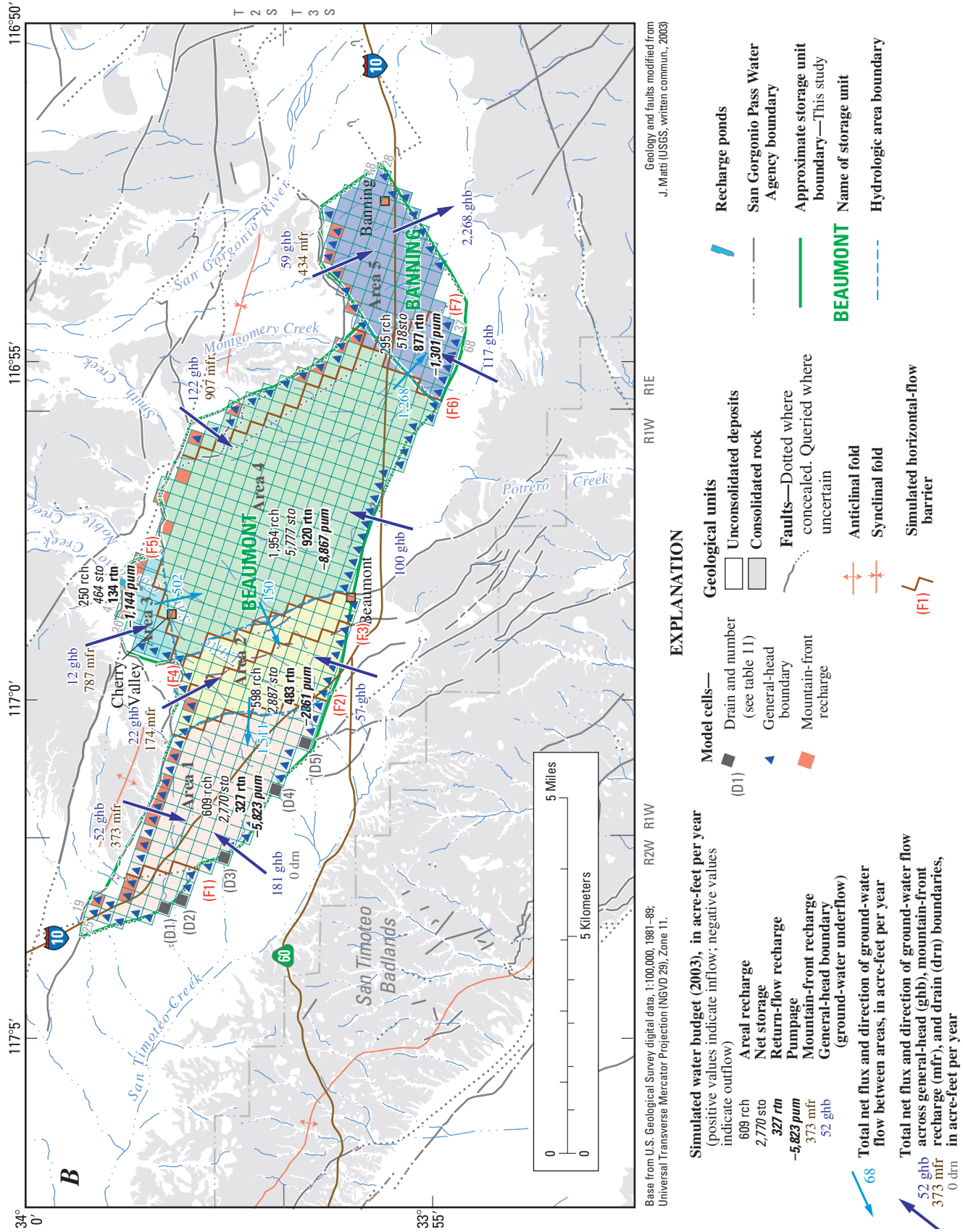


Figure 53. Continued.

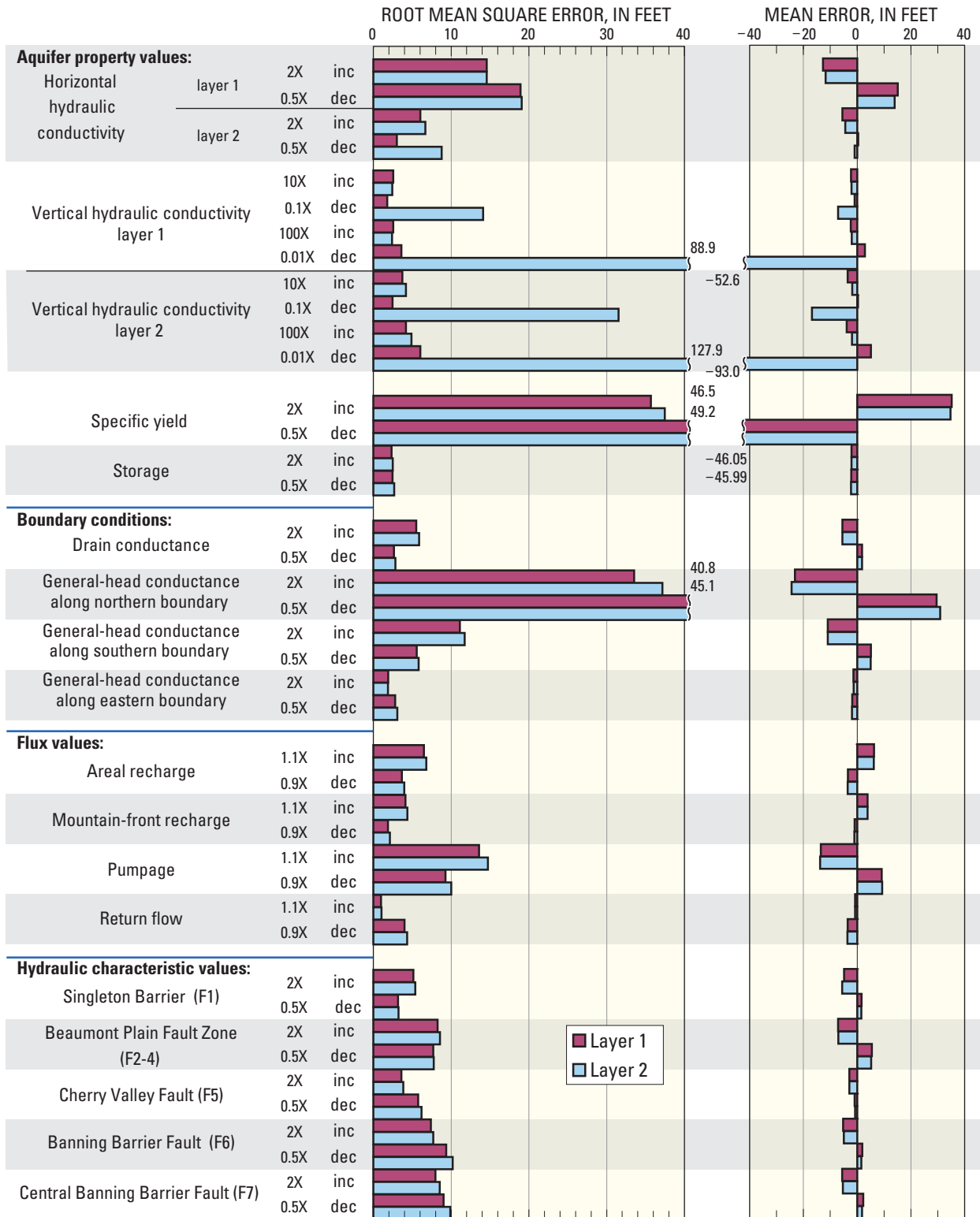


Figure 54. Graph showing the sensitivity of selected ground-water model parameters, San Gorgonio Pass area, Riverside County, California.

Model Limitations

A ground-water flow model is a numeric representation of a conceptual model of the ground-water system. Furthermore, the conceptual model is a simplified version of reality based on the modeler's understanding of the ground-water system. The conceptualization of the ground-water system introduces potential errors because the conceptual model may be based on incomplete or erroneous data and analyses.

Perhaps the greatest limitation of the modeling approach used in this study is the ability of zonal heterogeneity to represent a complex hydrogeologic setting. The capability of the model to reliably project aquifer responses also is related to the accuracy of the calibration data, and it is inversely related to the magnitude of the proposed changes in aquifer stresses and the length of the simulation horizon.

In this study, the model was calibrated using trial-and-error techniques. Owing to the complexity and unknowns of the system being represented, it is worth noting that model construction and calibration results in a non-unique model and model predictions can be subject to large errors (Konikow and Bredehoeft, 1992). Automated model-calibration techniques have been used in subsequent studies to quantify uncertainties in the model-calibrated parameters that could improve the fit of the model to calibration data (Yeh, 1986).

As with all models, uncertainties in the input data may affect the calibration results. For example, uncertainties are introduced by the temporal averaging of recharge, spatial averaging of horizontal and vertical hydraulic properties over large areas, estimation of pumpage, as well as errors in measuring and interpreting data.

Faults can have a significant barrier effect on the flow of ground water in the Beaumont and Banning storage units. Therefore, in order to accurately simulate ground-water flow, the location and hydrologic properties of the faults must be known. However, the locations and geometries of faults within the model domain are uncertain because limited data are available over most of the study area. As more information becomes available, the simulated locations of faults may need to be changed and new faults may need to be added to the model.

In the neighboring lower Coachella Valley, measured water-level declines similar to those observed in the study area have caused land subsidence (Sneed and others, 2001). Land subsidence is often related to the compaction of fine-grained sediments resulting primarily from ground-water withdrawals. In this study, compaction is not modeled because there is no evidence of subsidence and the aquifer deposits are considered less susceptible to compaction than those experiencing compaction in the Coachella Valley. Compaction of the aquifer system and land subsidence could occur in the future if water levels decline below critical thresholds that are not yet defined.

Particle-Tracking and Flow Paths

The ground-water ages determined from the tritium and ^{14}C data collected at selected wells were compared with the simulated travel time for imaginary particles to travel from model cells representing the selected wells (*table 14*) to recharge zones, thereby verifying that the model reasonably simulates the ground-water flow system. As described in the "Source and Age of Ground Water" section of this report, selected wells were sampled for tritium and (or) ^{14}C to determine the age, or time since recharge, of the ground water in the Beaumont and Banning storage units (*fig. 36*). The estimated age of the sampled ground water ranges from less than 50 years to as old as 17,500 years old (uncorrected age). As stated in the "Source and Age of Ground Water" section, uncorrected ^{14}C ages generally are older than the actual age of the associated water.

A backward-tracking analysis was completed under steady-state conditions using the particle-tracking program MODPATH (Pollock, 1994) to determine the travel time of water to 11 production wells where both tritium ^{14}C data were collected (*table 14*). For this report, traveltime is assumed to be the simulated age of the ground water at the well. MODPATH is a three-dimensional particle-tracking post-processing program designed for use with MODFLOW simulation results. The results from this program represent ground-water travel times and pathlines for advective transport only. MODPATH requires selected MODFLOW input and output files, including cell-by-cell flows for each time step. Additional required inputs include porosity, top and bottom elevations of model layers, and particle-starting locations. A complete description of the theoretical development, solution techniques, and limitations of MODPATH is presented by Pollock (1994).

A porosity of 0.30 was assumed for both model layers, which is within the range of reported porosity values for sand and gravel aquifers (Davis and DeWeist, 1966). Ground water moves more slowly if the porosity is higher; therefore, simulated travel times will be greater in an aquifer with a high porosity than in an aquifer with a low porosity, if the gradient and transmissivity along the flow path within the two aquifers are the same.

To allow for variations in travel times among particle paths starting at different locations within a model cell, 30 to 100 particles were evenly distributed along a vertical column in the cell node representing the well with estimated age data. The particles were distributed in each model layer based on the reported screened interval of the well being simulated (*table 14*). *Figure 55* shows the lateral extent of the particle paths under steady-state conditions.

Table 14. Estimated and simulated residence times of ground water in selected cells during steady-state conditions using backward particle tracking, San Geronio Pass area, Riverside County, California.

Well no.	Layer	Model node (row, column)	Number of particles per layer	Ages				Screened interval altitudes (in feet)			
				Estimated age (in years)		Simulated age (in years)		Layer 1	Layer 2		
				Tritium	Carbon-14	Minimum	Maximum			Mean	Median
Area 1											
2S/1W-32M001	1	33,34	100	>50	954	4	3,204	879	384	2,111–1,822	1,822–1,469
	2		100			81	4,611	1,668	1,607		
Area 2											
2S/1W-33L001	1	31,40	100	<50	1,680	15	558	191	139	2,164–1,776	1,776–1,362
	2		100			82	3,516	995	809		
Area 3											
2S/1W-22P003	1	21,43	100	<50	608	10	46	25	22	2,279–2,239	—
2S/1W-27B001	1	21,45	100	>50	963	4	30	14	11	2,357–2,109	—
Area 4											
3S/1W-03K001	1	33,48	100	>50	1,237	31	1,122	391	372	2,198–1,975	—
2S/1W-35J001	1	26,53	30	>50	1,470	75	270	173	192	1,897–1,877	—
2S/1W-35J002	1	26,53	30	>50	1,772	75	238	169	192	2,027–2,007	—
2S/1W-35J003	1	26,53	30	>50	1,304	75	207	153	167	2,167–2,147	—
3S/1W-12K001	1	35,60	100	<50	3,043	11	929	328	279	2,145–1,921	1,921–1,587
	2		100			8	7,669	1,252	1,035		
3S/1E-07E002	1	33,61	100	<50	1,896	9	706	237	206	2,120–1,817	1,817–1,520
	2		100			5	17,661	1,568	791		
3S/1E-18D001	1	37,63	100	>50	6,786	16	980	395	315	2,099–2,043	—

[—, no screened interval in model layer 2; altitude shown in National Geodetic Vertical Datum of 1927; <, less than; >, greater than]

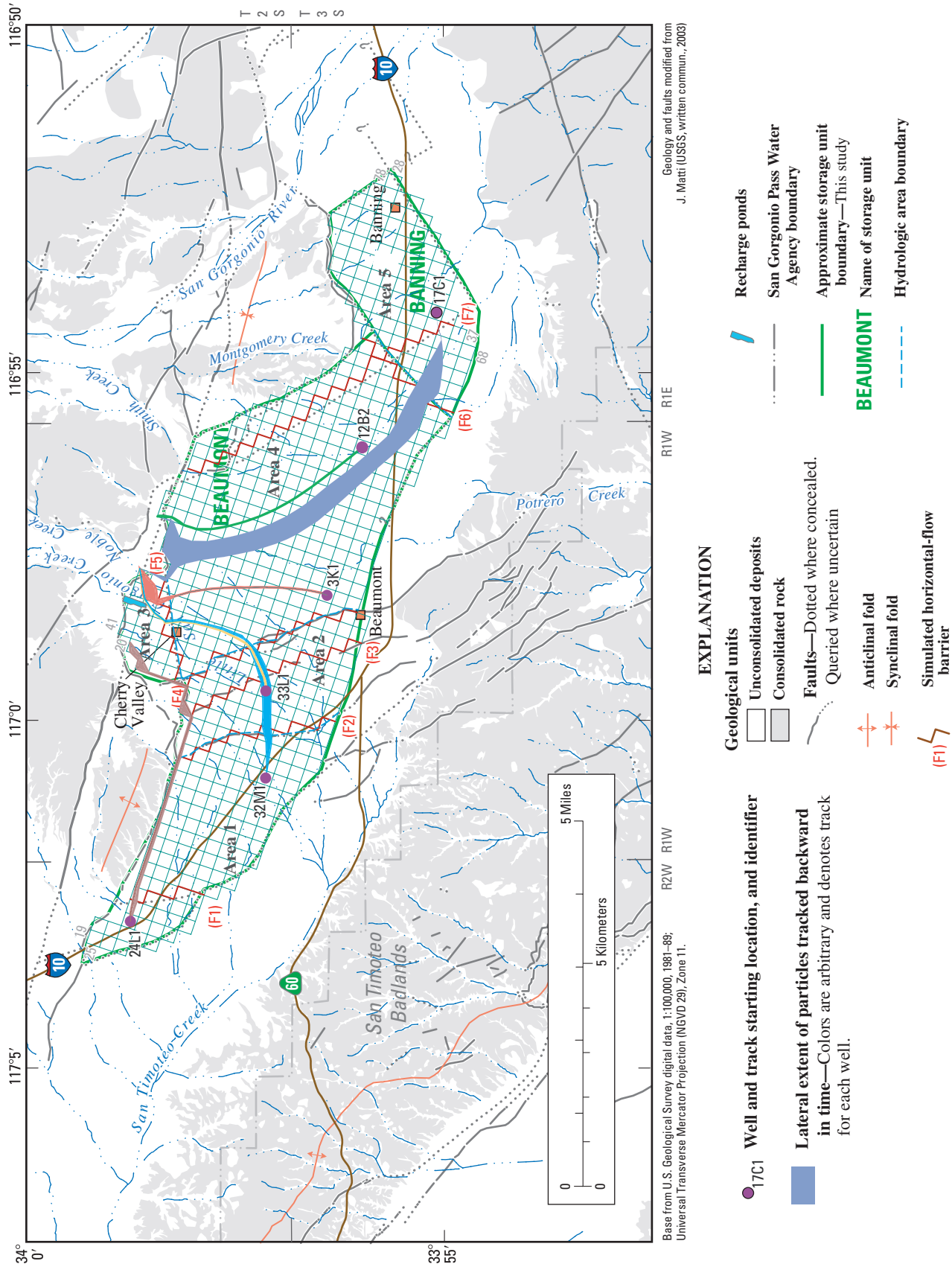


Figure 55. Map showing backward particle tracking of particles under steady-state conditions starting at selected production wells, San Gorgonio Pass area, Riverside County, California.

In general, the simulated ages based on travel times are younger than the uncorrected ^{14}C ages. The median simulated ages for ground water at the 11 production wells range from 11 years old to 1,607 years old; whereas, the estimated age of the ground water from these wells ranges from less than 50 years old to 6,786 years old (*table 14*). The greatest discrepancies between simulated ages and estimated ground-water age is for wells that are perforated only in model layer 1. Note, the travel time through the unsaturated zone was not accounted for in the particle-tracking simulation. To more accurately simulate the travel time through the aquifer would require simulating the flow through the unsaturated zone and adding additional layers in the upper aquifer to simulate the interbedded silt and clay layers that retard the downward migration of the recharge water.

Simulation of Future Water-Management Scenarios

The SGPWA has the authority to artificially recharge the San Geronio Pass area using imported water from the State Water Project (SWP) and has constructed a pipeline to deliver SWP water into the Cherry Valley area (*fig. 2*) for recharge and possibly for irrigation supply. The calibrated ground-water flow model was used to simulate the effects of four water-management scenarios being considered by SGPWA (Steve Stockton, General Manager, San Geronio Pass Water Agency, written commun., 2002) to artificially recharge the Beaumont storage unit with imported water from the SWP and utilize water from the SWP in lieu of pumping ground water for agricultural supply in the Beaumont storage unit. The SWP water was assumed to recharge model layer 1. The simulation period for these scenarios was 2004–13.

The four water-management scenarios assumed that the total basin-wide areal recharge and mountain-front recharge remained constant at about 4,300 acre-ft/yr and about 2,670 acre-ft/yr; respectively. The recharge simulated by the urban-modified INFILv3 model (about 4,300 acre-ft/yr) was assumed representative of areal recharge for the four-management scenarios. The urban-modified areal recharge rate is about 600 acre-ft/yr greater than the areal recharge rate of about 3,710 acre-ft/yr used for the transient simulation (1926–2003) and resulted in a maximum increase of about 5.5 ft in simulated hydraulic head for the water-management scenarios over that of the transient-simulation recharge rate for the scenarios. Recall that the estimated travel time for natural recharge to reach the water table ranges from 50 to 250 years. The model area has been urbanized since about the 1950s; consequently, the additional water simulated by INFILv3 resulting from urbanization may reach the water table during the predictive period. Mountain-front recharge was assumed the same as that simulated during the transient simulation.

Artificial recharge from return flows of crop, golf course, and landscape irrigation and septic-tank seepage was estimated from pumpage, similar to the transient calibration, and ranged

from a low of about 2,750 acre-ft/yr in 2005 to a high of about 3,130 acre-ft/yr in 2012 (reported as return flow on *table 15*). The artificial recharge from return flows is variable during the predictive period because this flux is based on pumpage that occurred 23 to 71 years prior to the year being simulated.

Water-Management Scenario 1

Water-management scenario 1, considered the base case, evaluated the response of the ground-water system assuming no SWP water was available for artificial recharge. This scenario used reported ground-water pumpage for 2001–03 (*table 15A*) and an assumed pumpage of about 20,000 acre-ft/yr for 2004–13. The assumed pumpage was distributed among water-supply wells that were in use in 2003, based on the percentage of the total 2003 pumpage pumped from each active water-supply well (for example, if well A pumped 10 percent of the total 2003 pumpage, then 10 percent of 20,000 acre-ft/yr will be assigned to well A). All the other water-management scenarios were compared with the base case.

The model results indicate that for scenario 1, simulated hydraulic heads declined about 50 ft in the Beaumont storage unit and about 25 ft in the Banning storage unit compared with that for 2003 conditions (*fig. 56A*). The large simulated hydraulic-head declines in area 1 since 2003 are the result of large increases in golf-course irrigation pumpage that began in 2000 (*Appendix table 3*). These simulated hydraulic-head declines are in addition to the hydraulic-head declines that already occurred in the Beaumont and Banning storage units from 1926–2003 (*fig. 51*). From 1926–2013, the maximum simulated decline in hydraulic head is about 180 ft, which occurs in the southeastern part of area 4.

Water-Management Scenario 2

Water-management scenario 2 simulates artificial recharge of imported water from the SWP in area 3 starting in 2003 and assumes the same pumping distribution and rates as scenario 1 (*table 15B*). In scenarios 2A–C, the SWP water is equally distributed in model cells (20, 43) and (21, 43). The total imported water recharged was 2,000 acre-ft/yr, 3,000 acre-ft/yr, and 5,000 acre-ft/yr for scenarios 2A–C, respectively. Recharge is assumed to reach the water table instantaneously; however, in reality, there would probably be a delay in the recharge water reaching the water table.

In comparison with scenario 1, by 2013 scenarios 2A–C resulted in simulated increases in a range of hydraulic heads in area 3 of about 75 ft for scenario 2A to about 225 ft for scenario 2C (*fig. 56B*). In addition, there is less than a 50-ft change in simulated hydraulic head in areas 2 and 4 and almost no change in areas 1 and 5 (*fig. 56B*). The increases in simulated hydraulic heads are confined to area 3 because the Cherry Valley Fault (F4) restricts hydraulic communication between the areas 3 and 4.

Table 15A. Simulated water budgets for water management scenario 1 for the San Geronio Pass area, Riverside County, California.

[acre-ft/yr, acre feet per year]

	Scenario 1: no artificial recharge											
	Stress period (year)											
	78 (2003)	79 (2004)	80 (2005)	81 (2006)	82 (2007)	83 (2008)	84 (2009)	85 (2010)	86 (2011)	87 (2012)	88 (2013)	
Inflow (in acre-ft/yr)												
Storage	12,409	12,186	12,042	11,753	11,361	11,525	11,248	11,215	10,763	10,508	10,613	
General head ¹	805	942	1,085	1,224	1,361	1,494	1,624	1,751	1,873	1,991	2,107	
Return flow	2,741	2,784	2,751	2,870	3,098	2,754	2,864	2,728	3,024	3,133	2,881	
Mountain front recharge	2,681	2,681	2,681	2,681	2,681	2,681	2,681	2,681	2,681	2,681	2,681	
Areal recharge	3,707	3,707	3,707	3,707	3,707	3,707	3,707	3,707	3,707	3,707	3,707	
Artificial recharge	0	0	0	0	0	0	0	0	0	0	0	
Total IN to the system	22,343	22,300	22,266	22,235	22,208	22,161	22,123	22,082	22,047	22,019	21,988	
Outflow (in acre-ft/yr)												
Storage	0	0	0	0	0	0	0	0	0	0	0	
General head	2,346	2,303	2,269	2,237	2,211	2,163	2,126	2,085	2,050	2,022	1,991	
Pumpage	19,996	19,996	19,996	19,996	19,996	19,996	19,996	19,996	19,996	19,996	19,996	
Drains ²	0	0	0	0	0	0	0	0	0	0	0	
Total OUT from the system	22,342	22,299	22,265	22,233	22,207	22,159	22,122	22,081	22,046	22,018	21,987	
Difference: IN-OUT	1	1	1	2	1	2	1	1	1	1	1	

¹Ground-water underflow.

²Ground-water outflow to stream channels draining the San Timoteo storage unit.

Table 15B. Simulated water budgets for water management scenario 2 for the San Gorgonio Pass area, Riverside County, California.

[acre-ft/yr, acre feet per year]

Scenario 2A: 2,000 acre-ft of artificial recharge												
Stress period (year)												
	78	79	80	81	82	83	84	85	86	87	88	
	(2003)	(2004)	(2005)	(2006)	(2007)	(2008)	(2009)	(2010)	(2011)	(2012)	(2013)	
Inflow (in acre-ft/yr)												
Storage	12,409	11,375	10,854	10,302	9,705	9,745	9,373	9,264	8,810	8,566	8,684	
General head ¹	805	941	1,081	1,217	1,349	1,476	1,597	1,716	1,829	1,936	2,042	
Return flow	2,741	2,784	2,751	2,870	3,098	2,754	2,864	2,728	3,024	3,133	2,881	
Mtn Front recharge	2,681	2,681	2,681	2,681	2,681	2,681	2,681	2,681	2,681	2,681	2,681	
Areal recharge	3,707	3,707	3,707	3,707	3,707	3,707	3,707	3,707	3,707	3,707	3,707	
Artificial recharge	0	2000	2000	2000	2000	2000	2000	2000	2000	2000	2000	
Total IN to the system	22,343	23,488	23,074	22,777	22,540	22,363	22,222	22,097	22,050	22,024	21,995	
Outflow (in acre-ft/yr)												
Storage	0	1,188	808	542	332	202	98	13	0	0	0	
General head	2,346	2,303	2,269	2,237	2,211	2,164	2,127	2,087	2,053	2,026	1,997	
Pumpage	19,996	19,996	19,996	19,996	19,996	19,996	19,996	19,996	19,996	19,996	19,996	
Drains ²	0	0	0	0	0	0	0	0	0	0	0	
Total OUT from the system	22,342	23,487	23,074	22,776	22,539	22,361	22,221	22,096	22,049	22,022	21,993	
Difference: IN-OUT	1	1	0	1	1	2	1	1	1	2	2	

¹Ground-water underflow.

²Ground-water outflow to stream channels draining the San Timoteo storage unit.

Table 15B. Simulated water budgets for water management scenario 2 for the San Geronio Pass area, Riverside County, California—Continued.
[acre-ft/yr, acre feet per year]

	Scenario 2B: 3,000 acre-ft of artificial recharge										
	Stress period (year)										
	78 (2003)	79 (2004)	80 (2005)	81 (2006)	82 (2007)	83 (2008)	84 (2009)	85 (2010)	86 (2011)	87 (2012)	88 (2013)
Inflow (in acre-ft/yr)											
Storage	12,409	11,132	10,420	9,727	9,027	8,993	8,569	8,426	7,902	7,601	7,721
General head ¹	805	940	1,080	1,213	1,343	1,466	1,584	1,698	1,806	1,908	2,008
Return flow	2,741	2,784	2,751	2,870	3,098	2,754	2,864	2,728	3,024	3,133	2,881
Mtn Front recharge	2,681	2,681	2,681	2,681	2,681	2,681	2,681	2,681	2,681	2,681	2,681
Areal recharge	3,707	3,707	3,707	3,707	3,707	3,707	3,707	3,707	3,707	3,707	3,707
Artificial recharge	0	3000	3000	3000	3000	3000	3000	3000	3000	3000	3000
Total IN to the system	22,343	24,244	23,639	23,198	22,856	22,601	22,405	22,240	22,119	22,030	21,997
Outflow (in acre-ft/yr)											
Storage	0	1,944	1,373	964	648	440	280	155	67	5	0
General head	2,346	2,303	2,269	2,237	2,211	2,164	2,127	2,088	2,055	2,028	2,001
Pumpage	19,996	19,996	19,996	19,996	19,996	19,996	19,996	19,996	19,996	19,996	19,996
Drains ²	0	0	0	0	0	0	0	0	0	0	0
Total OUT from the system	22,342	24,243	23,638	23,197	22,854	22,600	22,403	22,239	22,118	22,029	21,997
Difference: IN-OUT	1	1	1	1	2	1	2	1	1	1	0

¹Ground-water underflow.

²Ground-water outflow to stream channels draining the San Timoteo storage unit.

Table 15B. Simulated water budgets for water management scenario 2 for the San Gorgonio Pass area, Riverside County, California—Continued.
[acre-ft/yr, acre feet per year]

	Scenario 2C: 5,000 acre-ft of artificial recharge										
	Stress period (year)										
	78 (2003)	79 (2004)	80 (2005)	81 (2006)	82 (2007)	83 (2008)	84 (2009)	85 (2010)	86 (2011)	87 (2012)	88 (2013)
Inflow (in acre-ft/yr)											
Storage	12,409	10,634	9,525	8,536	7,623	7,440	6,914	6,703	6,138	5,813	5,876
General head ¹	805	939	1,076	1,206	1,330	1,447	1,556	1,661	1,757	1,848	1,936
Return flow	2,741	2,784	2,751	2,870	3,098	2,754	2,864	2,728	3,024	3,133	2,881
Mtn Front recharge	2,681	2,681	2,681	2,681	2,681	2,681	2,681	2,681	2,681	2,681	2,681
Areal recharge	3,707	3,707	3,707	3,707	3,707	3,707	3,707	3,707	3,707	3,707	3,707
Artificial recharge	0	5000	5000	5000	5000	5000	5000	5000	5000	5000	5000
Total IN to the system	22,343	25,745	24,741	24,000	23,439	23,028	22,721	22,480	22,307	22,183	22,082
Outflow (in acre-ft/yr)											
Storage	0	3,445	2,475	1,765	1,231	866	596	394	252	152	77
General head	2,346	2,303	2,269	2,237	2,211	2,164	2,128	2,090	2,058	2,033	2,007
Pumpage	19,996	19,996	19,996	19,996	19,996	19,996	19,996	19,996	19,996	19,996	19,996
Drains ²	0	0	0	0	0	0	0	0	0	0	0
Total OUT from the system	22,342	25,744	24,740	23,999	23,438	23,026	22,720	22,479	22,306	22,181	22,080
Difference: IN-OUT	1	1	1	1	1	2	1	1	1	2	2

¹Ground-water underflow.

²Ground-water outflow to stream channels draining the San Timoteo storage unit.

Table 15C. Simulated water budgets for water management scenario 3 for the San Geronio Pass area, Riverside County, California.

[acre-ft/yr, acre feet per year]

	Scenario 3A: No artificial recharge										
	78 (2003)	79 (2004)	80 (2005)	81 (2006)	82 (2007)	83 (2008)	84 (2009)	85 (2010)	86 (2011)	87 (2012)	88 (2013)
Inflow (in acre-ft/yr)											
Storage	12,445	10,006	9,910	9,666	9,317	9,522	9,285	9,290	8,874	8,653	8,792
General head	802	904	1,000	1,088	1,179	1,269	1,360	1,450	1,536	1,620	1,704
Return flow	2,741	2,784	2,751	2,870	3,098	2,754	2,864	2,728	3,024	3,133	2,881
Mountain front recharge	2,681	2,681	2,681	2,681	2,681	2,681	2,681	2,681	2,681	2,681	2,681
Areal recharge	3,707	3,707	3,707	3,707	3,707	3,707	3,707	3,707	3,707	3,707	3,707
Artificial recharge	0	0	0	0	0	0	0	0	0	0	0
Total IN to the system	22,376	20,082	20,049	20,012	19,982	19,933	19,896	19,856	19,822	19,795	19,765
Outflow (in acre-ft/yr)											
Storage	0	0	0	0	0	0	0	0	0	0	0
General head	2,380	2,346	2,313	2,276	2,247	2,197	2,161	2,121	2,086	2,059	2,029
Pumpage	19,996	17,735	17,735	17,735	17,735	17,735	17,735	17,735	17,735	17,735	17,735
Drains	0	0	0	0	0	0	0	0	0	0	0
Total OUT from the system	22,376	20,081	20,048	20,011	19,982	19,932	19,896	19,856	19,821	19,794	19,764
Difference: IN-OUT	0	1	1	1	0	1	0	0	1	1	1

¹Ground-water underflow.²Ground-water outflow to stream channels draining the San Timoteo storage unit.

Table 15C. Simulated water budgets for water management scenario 3 for the San Geronio Pass area, Riverside County, California—Continued.

[acre-ft/yr, acre feet per year]

Scenario 3B: 2,000 acre-ft of artificial recharge												
Stress period												
	78	79	80	81	82	83	84	85	86	87	88	
	(2003)	(2004)	(2005)	(2006)	(2007)	(2008)	(2009)	(2010)	(2011)	(2012)	(2013)	
Inflow (in acre-ft/yr)						(in ac-ft/yr)						
Storage	12,445	9,109	8,663	8,179	7,643	7,739	7,416	7,354	6,922	6,713	6,864	
General head ¹	802	903	997	1,081	1,167	1,251	1,333	1,415	1,491	1,565	1,638	
Return flow	2,741	2,784	2,751	2,870	3,098	2,754	2,864	2,728	3,024	3,133	2,881	
Mountain front recharge	2,681	2,681	2,681	2,681	2,681	2,681	2,681	2,681	2,681	2,681	2,681	
Areal recharge	3,707	3,707	3,707	3,707	3,707	3,707	3,707	3,707	3,707	3,707	3,707	
Total IN to the system	22,376	21,184	20,799	20,518	20,296	20,131	20,001	19,885	19,825	19,799	19,771	
Outflow (in acre-ft/yr)												
Storage	0	1,101	749	506	314	197	104	27	0	0	0	
General head	2,380	2,346	2,314	2,276	2,247	2,198	2,161	2,122	2,089	2,063	2,035	
Pumpage	19,996	17,735	17,735	17,735	17,735	17,735	17,735	17,735	17,735	17,735	17,735	
Drains ²	0	0	0	0	0	0	0	0	0	0	0	
Total OUT from the system	22,376	21,182	20,798	20,518	20,295	20,130	20,000	19,884	19,824	19,798	19,770	
Difference: IN-OUT	0	2	1	0	1	1	1	1	1	1	1	

¹Ground-water underflow.²Ground-water outflow to stream channels draining the San Timoteo storage unit.

Table 15C. Simulated water budgets for water management scenario 3 for the San Gorgonio Pass area, Riverside County, California—Continued.

[acre-ft/yr, acre feet per year]

	Scenario 3C: 3,000 acre-ft of artificial recharge										
	Stress period										
	78 (2003)	79 (2004)	80 (2005)	81 (2006)	82 (2007)	83 (2008)	84 (2009)	85 (2010)	86 (2011)	87 (2012)	88 (2013)
Inflow (in acre-ft/yr)											
Storage	12,445	8,864	8,227	7,603	6,964	6,987	6,612	6,514	6,033	5,772	5,902
General head ¹	802	902	995	1,078	1,161	1,241	1,319	1,396	1,468	1,536	1,603
Return flow	2,741	2,784	2,751	2,870	3,098	2,754	2,864	2,728	3,024	3,133	2,881
Mountain front recharge	2,681	2,681	2,681	2,681	2,681	2,681	2,681	2,681	2,681	2,681	2,681
Areal recharge	3,707	3,707	3,707	3,707	3,707	3,707	3,707	3,707	3,707	3,707	3,707
Artificial recharge	0	3000	3000	3000	3000	3000	3000	3000	3000	3000	3000
Total IN to the system	22,376	21,938	21,362	20,939	20,611	20,369	20,183	20,027	19,912	19,829	19,774
Outflow (in acre-ft/yr)											
Storage	0	1,856	1,312	926	628	435	285	168	86	28	0
General head	2,380	2,346	2,314	2,277	2,247	2,198	2,162	2,123	2,091	2,065	2,039
Pumpage	19,996	17,735	17,735	17,735	17,735	17,735	17,735	17,735	17,735	17,735	17,735
Drains ²	0	0	0	0	0	0	0	0	0	0	0
Total OUT from the system	22,376	21,937	21,361	20,938	20,610	20,368	20,182	20,026	19,912	19,828	19,774
Difference: IN-OUT	0	1	1	1	1	1	1	1	0	1	0

¹Ground-water underflow.²Ground-water outflow to stream channels draining the San Timoteo storage unit.

Table 15C. Simulated water budgets for water management scenario 3 for the San Geronio Pass area, Riverside County, California—Continued.

[acre-ft/yr, acre feet per year]

Scenario 3D: 5,000 acre-ft of artificial recharge												
Stress period												
	78	79	80	81	82	83	84	85	86	87	88	
	(2003)	(2004)	(2005)	(2006)	(2007)	(2008)	(2009)	(2010)	(2011)	(2012)	(2013)	
Inflow (in acre-ft/yr)												
Storage	12,445	6,976	6,326	5,711	5,080	5,110	4,745	4,658	4,189	3,941	4,067	
General head ¹	802	901	987	1,061	1,133	1,201	1,267	1,331	1,389	1,444	1,498	
Return flow	2,741	2,784	2,751	2,870	3,098	2,754	2,864	2,728	3,024	3,133	2,881	
Mountain front recharge	2,681	2,681	2,681	2,681	2,681	2,681	2,681	2,681	2,681	2,681	2,681	
Areal recharge	3,707	3,707	3,707	3,707	3,707	3,707	3,707	3,707	3,707	3,707	3,707	
Artificial recharge	0	5000	5000	5000	5000	5000	5000	5000	5000	5000	5000	
Total IN to the system	22,376	22,048	21,453	21,030	20,699	20,453	20,264	20,105	19,990	19,906	19,834	
Outflow (in acre-ft/yr)												
Storage	0	1,966	1,403	1,017	715	517	363	241	156	94	45	
General head	2,380	2,346	2,314	2,278	2,248	2,200	2,165	2,128	2,099	2,076	2,053	
Pumpage	19,996	17,735	17,735	17,735	17,735	17,735	17,735	17,735	17,735	17,735	17,735	
Drains ²	0	0	0	0	0	0	0	0	0	0	0	
Total OUT from the system	22,376	22,047	21,452	21,029	20,698	20,452	20,263	20,105	19,989	19,905	19,833	
Difference: IN-OUT	0	1	1	1	1	1	1	0	1	1	1	

¹Ground-water underflow.²Ground-water outflow to stream channels draining the San Timoteo storage unit.

Table 15D. Simulated water budgets for water management scenario 4 for the San Gorgonio Pass area, Riverside County, California.

[acre-ft/yr, acre feet per year]

Scenario 4A: No artificial recharge											
Stress period											
	78	79	80	81	82	83	84	85	86	87	88
	(2003)	(2004)	(2005)	(2006)	(2007)	(2008)	(2009)	(2010)	(2011)	(2012)	(2013)
Inflow (in acre-ft/yr)											
Storage	12,445	8,731	8,417	8,153	7,843	8,085	7,882	7,920	7,534	7,343	7,508
General head ¹	802	885	950	1,004	1,053	1,103	1,152	1,209	1,263	1,317	1,372
Return flow	2,741	2,784	2,751	2,870	3,098	2,754	2,864	2,728	3,024	3,133	2,881
Mountain front recharge	2,681	2,681	2,681	2,681	2,681	2,681	2,681	2,681	2,681	2,681	2,681
Areal recharge	3,707	3,707	3,707	3,707	3,707	3,707	3,707	3,707	3,707	3,707	3,707
Artificial recharge	0	0	0	0	0	0	0	0	0	0	0
Total IN to the system	22,376	18,788	18,507	18,415	18,382	18,329	18,286	18,244	18,209	18,181	18,149
Outflow (in acre-ft/yr)											
Storage	0	319	60	0	0	0	0	0	0	0	0
General head	2,380	2,354	2,332	2,300	2,267	2,214	2,171	2,130	2,095	2,066	2,034
Pumpage	19,996	16,114	16,114	16,114	16,114	16,114	16,114	16,114	16,114	16,114	16,114
Drains ²	0	0	0	0	0	0	0	0	0	0	0
Total OUT from the system	22,376	18,787	18,506	18,414	18,381	18,328	18,285	18,244	18,209	18,180	18,148
Difference: IN-OUT	0	1	1	1	1	1	1	0	0	1	1

¹Ground-water underflow.

²Ground-water outflow to stream channels draining the San Timoteo storage unit.

Table 15D. Simulated water budgets for water management scenario 4 for the San Gorgonio Pass area, Riverside County, California—Continued.

	Scenario 4B: 2,000 acre-ft of artificial recharge												
	Stress period												
	78	79	80	81	82	83	84	85	86	87	88		
	(2003)	(2004)	(2005)	(2006)	(2007)	(2008)	(2009)	(2010)	(2011)	(2012)	(2013)		
Inflow (in acre-ft/yr)													
Storage	12,445	7,837	7,179	6,671	6,175	6,310	6,024	5,996	5,582	5,403	5,581		
General head ¹	802	884	947	997	1,042	1,086	1,129	1,174	1,219	1,262	1,306		
Return flow	2,741	2,784	2,751	2,870	3,098	2,754	2,864	2,728	3,024	3,133	2,881		
Mountain front recharge	2,681	2,681	2,681	2,681	2,681	2,681	2,681	2,681	2,681	2,681	2,681		
Areal recharge	3,707	3,707	3,707	3,707	3,707	3,707	3,707	3,707	3,707	3,707	3,707		
Total IN to the system	22,376	19,893	19,266	18,926	18,704	18,538	18,404	18,286	18,213	18,186	18,157		
Outflow (in acre-ft/yr)													
Storage	0	1,424	819	510	320	206	114	39	0	0	0		
General head	2,380	2,354	2,332	2,301	2,269	2,217	2,175	2,132	2,098	2,071	2,042		
Pumpage	19,996	16,114	16,114	16,114	16,114	16,114	16,114	16,114	16,114	16,114	16,114		
Drains ²	0	0	0	0	0	0	0	0	0	0	0		
Total OUT from the system	22,376	19,892	19,265	18,925	18,703	18,536	18,404	18,285	18,212	18,185	18,156		
Difference: IN-OUT	0	1	1	1	1	2	0	1	1	1	1		

¹Ground-water underflow.²Ground-water outflow to stream channels draining the San Timoteo storage unit.

Table 15D. Simulated water budgets for water management scenario 4 for the San Geronio Pass area, Riverside County, California—Continued.

[acre-ft/yr, acre feet per year]

	Scenario 4C: 3,000 acre-ft of artificial recharge												
	78 (2003)	79 (2004)	80 (2005)	81 (2006)	82 (2007)	83 (2008)	84 (2009)	85 (2010)	86 (2011)	87 (2012)	88 (2013)		
Inflow (in acre-ft/yr)													
Storage	12,445	7,593	6,748	6,094	5,496	5,558	5,220	5,157	4,708	4,477	4,619		
General head ¹	802	884	946	994	1,037	1,078	1,116	1,156	1,195	1,233	1,272		
Return flow	2,741	2,784	2,751	2,870	3,098	2,754	2,864	2,728	3,024	3,133	2,881		
Mountain front recharge	2,681	2,681	2,681	2,681	2,681	2,681	2,681	2,681	2,681	2,681	2,681		
Areal recharge	3,707	3,707	3,707	3,707	3,707	3,707	3,707	3,707	3,707	3,707	3,707		
Artificial recharge	0	3,000	3,000	3,000	3,000	3,000	3,000	3,000	3,000	3,000	3,000		
Total IN to the system	22,376	20,649	19,833	19,346	19,019	18,777	18,588	18,429	18,315	18,232	18,160		
Outflow (in acre-ft/yr)													
Storage	0	2,180	1,386	930	635	443	296	180	100	43	0		
General head ²	2,380	2,354	2,332	2,301	2,270	2,218	2,177	2,134	2,100	2,074	2,046		
Pumpage	19,996	16,114	16,114	16,114	16,114	16,114	16,114	16,114	16,114	16,114	16,114		
Drains	0	0	0	0	0	0	0	0	0	0	0		
Total OUT from the system	22,376	20,648	19,832	19,345	19,018	18,775	18,587	18,428	18,314	18,231	18,160		
Difference: IN-OUT	0	1	1	1	1	2	1	1	1	1	0		

¹Ground-water underflow.²Ground-water outflow to stream channels draining the San Timoteo storage unit.

Table 15D. Simulated water budgets for water management scenario 4 for the San Geronio Pass area, Riverside County, California—Continued.

[acre-ft/yr, acre feet per year]

Scenario 4D: 5,000 acre-ft of artificial recharge											
Stress period											
	78	79	80	81	82	83	84	85	86	87	88
	(2003)	(2004)	(2005)	(2006)	(2007)	(2008)	(2009)	(2010)	(2011)	(2012)	(2013)
Inflow (in acre-ft/yr)											
Storage	12,445	5,724	4,881	4,202	3,612	3,681	3,353	3,301	2,864	2,647	2,802
General head ¹	802	882	939	980	1,013	1,044	1,071	1,099	1,124	1,147	1,170
Return flow	2,741	2,784	2,751	2,870	3,098	2,754	2,864	2,728	3,024	3,133	2,881
Mountain front recharge	2,681	2,681	2,681	2,681	2,681	2,681	2,681	2,681	2,681	2,681	2,681
Areal recharge	3,707	3,707	3,707	3,707	3,707	3,707	3,707	3,707	3,707	3,707	3,707
Artificial recharge	0	5000	5000	5000	5000	5000	5000	5000	5000	5000	5000
Total IN to the system	22,376	20,778	19,959	19,440	19,111	18,867	18,676	18,516	18,399	18,315	18,240
Outflow (in acre-ft/yr)											
Storage	0	2,309	1,511	1,021	722	526	374	254	170	109	61
General head	2,380	2,354	2,333	2,304	2,275	2,226	2,188	2,147	2,115	2,090	2,065
Pumpage	19,996	16,114	16,114	16,114	16,114	16,114	16,114	16,114	16,114	16,114	16,114
Drains ²	0	0	0	0	0	0	0	0	0	0	0
Total OUT from the system	22,376	20,777	19,958	19,439	19,111	18,866	18,676	18,515	18,399	18,313	18,240
Difference: IN-OUT	0	1	1	1	0	1	0	1	0	2	0

¹Ground-water underflow.

²Ground-water outflow to stream channels draining the San Timoteo storage unit.

A Water-management scenario 1 2004–2013

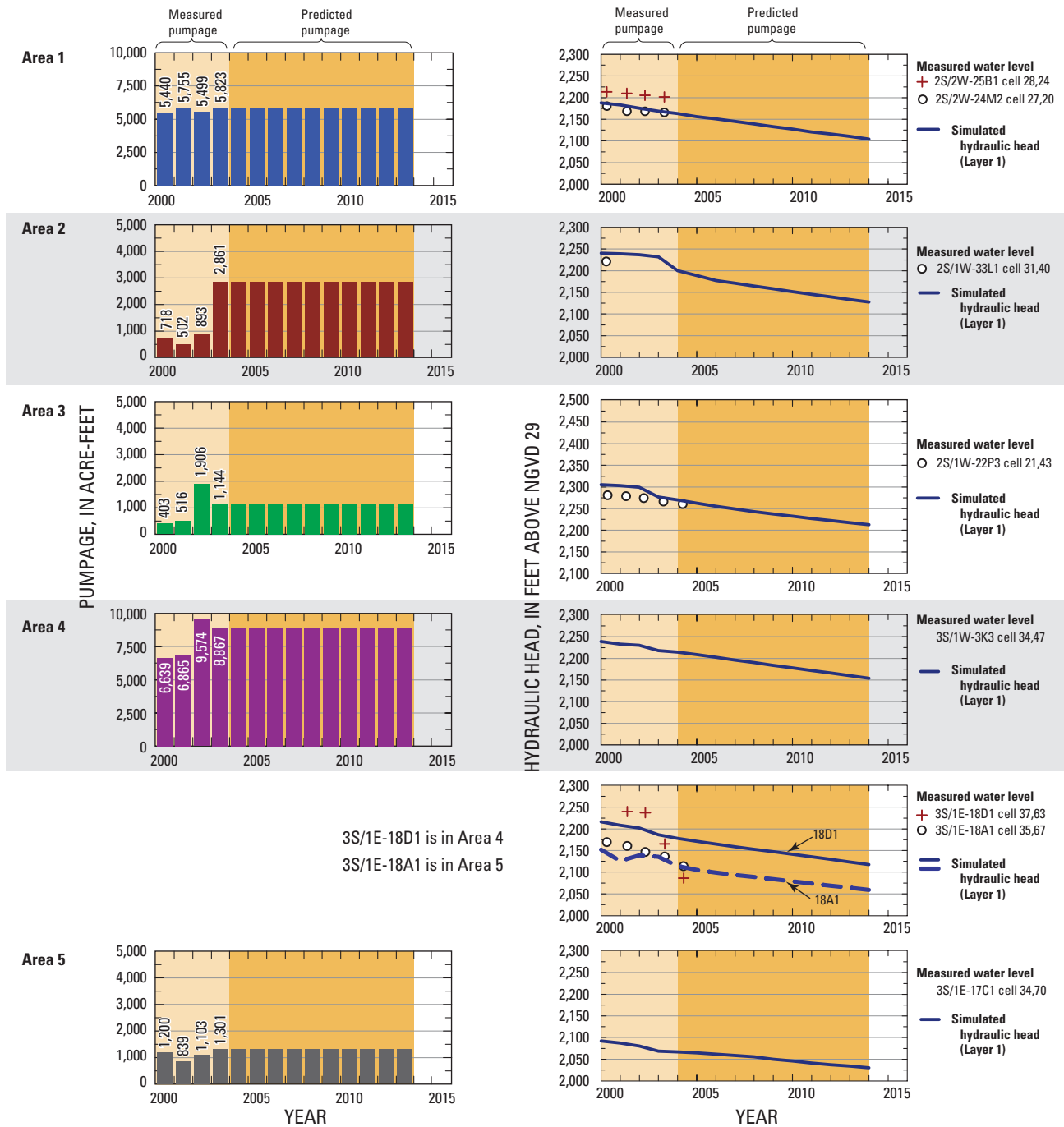


Figure 56. Graphs showing pumpage and simulated hydraulic heads from 2000–2013 for water-management (A) scenario 1, (B) scenario 2, (C) scenario 3, and (D) scenario 4, San Gorgonio Pass area, Riverside County, California.

B Water-management scenario 2 2004–2013

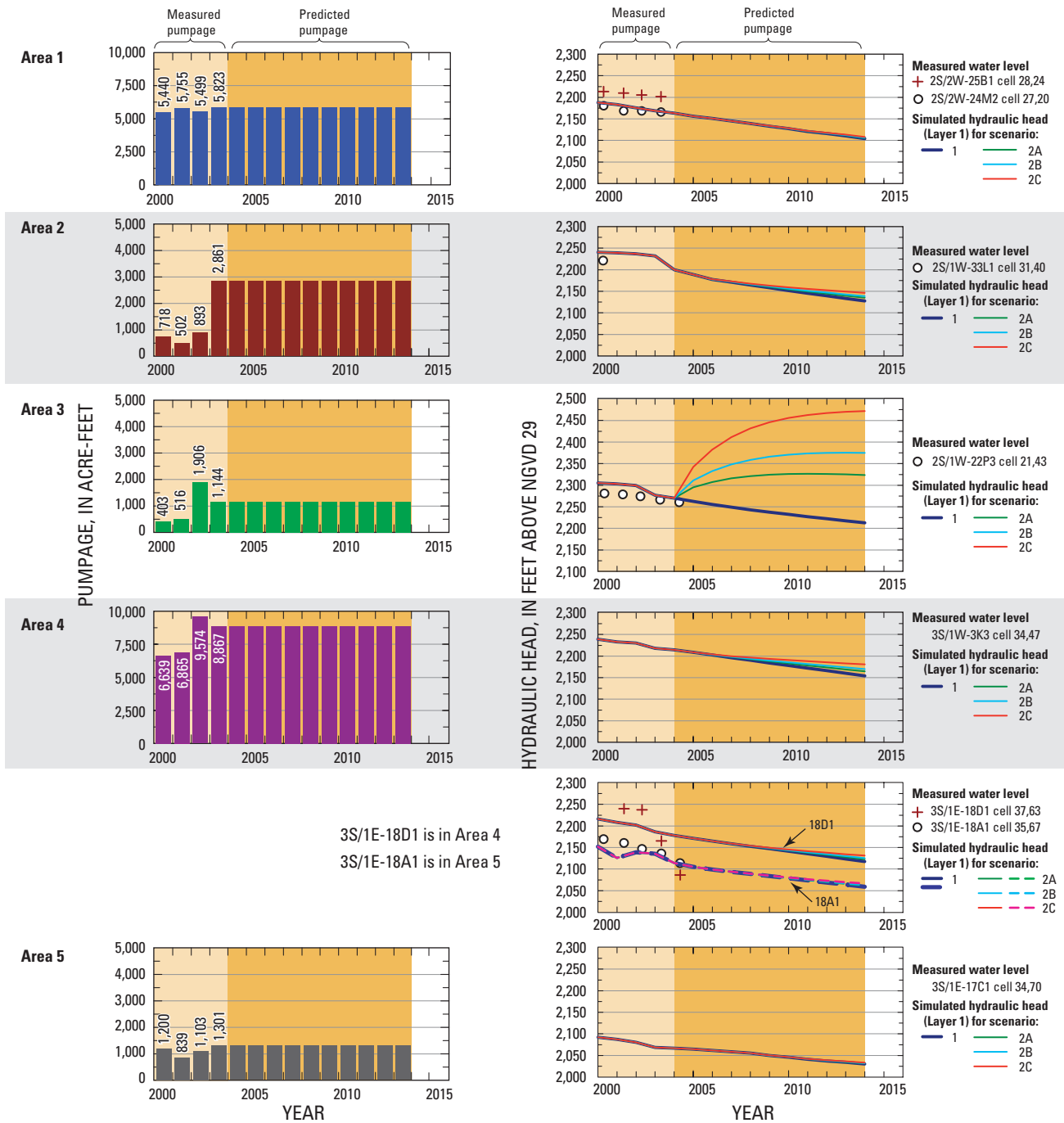


Figure 56. Continued.

C Water-management scenario 3 2004-2013

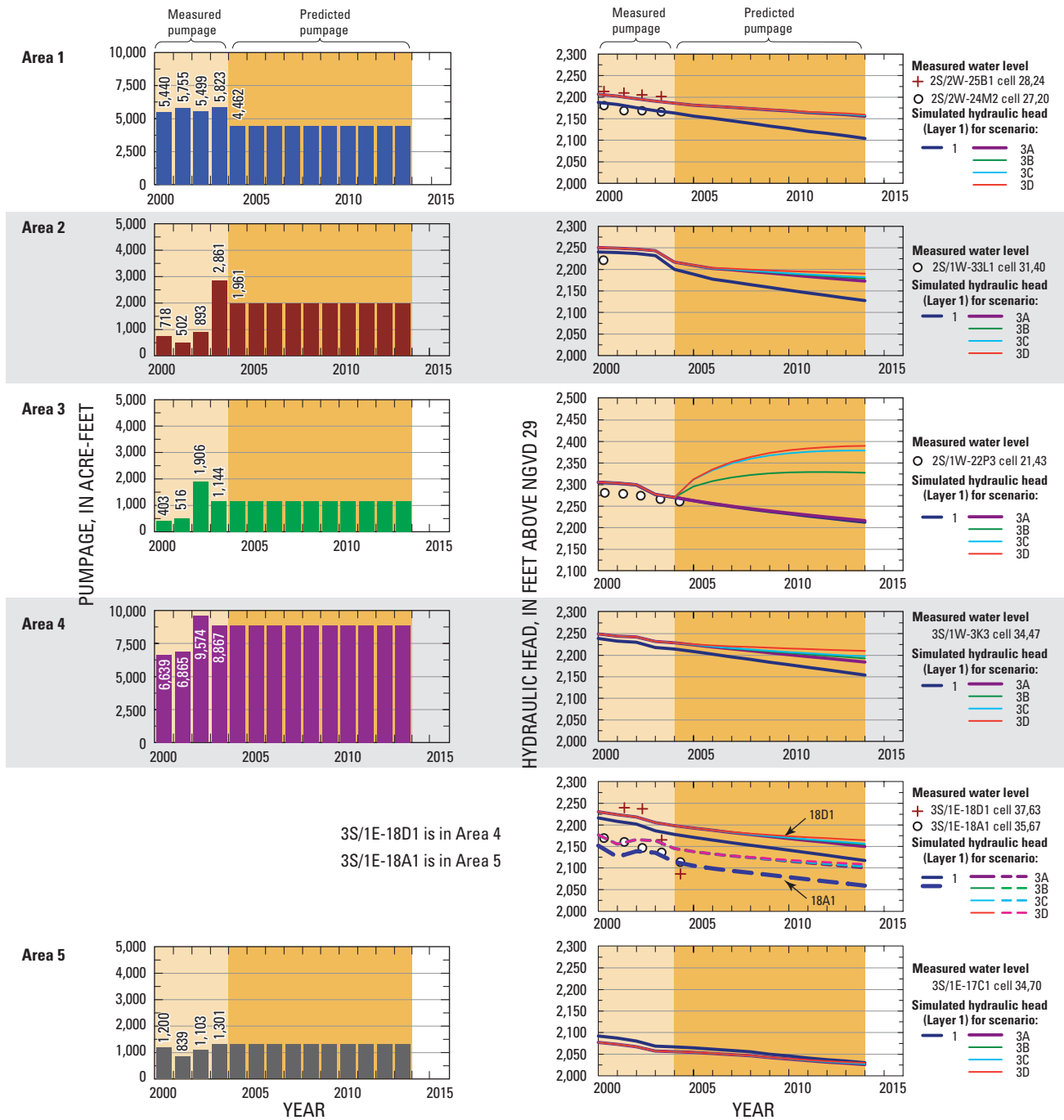


Figure 56. Continued.

D Water-management scenario 4 2004–2013

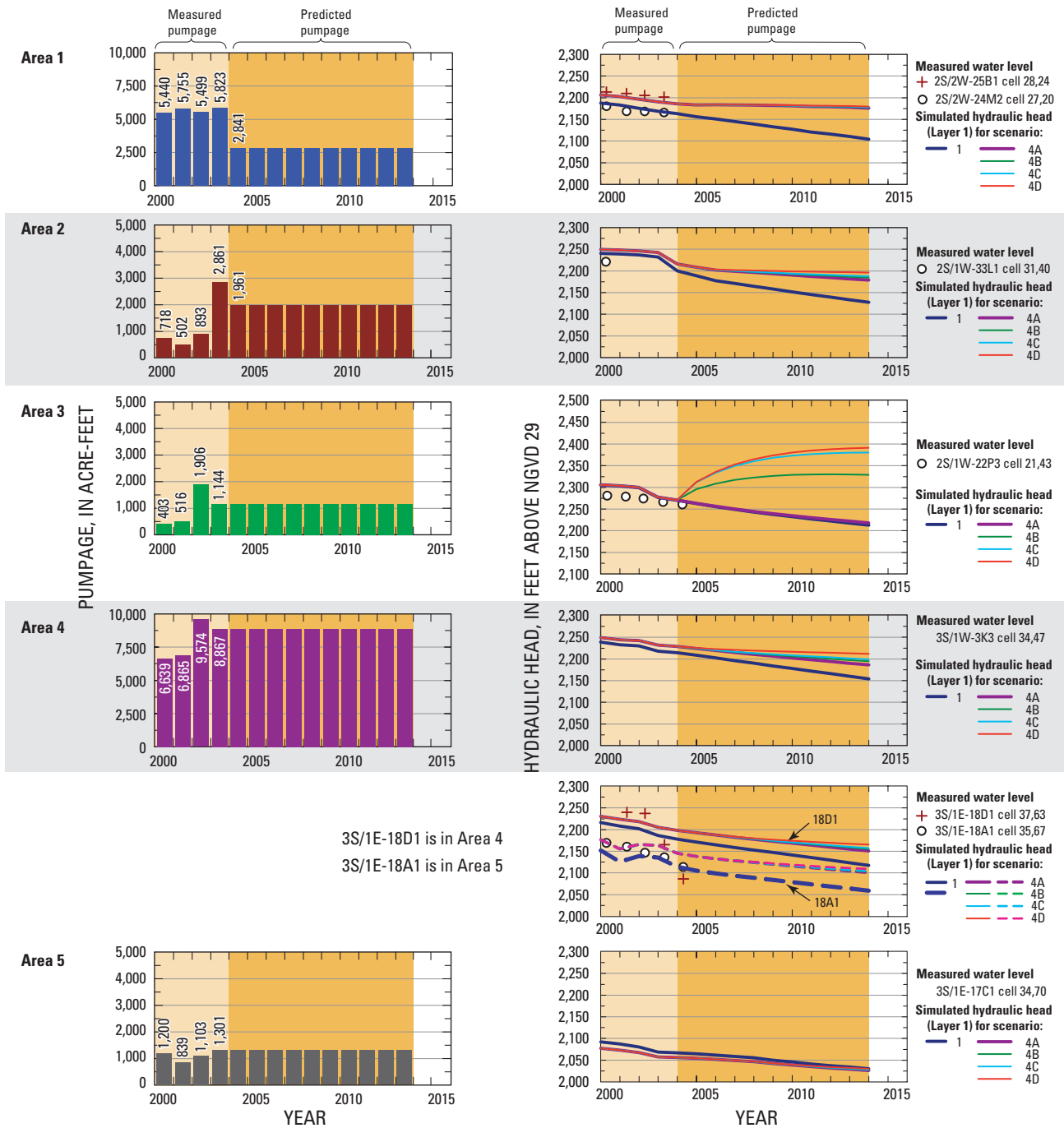


Figure 56. Continued.

Water-Management Scenario 3

Water-management scenario 3 assumes that SWP water is used for golf course irrigation in areas 1 and 2 in lieu of ground water starting in 2004; that is, ground-water pumpage is reduced by the amount of SWP water used for irrigation. In scenario 3A, pumpage was reduced by a total of about 2,000 acre-ft/yr (about 1,450 acre-ft/yr in area 1 and about 550 acre-ft/yr in area 2) and no SWP water was artificially recharged in area 3. In scenarios 3B–C, the pumpage was the same as that for scenario 3A; however, the SWP water was artificially recharged in area 3 as in scenarios 2A–B (*table 15C*). In scenario 3D, the pumpage was the same as that for scenario 3A; however, 3,000 acre-ft/yr of SWP water was equally distributed in model cells (20, 43) and (21, 43) in area 3 and 2,000 acre-ft/yr of SWP water was equally distributed in model cells (25, 44) and (26, 44) in area 4.

In comparison with scenario 1, by 2013 scenario 3A (reduction in golf course pumpage only) results in about a 50-ft increase in simulated hydraulic heads in area 1, about a 25-ft increase in area 2, about a 0 to 10-ft increase in areas 3 and 4, and no change in area 5 (*fig. 56C*). The simulated hydraulic heads for scenarios 3B–D reflect the effects of reduced pumpage in areas 1 and 2 and the increased artificial recharge of SWP water in areas 3 (scenarios 3B–D) and 4 (scenario 3D only) with simulated hydraulic heads increasing in all areas except for the eastern part of area 5 (*fig. 56C*). There was little increase in simulated hydraulic heads in area 5 because simulated fault F6 restricted ground-water flow between areas 4 and 5. The changes in simulated hydraulic heads in scenarios 3B–C are essentially the result of the changes in simulated hydraulic head from the reduced pumpage (scenario 3A) plus the changes in hydraulic head from artificially recharging SWP water (scenarios 2A–B). The scenario 3D simulated hydraulic heads in area 3 are lower than the scenario 2D simulated hydraulic heads because 2,000 acre-ft of artificially recharged SWP water was moved from area 3 to area 4.

Water-Management Scenario 4

In water-management scenario 4, ground water pumped for golf course irrigation in areas 1 and 2 (about 2,000 acre-ft/yr), as well as ground water pumped for use by Sunny-Cal Poultry in area 1 (about 2,200 acre-ft/yr), would be supplied by direct delivery of SWP water. In scenario 4A, pumpage was reduced by a total of about 4,200 acre-ft/yr (about 3,650 acre-ft/yr in area 1 and about 550 acre-ft/yr in area 2) starting in 2004. Scenarios 4B–D have the same pumpage as scenario 4A; however, the recharge distribution of SWP water is the same as that for scenarios 3B–D (*table 15D*).

In comparison with scenario 1, scenario 4A (reduction in pumpage only) results in about a 50-ft increase in simulated hydraulic heads in area 1, about a 30-ft increase in area 2, about a 10-ft increase in areas 3 and 4, and little to no change in area 5 (*fig. 56D*). The simulated hydraulic heads

for scenarios 4B–D reflect the effects of reduced pumpage in areas 1 and 2 and the artificially recharged SWP water in areas 3 (scenarios 4B–D) and 4 (scenario 4D only), with simulated hydraulic heads increasing in all areas except for area 5, where there is little to no change (*fig. 56D*). As observed in scenario 3, simulated fault F6 restricted ground-water movement between areas 4 and 5. The changes in simulated hydraulic heads in scenarios 4B–C are essentially the result of the changes in simulated hydraulic head from reducing pumpage (scenario 4A) plus the changes in hydraulic head from artificially recharging SWP water (scenarios 2A–B). Again, the scenario 4D simulated hydraulic heads in area 3 are lower than the scenario 2D simulated hydraulic heads because 2,000 acre-ft of artificially recharged SWP water was moved from area 3 to area 4.

Summary and Conclusions

Ground water has been the only source of potable water supply for residential, industrial, and agricultural users in the Beaumont and Banning storage units of the San Gorgonio Pass area, Riverside County, California. Ground-water levels in the Beaumont storage unit declined as much as 100 ft between the early 1920s and early 2000s, and numerous natural springs have stopped flowing in the western part of the Beaumont storage unit. In 1961, the San Gorgonio Pass Water Agency (SGPWA) entered into a contract with the California State Department of Water Resources to receive 17,300 acre-ft/yr of water to be delivered by the California State Water Project (SWP) to supplement natural recharge. Currently (2005), a pipeline is delivering SWP water into the area; SGPWA is using the water to artificially recharge the ground-water system using recharge ponds located along Little San Gorgonio Creek in the Cherry Valley area. In addition to this artificial recharge, SGPWA is considering the direct delivery of SWP water for the irrigation of local golf courses and for agricultural supply in lieu of ground-water pumpage. SGPWA is concerned about the effects of these water-management alternatives on ground-water levels and movement in the Beaumont and Banning storage units.

To better understand the potential hydrologic effects of different water-management alternatives on ground-water levels and movement in the Beaumont and Banning storage units, the USGS compiled existing geohydrologic and geochemical data; collected new data from a basin-wide ground-water level and water-quality monitoring network; installed monitoring wells near the Little San Gorgonio Creek recharge ponds; defined the geology, ground-water hydrology, and geochemistry of the Beaumont and Banning storage units from the data compiled and collected for this study; and developed a ground-water flow simulation model. The calibrated ground-water flow model was used to evaluate the potential effects of four different water-management alternatives.

The San Gorgonio Pass area was divided into the Beaumont, Banning, Cabazon, Calimesa, San Timoteo, South Beaumont, Banning Bench, Singleton, and Canyon (Edgar Canyon, Banning Canyon, Hathaway Canyon, Potrero Canyon, and Millard Canyon) storage units on the basis of faults mapped or inferred by previous investigators. This study addresses primarily the Beaumont and Banning storage units. The study area is about 11 miles long, trending northwest to southeast, and as much as 3 miles wide, with the San Bernardino Mountains to the north, the San Jacinto Mountains to the south, and the San Timoteo Badlands to the southwest.

The geologic units in the study area were generalized into crystalline basement rocks and sedimentary deposits. Crystalline rocks occur beneath and around the margins of the Beaumont and Banning storage units and are referred to as basement rock and are considered non-water bearing. The sedimentary deposits were grouped into three major units: (1) older sedimentary deposits, (2) younger sedimentary deposits, and (3) surficial deposits. The older sedimentary deposits are generally impermeable, yielding only small quantities of water to wells. The younger sedimentary deposits and the surficial deposits are the main water-bearing deposits in the San Gorgonio Pass area.

On the basis of lithologic and downhole geophysical logs, the water-bearing deposits were divided into three aquifers: (1) the perched aquifer, (2) the upper aquifer, and (3) the lower aquifer. The perched aquifer is present in the surficial deposits in the Cherry Valley area. The upper aquifer is present in the upper part of the younger sedimentary deposits and consists mainly of unconsolidated to slightly consolidated sand and gravel with interbedded silt and clay. The lower aquifer is present in the lower part of the younger sedimentary deposits and consists mainly of poorly consolidated to consolidated sand, silt, and clay.

A deterministic, distributed-parameter precipitation-runoff model, INFILv3, was used to estimate the spatial and temporal distribution of natural recharge in the study area for predevelopment and urbanized conditions. INFILv3 results indicate that the total potential natural recharge in the Beaumont and Banning storage units is 9,890 acre-ft/yr: the sum of recharge simulated in the Beaumont and Banning storage units (about 3,710 acre-ft/yr) and recharge simulated in the 28 upstream sub-drainage basins (about 6,180 acre-ft/yr). Incorporation of an assumed decrease in ground-surface (soil) permeability (saturated hydraulic conductivity) caused by urbanization into the INFILv3 model results in an increase in simulated runoff from the urbanized areas and an increase in simulated recharge in areas downstream of the urbanized areas. In the Beaumont and Banning storage units, the increase in simulated average annual natural recharge is about 600 acre-ft/yr.

The water supply for the Beaumont and Banning storage units is supplied by pumping ground water from wells in the Canyon (Edgar and Banning Canyons), Banning Bench, Beaumont, and Banning storage units. Ground-water pumpage was compiled for 1927–2003 for this study from various sources and total annual pumpage from the Beaumont and Banning storage units ranged from about 1,630 acre-ft in 1936 to about 20,000 acre-ft in 2003.

Since ground-water development began in the San Gorgonio Pass area, there have been several sources of artificial recharge to the basin, including return flow from water applied on crops, golf courses, and landscape; septic-tank seepage; and infiltration of diverted storm runoff and imported SWP water into recharge ponds. Potential artificial recharge was estimated for 1927–2003 for this study. Because of the great depth of water in much of study area (150 to 465 ft), the artificial recharge is estimated to take years to decades to reach the water table. The estimated vertical travel times for artificial recharge to reach the water table ranged from about 23, 40, 71, 56, and 52 years in areas 1–5, respectively. Estimated annual rates of artificial recharge applied at land surface reached a maximum of about 8,100 acre-ft in 2003; with a 1927–2003 cumulative total of about 224,000 acre-ft. However, only 37,000 acre-ft of artificial recharge applied to the land surface during 1927–2003 is estimated to reach the water table by 2003, due to the long travel times from land surface to the water table. The remainder of the artificial recharge applied to the land surface during this period is estimated to reach the water table between 2004 and 2074.

Ground-water conditions in the Beaumont and Banning storage units were evaluated using water-level maps from 1926–27, 1955, 1967, and 2000 as well as long-term hydrographs for selected wells. The maps and hydrographs indicate that water-levels declined as much as 100 ft in the Beaumont storage unit from 1926–2000.

The geochemistry of the Beaumont, Banning, and surrounding storage units was defined by collecting samples from a monitoring network consisting of more than 35 wells in the storage units and surrounding area. In general, the ground water is of good quality in the Beaumont, Banning, and surrounding storage units with dissolved-solids concentrations ranging from 177 mg/L in the Banning storage unit to 823 mg/L in Edgar Canyon. In general, wells in the Beaumont storage unit yield calcium/magnesium-bicarbonate type water and wells in the Banning storage unit yield sodium-bicarbonate type water. The chemical character of wells screened opposite both the upper and lower aquifers indicates that the upper aquifer contributes more than 75 percent of the water pumped from most wells in the Beaumont storage unit.

The stable-isotope data indicate that the source of ground-water recharge was precipitation from storms passing through the San Gorgonio Pass as opposed to runoff from the higher altitudes of the San Bernardino Mountains. In addition, these data indicate that little if any of the ground water in the fractured crystalline rocks flows across the Banning Fault into the Beaumont storage unit. Tritium concentrations indicate that little to no recharge has reached the water table since 1952 in most areas of the Beaumont and Banning storage units. Excluding the samples from wells in the southeastern part of the Beaumont storage area and in the Banning storage unit, ^{14}C activities in ground water sampled from wells in the Beaumont, Banning, and surrounding storage units ranged from about 82 to 95 pmc, representing uncorrected ^{14}C ages of about 1,800 to 400 years before present, respectively. The samples from wells in the southeastern part of the Beaumont storage unit and in the Banning storage unit had ^{14}C activities ranging from 12 to 79 pmc corresponding to uncorrected ^{14}C ground-water ages ranging from 17,500 to 1,900 years before present, respectively. The lowest carbon activities were in samples from the Banning storage unit, which probably indicate mixing with ground water from the older sedimentary deposits.

To better understand the dynamics of ground-water flow and the potential effects of water-level changes resulting from artificial recharge, and for use as a tool to help manage ground-water resources in the San Gorgonio Pass area, a regional-scale, numerical ground-water flow model was developed using MODFLOW-96. The active model domain includes the Beaumont and Banning storage units, discretized areally using square 1,000-ft cells. The aquifer system was vertically discretized into two layers to simulate vertical flow through the ground-water system. Model layer 1 simulates the upper aquifer and was simulated as an unconfined aquifer. Model layer 2 simulates the lower aquifer and was simulated as a convertible (confined/unconfined) aquifer. The model was calibrated to steady-state (pre-1927) and transient-state (1926–2003) conditions using a trial-and-error approach. The transient-state simulation was made using 1-year stress periods.

Results of the steady-state simulation indicate that the total inflow rate, or recharge, was about 6,590 acre-ft/yr with about 3,710 acre-ft/yr from areal recharge, about 2,670 acre-ft/yr from mountain-front recharge, and about 210 acre-ft/yr from general-head boundaries (the surrounding older sedimentary deposits). The steady-state results also indicate that the outflow rate, or discharge, was about 6,590 acre-ft/yr with about 2,865 acre-ft/yr as ground-water underflow from the Banning storage unit to the Cabazon storage unit, about 2,035 acre-ft/yr as ground-water underflow to the surrounding older sedimentary deposits along the southern boundary of the model, and about 1,690 acre-ft/yr to drain boundaries

that simulate the discharge to stream channels draining the San Timoteo storage unit. The total discharge value is similar to estimates by previous investigators.

The transient-state simulated hydraulic heads reasonably matched measured water levels throughout the model area. The root mean square error for the model is 14.5 ft, and the relative error of the residuals is 4.3 percent. The simulated water budget for 1926–2003 indicates that of the total simulated volume of water pumped from the aquifer (450,160 acre-ft), about 50 percent was derived from depletion of ground-water storage (222,660 acre-ft), about 21 percent was derived from the reduction of underflow to the Cabazon and San Timoteo storage units (about 96,280 acre-ft), about 19 percent was derived from a reduction of ground-water outflow to the stream channels draining the San Timoteo storage unit (about 86,030 acre-ft), about 8 percent was derived from irrigation return flows and septic-tank seepage (about 36,780 acre-ft), and about 2 percent was derived from an increase in ground-water underflow from the surrounding older sedimentary deposits (about 8,410 acre-ft).

A backward-tracking analysis was completed under steady-state conditions using the particle-tracking program MODPATH to determine the travel time of water to 11 production wells where both tritium and ^{14}C data were collected. The travel time is assumed to be the simulated age of ground water at the well. To allow for variations in travel times among particle paths starting at different locations within a model cell, 30 to 100 particles were evenly distributed along a vertical column through the cell node representing the well with estimated age data. The particles were distributed in each model layer based on the reported screened interval of the well being simulated. In general, the simulated ages based on travel times are younger than the uncorrected ^{14}C ages. The median simulated ages for ground water at the 11 production wells range from 11 years old to 1,607 years old; whereas, the estimated age of the ground water sampled from these wells ranges from less than 50 years old to 6,786 years old. The greatest discrepancies between simulated ages and estimated ground-water age is for wells that are perforated only in model layer 1.

The calibrated ground-water flow model was used to simulate the effects of four water-management scenarios being considered by SGPWA for the period 2004–13. Scenario 1, considered the base case, evaluated the response of the ground-water system assuming no SWP water was available. Scenario 2 assumed 2,000 to 5,000 acre-ft/yr of SWP water was available to artificially recharge the Cherry Valley area, north of the Cherry Valley Fault. Scenarios 3 and 4 assumed that 2,000 to 5,000 acre-ft/yr of SWP water was available to artificially recharge the Cherry Valley area and 2,000 to 4,200 acre-ft/yr of SWP water was available to utilize in lieu of ground water pumped for golf course irrigation and agricultural use in the western part of the Beaumont storage unit.

The model results for scenario 1 indicates that hydraulic heads declined throughout the Beaumont and Banning storage units compared with that for 2003 conditions, with the largest declines (more than 50 ft by 2013) occurring in the western part of the Beaumont storage unit (area 2) due to large increases in golf-course irrigation pumpage that began in 2000. In general, the results of the water-management scenarios 2–4 indicate that artificial recharge in the Little San Gorgonio Creek recharge ponds benefits primarily the area north of the Cherry Valley Fault because the fault limits ground-water flow to the aquifer system south of the fault. Utilizing SWP water in lieu of ground water pumped for golf course irrigation and agricultural use in the western part of the Beaumont storage unit (areas 1 and 2) results in increases in hydraulic head of about 50 feet in this area, compared with hydraulic head for the base case, owing to the reduction of pumpage in this area. None of the water-management scenarios significantly benefited the Banning storage unit.

References Cited

- Albright, L.B., 1997, Geochronology and vertebrate paleontology of the San Timoteo Badlands, southern California: Riverside, University of California, unpublished Ph.D. thesis, 328 p.
- Albright, L.B., 1999, Magnetostratigraphy and biochronology of the San Timoteo Badlands, southern California, with implications for local Pliocene-Pleistocene tectonic and depositional patterns: *Geological Society of America Bulletin*, v. 111, p. 1265–1293.
- Allen, C.R., 1957, San Andreas fault zone in San Gorgonio Pass, southern California: *Geological Society of America Bulletin*, v. 68, p. 319–350.
- Blanck, E.L., Jr., 1987, Geologic structure of the Beaumont-Banning area, California, from gravity profiles: Los Angeles, California State University, unpublished M.S. thesis, 84 p., scale 1:24,000.
- Bloyd, R.M., 1971, Underground storage of imported water in the San Gorgonio Pass area, Southern California: U.S. Geological Survey Water-Supply Paper 1999-D, 37 p.
- Bookman-Edmonston Engineering, Inc., 1991, Investigation for the establishment of zones of benefit: Draft consultant report prepared for Mojave Water Agency, Glendale, California, 34 p.
- Bouwer, Herman, 1980, Deep percolation and groundwater management, in *Proceedings of the deep percolation symposium*: Arizona Department of Water Resources Report No. 1, 118 p.
- Boyle Engineering Corporation, 1990, Well completion report, test well no. 1, San Gorgonio Pass Water Agency: San Bernardino, California, 30 p.
- Boyle Engineering Corporation, 1992, Water importation program, Beaumont-Calimesa Groundwater Storage Project, artificial recharge feasibility investigation, Phase 1, feasibility of surface spreading: Newport Beach, California, 75 p.
- Boyle Engineering Corporation, 1995, Safe Yield Study, Beaumont Storage Unit: Newport Beach, California, 55 p.
- California Department of Finance, 2006, Historical county and state population estimates, 1991–2000, with 1990 and 2000 census counts: Available on the World Wide Web, accessed April 2006 at <http://www.dof.ca.gov/html/demograp/newhist%5Fe%2D4.xls>
- California Department of Water Resources, 1947, South Coastal Basin investigation—Overdraft on ground water basins, California State printing office, (formerly California Department of Public Works, Division of Water Resources), 256 p.
- California Department of Water Resources, 1963, Feasibility of serving the San Gorgonio Pass Water Agency from the State water facilities: California Department of Water Resources Bulletin 119-2, 80 p.
- California Irrigation Management Information System, 2002, California ERO zones map: California Department of Water Resources data available on the World Wide Web, accessed July, 2002, at <http://www.cimis.water.ca.gov/>
- Catchings, R.D., Gandhok, G., Goldman, M.R., Horta, E., Rymer, M.J., Martin, P., and Christensen, A., 1999, Subsurface, high-resolution, seismic images from Cherry Valley, San Bernardino County, California—Implications for water resources and earthquake hazards: U.S. Geological Survey Open-File Report 99-26, 57 p.
- Cement Association of Canada, 2005, Testing hardened concrete-permeability, accessed at URL <http://www.cement.ca/cement.nsf/ep/6990436cd2803a4f852569140068e1d8?opendocument>
- Christensen, A.H., 2000, Structural analysis of the San Gorgonio Pass near Banning, California, using gravity profiles, San Diego, California State University, unpublished M.S. thesis, 138 p.
- Craig, Harmon, 1961, Isotope variations in meteoric water: *Science*, v. 133, p. 1702–1703.
- Davis, S.N. and Dewiest, R.J.M., 1966, *Hydrogeology*: New York, N.Y., John Wiley & Sons, 463 p.

- Dibblee, T.W., Jr., 1964, Geologic map of the San Gorgonio Mountain quadrangle, San Bernardino and Riverside Counties, California: U.S. Geological Survey Miscellaneous Geologic Investigations Map I-431, scale 1:62,500.
- Dibblee, T.W., Jr., 1968, Displacements on San Andreas Fault system in San Gabriel, San Bernardino, and San Jacinto Mountains, southern California, *in* Dickinson, W.R., and Grantz, Arthur, eds., Proceedings of conference on geologic problems of San Andreas Fault system: Stanford University Publications in Geological Sciences, v. XI, p. 269–278.
- Dibblee, T.W., Jr., 1975, Late Quaternary uplift of the San Bernardino Mountains on the San Andreas and related faults, *in* Crowell, J.C., ed., San Andreas Fault in southern California: California Division of Mines and Geology Special Report 118, p. 127–135.
- Dibblee, T.W., Jr., 1982, Geology of the San Bernardino Mountains, southern California, *in* Fife, D.L., and Minch, J.A., eds., Geology and mineral wealth of the California Transverse Ranges: South Coast Geological Society Guidebook no. 10 (Mason Hill volume), p. 148–169.
- EarthInfo Inc., 2004, NCDC Summary of the Day. West: Boulder, Colo., Earth Info, Inc., CD ROM West 1.
- Ellett, K.M., 2002, Hydrologic characterization of the deep vadose zone of the San Gorgonio Pass area for artificial recharge and natural recharge analysis: Davis, University of California, unpublished M.S. thesis, 123 p.
- English, H.D., 1953, The geology of the San Timoteo Badlands: Claremont, California, unpublished M.S. thesis, 159 p.
- Fetter, C.W., 1994, Applied Hydrology (3d ed.): Englewood Cliffs, N.J., Prentice Hall, 691 p.
- Flint, A.L. and Ellett, K.M., 2004, The role of the unsaturated zone in artificial recharge at San Gorgonio Pass, California: *Vadose Zone Journal*, 2004, v. 3, p. 763–774.
- Freeze, R.A., and Cherry, J.A., 1979, Groundwater: Englewood Cliffs, N.J., Prentice Hall, 604 p.
- Fraser, D.M., 1931, Geology of San Jacinto Quadrangle south of San Gorgonio Pass: California Journal of Mines and Geology, v. 27, no. 4, p. 494–540.
- Frick, Childs, 1921, Extinct vertebrate fauna of the badlands of Bautista Creek and San Timoteo Canyon, southern California: University of California, Department of Geology, Bulletin, v. 12, no. 5, p. 277–424.
- Friedman, I., Smith, G.I., Gleason, J.D., Warden, A., and Harris, J.M., 1992, Stable isotope composition of waters in southeastern California 1: Modern precipitation: *Journal of Geophysical Research*, v. 97, p. 5795–5812.
- Gandhok, G., Catchings, R.D., Goldman, M.R., Horta, E., Rymer, M.J., Christensen, A., and Martin, P., 2000, High-resolution seismic-reflection/refraction imaging from Interstate 10 to Cherry Valley Boulevard, Cherry Valley, Riverside County, California: Implications for water resources and earthquake hazards: U.S. Geological Survey Open-File Report 99-320, 59 p.
- Geoscience Support Services, 1991, Water wells C-4, C-5, C-6, and R-1 results of drilling, testing, and recommended pump design: Claremont, California, variously paged.
- Gonfiantini, Roberto, 1978, Standards for stable isotope measurements in natural compounds: *Nature*, v. 271, p. 534–536.
- Hanson, R.T., Martin, Peter, and Koczot, K.M., 2003, Simulation of Ground-water/surface-water flow in the Santa Clara-Calleguas ground-water basin, Ventura County, California: U.S. Geological Survey Water-Resources Investigations Report 02-4136, 214 p.
- Hehn, V.N., MacFadden, B.J., Albright, L.B., and Woodburne, M.O., 1996, Magnetic polarity stratigraphy and possible differential tectonic rotation of the Miocene-Pliocene mammal-bearing San Timoteo Badlands, southern California: *Earth and Planetary Science Letters*, v. 141, p. 35–49.
- Hem, J.D., 1992, Study and interpretation of the chemical characteristics of natural water (3d ed.): U.S. Geological Survey Water-Supply Paper 2254, 263 p.
- Hevesi, J.A., Flint, A.L., and Flint, L.E., 2003, Simulation of net infiltration and potential recharge using the distributed-parameter watershed model, INFILv3, of the Death Valley Regional Flow System, Nevada and California: U.S. Geological Survey Water-Resources Investigations Report 03-4090, 171 p.
- Hill, M.C., 1990, Preconditioned Conjugate-Gradient 2 (PCG2), a computer program for solving ground-water flow equations: U.S. Geological Survey Water-Resources Investigations Report 90-4048, 43 p.
- Hill, R.I., 1984, Petrology and petrogenesis of batholithic rocks, San Jacinto Mountains, southern California: Pasadena, California Institute of Technology, Ph.D. thesis, 660 p.
- Hill, R.I., 1988, San Jacinto intrusive complex: 1. Geology and mineral chemistry, and a model for intermittent recharge of tonalitic magma chambers: *Journal of Geophysical Research*, v. 93, no. B9, p. 10325–10348.
- Hill, R.I., Chappell, B.W., and Silver, L.T., 1988, San Jacinto intrusive complex: 2. Geochemistry: *Journal of Geophysical Research*, v. 93, no. B9, p. 10349–10372.

- Hill, R.I., and Silver, L.T., 1988, San Jacinto intrusive complex: 3. Constraints on crustal magma chamber processes from strontium isotope heterogeneity: *Journal of Geophysical Research*, v. 93, no. B9, p. 10373–10388.
- Hsieh, P.A., and Freckleton, J.R., 1993, Documentation of a computer program to simulate horizontal-flow barriers using the U.S. Geological Survey's modular three-dimensional finite-difference ground-water flow model: U.S. Geological Survey Open-File Report 92-0477, 32 p.
- Izbicki, J.A., Martin, Peter, and Michel, R.L., 1995, Source, movement, and age of groundwater in the upper part of the Mojave River Basin, California, U.S.A., in: Adar, E.M., and Leibundgut, Christian, eds., *Application of tracers in arid zone hydrology: International Association of Hydrological Sciences*, no. 232, p. 43–56.
- Izbicki, J.A., Christensen, A.H., Hanson, R.T., 1999, U.S. Geological Survey combined well-bore flow and depth-dependent water sampler: U.S. Geological Survey Fact Sheet 196-99, 2 p.
- Jennings, C.W., 1977, *Geologic map of California*, California Division of Mines and Geology.
- Kalin, R.M., 2000, Radiocarbon dating of groundwater systems, in Cook, P.G., and Herczeg, A.L., (eds.), Chapter 4: Environmental tracers in subsurface hydrology, Boston, Kluwer Academic Publishers, p. 111–144.
- Kendrick, K.J., 1999, Quaternary geologic evolution of the northern San Jacinto fault zone: Understanding evolving strike-slip faults through geomorphic and soil stratigraphic analysis: Riverside, University of California, unpublished Ph.D. dissertation, 301 p.
- Kendrick, K.J., Morton, D.M., Wells, S.G., and Simpson, R.W., 2002, Spatial and temporal deformation along the northern San Jacinto fault, southern California; implications for slip rates: *Bulletin of the Seismological Society of America*, v. 92, no. 7, p. 2782–2802.
- Larsen, N.R., 1962, *Geology of the Lamb Canyon area, Beaumont, California*: Claremont, California, unpublished M.S. thesis, 93 p., scale 1:12,000.
- Konikow, L.F., and Bredehoeft, J.D., 1992, Validation of geohydrological models: part 1: *Advances in Water Resources*, v. 15, no. 1, p. 75–83.
- Langenheim, V.E., Jachens, R.C., Matti, J.C., Morton, D.M., Hauksson, E., and Christensen, A., 2005, Geophysical evidence for wedging in the San Gorgonio Pass structural knot, southern San Andreas Fault zone, southern California: *Geological Society of America Bulletin*, v. 117, p. 1554–1572; doi: 10.1130/B25760.1
- Lohman, S.W., 1972, *Ground-water hydraulics*: U.S. Geological Survey Professional Paper 708, 70 p.
- Matti, J.C., and Morton, D.M., 1993, Paleogeographic evolution of the San Andreas Fault in Southern California; a reconstruction based on a new cross-fault correlation, in Powell, R.E., Weldon, R.J., II, Matti, Jonathan, eds., *The San Andreas fault system; displacement, palinspastic reconstruction, and geologic evolution: Memoir—Geological Society of America*, v. 178, p.107–159.
- Matti, J.C., Morton, D.M., and Cox, B.F., 1985, Distribution and geologic relations of fault systems in the vicinity of the central Transverse Ranges, southern California: U.S. Geological Survey Open-File Report 85-365, 27 p., scale 1:250,000.
- Matti, J.C., Morton, D.M., and Cox, B.F., 1992, *The San Andreas Fault system in the vicinity of the central Transverse Ranges province, southern California*: U.S. Geological Survey Open-File Report 92-354, 40 p., scale 1:250,000.
- May, S.R., and Reppening, C.A., 1982, New evidence for the age of the Mount Eden fauna, southern California: *Journal of Vertebrate Paleontology*, v. 2, no. 1, p. 109–113.
- McDonald, M.G., and Harbaugh, A.W., 1988, A modular three-dimensional finite-difference ground-water flow model: U.S. Geological Survey Techniques of Water-Resources Investigations, book 6, chap. A1, 586 p.
- McDonald, M.G., Harbaugh, A.W., Orr, B.R., and Ackerman, D.J., 1992, A method of converting no-flow cells to variable-head cells for the U.S. Geological Survey modular finite-difference ground-water flow model: U.S. Geological Survey Open-File Report 91-536, 99 p.
- McDonald, M.G., and Harbaugh, A.W., 1996; User's documentation of MODFLOW-96, an update to the U.S. Geological Survey modular finite-difference groundwater flow model: U.S. Geological Survey Open-File Report 96-485, 56 p.
- Michel, R.L., 1976, Tritium inventories of the world oceans and their implications: *Nature*, v. 263, p. 103–106.
- Mook, W.G., 1980, The dissolution-exchange model for dating of groundwater with ¹⁴C, in Fritz, P. and Fontes, J.C., eds., *Handbook of Environmental Isotopes Geochemistry*, v. 1, Amsterdam, Elsevier, p. 50–74.
- Morton, D.M., 1999, compiler, Preliminary digital geologic map of the Santa Ana 30' × 60' quadrangle, Southern California, version 1.0: U.S. Geological Survey Open-File Report 99-172 (<http://wrgis.wr.usgs.gov/open-file/of99-172/>), scale 1:100,000.

- Morton, D.M., Sadler, P.M., and Matti, J.C., 1990, Constant watershed growth and fault offset in the San Timoteo Badlands, southern California: Geological Society of America Abstracts with Programs, v. 22, no. 3, p. 70.
- National Atmospheric and Oceanic Administration, 1994, The International Tree Ring Data Base, NOAA's World Data Center-A for Paleoclimatology, Boulder, Colorado, 1994.
- National Oceanic and Atmospheric Association, 2006, Beaumont historical precipitation, 1906–71: Available on the World Wide Web, accessed April 2006, at <http://wf.ncdc.noaa.gov/oa/climate/climateproducts.html>
- Nishikawa, Tracy, J.A. Izbicki, J.A. Hevesi, C.L. Stamos, and Martin, Peter, 2004, Evaluation of geohydrologic framework, recharge estimates, and ground-water flow of the Joshua Tree area, San Bernardino County, California: U.S. Geological Survey Scientific Investigations Report 2004-5267, 118 p.
- Piper, A.M., 1944, A graphic procedure in the geochemical interpretation of water analyses: American Geophysical Union Transactions, v. 25, p. 914–923
- Pollock, D.A., 1994, User's guide for MODPATH/MODPATH_PLOT, Version 3: A particle tracking post-processing package for MODFLOW, the U.S. Geological Survey finite-difference ground-water flow model: U.S. Geological Survey Open-File Report 94-464, 245 p.
- Rasmussen, G.S., and Associates, 1978, Engineering geology investigation tentative Tract 9209, Lots 1–337, San Bernardino County, California: consulting report on file with San Bernardino County Planning Department, 29 p.
- Reynolds, R.E., and Reeder, W.A., 1986, Age and fossil assemblages of San Timoteo Formation, Riverside County, California, in Kooser, M.A. and Reynolds, R.E., editors, Geology around the margins of the eastern San Bernardino Mountains: Redlands, California, Publications of the Inland Geological Society, v. 1, p. 51–56.
- Reynolds, R.E., and Reeder, W.A., 1991, The San Timoteo Formation, Riverside County, California: Redlands, California, San Bernardino County Museum Quarterly, v. 39, p. 44–48.
- Riley, F.S., and Worts, G.F., Jr., 2001, Geologic reconnaissance and test-well drilling program, Marine Corps Training Center, Twentynine Palms, California: U.S. Geological Survey Open-File Report 98-166, 64 p.
- Rogers, T.H., compiler, 1965, Santa Ana sheet of geologic map of California: California Division of Mines and Geology, scale 1:250,000.
- Shuler, E.H., 1953, Geology of a portion of the San Timoteo Badlands near Beaumont, California: Los Angeles, University of Southern California, unpublished M.S. Thesis, 106 p.
- Sneed, Michelle, Ikehara, Marti E., Galloway, D.L., and Falk Amelung, 2001, Detection and measurement of land subsidence using global positioning system and interferometric synthetic aperture radar, Coachella Valley, California, 1996–98: U.S. Geological Survey Water-Resources Investigations Report 01-4193, 26 p.
- Solomon, K.H., 1988, Irrigation system selection: California State University, Fresno, California, Center for Irrigation Technology Irrigation Notes, accessed September 17, 2002, at <http://www.wateright.org/site2/publications/880105.asp>.
- Stiff, H.A., Jr., 1951, The interpretation of chemical water analysis by means of patterns: Journal of Petroleum Technology, v. 3, p. 15–17.
- Thomasson, H.G., Jr., Olmsted, F.H., and LeRoux, E.F., 1960, Geology, water resources, and usable ground-water storage capacity of part of Solano County, California: U.S. Geological Survey Water-Supply Paper 1464, 603 p.
- U.S. Department of Agriculture, 1994, State Soil Geographic (STATSGO) Data Base—Data use information, Misc. Pub. no. 1492.
- U.S. Environmental Protection Agency, 2005, List of contaminants and their MCLs: U.S. Environmental Protection Agency data available on the World Wide Web, accessed on July 14, 2005, at URL <http://www.epa.gov/safewater/mcl.html#mcls>
- U.S. Geological Survey, National Land Cover Database—Zone 60 Imperviousness layer: U.S. Geological Survey data available on the World Wide Web, accessed May 16, 2005, at <http://seamless.usgs.gov>
- Vaughan, F.E., 1922, Geology of the San Bernardino Mountains north of San Gorgonio Pass: California University Publications in Geological Sciences, v. 13, p. 319–411.
- Western Regional Climate Center, Desert Research Institute, 2006a, Beaumont 1 E, California (040609). Period of record monthly climate summary, 1948 to 2001: Available on the World Wide Web, accessed April 2006, at <http://www.wrcc.dri.edu/cgi-bin/cliMAIN.pl?cabeau+sca>
- Western Regional Climate Center, Desert Research Institute, 2006b, Remote Automated Weather Station Beaumont 1 E, Monthly Summary [precipitation], Beaumont California, August 2003–April 2006: Available on the World Wide Web, accessed April 2006, at <http://www.wrcc.dri.edu/cgi-bin/rawMAIN.pl?caCBEU>

- Willingham, R.C., 1981, Gravity anomaly patterns and fault interpretations in the San Bernardino Valley and western San Gorgonio Pass area, southern California, in Brown, A.R., and Ruff, R.W., eds., *Geology of the San Jacinto Mountains: Santa Ana, California*, South Coast Geological Society, Annual Field trip guidebook, no. 9, p. 164–174.
- Yeh, W. W-G., 1986, Review of parameter identification procedures in groundwater hydrology: the inverse problem: *Water Resources Research*, v. 22, no. 1, p. 95–108.A

Appendix

Appendix Table 1. Well construction data for selected wells, San Geronio Pass area, Riverside County, California.

[NGVD 27, National Geodetic Vertical Datum of 1927. Water use: Agr, agricultural well; Dom, domestic well; M&I, municipal and industrial well; Obs, observation well; Oil, oil well. Data used in study: G, geology; P, pumpage; Q, water quality; W, water levels; S, specific capacity; Y, yes indicates availability of a log. Agency archive: 1, U.S. Geological Survey archives; 2, San Geronio Pass Water Agency archives; 3, California Department of Water Resources (1957). ft, foot; <, actual value is less than value shown]

State well number	Storage Unit	Water use	Year drilled	Land-surface altitude (in feet above NGVD 27)	Hole depth (ft)	Well depth (ft)	Well diameter (in.)	Perforation intervals (ft)	Driller's log	Electric log	Data used in study	Agency archive
2S/1W-22G2	Edgar Canyon	Obs	2000	3,050	425	400	8	200-400	Y	Y	G,Q,W	1,2
2S/1W-22G3	Edgar Canyon	Obs	2000	3,031	320	320	2	300-320	Y	Y	G,Q,W	1
2S/1W-22G4	Edgar Canyon	Obs	2000	3,031	320	158	2	138-158	Y	Y	G,Q,W	1
2S/1W-22G5	Edgar Canyon	Obs	2000	3,031	136	136	2	115-135	Y	Y	G,Q,W	1
2S/1W-22H2	Edgar Canyon	M&I	1929	3,124	458	444	16	58-434	Y	Y	G,Q,W	1,2
2S/1W-22P3	Beaumont	Obs	1999	2,909	672	672	2	632-672	Y	Y	G,Q,W	1
2S/1W-22P7	Beaumont	Obs		2,909	672	234	<1	234-234	Y	Y	G,Q,W	1
2S/1W-22Q3	Beaumont	Obs	1990	2,926	1,002	1,000	6	200-980 with gaps	Y	Y	G,S,W	1,2
2S/1W-22Q4	Beaumont	Obs		2,926	1,002	660	2	640-660	Y	Y	G,Q,W	1
2S/1W-27B1	Beaumont	M&I	1961	2,887	1,143	1,143	16	530-694;710-725	Y	Y	G,S,P,Q,W	1,2
2S/1W-27L1	Beaumont	Obs	1989	2,809	1,106	1,030	6	1,000-1,020	Y	Y	G,S,W	1,2
2S/1W-27P1	Beaumont	M&I	2001	2,734	1,522	1,500	18	650-1,480	Y	Y	Q,W	1
2S/1W-28A1	Singleton	Dom	2001	2,755	800		6		Y	Y	Q	1
2S/1W-28M1	Beaumont	Dom	1979	2,658	600	595	10	455-595	Y	Y	G,W	1,2
2S/1W-29L1	Singleton	Dom	1961	2,596	517	517	6	392-517	Y	Y	S	1,2
2S/1W-29M1	Beaumont	Agr	1921	2,590	359	359	10		Y	Y	G,W	1,2
2S/1W-29M2	Beaumont	Dom	1961	2,560	496	496	6	375-496	Y	Y	S,W	1,2
2S/1W-29M3	Beaumont	Dom	1967	2,595	495	456	6	375-456	Y	Y	S	1,2
2S/1W-29M4	Beaumont	Agr	1968	2,580	603	603	12	385-585	Y	Y	G,P,W	1,2
2S/1W-29M8	Beaumont	Dom,Agr	1984	2,550	585	585	5	385-585	Y	Y	S	1,2
2S/1W-29N1	Beaumont	Agr	1951	2,535	240				Y	Y	P,W	1,2
2S/1W-30E1	Beaumont	Agr	1927	2,350		220	10	210-220			W	1,2,3
2S/1W-30F1	Beaumont	Agr	1984	2,400		350	6	250-350	Y	Y	S	1,2
2S/1W-30F2	Beaumont	Agr	1973	2,390		415	12	209-409	Y	Y	S	1
2S/1W-30J1	Beaumont	Agr	1990	2,565	1,413	1,410	20	500-1,400	Y	Y	G,S,P,W	1,2
2S/1W-30J2	Beaumont	Agr	1974	2,550	750	750	16	550-750	Y	Y	G,S,P	1
2S/1W-30L1	Beaumont	Agr	1946	2,377	232		8	80-232			P,W	1,2
2S/1W-30M1	Beaumont	Agr	1917	2,410	201		12		Y	Y	W	1,2
2S/1W-30N1	Beaumont	Agr	1947	2,400	454		12	209-409	Y	Y	G,P	1,2
2S/1W-31G1	Beaumont		1962	2,480	500		8				P,W	1,2
2S/1W-31G2	Beaumont	Agr	1962	2,476	560	550	10	140-360			S	1,2
2S/1W-31H1	Beaumont	Agr	1970	2,510	650	650	13	550-650			S,P,W	1,2
2S/1W-31L1	Beaumont	M&I	1999	2,405	1,138	1,110	16	180-540; 870-1,090	Y	Y	G,S,Q,W	1

Appendix Table 1. Well construction data for selected wells, San Geronimo Pass area, Riverside County, California — Continued.

[NGVD 27, National Geodetic Vertical Datum of 1927. Water use: Agr, agricultural well; Dom, domestic well; M&I, municipal and industrial well; Obs, observation well; Oil, oil well. Data used in study: G, geology; P, pumpage; Q, water quality; W, water levels; S, specific capacity; Y, yes indicates availability of a log. Agency archive: 1, U.S. Geological Survey archives; 2, San Geronimo Pass Water Agency archives; 3, California Department of Water Resources (1957). ft, foot; <, actual value is less than value shown]

State well number	Storage Unit	Water use	Year drilled	Land-surface altitude (in feet above mean sea level, NGVD 1927)	Hole depth (ft)	Well depth (ft)	Well diameter (in.)	Perforation intervals (ft)	Driller's log	Electric log	Data used in study	Agency archive
2S/1W-32B1	Beaumont			2,581			6				W	1,2
2S/1W-32G1	Beaumont	Dom	1929	2,491		231	12				W	1,2
2S/1W-32M1	Beaumont	Agr	1999	2,468	1,505	1,135	16	360–550; 570–1,040; 1,095–1,135	Y	Y	S,Q,W	1
2S/1W-33L1	Beaumont	M&I	1989	2,566	1,400	1,370	16	400–1,370	Y	Y	G,S,P,Q,W	1
2S/1W-33R1	Beaumont			2,600	600		8	420–595			Q,W	1
2S/1W-33R2	Beaumont	M&I	2000	2,617	640	620	12	500–600	Y		G,Q,W	1
2S/1W-34A1	Beaumont	Agr	1969	2,747	1,087	708	6	558–708	Y		G,Q,W	1,2
2S/1W-34A2	Beaumont	M&I	1970	2,747	1,010	1,000	20	550–980	Y		G,S,P,W	1,2
2S/1W-34E1	Beaumont	Agr	1944	2,658	427	427	12	230–425	Y		G,P	1,2
2S/1W-34E2	Beaumont		2000	2,655	576	576	8	276–576	Y	Y	G,W	1
2S/1W-34M1	Beaumont	Agr		2,650		500		427–500			Q,W	1,2
2S/1W-34Q1	Beaumont	M&I	1955	2,665	910	910	12	420–595		Y	S,P,Q,W	1,2
2S/1W-35J1	Beaumont	Obs	2001	2,774	904	900	2	880–900	Y	Y	G,Q,W	1
2S/1W-35J2	Beaumont	Obs	2001	2,774	904	770	2	750–770	Y	Y	G,Q,W	1
2S/1W-35J3	Beaumont	Obs	2001	2,774	904	630	2	610–630	Y	Y	G,Q,W	1
2S/1W-35J4	Beaumont	Obs	2001	2,774	904	260	2	240–260	Y	Y	G,W	1
2S/2W-14R3	Beaumont	M&I	1968	2,334	1,000	1,000	16	352–976	Y		G,Q	1,2
2S/2W-23H1	Beaumont	Agr	1924	2,387	285	285	12	182–284 with gaps	Y		G,W	1,2
2S/2W-23J6	Beaumont	M&I	1959	2,280							P	1,2
2S/2W-23R1	Beaumont	Agr	1955	2,230		781	14				P	1,2
2S/2W-24E2	Beaumont	M&I	1957	2,440	1,000	740	14	170–800			P,Q,W	1,2
2S/2W-24E3	Beaumont	M&I	1957	2,315	1,000	800	14	120–800	Y		G,P,W	1,2
2S/2W-24J1	Beaumont	Dom	1954	2,420	282	282	10	113–118; 150–161; 252–275	Y		S	1,2
2S/2W-24K1	Beaumont	Dom	1956	2,365	200	200	10	115–200	Y		G	1,2
2S/2W-24K2	Beaumont	Dom	1978	2,334	260	260	5	170–250	Y		G,W	1,2
2S/2W-24L1	Beaumont	M&I	1990	2,317	1,230	1,180	16	380–870; 930–1,160	Y	Y	P,Q,W	1,2
2S/2W-24M2	Beaumont	Dom,Agr	1926	2,274		190	12				W	1,2
2S/2W-24R2	Beaumont	Dom	1985	2,360	300	300	4		Y		G,W	1,2
2S/2W-25B1	Beaumont	M&I	1920	2,300	416	416	16	56–416	Y		G,W	1,2
2S/2W-25B2	Beaumont	Agr		2,330		120					P	1,2
2S/2W-25B3	Beaumont	Dom,Agr		2,320		160	4				P	1,2

Appendix Table 1. Well construction data for selected wells, San Geronio Pass area, Riverside County, California — Continued.

[NGVD 27, National Geodetic Vertical Datum of 1927. Water use: Agr, agricultural well; Dom, domestic well; M&I, municipal and industrial well; Obs, observation well; Oil, oil well. Data used in study: G, geology; P, pumpage; Q, water quality; W, water levels; S, specific capacity; Y, yes indicates availability of a log. Agency archive: 1, U.S. Geological Survey archives; 2, San Geronio Pass Water Agency archives; 3, California Department of Water Resources (1957). ft, foot; <, actual value is less than value shown]

State well number	Storage Unit	Water use	Year drilled	Land-surface altitude (in feet above mean sea level, NGVD 1927)	Hole depth (ft)	Well depth (ft)	Well diameter (in.)	Perforation intervals (ft)	Driller's log	Electric log	Data used in study	Agency archive
2S/2W-25B4	Beaumont	Agr	1981	2,276	300	300	16	80-180; 240-280	Y		P	1,2
2S/2W-25B5	Beaumont	Dom	1980	2,394	304	300	16	150-290	Y		P,W	1,2
2S/2W-25C1	Beaumont	M&I		2,260	973	950	16	600-973			P,W	1,2
2S/2W-25C2	Beaumont	Dom	1962	2,264	180	180	10	50-180	Y		G,P	1,2
2S/2W-25D1	Beaumont	Agr	1924	2,249	288	288	16	95-286	Y		G,P,W	1,2,3
2S/2W-25D2	Beaumont	Agr	1937	2,239	319	319	16	130-315	Y		P,W	1,2,3
2S/2W-25D3	Beaumont	Agr	1938	2,235	1,001	1,001	16	862-980	Y		P,W	1,2,3
2S/2W-25D5	Beaumont	Agr		2,235							P	1,2
2S/2W-25D6	Beaumont	Agr	1924	2,275	923		16	120-380; 600-882	Y		G,P,W	1,2
2S/2W-25F1	Beaumont	Agr	1919	2,260	387	360	16	131-221; 290-360	Y		G,P,W	1,2,3
2S/2W-25F2	Beaumont	Dom	1986	2,290	250	250	4	70-250	Y		S	1,2
2S/2W-25F3	Beaumont		1989	2,290	250	250	6	170-250	Y		S	1,2
2S/2W-25G1	Beaumont	Agr	1973	2,290	440	415	12	209-409	Y		G,S,P	1,2
2S/2W-25H1	Beaumont	Agr		2,320	232						P	1,2
2S/2W-25J1	Beaumont		1977	2,360	358	358	14	197-358			S	1,2
2S/2W-25J2	Beaumont		1977	2,380		403	14	240-403			S	1,2
2S/2W-26A3	Beaumont	M&I		2,210			10				P	1,2
2S/2W-28C2	San Timoteo	Agr	1921	1,943			10				Q,W	1,2
3S/1E-04A1	Banning Bench	M&I	1968	2,675	171	171	10	100-160	Y		G,W	1,2
3S/1E-06M1	Beaumont	M&I		2,591		487	12				P,W	1,2
3S/1E-06N1	Beaumont	M&I	1959	2,555	920	900	14	360-900	Y		G,S,P,W	1,2
3S/1E-06N2	Beaumont	M&I	1987	2,550	1,200	1,200	14	600-1,200	Y		G,P,Q,W	1,2
3S/1E-06P1	Beaumont	M&I	1965	2,542	1,000	1,000	16	360-1,000	Y		G,P,Q,W	1,2
3S/1E-07E1	Beaumont	M&I	1952	2,520	744	710	16	50-710			S,P,W	1,2
3S/1E-07E2	Beaumont	M&I	1984	2,522	1,002	1,000	20	400-1,000	Y		G,S,P,Q	1,2
3S/1E-08P1	Banning	M&I	1951	2,415	800	800	12	150-800			P,W	1,2
3S/1E-10N1	Banning	M&I	1990	2,295	1,180	1,130	18	580-860; 950-1,110			Q,W	1,2
3S/1E-17C1	Banning	M&I	1990	2,387	1,440	1,420	18	460-930; 1,000-1,400	Y	Y	G,S,P,Q,W	1,2
3S/1E-18A1	Banning		1988	2,422	1,000	1,000	14	600-1,000			P,Q,W	1
3S/1E-18B1	Banning	M&I	1990	2,464	1,000	1,000	14	300-980	Y		G,S,W	1,2
3S/1E-18C1	Banning	M&I	1988	2,455	1,000	1,000	14	400-1,000			W	1,2
3S/1E-18D1	Beaumont	M&I	1978	2,496	1,020	1,000	16	400-1,000	Y		G,P,Q,W	1,2
3S/1W-01N1	Beaumont	Oil		2,606	450	366	14				W	1,2

Appendix Table 1. Well construction data for selected wells, San Geronio Pass area, Riverside County, California — Continued.

[NGVD 27, National Geodetic Vertical Datum of 1927. Water use: Agr, agricultural well; Dom, domestic well; M&I, municipal and industrial well; Obs, observation well; Oil, oil well. Data used in study: G, geology; P, pumpage; Q, water quality; W, water levels; S, specific capacity; Y, yes indicates availability of a log. Agency archive: 1, U.S. Geological Survey archives; 2, San Geronio Pass Water Agency archives; 3, California Department of Water Resources (1957). ft, foot; <, actual value is less than value shown]

State well number	Storage Unit	Water use	Year drilled	Land-surface altitude (in feet above mean sea level, NGVD 1927)	Hole depth (ft)	Well depth (ft)	Well diameter (in.)	Perforation intervals (ft)	Driller's log	Electric log	Data used in study	Agency archive
3S/1W-01Q1	Beaumont	M&I	1961	2,583	1,210	1,152	16	420–1,152	Y		G,S,P,W	1,2
3S/1W-03K1	Beaumont	M&I	1947	2,642	800	800	20	445–782 with gaps	Y		G,S,P,Q,W	1,2
3S/1W-03K2	Beaumont	M&I	1952	2,641	812	812	18	232–604; 604–812	Y		G,S,P,Q,W	1,2
3S/1W-03K3	Beaumont	M&I	1936	2,634	1,000	946	20	320–694	Y		G,S,P,W	1,2
3S/1W-04A1	Beaumont	Agr	1926	2,605		311	10				W	1,2
3S/1W-04L1	Beaumont	Agr	1958	2,565		1,260	14	400–1,100			P,W	1,2
3S/1W-04Q1	Beaumont	Agr		2,565	244						W	1,2,3
3S/1W-04Q2	Beaumont	Dom,Agr	1953	2,575	819	819	12	350–806	Y		S,P,W	1,2
3S/1W-05B1	Beaumont	Dom	1921	2,453	170						W	1,2
3S/1W-05Q1	South Beaumont	Dom	1926	2,533	1,300	1,300	16	384–388; 454–494	Y		G,W	1,2,3
3S/1W-10R3	South Beaumont	Agr	1961	2,564	304	290	8	70–290	Y		G,Q,W	1,2
3S/1W-11A2	Beaumont	M&I	1951	2,580	390		10	270–480 with gaps	Y		P,W	1,2
3S/1W-12A2	Beaumont	Oil	1922	2,557	2,236						G,W	1,2
3S/1W-12B1	Beaumont	Dom	1927	2,572		480	10				W	1,2
3S/1W-12B2	Beaumont	Oil	1990	2,569	1,065	1,030	18	390–1,010	Y	Y	G,S,P,Q,W	1,2
3S/1W-12D1	Beaumont	Dom	1927	2,582		390	10				W	1,2,3
3S/1W-12E1	Beaumont	Obs	1951	2,580	529	480	12	270–480	Y		G,S,W	1,2
3S/1W-12K1	Beaumont	M&I	1986	2,534	1,104	1,050	16	380–1,040 with gaps	Y	Y	G,P,Q,W	1
3S/1W-12G1	Beaumont	M&I		2,555							P	1
3S/2W-01C1	San Timoteo	Agr	1999	2,241	1,167	1,130	16	80–1,110 with gaps	Y	Y	G,Q,W	1

¹Records show well was either deepened or redrilled.

Appendix Table 2. Well construction, specific capacity, and transmissivity data for selected wells, San Gorgonio Pass area, Riverside County, California.

[T, transmissivity equals specific capacity times 230. Depths and perforated interval in feet below land surface. Land-surface and screen altitudes in feet above NVDG 27 (National Geodetic Vertical Datum of 1927). Shaded drawdown measurements may have been taken after the recovery period rather than immediately at the time pumping was discontinued. unk, unknown; lo, lower aquifer; up, upper aquifer; b, both upper and lower aquifers. na, not available; ft, foot; gal/min, gallon per minute; gal/min/ft, gallon per minute per foot; in., inches; ft²/d, square foot per day]

Source of data:

- 1 Driller's log
- 2 San Gorgonio Pass Water Agency (SGPWA) (795 E. Sixth Street, Beaumont CA 92223)
- 3 Files of SGPWA: Southern California Edison letter to owner 9/19/61
- 4 Files of SGPWA: Southern California Edison letter to owner 11/14/67
- 5 Boyle Engineering Inc. (1991)
- 6 Files of SGPWA: Southern California Edison letter to owner 9/12/61
- 7 Files of SGPWA: Southern California Edison letter to owner 1/26/66
- 8 Files of SGPWA: Southern California Edison letter to owner 1/25/66
- 9 GeoSciences, Inc. (1991)
- 10 Files of SGPWA: Southern California Edison letter to owner 9/21/61

State well number	Source of data	Year drilled	Well depth (ft)	Land-surface altitude (ft)	Well diameter (in.)	Screen perforated interval (ft)	Aquifer system perforated	Screen altitude	
								Top (ft)	Bottom (ft)
Area 1									
2S/1W-29L1	1, 2	1961	517	2,596	6	392–517	unk	2,204	2,079
2S/1W-29M2	1, 2	1961	496	2,560	6	375–496	lo	2,185	2,064
2S/1W-29M3	1, 2	1967	456	2,595	6	375–456	lo	2,220	2,139
2S/1W-29M8	1, 2	1984	585	2,550	5	385–585	up	2,165	1,965
2S/1W-30F1	1, 2	1984	350	2,400	6	250–350	up	2,150	2,050
2S/1W-30F2	1, 2	1973	415	2,390	12	209–409	b	2,181	1,981
2S/1W-30J1	1, 2	1990	1,410	2,565	20	500–1,400	b	2,065	1,165
2S/1W-30J2	1, 2	1974	750	2,550	16	550–750	b	2,000	1,800
2S/1W-31G2	1, 2	1962	550	2,476	10	190–360	b	2,286	2,116
2S/1W-31H1	1, 2	1970	650	2,510	13	550–650	b	1,960	1,860
2S/1W-31L1	1, 2	1999	1,110	2,405	16	180–540; 870–1,090	b	2,225	1,315
2S/1W-32M1	1, 2	1999	1,135	2,468	16	360–550; 570–1,040; 1,095–1,135	b	2,108	1,333
2S/2W-24J1	1, 2	1954	282	2,440	10	113–118; 150–161; 252–275	up	2,327	2,165
2S/2W-25F2	1, 2	1986	250	2,290	4	70–250	up	2,220	2,040
2S/2W-25F3	1, 2	1989	250	2,290	6	170–250	up	2,320	2,240
2S/2W-25G1	1, 2	1973	415	2,290	12	209–409	b	2,081	1,881
2S/2W-25J1	1, 2	1977	358	2,360	14	197–358	up	2,163	2,002
2S/2W-25J2	1, 2	1977	403	2,380	14	240–403	unk	2,140	1,977
Area 2									
2S/1W-33L1	1, 2	1999	1,400	2,566	16	400–1,370	b	2,166	1,196
3S/1W-04Q2	1, 2	1953	819	2,575	12	350–806	b	2,225	1,769
Area 3									
2S/1W-22Q3	1, 2	1990	1,000	2,926	6	200–220; 280–300; 340–360; 480–500; 540–560; 960–980	up	2,726	1,946
2S/1W-27B1	1, 2	1961	788	2,887	16	530–694; 710–725	up	2,357	2,162
	3								
	4								
	5	1991	1,143	2,887	16	(well deepened) 530–1,143	b	2,357	1,744
Area 4									
2S/1W-34A2	1, 2	1970	1,000	2,747	20	550–980	b	2,197	1,767
3S/1W-34Q1	1, 2	1955	910	2,665	12	420–595	up	2,245	2,070
	6								
	7								
3S/1E-06N1	1, 2	1959	900	2,555	14	360–900	b	2,195	1,655
3S/1E-07E1	1, 2	1951	744	2,520	20	50–710	b	2,470	1,810
3S/1E-07E2	1, 2	1984	1,000	2,522	20	400–1,000	b	2,122	1,522
3S/1W-01Q1	1, 2	1961	1,152	2,583	16	420–1,152	b	2,163	1,431
3S/1W-03K1	1, 2	1947	800	2,642	20	445–782	up	2,197	1,860
	8								
3S/1W-03K2	1, 2	1952	812	2,641	20	232–604; 604–812	up	2,409	1,829
	3								
	4								
3S/1W-03K3	1, 2	1936	946	2,634	20	320–694	up	2,314	1,940
	8								
3S/1W-12B2	1, 2, 9	1990	1,030	2,569	18	390–1,010	b	2,179	1,559
3S/1W-12E1	1, 2, 10	1951	529	2,580	12	270–332; 375–396; 422–444; 472–480	up	2,310	2,100
	7								
Area 5									
3S/1E-17C1	1, 2, 9	1990	1,420	2,387	18	460–930; 1,000–1,400	b	1,927	987
3S/1E-18B1	1, 2	1990	1,000	2,464	14	300–980	b	2,164	1,484

Appendix Table 2. Well construction, specific capacity, and transmissivity data for selected wells, San Gorgonio Pass area, Riverside County, California—Continued.

[T, transmissivity equals specific capacity times 230. Depths and perforated interval in feet below land surface. Land-surface and screen altitudes in feet above NVDG 27 (National Geodetic Vertical Datum of 1927). Shaded drawdown measurements may have been taken after the recovery period rather than immediately at the time pumping was discontinued. unk, unknown; lo, lower aquifer; up, upper aquifer; b, both upper and lower aquifers. na, not available; ft, foot; gal/min, gallon per minute; gal/min/ft, gallon per minute per foot; in., inches; ft²/d, square foot per day]

Perforation length (ft)	Discharge (gal/min)	Drawdown (ft)	Reported hours pumped	Reported specific capacity (gal/min/ft)	Calculated		Confidence in data (1 low–4 high)
					Specific capacity (gal/min/ft)	T (ft ² /d)	
125	70	2.0	24		35.0	8,050	1
121	70	2.0	24		35.0	8,050	1
81	100	14.0	8		7.1	1,650	2
200	40	250.0	2		0.2	50	2
100	15	40.0	2		0.4	100	2
200	1,010	30.0	21		33.7	7,750	2
900	4,000	3.0	33		1,333.3	306,650	1
200	600	24.0	25		25.0	5,750	2
170	410	160.0	12		2.6	600	2
100	650	89.0	24		7.3	1,700	2
910	1,800	205.0	12		8.8	2,000	2
775	3,100	60.0	24		51.7	11,900	2
162	10	70.0	16		0.1	50	2
180	60	23.0	4		2.6	600	2
80	200	20.0	1		10.0	2,300	2
200	1,010	30.0	21		33.7	7,750	2
161	1,500	6.0	24		250.0	57,500	1
163	1,500	44.0	24		34.1	7,850	2
970	2,300	30.0	na		76.7	17,650	2
456	1,080	62.0	na		17.4	4,000	2
760	15	1.0	24		15.0	3,450	2
195	488	95.0	75		5.1	1,200	2
	329	41.3	na	8.0	8.0	1,850	3
	385	103.4	na	3.7	3.7	850	3
613	1,230	75.0	1	16.4	16.4	3,750	4
430	2,575	138.0	na		18.7	4,300	2
175	na	na	na				2
	994	17.4	na	57.1	57.1	13,150	3
	1,019	16.9	na	60.3	60.3	13,850	3
540	2,000	124.0	12		16.1	3,700	2
600	2,500	1.0	72		2,500.0	575,000	1
600	2,500	1.0	72		2,500.0	575,000	1
732	2,130	152.0	50		14.0	3,200	2
337	1,343	25.2	na	53.3	53.3	12,250	2
	1,402	25.9	na	54.1	54.1	12,450	3
580	2,725	62.0	58		44.0	10,100	2
	1,674	38.2	na	43.8	43.8	10,100	3
	1,964	35.1	na	55.9	56.0	12,850	3
374	1,087	28.2	na	38.5	38.5	8,850	2
	1,114	25.4	na	43.8	43.9	10,100	3
620	700	31.0	2		22.6	5,200	4
210	169	12.0	na	14.1	14.1	3,250	3
	121	13.2	na	9.2	9.2	2,100	3
940	1,100	116.0	24		9.5	2,200	2
680	2,000	11.0	36		181.8	41,800	1

Appendix Table 3. Reported or estimated pumpage for wells in the Beaumont and Banning Storage Units and total pumpage for the Edgar Canyon, Banning Bench and Banning Canyon Storage Units, San Geronio Pass, Riverside County, California, 1927–2003—Continued.

[All pumpage values are in acre-feet per year. PGA, Professional Golf Association. —, Prior to well being drilled. Shaded values are estimates]

State Well number	Owner and well name/number	Model node Pumpage fraction		Pumpage										
		(row,column) Layer1	Layer2	1947	1948	1949	1950	1951	1952	1953	1954	1955	1956	
Area 4														
2S/1W-34A2	BCVWD 21	95	5	—	—	—	—	—	—	—	—	—	—	—
2S/1W-34E1	Manheim, M. Wilkins	100	—	97	97	97	97	97	97	97	97	97	97	84
2S/1W-34Q1	BCVWD 22 @ Old 55	100	—	—	—	—	—	—	—	—	—	—	109	640
3S/1E-06M1	Mountain Water Co. 1	100	—	—	—	—	—	—	—	—	—	—	—	—
3S/1E-06N1	Mountain Water Co. 2	75	25	—	—	—	—	—	—	—	—	—	—	—
3S/1E-06N2	Mountain Water Co. 9	100	—	—	—	—	—	—	—	—	—	—	—	—
3S/1E-06P1	Mountain Water Co. 3	67	33	—	—	—	—	—	—	—	—	—	—	—
3S/1E-07E1	Banning City Water C-2	94	6	—	—	—	—	—	—	320	800	990	960	850
3S/1E-07E2	Banning City Water C-2A	33,61	28	73	—	—	—	—	—	—	—	—	—	—
3S/1E-18D1	Banning City Water 7	37,63	89	11	—	—	—	—	—	—	—	—	—	—
3S/1W-01Q1		32,59	61	39	—	—	—	—	—	—	—	—	—	—
3S/1W-03K1	BCVWD 2	33,48	100	0	864	859	1,030	1,076	1,029	1,029	835	822	721	705
3S/1W-03K2	BCVWD 3	34,48	100	—	—	—	—	—	12	389	455	484	403	403
3S/1W-03K3	BCVWD 1	34,47	100	1,624	1,737	1,930	1,839	1,919	2,017	2,017	1,681	1,894	1,887	1,401
3S/1W-11A2	BCVWD Old 15	35,55	100	—	—	—	—	21	21	21	21	21	21	21
3S/1W-12B2	Banning City Water C-4	33,59	69	—	—	—	—	—	—	—	—	—	—	—
3S/1W-12G1		35,59	100	0	0	0	0	0	0	0	0	0	0	0
3S/1W-12K1	Banning City Water C-3 Sunland	35,60	90	10	—	—	—	—	—	—	—	—	—	—
Annual area pumpage				1,721	2,698	2,886	2,966	3,113	3,496	3,823	4,279	4,279	4,279	4,104
Area 5														
3S/1E-08P1	Banning City Water C-1	34,69	83	17	—	—	—	—	—	—	—	—	—	16
3S/1E-17C1	Banning City Water C-5	34,70	100	—	—	—	—	—	—	—	—	—	—	—
3S/1E-18A1	Banning City Water 10	35,67	40	60	—	—	—	—	—	—	—	—	—	—
Annual area pumpage				0	0	0	0	0	0	0	0	0	0	16
Total Beaumont and Banning storage basin pumpage				2,655	3,637	3,825	5,381	6,035	6,334	7,466	6,982	5,910	6,003	6,003
Total Edgar Canyon pumpage				1,139	832	1,160	1,336	1,475	1,824	979	848	839	1,295	1,295
Total Banning Bench and Banning Canyon pumpage				6,550	4,700	4,425	3,945	2,575	4,095	4,155	3,986	3,835	4,062	4,062

Appendix Table 3. Reported or estimated pumpage for wells in the Beaumont and Banning Storage Units and total pumpage for the Edgar Canyon, Banning Bench and Banning Canyon Storage Units, San Geronio Pass, Riverside County, California, 1927–2003—Continued.

[All pumpage values are in acre-feet per year. PGA, Professional Golf Association. —, Prior to well being drilled. Shaded values are estimates]

State Well number	Owner and well name/number	Model node Pumpage fraction		Pumpage											
		(row,column) Layer 1	Layer 2	1957	1958	1959	1960	1961	1962	1963	1964	1965	1966		
Area 1															
2S/1W-30J2	SunnyCal Egg & Poultry 3	100		0	0	0	0	0	0	0	0	0	0	0	
2S/1W-29M4	SunnyCal Egg & Poultry 1	90	10	0	0	0	0	0	0	0	0	0	0	0	
2S/1W-29N1	SunnyCal Egg & Poultry 2	100		—	—	—	—	—	—	—	—	—	—	—	
2S/1W-30J1	SunnyCal Egg & Poultry 4	74	26	0	0	0	0	0	0	0	0	0	0	0	
2S/1W-30L1	Tyson, E Landholm	100		33	33	0	19	21	22	24	25	23	23	23	
2S/1W-30N1	Riedman, F.	100		438	738	738	738	738	738	738	738	350	350	350	
2S/1W-31G1	Southern California PGA (A)	74	26	—	—	—	—	—	—	—	—	—	—	—	
2S/1W-31H1	Southern California PGA (D)	74	26	—	—	—	—	—	—	—	—	—	—	—	
2S/2W-23J6	Brown Concrete	98	2	—	—	11	19	21	22	24	25	23	23	23	
2S/2W-23R1		98	2	520	520	520	520	520	520	516	516	516	516	516	
2S/2W-24E2	Yucaipa Valley Water Dist. 34 {Gard2}	24	76	120	100	100	100	100	400	400	408	360	619	619	
2S/2W-24E3	Yucaipa Valley Water Dist. 35 {Gard1}	90	10	420	400	400	400	400	400	323	0	102	0	0	
2S/2W-24L1	Yucaipa Valley Water Dist. 48	27,22	100	—	—	—	—	—	—	—	—	—	—	—	
2S/2W-25B4	Murray, C.	100		—	—	—	—	—	—	—	—	—	—	—	
2S/2W-25B5	Murray, C.	100		—	—	—	—	—	—	—	—	—	—	—	
2S/2W-25C1	Moreno Mutual 8	29,23	100	0	0	0	0	0	0	0	0	0	0	0	
2S/2W-25C2	Rogers, M.	28,22	100	31	0	1,150	672	802	654	537	537	0	0	0	
2S/2W-25D1	Moreno Mutual 5	29,21	99	570	570	570	466	0	480	467	470	470	0	0	
2S/2W-25D2	Moreno Mutual 7	29,21	100	40	40	25	0	0	0	0	0	0	0	0	
2S/2W-25D3	Moreno Mutual 9 E233Q	29,21	96	0	0	0	0	0	0	0	0	0	0	0	
2S/2W-25D5	Moreno Mutual	29,21	99	—	—	—	—	—	—	—	—	—	—	—	
2S/2W-25D6	Moreno Mutual 3	28,22	100	0	0	0	0	0	0	0	0	0	0	0	
2S/2W-25F1	Moreno Mutual	29,23	100	0	0	0	0	0	0	0	0	0	0	0	
2S/2W-25G1	Oak Valley Partners	29,24	91	—	—	—	—	—	—	—	—	—	—	—	
2S/2W-25H1	Downing, R.	29,26	100	0	0	0	0	0	500	250	0	25	0	0	
2S/2W-26A3	Moreno Mutual	29,20	100	145	145	145	0	0	489	467	0	0	0	0	
Annual area pumpage				2,317	2,546	3,659	2,934	2,602	4,225	3,346	2,719	1,869	1,531		
Area 2															
2S/1W-33L1	California Oak Valley Management	96	4	—	—	—	—	—	—	—	—	—	—	—	
3S/1W-04L1	Coscam/Stewart 3	35,42	99	291	230	275	254	325	322	252	424	341	0	0	
3S/1W-04Q2	Coscam/Stewart 2	36,44	100	291	263	316	323	369	317	323	151	235	0	0	
Annual area pumpage				582	493	591	577	694	639	575	575	576	0	0	
Area 3															
2S/1W-27B1	BCVWD 16	21,45	100	—	—	—	—	132	130	309	296	210	247	247	
Annual area pumpage				0	0	0	0	132	130	309	296	210	247	247	

Appendix Table 3. Reported or estimated pumpage for wells in the Beaumont and Banning Storage Units and total pumpage for the Edgar Canyon, Banning Bench and Banning Canyon Storage Units, San Geronimo Pass, Riverside County, California, 1927–2003—Continued.

[All pumpage values are in acre-feet per year. PGA, Professional Golf Association. —, Prior to well being drilled. Shaded values are estimates]

State Well number	Owner and well name/number	Model node (row,column)	Pumpage fraction		Pumpage										
			Layer 1	Layer 2	1957	1958	1959	1960	1961	1962	1963	1964	1965	1966	
Area 4															
2S/1W-34A2	BCVWD 21	26,47	95	5	—	—	—	—	—	—	—	—	—	—	—
2S/1W-34E1	Manheim, M. Wilkins	29,44	100	—	84	84	84	84	84	84	84	84	84	84	84
2S/1W-34Q1	BCVWD 22 @Old 55	31,48	100	—	886	964	896	1,007	883	1,007	708	535	771	831	831
3S/1E-06M1	Mountain Water Co. 1	30,60	100	—	—	—	—	—	—	—	—	—	11	10	—
3S/1E-06N1	Mountain Water Co. 2	31,61	75	25	—	—	—	—	6	6	11	19	26	36	36
3S/1E-06N2	Mountain Water Co. 9	31,61	100	—	—	—	—	—	—	—	—	—	—	—	—
3S/1E-06P1	Mountain Water Co. 3	31,62	67	33	—	—	—	—	—	—	—	—	—	—	—
3S/1E-07E1	Banning City Water C-2	33,61	94	6	—	—	—	—	—	—	—	—	—	—	—
3S/1E-07E2	Banning City Water C-2A	33,61	28	73	—	—	—	—	—	—	—	—	—	—	—
3S/1E-18D1	Banning City Water 7	37,63	89	11	—	—	—	—	—	—	—	—	—	—	—
3S/1W-01Q1		32,59	61	39	—	—	—	—	—	—	—	—	—	—	360
3S/1W-03K1	BCVWD 2	33,48	100	—	982	296	272	595	754	595	644	614	362	645	645
3S/1W-03K2	BCVWD 3	34,48	100	—	525	434	1,191	942	1,098	942	330	622	440	294	294
3S/1W-03K3	BCVWD 1	34,47	100	—	552	1,122	534	602	494	602	547	669	618	729	729
3S/1W-11A2	BCVWD Old 15	35,55	100	—	21	21	7	29	28	29	1	6	2	3	3
3S/1W-12B2	Banning City Water C-4	33,59	69	31	—	—	—	—	—	—	—	—	—	—	—
3S/1W-12G1		35,59	100	—	0	0	0	0	0	0	0	0	0	0	0
3S/1W-12K1	Banning City Water C-3 Sunland	35,60	90	10	—	—	—	—	—	—	—	—	—	—	—
Annual area pumpage					3,050	2,921	2,984	3,259	3,347	3,265	2,325	2,549	2,314	2,992	2,992
Area 5															
3S/1E-08P1	Banning City Water C-1	34,69	83	17	707	767	652	574	1,090	1,174	1,185	1,144	902	902	902
3S/1E-17C1	Banning City Water C-5	34,70	100	—	—	—	—	—	—	—	—	—	—	—	—
3S/1E-18A1	Banning City Water 10	35,67	40	60	—	—	—	—	—	—	—	—	—	—	—
Annual area pumpage					707	767	652	574	1,090	1,174	1,185	1,144	902	902	902
Total Beaumont and Banning storage basin pumpage					6,656	6,727	7,886	7,344	7,865	9,433	7,740	7,283	5,871	5,672	5,672
Total Edgar Canyon pumpage					1,452	964	1,173	994	882	985	1,482	1,212	768	700	700
Total Banning Bench and Banning Canyon pumpage					3,114	3,587	3,353	3,675	3,406	3,176	4,122	3,287	3,187	3,301	3,301

Appendix Table 3. Reported or estimated pumpage for wells in the Beaumont and Banning Storage Units and total pumpage for the Edgar Canyon, Banning Bench and Banning Canyon Storage Units, San Geronio Pass, Riverside County, California, 1927–2003—Continued.

[All pumpage values are in acre-feet per year. PGA, Professional Golf Association. —, Prior to well being drilled. Shaded values are estimates]

State Well number	Owner and well name/number	Model node Pumpage fraction		Pumpage												
		(row,column) Layer 1	Layer 2	1967	1968	1969	1970	1971	1972	1973	1974	1975	1976			
Area 1																
2S/1W-30J2	SunnyCal Egg & Poultry 3	100	28,32	0	0	0	0	0	0	0	0	0	0	0		
2S/1W-29M4	SunnyCal Egg & Poultry 1	90	28,32	0	0	0	0	0	0	0	0	0	0	0		
2S/1W-29N1	SunnyCal Egg & Poultry 2	100	29,33	—	—	—	—	—	—	—	—	—	—	—		
2S/1W-30I1	SunnyCal Egg & Poultry 4	74	28,31	0	0	0	0	0	0	0	0	0	0	0		
2S/1W-30L1	Tyson, E Landholm	100	28,29	25	24	0	0	0	0	0	0	0	0	0		
2S/1W-30N1	Riedman, F.	100	31,28	0	28	51	165	0	160	140	246	300	344	—		
2S/1W-31G1	Southern California PGA (A)	74	32,33	—	—	—	—	—	—	—	—	—	—	—		
2S/1W-31H1	Southern California PGA (D)	74	32,31	—	—	—	—	—	—	—	—	—	—	—		
2S/2W-23J6	Brown Concrete	98	28,30	25	24	24	24	0	0	0	0	0	0	0		
2S/2W-23R1		98	28,20	516	516	516	516	516	0	330	330	330	330	330		
2S/2W-24E2	Yucaipa Valley Water Dist. 34 { Gard2}	24	25,30	302	375	324	373	494	672	671	0	82	199	—		
2S/2W-24E3	Yucaipa Valley Water Dist. 35 { Gard1}	90	26,20	302	250	324	372	124	73	70	0	437	463	—		
2S/2W-24L1	Yucaipa Valley Water Dist. 48	100	27,22	—	—	—	—	—	—	—	—	—	—	—		
2S/2W-25B4	Murray, C.	100	28,24	—	—	—	55	52	65	46	52	51	46	—		
2S/2W-25B5	Murray, C.	100	28,25	—	—	—	8	8	8	8	8	8	8	—		
2S/2W-25C1	Moreno Mutual 8	100	29,23	0	0	0	0	0	0	0	0	0	0	0		
2S/2W-25C2	Rogers, M.	100	28,22	0	0	0	0	0	0	0	0	0	0	0		
2S/2W-25D1	Moreno Mutual 5	99	29,21	0	470	470	470	0	0	0	0	0	0	0		
2S/2W-25D2	Moreno Mutual 7	100	29,21	0	0	0	0	0	0	0	0	0	0	0		
2S/2W-25D3	Moreno Mutual 9 E233Q	96	29,21	0	0	0	0	0	0	0	0	0	0	0		
2S/2W-25D5	Moreno Mutual	99	29,21	—	—	—	—	—	—	—	—	—	—	—		
2S/2W-25D6	Moreno Mutual 3	100	28,22	0	0	0	0	0	0	0	0	0	0	0		
2S/2W-25F1	Moreno Mutual	100	29,23	0	0	0	0	0	0	0	0	0	0	0		
2S/2W-25G1	Oak Valley Partners	91	29,24	—	—	—	—	—	—	—	138	138	150	—		
2S/2W-25H1	Downing, R.	100	29,26	0	0	0	0	0	0	0	0	0	0	0		
2S/2W-26A3	Moreno Mutual	100	29,20	0	0	0	0	0	0	0	0	0	0	0		
Annual area pumpage				1,170	1,687	1,709	1,983	1,194	978	1,265	774	1,346	1,540	—		
Area 2																
2S/1W-33L1	California Oak Valley Management	96	31,40	—	—	—	—	0	0	0	0	0	0	0		
3S/1W-04L1	Coscan/Stewart 3	99	35,42	376	340	254	253	258	288	274	257	460	468	—		
3S/1W-04Q2	Coscan/Stewart 2	100	36,44	159	191	298	263	301	294	285	255	239	677	—		
Annual area pumpage				535	531	552	516	559	582	559	512	699	1,145	—		
Area 3																
2S/1W-27B1	BCVWD 16	100	21,45	170	165	98	92	106	127	64	11	29	121	—		
Annual area pumpage				170	165	98	92	106	127	64	11	29	121	—		

Appendix Table 3. Reported or estimated pumpage for wells in the Beaumont and Banning Storage Units and total pumpage for the Edgar Canyon, Banning Bench and Banning Canyon Storage Units, San Geronio Pass, Riverside County, California, 1927–2003—Continued.

[All pumpage values are in acre-feet per year. PGA, Professional Golf Association. —, Prior to well being drilled. Shaded values are estimates]

State Well number	Owner and well name/number	Model node (row,column)	Pumpage fraction		Pumpage											
			Layer 1	Layer 2	1967	1968	1969	1970	1971	1972	1973	1974	1975	1976		
Area 4																
2S/1W-34A2	BCVWD 21	26,47	95	5	—	—	—	—	40	787	1,076	537	677	687	850	
2S/1W-34E1	Manheim, M. Wilkins	29,44	100	—	84	84	84	84	84	84	84	0	0	0	0	
2S/1W-34Q1	BCVWD 22 @ Old 55	31,48	100	—	539	607	901	691	657	559	651	804	560	797	797	
3S/1E-06M1	Mountain Water Co. 1	30,60	100	—	9	3	9	3	3	3	3	1	1	0	0	
3S/1E-06N1	Mountain Water Co. 2	31,61	75	25	33	40	29	57	52	73	61	60	79	80	80	
3S/1E-06N2	Mountain Water Co. 9	31,61	100	—	—	—	—	—	—	—	—	—	—	—	—	
3S/1E-06P1	Mountain Water Co. 3	31,62	67	33	3	14	20	9	15	12	24	31	21	23	23	
3S/1E-07E1	Banning City Water C-2	33,61	94	6	—	—	—	—	—	—	—	443	403	339	339	
3S/1E-07E2	Banning City Water C-2A	33,61	28	73	—	—	—	—	—	—	—	—	—	—	—	
3S/1E-18D1	Banning City Water 7	37,63	89	11	—	—	—	—	—	—	—	—	—	—	—	
3S/1W-01Q1	—	32,59	61	39	360	360	360	360	360	360	360	360	360	360	400	
3S/1W-03K1	BCVWD 2	33,48	100	—	579	657	755	653	584	675	758	744	691	463	463	
3S/1W-03K2	BCVWD 3	34,48	100	—	285	409	307	374	86	125	63	53	50	66	66	
3S/1W-03K3	BCVWD 1	34,47	100	—	629	957	656	593	515	369	394	437	381	407	407	
3S/1W-11A2	BCVWD Old 15	35,55	100	—	1	4	4	4	4	4	0	6	0	6	6	
3S/1W-12B2	Banning City Water C-4	33,59	69	31	—	—	—	—	—	—	—	—	—	—	—	
3S/1W-12G1	—	35,59	100	—	0	0	0	0	0	2,698	347	0	0	0	0	
3S/1W-12K1	Banning City Water C-3 Sunland	35,60	90	10	—	—	—	—	—	—	—	—	—	—	—	
Annual area pumpage					2,522	3,135	3,125	2,868	3,147	6,038	3,196	3,616	3,232	3,431	3,431	
Area 5																
3S/1E-08P1	Banning City Water C-1	34,69	83	17	41	217	325	300	333	0	0	0	0	0	0	
3S/1E-17C1	Banning City Water C-5	34,70	100	—	—	—	—	—	—	—	—	—	—	—	—	
3S/1E-18A1	Banning City Water 10	35,67	40	60	—	—	—	—	—	—	—	—	—	—	—	
Annual area pumpage					41	217	325	300	333	0	0	0	0	0	0	
Total Beaumont and Banning storage basin pumpage					4,438	5,735	5,809	5,759	5,339	7,725	5,084	4,913	5,306	6,237	6,237	
Total Edgar Canyon pumpage					1,225	841	1,003	1,823	1,709	3,116	1,984	1,765	1,858	1,664	1,664	
Total Banning Bench and Banning Canyon pumpage					3,667	3,452	3,623	4,485	4,301	3,658	2,505	5,301	4,838	4,376	4,376	

Appendix Table 3. Reported or estimated pumpage for wells in the Beaumont and Banning Storage Units and total pumpage for the Edgar Canyon, Banning Bench and Banning Canyon Storage Units, San Geronio Pass, Riverside County, California, 1977–2003—Continued.

[All pumpage values are in acre-feet per year. PGA, Professional Golf Association. —, Prior to well being drilled. Shaded values are estimates]

State Well number	Owner and well name/number	Model node Pumpage fraction		Pumpage												
		Layer 1	Layer 2	1977	1978	1979	1980	1981	1982	1983	1984	1985	1986			
Area 1																
2S/1W-30J2	SunnyCal Egg & Poultry 3	100		0	0	0	0	0	0	0	0	0	0	0		
2S/1W-29M4	SunnyCal Egg & Poultry 1	90	10	0	0	0	0	0	0	0	0	0	0	0		
2S/1W-29N1	SunnyCal Egg & Poultry 2	100		0	0	0	0	0	0	0	0	0	0	0		
2S/1W-30J1	SunnyCal Egg & Poultry 4	74	26	0	0	0	0	0	0	0	0	0	0	0		
2S/1W-30L1	Tyson, E Landholm	100		0	0	0	0	0	0	0	0	0	0	0		
2S/1W-30N1	Riedman, F.	100		0	351	355	390	400	410	430	400	390	420	420		
2S/1W-31G1	Southern California PGA (A)	74	26	—	—	—	—	—	—	—	—	—	—	—		
2S/1W-31H1	Southern California PGA (D)	74	26	—	—	—	—	—	—	—	—	—	—	—		
2S/2W-23J6	Brown Concrete	98	2	0	0	0	0	0	0	0	0	0	0	0		
2S/2W-23R1		98	2	330	0	410	300	300	240	200	1	0	0	0		
2S/2W-24E2	Yucaipa Valley Water Dist. 34 {Gard2}	24	76	130	0	97	99	114	120	267	426	443	664	664		
2S/2W-24E3	Yucaipa Valley Water Dist. 35 {Gard1}	90	10	379	0	529	568	600	441	242	237	253	46	46		
2S/2W-24L1	Yucaipa Valley Water Dist. 48	27,22	100	—	—	—	—	—	—	—	—	—	—	—		
2S/2W-25B4	Murray, C.	100		39	40	40	65	0	44	58	51	59	54	54		
2S/2W-25B5	Murray, C.	100		8	8	8	0	0	18	8	8	13	7	7		
2S/2W-25C1	Moreno Mutual 8	100		0	0	0	0	0	0	0	0	0	0	0		
2S/2W-25C2	Rogers, M.	100		0	0	0	0	0	0	0	0	0	0	0		
2S/2W-25D1	Moreno Mutual 5	99	1	0	0	0	0	0	0	0	0	0	0	0		
2S/2W-25D2	Moreno Mutual 7	100		0	0	0	0	0	0	0	0	0	0	0		
2S/2W-25D3	Moreno Mutual 9 E233Q	96	4	0	0	0	0	0	0	0	0	0	0	0		
2S/2W-25D5	Moreno Mutual	99	1	—	—	—	—	—	—	—	—	—	—	—		
2S/2W-25D6	Moreno Mutual 3	28,22	100	0	0	0	0	0	0	0	0	0	0	0		
2S/2W-25F1	Moreno Mutual	29,23	100	0	0	0	0	0	0	0	0	0	0	0		
2S/2W-25G1	Oak Valley Partners	29,24	9	150	138	113	275	900	0	750	750	750	750	750		
2S/2W-25H1	Downing, R.	29,26	100	0	0	0	0	0	0	0	0	0	0	0		
2S/2W-26A3	Moreno Mutual	29,20	100	0	0	0	0	0	0	0	0	0	0	0		
Annual area pumpage				1,036	537	1,552	1,697	2,314	1,273	1,955	1,873	1,908	1,941	1,941		
Area 2																
2S/1W-33L1	California Oak Valley Management	96	4	0	0	0	0	0	0	0	0	0	0	0		
3S/1W-04L1	Coscan/Stewart 3	35,42	1	241	118	148	232	470	379	344	440	373	308	308		
3S/1W-04Q2	Coscan/Stewart 2	36,44	100	385	249	220	249	557	313	185	257	192	201	201		
Annual area pumpage				626	367	368	481	1,027	692	529	697	565	509	509		
Area 3																
2S/1W-27B1	BCVWD 16	21,45	100	31	0	0	0	0	203	0	0	0	0	0		
Annual area pumpage				31	0	0	0	203	0	0	0	0	0	0		

Appendix Table 3. Reported or estimated pumpage for wells in the Beaumont and Banning Storage Units and total pumpage for the Edgar Canyon, Banning Bench and Banning Canyon Storage Units, San Geronimo Pass, Riverside County, California, 1927–2003—Continued.

[All pumpage values are in acre-feet per year. PGA, Professional Golf Association. —, Prior to well being drilled. Shaded values are estimates]

State Well number	Owner and well name/number	Model node (row,column)	Pumpage fraction		Pumpage											
			Layer 1	Layer 2	1977	1978	1979	1980	1981	1982	1983	1984	1985	1986		
Area 4																
2S/1W-34A2	BCVWD 21	26,47	95	5	923	1,077	1,028	1,166	573	491	416	856	1,786	1,442		
2S/1W-34E1	Manheim, M. Wilkins	29,44	100		0	0	0	0	0	0	0	0	0	0		
2S/1W-34Q1	BCVWD 22 @Old 55	31,48	100		473	508	756	140	0	0	0	0	0	0		
3S/1E-06M1	Mountain Water Co. 1	30,60	100		0	0	0	0	0	0	0	0	0	0		
3S/1E-06N1	Mountain Water Co. 2	31,61	75	25	88	112	0	120	130	135	129	130	86	71		
3S/1E-06N2	Mountain Water Co. 9	31,61	100		0	0	0	0	0	0	0	0	0	0		
3S/1E-06P1	Mountain Water Co. 3	31,62	67	33	26	13	14	67	74	72	35	67	113	120		
3S/1E-07E1	Banning City Water C-2	33,61	94	6	224	289	91	93	10	915	1	0	13	0		
3S/1E-07E2	Banning City Water C-2A	33,61	28	73	—	—	—	—	—	—	—	—	—	64		
3S/1E-18D1	Banning City Water 7	37,63	89	11	—	2	0	0	25	25	20	30	41	57		
3S/1W-01Q1		32,59	61	39	300	200	175	0	0	0	0	0	0	0		
3S/1W-03K1	BCVWD 2	33,48	100		759	959	553	627	664	169	24	24	57	83		
3S/1W-03K2	BCVWD 3	34,48	100		29	22	100	0	0	0	0	109	630	747		
3S/1W-03K3	BCVWD 1	34,47	100		353	597	474	474	358	142	23	30	6	94		
3S/1W-11A2	BCVWD Old 15	35,55	100		0	0	0	0	0	0	0	0	0	0		
3S/1W-12B2	Banning City Water C-4	33,59	69	31	—	—	—	—	—	—	—	—	—	—		
3S/1W-12G1		35,59	100		0	0	0	0	0	0	0	0	0	0		
3S/1W-12K1	Banning City Water C-3 Sunland	35,60	90	10	—	—	—	—	—	—	—	—	—	—		
Annual area pumpage					3,175	3,779	3,191	2,687	1,834	1,949	648	1,246	2,732	2,678		
Area 5																
3S/1E-08P1	Banning City Water C-1	34,69	83	17	0	0	0	0	0	0	0	0	0	0		
3S/1E-17C1	Banning City Water C-5	34,70	100		—	—	—	—	—	—	—	—	—	—		
3S/1E-18A1	Banning City Water 10	35,67	40	60	—	—	—	—	—	—	—	—	—	—		
Annual area pumpage					0	0	0	0	0	0	0	0	0	0		
Total Beaumont and Banning storage basin pumpage					4,868	4,683	5,111	4,865	5,378	3,914	3,132	3,816	5,205	5,128		
Total Edgar Canyon pumpage					1,293	1,414	1,044	2,180	3,159	3,069	3,102	3,357	1,509	2,336		
Total Banning Bench and Banning Canyon pumpage					4,042	5,698	5,255	6,182	6,408	5,396	7,163	6,567	6,523	6,382		

Appendix Table 3. Reported or estimated pumpage for wells in the Beaumont and Banning Storage Units and total pumpage for the Edgar Canyon, Banning Bench and Banning Canyon Storage Units, San Geronio Pass, Riverside County, California, 1972–2003—Continued.

[All pumpage values are in acre-feet per year. PGA, Professional Golf Association. —, Prior to well being drilled. Shaded values are estimates]

State Well number	Owner and well name/number	Model node Pumpage fraction		Pumpage										
		Layer 1	Layer 2	1987	1988	1989	1990	1991	1992	1993	1994	1995	1996	
Area 1														
2S/1W-30J2	SunnyCal Egg & Poultry 3	100	0	0	0	0	0	0	0	0	0	0	0	403
2S/1W-29M4	SunnyCal Egg & Poultry 1	90	10	0	0	0	0	0	0	0	0	0	0	75
2S/1W-29N1	SunnyCal Egg & Poultry 2	100	0	0	0	0	0	0	0	0	0	0	0	25
2S/1W-30J1	SunnyCal Egg & Poultry 4	74	26	0	0	0	0	0	0	0	0	0	0	1
2S/1W-30L1	Tyson, E Landholm	100	0	0	0	0	0	0	0	0	0	0	0	0
2S/1W-30N1	Riedman, F.	100	420	490	470	470	470	480	490	490	475	500	550	525
2S/1W-31G1	Southern California PGA (A)	74	26	—	—	—	—	—	—	—	—	—	1	0
2S/1W-31H1	Southern California PGA (D)	74	26	—	—	—	—	—	—	—	—	—	—	—
2S/2W-23J6	Brown Concrete	98	2	0	0	0	0	0	0	0	0	0	0	0
2S/2W-23R1		98	2	0	0	0	0	0	0	0	0	0	0	0
2S/2W-24E2	Yucaipa Valley Water Dist. 34 { Gard2 }	24	76	626	754	749	743	673	777	763	763	244	0	0
2S/2W-24E3	Yucaipa Valley Water Dist. 35 { Gard1 }	90	10	61	20	73	56	83	4	29	430	11	11	11
2S/2W-24L1	Yucaipa Valley Water Dist. 48	100	100	—	—	—	—	—	—	—	140	854	912	0
2S/2W-25B4	Murray, C.	100	62	59	70	67	67	69	71	65	73	75	73	73
2S/2W-25B5	Murray, C.	100	13	10	18	20	20	25	26	24	29	28	26	26
2S/2W-25C1	Moreno Mutual 8	100	100	0	0	0	0	0	0	0	0	0	0	0
2S/2W-25C2	Rogers, M.	100	0	0	0	0	0	0	0	0	0	0	0	0
2S/2W-25D1	Moreno Mutual 5	99	1	0	0	0	0	0	0	0	0	0	0	0
2S/2W-25D2	Moreno Mutual 7	100	0	0	0	0	0	0	0	0	0	0	0	0
2S/2W-25D3	Moreno Mutual 9 E233Q	96	4	0	0	0	0	0	0	0	0	0	0	0
2S/2W-25D5	Moreno Mutual	99	1	—	—	—	375	375	375	325	325	325	330	330
2S/2W-25D6	Moreno Mutual 3	100	0	0	0	0	0	0	0	0	0	0	0	0
2S/2W-25F1	Moreno Mutual	100	0	0	0	0	0	0	0	0	0	0	0	0
2S/2W-25G1	Oak Valley Partners	91	9	750	15	750	750	750	750	0	750	10	10	10
2S/2W-25H1	Downing, R.	100	0	0	0	0	0	0	0	0	0	0	0	0
2S/2W-26A3	Moreno Mutual	100	0	0	0	0	0	0	0	0	0	0	0	0
Annual area pumpage				1,932	1,348	2,130	2,481	1,704	2,493	1,681	2,491	1,859	2,391	
Area 2														
2S/1W-33L1	California Oak Valley Management	96	4	0	0	0	700	650	675	740	640	850	863	863
3S/1W-04L1	Coscan/Stewart 3	99	1	293	235	98	100	71	114	0	0	0	0	0
3S/1W-04Q2	Coscan/Stewart 2	100	0	311	384	62	100	0	72	65	65	13	0	0
Annual area pumpage				604	619	160	900	721	860	805	705	863	863	
Area 3														
2S/1W-27B1	BCVWD 16	100	0	0	0	0	134	416	432	167	272	146	252	252
Annual area pumpage				0	0	0	134	416	432	167	272	146	252	

Appendix Table 3. Reported or estimated pumpage for wells in the Beaumont and Banning Storage Units and total pumpage for the Edgar Canyon, Banning Bench and Banning Canyon Storage Units, San Geronimo Pass, Riverside County, California, 1927–2003—Continued.

[All pumpage values are in acre-feet per year. PGA, Professional Golf Association. —, Prior to well being drilled. Shaded values are estimates]

State Well number	Owner and well name/number	Model node (row,column)	Pumpage fraction		Pumpage									
			Layer 1	Layer 2	1987	1988	1989	1990	1991	1992	1993	1994	1995	1996
Area 4														
2S/1W-34A2	BCVWD 21	26,47	95	5	1,432	2,389	2,124	1,927	1,726	1,321	1,044	942	732	970
2S/1W-34E1	Manheim, M. Wilkins	29,44	100		0	0	0	0	0	0	0	0	0	0
2S/1W-34Q1	BCVWD 22 @Old 55	31,48	100		0	0	0	8	541	362	76	41	3	0
3S/1E-06M1	Mountain Water Co. 1	30,60	100		0	0	0	0	0	0	0	0	0	0
3S/1E-06N1	Mountain Water Co. 2	31,61	75	25	73	118	115	119	99	0	55	49	36	55
3S/1E-06N2	Mountain Water Co. 9	31,61	100		9	35	39	42	2	0	5	155	8	9
3S/1E-06P1	Mountain Water Co. 3	31,62	67	33	118	163	186	189	144	0	143	133	147	165
3S/1E-07E1	Banning City Water C-2	33,61	94	6	0	0	0	0	0	0	0	0	0	0
3S/1E-07E2	Banning City Water C-2A	33,61	28	73	89	0	1,365	1,303	1,152	645	407	356	3	4
3S/1E-18D1	Banning City Water 7	37,63	89	11	58	58	60	64	64	0	36	39	4	5
3S/1W-01Q1		32,59	61	39	0	0	0	0	0	0	0	0	0	0
3S/1W-03K1	BCVWD 2	33,48	100		241	176	730	709	784	949	652	525	339	497
3S/1W-03K2	BCVWD 3	34,48	100		1,409	1,100	1,193	1,176	637	527	173	282	75	187
3S/1W-03K3	BCVWD 1	34,47	100		36	156	289	369	117	40	35	6	0	1
3S/1W-11A2	BCVWD Old 15	35,55	100		0	0	0	0	0	0	0	0	0	0
3S/1W-12B2	Banning City Water C-4	33,59	69	31	—	—	—	—	—	315	472	1,174	823	330
3S/1W-12G1		35,59	100		0	0	0	0	0	0	0	0	0	0
3S/1W-12K1	Banning City Water C-3 Sunland	35,60	90	10	403	792	1,453	1,711	1,721	830	822	163	106	166
Annual area pumpage					3,868	4,987	7,554	7,617	6,986	4,989	3,920	3,865	2,276	2,389
Area 5														
3S/1E-08P1	Banning City Water C-1	34,69	83	17	0	0	0	0	0	0	0	0	0	0
3S/1E-17C1	Banning City Water C-5	34,70	100		—	—	—	—	—	429	461	58	225	115
3S/1E-18A1	Banning City Water 10	35,67	40	60	—	—	46	42	2	0	0	0	0	98
Annual area pumpage					0	0	46	42	2	429	461	58	225	213
Total Beaumont and Banning storage basin pumpage					6,404	6,954	9,890		9,828	9,203	7,034	7,391	5,369	6,108
Total Edgar Canyon pumpage					1,058	1,767	1,326	1,780	295	1,354	2,894	2,727	4,192	3,666
Total Banning Bench and Banning Canyon pumpage					6,256	5,673	4,716	3,680	4,623	5,531	6,017	5,508	6,297	8,050

Appendix Table 3. Reported or estimated pumpage for wells in the Beaumont and Banning Storage Units and total pumpage for the Edgar Canyon, Banning Bench and Banning Canyon Storage Units, San Geronio Pass, Riverside County, California, 1972–2003—Continued.

[All pumpage values are in acre-feet per year. PGA, Professional Golf Association. —, Prior to well being drilled. Shaded values are estimates]

State Well number	Owner and well name/number	Model node (row,column)	Pumpage fraction		Pumpage						Total pumpage and area	
			Layer 1	Layer 2	1997	1998	1999	2000	2001	2002		2003
Area 1												
2S/1W-30J2	SunnyCal Egg & Poultry 3	28,32	100		967	1,250	1,600	1,625	1,706	1,306	1,306	10,893
2S/1W-29M4	SunnyCal Egg & Poultry 1	28,32	90	10	47	57	61	63	78	79	79	1,967
2S/1W-29N1	SunnyCal Egg & Poultry 2	29,33	100		49	59	70	74	90	90	90	547
2S/1W-30I1	SunnyCal Egg & Poultry 4	28,31	74	26	47	56	126	130	144	146	146	1,596
2S/1W-30L1	Tyson, E Landholm	28,29	100		0	0	0	0	0	0	0	586
2S/1W-30N1	Riedman, F.	31,28	100		540	550	545	535	530	530	520	20,629
2S/1W-31G1	Southern California PGA (A)	32,33	74	26	0	0	0	355	124	233	284	997
2S/1W-31H1	Southern California PGA (D)	32,31	74	26	—	—	—	1,325	1,194	988	1,067	4,574
2S/2W-23J6	Brown Concrete	28,30	98	2	0	0	0	0	0	0	0	265
2S/2W-23R1		28,20	98	2	0	0	0	0	0	0	0	11,385
2S/2W-24E2	Yucaipa Valley Water Dist. 34 { Gard2 }	25,30	24	76	0	0	0	0	0	0	0	13,488
2S/2W-24E3	Yucaipa Valley Water Dist. 35 { Gard1 }	26,20	90	10	6	2	29	356	313	39	75	10,153
2S/2W-24L1	Yucaipa Valley Water Dist. 48	27,22	100		868	777	859	418	1,061	1,565	1,663	9,117
2S/2W-25B4	Murray, C.	28,24	100		6	2	29	75	99	99	99	1,910
2S/2W-25B5	Murray, C.	28,25	100		22	26	30	75	99	103	103	811
2S/2W-25C1	Moreno Mutual 8	29,23	100		0	0	0	0	0	0	0	3,136
2S/2W-25C2	Rogers, M.	28,22	100		0	0	0	0	0	0	0	4,551
2S/2W-25D1	Moreno Mutual 5	29,21	99	1	0	0	0	0	0	0	0	21,137
2S/2W-25D2	Moreno Mutual 7	29,21	100		0	0	0	0	0	0	0	3,701
2S/2W-25D3	Moreno Mutual 9 E233Q	29,21	96	4	0	0	0	136	91	73	143	10,207
2S/2W-25D5	Moreno Mutual	29,21	99	1	300	300	300	300	300	300	300	4,535
2S/2W-25D6	Moreno Mutual 3	28,22	100		0	0	0	0	0	0	0	11,217
2S/2W-25F1	Moreno Mutual	29,23	100		0	0	0	0	0	0	0	10,099
2S/2W-25G1	Oak Valley Partners	29,24	91	9	10	10	10	10	10	10	10	8,857
2S/2W-25H1	Downing, R.	29,26	100		0	0	0	0	0	0	0	1,701
2S/2W-26A3	Moreno Mutual	29,20	100		0	0	0	0	0	0	0	2,406
Annual area pumpage					2,862	3,089	3,659	5,476	5,839	5,561	5,885	170,461
Area 2												
2S/1W-33L1	California Oak Valley Management	31,40	96	4	852	558	558	718	502	893	900	10,099
3S/1W-04L1	Coscan/Stewart 3	35,42	99	1	0	0	0	0	0	0	944	10,849
3S/1W-04Q2	Coscan/Stewart 2	36,44	100		0	0	0	0	0	0	1,017	10,447
Annual area pumpage					852	558	558	718	502	893	2,861	31,395
Area 3												
2S/1W-27B1	BCVWD 16	21,45	100		367	175	329	403	516	1,906	1,144	9,200
Annual area pumpage					367	175	329	403	516	1,906	1,144	9,200

Appendix Table 3. Reported or estimated pumpage for wells in the Beaumont and Banning Storage Units and total pumpage for the Edgar Canyon, Banning Bench and Banning Canyon Storage Units, San Geronio Pass, Riverside County, California, 1927–2003—Continued.

[All pumpage values are in acre-feet per year. PGA, Professional Golf Association. —, Prior to well being drilled. Shaded values are estimates]

State Well number	Owner and well name/number	Model node (row,column)	Pumpage fraction		Pumpage					Total pumpage and area		
			Layer 1	Layer 2	1997	1998	1999	2000	2001		2002	2003
Area 4												
2S/1W-34A2	BCVWD 21	26,47	95	5	1,200	1,144	1,540	1,689	1,971	2,234	1,644	40,441
2S/1W-34E1	Manheim, M. Wilkins	29,44	100		0	0	0	0	0	0	0	2,301
2S/1W-34Q1	BCVWD 22 @Old 55	31,48	100		0	1	0	8	17	230	840	20,007
3S/1E-06M1	Mountain Water Co. 1	30,60	100		0	0	0	0	0	0	0	53
3S/1E-06N1	Mountain Water Co. 2	31,61	75	25	50	0	0	0	0	0	0	2,438
3S/1E-06N2	Mountain Water Co. 9	31,61	100		3	0	0	0	0	0	424	731
3S/1E-06P1	Mountain Water Co. 3	31,62	67	33	111	0	0	0	0	0	525	2,797
3S/1E-07E1	Banning City Water C-2	33,61	94	6	0	0	0	0	0	0	0	6,741
3S/1E-07E2	Banning City Water C-2A	33,61	28	73	1	0	0	748	1007	1,213	1,136	9,493
3S/1E-18D1	Banning City Water 7	37,63	89	11	4	0	0	0	0	303	344	1,239
3S/1W-01Q1		32,59	61	39	0	0	0	0	0	0	0	4,675
3S/1W-03K1	BCVWD 2	33,48	100		674	360	674	958	1041	1,631	1,017	36,135
3S/1W-03K2	BCVWD 3	34,48	100		292	169	288	513	462	891	934	22,324
3S/1W-03K3	BCVWD 1	34,47	100		1	0	1	67	0	50	6	52,660
3S/1W-11A2	BCVWD Old 15	35,55	100		0	0	0	0	0	0	0	306
3S/1W-12B2	Banning City Water C-4	33,59	69	31	725	1,049	1,144	1,548	1254	1,700	980	11,514
3S/1W-12G1		35,59	100		0	0	0	0	0	0	0	15,045
3S/1W-12K1	Banning City Water C-3 Sunland	35,60	90	10	20	155	817	1,108	1113	1,322	1,017	13,719
	Annual area pumpage				3,081	2,878	4,464	6,639	6,865	9,574	8,867	242,618
Area 5												
3S/1E-08P1	Banning City Water C-1	34,69	83	17	0	0	0	0	0	0	0	10,329
3S/1E-17C1	Banning City Water C-5	34,70	100		134	179	424	586	839	1,103	869	5,422
3S/1E-18A1	Banning City Water 10	35,67	40	60	78	0	0	614	0	0	432	1,312
	Annual area pumpage				212	179	424	1,200	839	1,103	1,301	15,751
Total Beaumont and Banning storage basin pumpage					7,374	6,879	9,434	14,436	14,561	19,037	20,058	469,425
Total Edgar Canyon pumpage					3,476	3,152	3,231	2,671	2,671	2,671	2,671	131,793
Total Banning Bench and Banning Canyon pumpage					7,848	7,102	6,652	5,550	5,550	5,550	5,550	276,511

This page intentionally left blank.

